

TECHNISCHE UNIVERSITÄT MÜNCHEN

Wissenschaftszentrum Weihenstephan
für Ernährung, Landnutzung und Umwelt

Lehrstuhl für Experimentelle Genetik

IN VIVO AND *IN VITRO* ANALYSIS OF DLL1 AND DLL4 FUNCTION IN ADULT PANCREATIC ISLETS

Marina Helga Fütterer

Vollständiger Abdruck der von der Fakultät Wissenschaftszentrum Weihenstephan für Ernährung, Landnutzung und Umwelt der Technischen Universität München zur Erlangung des akademischen Grades eines

Doktors der Naturwissenschaften

genehmigten Dissertation.

Vorsitzender: Univ.-Prof. Dr. S. Scherer

Prüfer der Dissertation:

1. Univ.-Prof. Dr. M. Hrabě de Angelis
2. Univ.-Prof. A. Schnieke, Ph.D.

Die Dissertation wurde am 16.05.2017 bei der Technischen Universität München eingereicht und durch die Fakultät Wissenschaftszentrum Weihenstephan für Ernährung, Landnutzung und Umwelt am 17.10.2017 angenommen.

I. TABLE OF CONTENTS

I. TABLE OF CONTENTS	I
II. FIGURES AND TABLES	V
III. ABBREVIATIONS	IX
1. SUMMARY/ZUSAMMENFASSUNG	1
2. INTRODUCTION	3
2.1. The Delta-Notch pathway	3
2.1.1. General	3
2.1.2. The role of the ligand intracellular domain	7
2.2. The pancreas and islets of Langerhans	9
2.2.1. The pancreatic development.....	9
2.2.2. Notch signaling in the pancreas	11
2.2.3. Islets of Langerhans	14
2.2.3.1. Pancreatic β -cells.....	14
2.2.3.2. Pancreatic α -cells	16
2.3. Glucose metabolism and insulin secretion	18
2.3.1. Regulation of glucose metabolism	18
2.3.2. Insulin secretion in pancreatic beta cells.....	20
2.4. β -cell deficiency in diabetes mellitus	22
2.5. Aim of this thesis.....	24
3. MATERIAL AND METHODS	25
3.1. Materials	25
3.1.1. Chemicals.....	25
3.1.2. Buffers and solutions.....	25
3.1.3. Antibodies	27
3.1.4. Molecular biology reagents.....	29

3.1.5.	Oligonucleotide primers	29
3.1.5.1.	Primers for genotyping.....	29
3.1.5.2.	Primers for qRT-PCR	30
3.1.6.	Consumables and kits.....	31
3.1.7.	Laboratory equipment.....	32
3.2.	Methods	34
3.2.1.	Mouse methods.....	34
3.2.1.1.	Animal housing	34
3.2.1.2.	Generation of β -D1/D4 knock-down mice	34
3.2.1.3.	Generation of β -DICD overexpressing mice	34
3.2.1.4.	Genotyping.....	34
3.2.1.5.	Blood plasma collection	35
3.2.1.6.	Blood glucose evaluation	35
3.2.1.7.	Intraperitoneal and oral glucose tolerance test.....	36
3.2.1.8.	NMR body composition analysis	36
3.2.1.9.	Food consumption analysis	36
3.2.2.	Cell culture methods	36
3.2.2.1.	Islet isolation and culture	36
3.2.2.2.	Glucose-stimulated insulin secretion	38
3.2.3.	Isolation and purification methods	39
3.2.3.1.	DNA isolation.....	39
3.2.3.2.	RNA isolation	39
3.2.3.2.1.	Islets	39
3.2.3.2.2.	Other tissues	40
3.2.4.	Molecular methods	41
3.2.4.1.	Polymerase Chain Reaction.....	41
3.2.4.2.	cDNA synthesis	41

3.2.4.3.	Quantitative real-time PCR (qRT-PCR).....	42
3.2.4.4.	Whole transcriptome microarray analysis	43
3.2.4.4.1.	RNA isolation	43
3.2.4.4.2.	Expression profiling	44
3.2.4.4.3.	Statistical transcriptome analysis.....	44
3.2.4.5.	ELISA.....	44
3.2.4.5.1.	Insulin	44
3.2.4.5.2.	Proinsulin.....	45
3.2.4.5.3.	C-Peptide.....	45
3.2.4.5.4.	Glucagon.....	46
3.2.5.	Immunohistochemistry	46
4.	RESULTS.....	48
4.1.	Loss of function studies of <i>Dll1</i> and <i>Dll4</i> in murine pancreatic β -cells.....	48
4.1.1.	DLL1 and DLL4 are predominately expressed in pancreatic β -cells.....	48
4.1.2.	Mouse models for β -cell specific deletion of <i>Dll1</i> and <i>Dll4</i>	50
4.1.3.	Effects of conditional deletion of <i>Dll1</i> in adult pancreatic β -cells	52
4.1.4.	Effects of conditional deletion of <i>Dll4</i> in adult pancreatic β -cells	56
4.1.5.	Conditional simultaneous deletion of <i>Dll1</i> and <i>Dll4</i> in adult pancreatic β -cells	60
4.1.5.1.	Histological analysis of islet morphology	60
4.1.5.2.	β -D1D4 mice have altered metabolic function in vivo and in vitro.....	66
4.1.5.3.	Expression analysis with whole genome transcriptomics	71
4.2.	Overexpression of DLL1ICD in pancreatic β -cells	76
4.2.1.	Metabolic physiology	76
4.2.2.	Molecular phenotyping	79
4.2.3.	Gene expression analysis.....	81
4.2.3.1.	The cardiovascular system in β -DICD islets	84
4.2.3.2.	Genes associated with islet function and diabetes	85
4.2.3.3.	β -DICD islets express less CTGF	86

5.	DISCUSSION.....	88
5.1.	DLL1- and DLL4 mediated signaling in pancreatic β -cells.....	88
5.1.1.	DLL1 and DLL4 are necessary for islet function, but not islet morphology	89
5.1.2.	Simultaneous deletion of <i>Dll1</i> and <i>Dll4</i> in pancreatic β -cells leads to hypoglycemia and hyperglucagonemia through increased insulin secretion	90
5.1.3.	Gene expression analysis.....	93
5.1.3.1.	Delta-Notch regulates the cell cycle arrest in pancreatic β -cells	93
5.1.3.2.	Genes associated with insulin secretion	95
5.1.3.3.	Mitochondrial dysfunction in β -D1D4 mice	97
5.1.4.	General remarks (Limitations of the project) and future perspective.....	98
5.2.	What is happening inside the β -cell – the DLL1 intracellular domain.....	100
5.2.1.	The DLL1 intracellular domain inhabits a function in β -cells.....	100
5.2.2.	Gene expression analysis.....	101
5.2.2.1.	Genes that state for a compensatory effect	103
5.2.3.	What is the mechanism behind Delta in islets?.....	105
5.2.4.	Conclusion and future perspectives	108
5.3.	Closing remarks.....	110
6.	APPENDIX.....	111
6.1.	Supplementary figures	111
6.2.	Supplementary tables	114
7.	REFERENCES	128
IV.	ACKNOWLEDGEMENTS	151
V.	AFFIRMATION.....	153
VI.	PUBLICATIONS, TALKS AND POSTERS.....	154
VII.	CURRICULUM VITAE	155

II. FIGURES AND TABLES

Figure 1: General overview of the Delta-Notch signaling pathway.....	5
Figure 2: Pancreatic organogenesis.....	10
Figure 3: Schematic representation of pancreatic development and the involvement of Notch signaling.	12
Figure 4: The pathways of insulin secretion.....	21
Figure 5: Immunohistochemical analysis of pancreata in 13-weeks old male C3HeB/FeJ mice.	48
Figure 6: Immunohistochemical analysis of pancreata in 13-weeks old male C3HeB/FeJ mice.	49
Figure 7: Schematic representation of the <i>Dll1</i> locus and its recombination in β -cells of the β -D1 mouse.	50
Figure 8: Proof of knock-down efficiency.....	52
Figure 9: Immunohistochemical analysis of pancreata in 8-weeks old male β -D1 and <i>Cre</i> -positive control mice.	53
Figure 10: Islet hormone content in 8-weeks old male β -D1 and <i>Cre</i> -positive control mice.....	54
Figure 11: qRT-PCR analysis of mRNA in isolated islets from 8-weeks old male β -D1 and <i>Cre</i> -positive control mice.	55
Figure 12: Metabolic phenotype of male β -D1 mice.....	56
Figure 13: Immunohistochemical analysis of pancreata in 8-weeks old male β -D4 and <i>Cre</i> -positive control mice.	57
Figure 14: Islet hormone content in 8-weeks old male β -D4 mice	58
Figure 15:qRT-PCR analysis of isolated islets from 8-weeks old male β -D4 and <i>Cre</i> -positive control mice.	58
Figure 16: Metabolic phenotype of male β -D4 mice.....	59
Figure 17: Immunohistochemical analysis of pancreata from 8-weeks old male β -D1D4 and <i>Cre</i> -positive control mice.	61
Figure 18: Islet hormone content in 8-weeks old male β -D1D4 and <i>Cre</i> -positive control mice.....	62
Figure 19: Immunohistochemical analysis for double positive cells in β -D1D4 and <i>Cre</i> -positive control islets.....	63
Figure 20: Immunohistochemical analysis for α -cell proliferation in β -D1D4 and <i>Cre</i> -positive control islets.....	64

Figure 21: Immunohistochemical analysis of islet maturity in β -D1D4 and <i>Cre</i> -positive control mice	65
Figure 22: Body weight and composition of male β -D1D4 compared to <i>Cre</i> -positive control mice	66
Figure 23: Blood glucose levels of male β -D1D4 compared to <i>Cre</i> -positive control mice	67
Figure 24: Glucose homeostasis in male β -D1D4 mice	68
Figure 25: Glucose stimulated insulin secretion of β -D1D4 and <i>Cre</i> -positive control islets.....	70
Figure 26: Individual daily food intake of β -D1D4 and <i>Cre</i> -positive control mice.....	71
Figure 27: qRT-PCR analysis of isolated islets from 8-weeks old β -D1D4 and <i>Cre</i> -positive control mice.	72
Figure 28: qRT-PCR analysis of insulin-secretion and cell-cycle marker genes in isolated islets from 8-weeks old male β -D1D4 and <i>Cre</i> -positive control mice.....	73
Figure 29: Body weight and blood glucose levels of β -D1CD mice	76
Figure 30: Glucose homeostasis in male β -D1CD mice compared to <i>Cre</i> -positive control animals..	77
Figure 31: Glucose stimulated insulin secretion of β -D1CD islets	78
Figure 32: Hormonal content in islets and plasma of male β -D1CD mice	78
Figure 33: Immunohistochemical analysis of pancreata from 8-weeks old male β -D1CD and <i>Cre</i> -positive control mice	80
Figure 34: qRT-PCR analysis of isolated islets from 8-weeks old male β -D1CD and <i>Cre</i> -positive control mice	81
Figure 35: The vascular system in 8-weeks old male β -D1CD and <i>Cre</i> -positive control mice	84
Figure 36: Ghrelin expression in islets from 8-weeks old male β -D1CD and <i>Cre</i> -positive control mice.	85
Figure 37: qRT-PCR analysis of $Tgf\beta$ components in isolated islets from 8-weeks old male β -D1CD and <i>Cre</i> -positive control mice.....	86
Figure 38: Immunohistochemical analysis of pancreata in 8-weeks old male β -D1CD and <i>Cre</i> -positive control mice.	87
Figure 39: Model of Slit–Robo signaling in pancreatic beta cells	107

Table 1: Overview of the enzymatic steps during glycolysis	18
Table 2: List of used chemicals	25
Table 3: List of used buffers, solutions and their preparation	25
Table 4: List of used primary and secondary antibodies	27
Table 5: List of primers used for mouse genotyping	29
Table 6: List of primers used for qRT-PCR	30
Table 7: List of used consumables.....	31
Table 8: List of used kits	32
Table 9: List of used laboratory equipment	32
Table 10: Components and amount for genotyping PCR	35
Table 11: PCR conditions	35
Table 12: Treatments for GSIS.....	38
Table 13: Components for the pre-annealing step	41
Table 14: Components for the enzymatic reaction	41
Table 15: Components and amount of the qRT-PCR master mix.....	43
Table 16: Reaction conditions	43
Table 17: Overrepresented downregulated diseases	73
Table 18: Overrepresented up regulated diseases.....	74
Table 19: Overrepresented signaling pathways up & down	74
Table 20: Overrepresented downregulated diseases	82
Table 21: Overrepresented upregulated diseases	83
Table 22: Down regulated signaling pathways.....	83
Table 23: Upregulated signaling pathways	84

Supplementary Figure 1: Protein expression of Notch ligands	111
Supplementary Figure 2: Protein expression of Notch receptors	112
Supplementary Figure 3: qRT-PCR analysis of the hypothalamus from 8-weeks old male β -D1D4 and Cre-positive control mice.	113
Supplementary Figure 4: Protein expression of MAGI proteins.....	113
Supplementary Table 1: Differentially expressed genes in isolated islets from 8-weeks old male β -D1D4 and Cre-positive control mice (4.1.5.3) filtered for a fold change of at least 1.3, FDR <10% and p<0.01	114
Supplementary Table 2: Differentially expressed genes in isolated islets from 8-weeks old male β -D1D4 and Control mice (4.2.2.1) filtered for a fold change of at least 1.2 and p<0.01.....	122
Supplementary Table 3: Genes that are differentially expressed in both (β -D1D4 and β -D1CD) data sets	127

III. ABBREVIATIONS

ABBREVIATION	FULL NAME
°C	degree celsius
μL	microliter
μM	micromolar
AC	Adenylyl cyclase
Acetyl CoA	acetyl coenzyme A
Adcy5	adenylate cyclase 5
AIR	Acute insulin response
ANK	Ankyrin
ANOVA	Analysis of variance
Arx	aristaless related homeobox
ATP	Adenosine triphosphate
AUC	Area under the curve
bHLH	basic-helix-loop-helix
bp	basepair
BSA	bovine albumin serum
Ca ²⁺	Calcium
cAMP	cyclic adenosine monophosphate
CDK8	cyclin-dependent kinase-8
cDNA	complementary DNA
CO ₂	Carbon dioxide
Cox	Cytochrom C oxidase
Cp	crossing point
CPA	carboxypeptidase
CSL	CBF1-SU(H)-LAG1
CTGF	connective tissue growth factor
DICD	DLL1 intracellular domain
DLL	Delta-like
DLL1	Delta-like protein 1
DLL4	Delta-like protein 4
DMSO	dimethyl sulfoxide
DNA	desoxyribonuclein acid
dNTPs	Desoxynucleotides
DSL	Delta, Serrate and Lag-2
DTT	Dithiothreitol
ECD	extracellular domain
EDTA	Ethylenediaminetetraacetic acid
EGF	epidermal growth factor
ELISA	Enzyme-linked immunosorbent assay
EPAC2	exchange protein activated by cAMP 2
ER	endoplasmic reticulum
FADH ₂	flavin adenine dinucleotide

FBS	Fetal bovine serum
FC	fold change
FDR	False discovery rate
FELASA	Federation of Laboratory Animal Science Associations
FGF	Fibroblast growth factor
Foxa	forkhead box A
Gcgr	glucagon receptor
GIP	glucose-dependent insulintropic peptide
GIPR	glucose-dependent insulintropic peptide receptor
GLP1	glucagon-like protein1
Glp1r	glucagon-like protein1 receptor
Glut2	glucose transporter 2
GPCR	G-protein coupled receptor
GSIS	glucose-stimulated insulin secretion
GTP	guanosine triphosphate
GTT	Glucose tolerance test
GWAS	genome wide association studies
h	hour
H2O	water
HAT	Histone actelyase
HCl	hydrogen chloride
HEPES	4-(2-hydroxyethyl)-1-piperazineethanesulfonic acid
HKG	Housekeeping gene
Hnf1 α	hepatocyte nuclear factor-1alpha
ICD	intracellular domain
ip	intraperitoneal
IP3	inositol 1,4,5-trisphosphate
JAG	Jagged
KRB	Krebs Ringer Buffer
L	liter
LN	Lin12-Notch
MafA	v-maf musculoaponeurotic fibrosarcoma oncogene family A
MafB	v-maf musculoaponeurotic fibrosarcoma oncogene family B
Mam	Mastmind
MIB	Mindbomb
min	minutes
mL	milliliter
mM	millimolar
MODY	maturity onset diabetes of the young.
MPC	multipotent progenitor cell
Msln	Mesothelin
NAADP	nicotinic acid-adenine dinucleotide phosphate
NAD	Nicotinamide adenine dinucleotide
NaOH	Sodium hydroxide
NEURL	Neutralized

NeuroD1	Neurogenic differentiation 1
Neurog3	Neurogenin 3
NICD	NOTCH intracellular domain
NLS	nuclear localization signal
nM	nanomolar
NMR	Nuclear magnetic resonance
NRR	negative regulatory domain
OCT	Optimum cutting temperature
oGTT	oral glucose tolerance test
PBS	Sodium perborate
PCR	polymerase chain reaction
Pdk	Pyruvate Dehydrogenase Kinase
Pdx1	pancreatic duodenal homeobox 1
PECAM-1	Platelet endothelial cell adhesion molecule
PFA	Paraformaldehyde
Pianp	PILR alpha associated neural protein
PKA	activating protein kinase A
Ptf1a	Pancreas-specific transcriptionfactor 1a
qRT-PCR	quantitative Real-time PCR
RAM	RBPJkappa-associated molecule
RCME	recombinase-mediated cassette exchange
RIN	RNA integrity number
RNA	ribonucleic acid
ROS	radical oxygen species
rpm	rounds per minute
RPMI	Roswell Park Memorial Insitute medium
RT	room temperature
s	seconds
S1	site 1
SDS	Sodium dodecyl Sulfate
SEM	Standard error of the mean
SH2	Src Homology 2
SNARE	small N-ethylmaleimide-sensitive factor receptor
SPF	Specific-pathogen-free
T1DM	type 1 diabetes mellitus
T2DM	type 2 diabetes mellitus
TACE	tumor-necrosis-factor α -converting enzyme
TCA	tricarboxylic acid cycle
TF	transcription factor
TMB	3,3',5,5'-Tetramethylbenzidine
Ucn3	Urocortin 3
USD	US Dollar
VEGF	Vascular endothelial growth factor
Wnt	wingless
α	alpha

β	beta
δ	delta
ϵ	epsilon

1. SUMMARY/ZUSAMMENFASSUNG

The Delta-Notch signaling pathway is involved in the regulation of many cellular processes and genes of the pathway are expressed in different cell types at different time points during embryonic development and adulthood. For example, the Notch ligand Delta-like 1 (DLL1) is important for the proper differentiation of the pancreatic endocrine cell lineage. The ligands DLL1 and DLL4 as well as other members of the pathway are also expressed in the adult pancreas. However, their role in adult tissue homeostasis is not well understood.

This study shows cell-type specific, distinct expression of DLL1 and DLL4 in the adult murine pancreas. Using ligand-specific conditional loss- and gain-of-function mouse models we demonstrate alterations in islet morphology and effects on blood-glucose regulation as well as other metabolic parameters. Mice lacking both DLL1- and DLL4- mediated signaling in β -cells display strong hypoglycemia and perform better during glucose challenge due to increased insulin secretion, while the total insulin content is unaltered. To compensate this phenotype, the mice produce more glucagon and have more α -cells due to an increased proliferation rate.

Furthermore, a possible gain-of-function of DLL1 was analyzed by overexpressing the intracellular domain of DLL1 (DICD) specifically in adult murine pancreatic β -cells. Those mice showed decreased body weight and higher blood glucose levels. Stimulation with glucose *in vivo* and *in vitro* demonstrated impaired glucose tolerance and insulin secretion. The underlying mechanism is still not revealed completely, but this study provides hints that it is independent of the canonical Delta-Notch signaling pathway. Instead an altered protein binding pattern, especially regarding the function of adenylyl cyclase is more likely. Possible target proteins might be among PDZ proteins like the MAGUK proteins or from the novel Slit-Robo pathway.

In conclusion, this study provides new insight into the relevance of Delta-Notch signaling in adult murine islets and shows the importance of the genes *Dll1* and *Dll4* for proper β -cell function.

Der Delta-Notch Signalweg ist an der Regulation von vielen zellulären Prozessen beteiligt und dessen Gene sind in verschiedensten Zelltypen und zu unterschiedlichsten Entwicklungsstadien bis hin zum Erwachsenenalter exprimiert. Der Notch Ligand Delta-like 1 (DLL1) ist zum Beispiel wichtig für die korrekte Differenzierung der endokrinen Zelllinie des Pankreas. Im adulten Pankreas sind neben den Liganden DLL1 und DLL4 auch weitere Mitglieder des Notch Signalweges vorhanden. Allerdings ist deren Funktion dort noch nicht ausführlich untersucht worden.

Diese Dissertation zeigt die zelltyp-spezifische und klare Proteinexpression von DLL1 und DLL4 im adulten Pankreas der Maus. Mittels liganden-spezifischen und konditionalen „Loss-of-function“ und „Gain-of-function“ Mausmodellen konnte eine Veränderung der Inselzellenmorphologie sowie Einflüsse auf die Blutglukoseregulation und andere metabolische Parameter demonstriert werden. Mäuse ohne DLL1- und DLL4-abhängiges Signalpotential in den β -Zellen schütten effektiver Insulin aus und zeigen daher eine ausgeprägte Hypoglykämie und eine bessere Performance während des Glukose Toleranz Tests. Die Gesamtmenge an Insulin bleibt dabei unverändert. Um diesen starken Phänotyp zu kompensieren, produzieren diese Mäuse außerdem deutlich mehr Glukagon und besitzen mehr α -Zellen auf Grund einer gesteigerten Proliferationsrate.

Zusätzlich wurde mittels einer Überexpression der intrazellulären Domäne von DLL1 (DICD) die potentielle „Gain-of-function“ von DLL1 in adulten pankreatischen β -Zellen analysiert. Diese Mäuse zeigten verringertes Körpergewicht und höhere Blutzuckerwerte. Die Stimulation mit Glukose *in vivo* und *in vitro* legte außerdem eine beeinträchtigte Glukosetoleranz und Insulin Ausschüttung dar. Der maßgebliche Mechanismus konnte zwar noch nicht vollständig aufgeklärt werden, allerdings gibt diese Arbeit Hinweise darauf, dass er vermutlich unabhängig vom kanonischen Delta-Notch Signalweges ist. Stattdessen ist eine veränderte Proteininteraktion, besonders im Bereich der Adenylylcyclase eher wahrscheinlich. Mögliche verantwortliche Proteine könnten zu den PDZ Proteinen z.B. die MAGUK Proteine oder zum neu entdeckten Slit-Robo Signalweg gehören.

Zusammenfassend liefert diese Dissertation einen neuen Einblick über die Rolle des Delta-Notch Signalweges in den adulten Inselzellen der Maus. Vor allem die Wichtigkeit der Gene *Dll1* und *Dll4* für eine korrekte Funktionsweise der β -Zellen konnte belegt werden.

2. INTRODUCTION

2.1. The Delta-Notch pathway

2.1.1. General

In multicellular organisms it is crucial that cells are communicating with each other. This is especially important during tissue development and organization as well as the regulation of growth and cell death. It is obvious that for these different processes several communication pathways are established and that such activities are strictly regulated, for example, in a tissue- and time-dependent manner. One of these signaling pathways is the Delta-Notch pathway, which is a highly conserved cell-cell-communication transducer and based on the binding of a ligand to a receptor on an adjacent cell. Moreover, it is often used to select between preexisting developmental programs and to specify cell differentiation during morphogenesis (Kopan et al. 2009, Guruharsha et al. 2012). The *Notch* gene was first described 1914 in the fruit fly *Drosophila melanogaster*, where haploinsufficiency of the gene display a serrated wing margin phenotype and homozygous loss-of-function leads to embryonic lethality (Dexter 1914, Poulson 1940). Several years later, the importance of Delta-Notch has also been proven in mammals. There, the Delta-Notch based cell-cell interaction is critical for nervous system development and somitogenesis (Bettenhausen et al. 1995, Hrabe de Angelis et al. 1997). Moreover, the pathway has been shown to be required for the development of the left-right asymmetry in vertebrates and therefore essential for the correct placement and orientation of the organs (Przemeck et al. 2003).

In mammals, the basic main elements of Delta-Notch signaling include the Notch receptors, the Delta-like (DLL) and Jagged (JAG) (or Serrate in *Drosophila*) ligands and the CBF1-SU(H)-LAG1(CSL) DNA-binding proteins (such as CBF1; also known as RBPJ κ) (Bray 2006, Guruharsha et al. 2012). Whereas only one Notch receptor exists in *Drosophila*, mammals possess four Notch paralogs (NOTCH 1-4), displaying all an unique function (Kopan et al. 2009). These receptors are large single-pass type I transmembrane proteins with a ligand-binding extracellular domain (ECD) and a signal-transducing intracellular domain (ICD) (Kopan et al. 2009). The extracellular domain of the Notch receptors contains 29-36 tandem epidermal growth factor (EGF) like repeats, from which 11-12 are sufficient to mediate successful interaction and ligand binding of a neighboring cell, which is called trans interaction

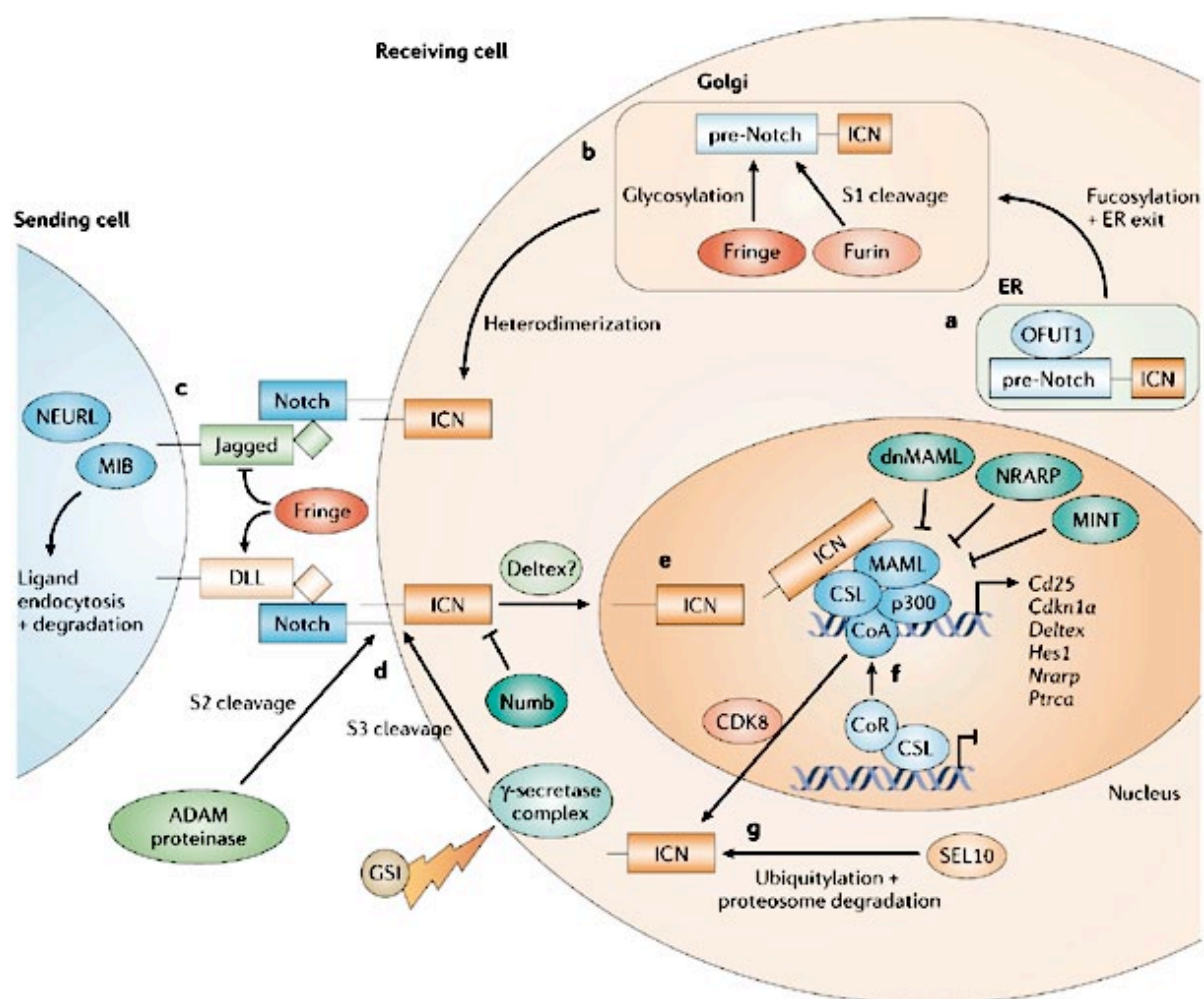
(Rebay et al. 1991, Kopan et al. 2009). Many EGF-like repeats bind to calcium ions, which play an important role in determining the structure and affinity of Notch in ligand binding and can affect signaling efficiency (Cordle et al. 2008). The EGF-repeats are followed by a negative regulatory region (NRR) consisting of three similarly arranged Lin12-Notch (LN) repeats and a heterodimerization domain. Both are unique to the Notch receptor family and required for preventing ligand-independent signaling (Kopan et al. 2009). The Notch intracellular domain (NICD) contains the RBPJk-associated molecule (RAM) region in the juxtamembrane region followed by seven Ankyrin repeats (ANK), a putative trans-activating domain and a C-terminal PEST motif (Kurooka et al. 1998, Kopan et al. 2009).

Aside from the concrete pathway with ligand binding, Notch signaling is controlled by a complex protein-processing mechanism that requires glycosylation for proper protein folding as well as trafficking to the plasma membrane (Haines et al. 2003, Kopan et al. 2009). Upon entering the secretory pathway through the trans-Golgi vesicles, translated Notch proteins get cleaved by furin-like convertases within the secretory pathway at site 1 (S1), which is located within an unstructured loop that protrudes from the heterodimerization domain (Blaumueller et al. 1997, Logeat et al. 1998). In addition to the cleavage, the receptor is glycosylated during its transit through the Golgi and these modifications have important consequences for the signaling competence. Many Notch EGF-repeats are fucosylated at serine or threonine residues by O-fucosyltransferase 1 and these fucosylated residues can be additionally further modified by other glycosyltransferases. These posttranslational modifications have important modulatory effects on the receptor-ligand interactions (Haines et al. 2003, Kopan et al. 2009).

The Notch ligands are members of the DSL (Delta, Serrate, Lag-2) family including DLL1, DLL3, DLL4 and JAG1, JAG2 in mammals. Like the Notch receptors they are type I transmembrane proteins consisting of several EGF-like repeats, a N-terminal DSL domain, and a short intracellular domain (Kopan et al. 2009). The two classes Delta and Serrate/Jagged differ in the presence of a cysteine-rich domain, which is only present in Serrate/Jagged (Watt et al. 2008).

Regulation of Delta-Notch signaling is not limited to the receptors alone. Also the ligands get post-transcriptional modified and their trafficking is controlled, so that their dynamic

expression contributes significantly to the differential activity of the pathway during development (Bray 2006). Endocytic trafficking of the ligands plays a critical role in enhancing ligand signaling activity (Le Borgne 2006) and is triggered by monoubiquitination mediated by the RING-type E3 ubiquitin ligases NEUTRALIZED (NEURL) and MINDBOMB (MIB). The internalization from the plasma membrane is an obligatory step for surface expression of active Notch ligands (Le Borgne 2006). Only when both, receptor and ligand, are expressed on neighboring cells the actual cell-cell communication and signaling pathway can take place (a graphical overview is shown in figure 1 (Grabher et al. 2006)).



Copyright © 2006 Nature Publishing Group
Nature Reviews | Cancer

Figure 1: General overview of the Delta-Notch signaling pathway

Shown is the Delta-Notch pathway including posttranslational protein modifications for regulatory activities as well as receptor processing and trafficking of the intracellular domain (here ICN) to the nucleus after ligand binding. Within the nucleus, ICN binds the CSL complex and mediates specific target gene expression. The graph is adopted from Grabher et al. 2006.

Upon ligand binding, Notch is sequentially cleaved by two different proteases at sites designated S2 and S3, resulting in the release of NICD. The S3 cleavage occurs only in response to a preceding S2 cleavage (Brou et al. 2000, Mumm et al. 2000, Fortini 2002) in which two metalloproteases, ADAM10 (Kuzbanian) and ADAM17 (tumor-necrosis-factor α -converting enzyme), seem to act partially redundant (Brou et al. 2000, Jarriault et al. 2005). The S2 cleavage releases the Notch extracellular domain (ECD), leaving the still membrane-bound ICD behind, which then leads to the ligand-independent cleavage at S3. The S3 cleavage occurs in the transmembrane helix and is catalyzed by the gamma secretase activity of the presenilin-nicastrin-Aph1-Pen2 protein complex (Brou et al. 2000). This releases Notch ICD (NICD), which is now able to enter the nucleus. In the nucleus, NICD interacts directly with members of the transcription factor (TF) CSL family (CBF1-SU(H)-LAG1) and participates in transcriptional activation of target genes. CSL is a constitutive repressor of Notch target genes and acts in association with transcriptional co-repressors (Ehebauer et al. 2006). To activate gene expression at the target gene promoter, the NICD binds to CSL and mediates a so called “transcriptional switch” (Kopan et al. 2009). Thereby, the NICD forms a trimeric complex with CSL and MASTERMIND (MAM), a protein which is required for recruiting the histone acetylase (HAT) P300, a coactivator of the complex (Petcherski et al. 2000, Wu et al. 2000, Fryer et al. 2002, Nam et al. 2006, Wilson et al. 2006). The histone acetylase promotes assembly of the transcription initiation and elongation complex and is therefore crucial for gene transcription (Wallberg et al. 2002). Among the Notch target genes, best characterized are the bHLH (basic-helix-loop-helix) genes of the E(spl)/HES family (Bray 2006). However, the response to Notch differs greatly between cell types. For example Notch promotes cell proliferation in some contexts and apoptosis in others (Radtke et al. 2003).

The CSL trimeric complex is also involved in the turnover of NICD by recruiting proteins that promote NICD phosphorylation like cyclin-dependent kinase-8 (CDK8). By this phosphorylation NICD becomes a substrate for the nuclear ubiquitin ligase SEL10 (Fryer et al. 2002, Fryer et al. 2004). Essential for this interaction is the C-terminal PEST domain. The destruction of NICD leads to dissociation of MAM and other co-activators (Bray 2006). The NICD turnover is essential, because aberrant stabilization of NICD can cause severe diseases like T-cell acute lymphoblastic leukemia in humans (Grabher et al. 2006).

Delta-Notch signaling occurs not only by trans-activation between neighboring cells. Several studies demonstrated that ligand-receptor interactions could also take place within the same cell. These interactions reduce the ability of a cell to respond to neighboring cells. This process is called cis-inhibition of the receptor by the ligand or vice versa (del Alamo et al. 2011). It is important to realize cell fate decisions during pattern formation, where one developing element prohibits the development of similar elements nearby. This mechanism, called lateral inhibition, establishes patterns through the activity of a negative intercellular feedback loop involving the receptor and their ligands (Axelrod 2010), whereby activated Notch signaling promotes transcriptional suppression of its ligands and cell fate regulators. Consequently, when either Notch or Delta is available in the same cell, a cell cannot interact with neighboring cells unless the other components are present in excess (Axelrod 2010).

2.1.2. The role of the ligand intracellular domain

Beside the Notch receptors also the ligands could be processed by proteases extracellularly (to promote endocytosis) as well as at the transmembrane region to release the intracellular domain (ICD) (Bland et al. 2003, Dyczynska et al. 2007).

In mammals, the ligand ICDs are relatively short sequences with, for example, 125 amino-acid residues in murine JAG1 and 153 residues in murine DLL1. They are not conserved in their primary amino-acid sequence. However, an alignment of the three mammalian Delta (DLL3, DLL3, DLL4) and two Jagged (JAG1, JAG2) proteins disclosed that some but not all ICDs contain at least one nuclear localization signal (DLL1, JAG1, JAG2) and/or a C-terminal PDZ-binding motif (DLL1, DLL4, JAG1), which are conserved among Delta and Jagged homologues (Pfister et al. 2003, Pfister 2005, Dissertation). Moreover, some of the ICDs (JAG1, DLL1, DLL3) contain in addition Src Homology (SH2) and/or SH3 domain interaction motives (Bland et al. 2003, Kolev et al. 2005, Pintar et al. 2007). All these components lead to the suggestion that the ICDs occupy certain functions, especially since the NLS enables the localization to the nucleus and therefore the potential for transcriptional regulation (Bland et al. 2003). For instance, it is known that DELTA variants missing the ICD can still bind to NOTCH but are unable to activate the pathway (Parks et al. 2006). Moreover, the ICD of Delta-like 1 (DICD) was shown to act as a negative regulator of Notch signaling by binding to NICD in the nucleus (Jung et al. 2011). It was also demonstrated that DICD induces cell growth arrest by upregulation of the cell cycle

inhibitor *p21* (*Cdkn1a*). Interestingly, this effect could be counterbalanced by constitutively active Notch1 (Kolev et al. 2005).

Several recent studies revealed a cytoplasmic interaction between DICD and different signaling pathways, which seem to be not dependent on nuclear localization. For instance, it was shown that DICD overexpression induces neuronal differentiation in embryonic carcinoma P19 cells by forming complexes with SMAD2/3 as components of the TGF β /activin cascade (Hiratochi et al. 2007). In a similar study in colon cancer cells, the overexpression of DICD increases not only the TGF β /activin activity but also the activity of wingless (Wnt) signaling-dependent reporters and endogenous connective tissue growth factor (CTGF) (Bordonaro et al. 2011).

However, these data are based exclusively on *in vitro* studies. Only one recent publication analyses the effects of constitutive DICD overexpression on embryonic development of mice (Redeker et al. 2013). The authors detected no effects on early Notch-dependent processes or expression of selected Notch target genes in transgenic embryos as well as no apparent phenotype, arguing against a signaling activity of the ICD in developing mouse embryos *in vivo*. To date, no further *in vivo* data on distinct processes have been published beyond embryonic development, making DICD interesting for further studies. Especially a potential involvement in the endocrine cell lineage of the pancreas seems to be attractive, which share plenty properties and gene expression patterns with neurons (Atouf et al. 1997). Moreover, the importance of Notch signaling in adult islets has been suggested for murine and human pancreatic islets (Dror et al. 2007).

2.2. The pancreas and islets of Langerhans

2.2.1. The pancreatic development

The pancreas is a multicellular tissue, composing of both exocrine as well as endocrine tissue and requires a complex developmental process. Like other organs of the gastrointestinal tract, the pancreas is derived from the endodermal germ layer during gastrulation, which is a critical process in the early development and forms not only the endoderm but also the ectoderm and mesoderm (Solnica-Krezel et al. 2012). The pancreas is built by two independent buds (dorsal and ventral) of the embryonic foregut at E9.5 in the mouse (Pictet et al. 1972, Piper et al. 2002), which are characterized by the expression of *Pdx1* (pancreatic duodenal homeobox 1) and *Ptf1a* (pancreas-specific transcription factor 1a) (Schwitzgebel et al. 2000, Gu et al. 2002) and build the so-called multipotent pancreatic progenitors (MPC) (Murtaugh et al. 2003). Around E11.5 the two buds start to grow finger-like epithelial protrusions into the surrounding mesenchyme and fuse into a single organ. This leads finally to highly branched structures and is usually referred to as primary transition, which lasts until E12.5 (Pictet et al. 1972, Zhou et al. 2007, Shih et al. 2013). In parallel, the cells start to proliferate and increase the size of the pancreatic buds rapidly (Pictet et al. 1972). At this state, the pancreatic buds did not yet develop into the mature organ with its macroscopic structure. The cells are still undifferentiated MPCs (Cano et al. 2013). These MPCs will give rise to the hormone-expressing endocrine cells, ductal cells and digestive enzyme-producing acinar cells of the exocrine tissue. To control this expansion process and maintain the pancreatic identity, many different pathways and transcription factors are necessary. For instance, the expressions of *Pdx1*, *Ptf1a* as well as *Sox9*, *Foxa1/2*, *Prox1*, *Tcf2*, *Onecut1*, *Hnf1b*, *Gata4/6* and *Hes1* are essential for forming the MPCs (Cano et al. 2013, Shih et al. 2013). In addition, pathways like Fibroblast Growth Factor (FGF), Wntless or Notch signaling have been shown to play important roles (Bhushan et al. 2001, Norgaard et al. 2003, Murtaugh 2008, Afelik et al. 2012). A graphical overview of the pancreatic development is shown in figure 2 (Shih et al. 2013).

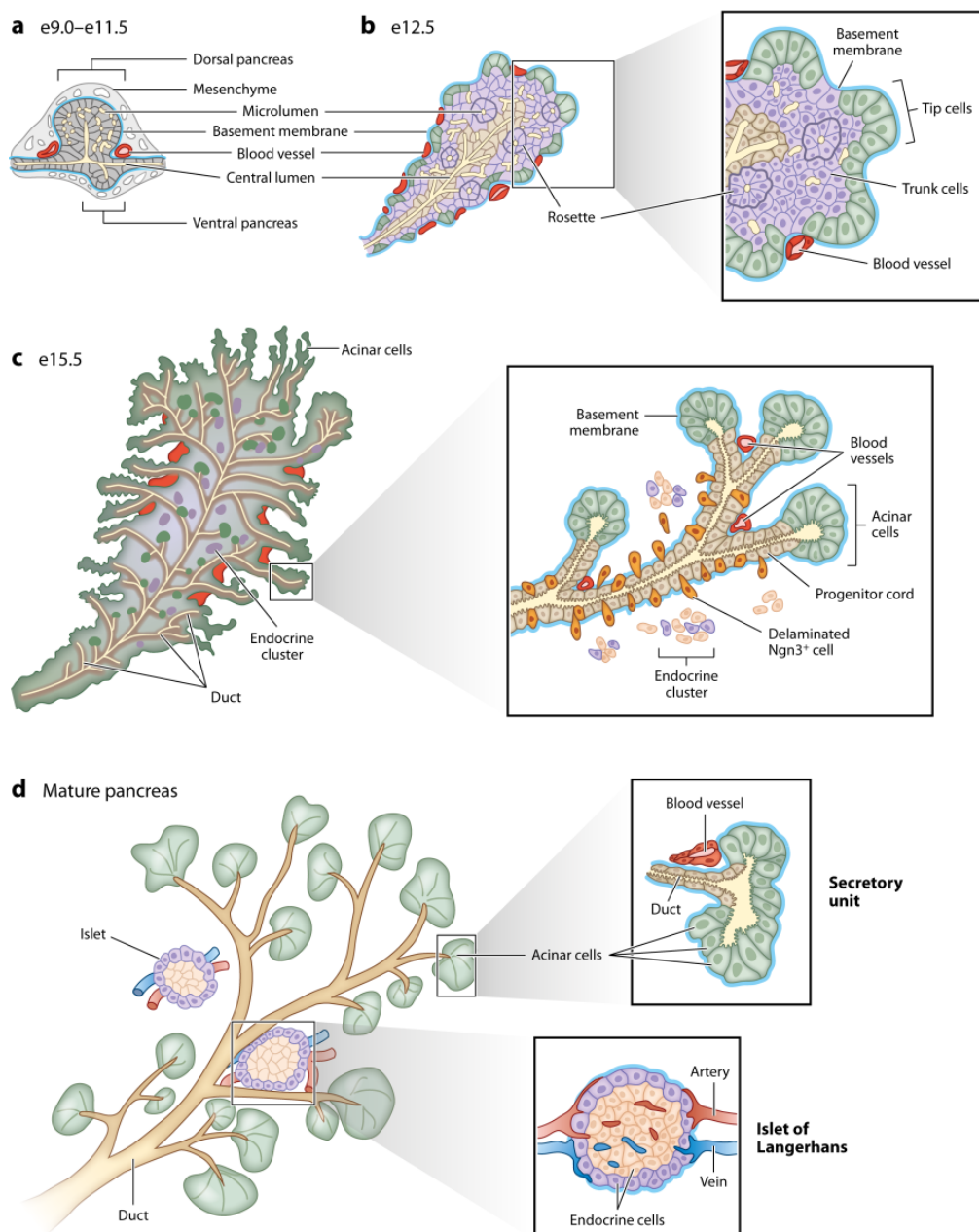


Figure 2: Pancreatic organogenesis

The pancreas is developing by combining dorsal and ventral epithelial cells between E9.0-11.5. After E12.5 the cells start to become either tip (green) or trunk (violet) cells that later determine the exocrine and endocrine cell fate. The expression of *Neurog3* in trunk cells is crucial for endocrine cell differentiation. During this early development, blood vessels are progressively intercalating the tissue. Illustration was adapted from Shih et al. 2013.

Starting at E12.5 until birth, the pancreatic epithelium continues to branch. A complex highly ordered tubular system is build and the cells start to lose their multipotency by undergoing endocrine and exocrine cell differentiation. This process is called secondary transition of pancreatic development. The first step of secondary transition is the segregation into the so-called “tip” and “trunk” domains (Zhou et al. 2007). Cells that are located at the “tips” of the

branching network can be identified by the expression of *Ptf1a*, *Myc* and *carboxypeptidase A* (*CPA*) and give rise to acinar cells (Zhou et al. 2007, Shih et al. 2013). In contrast, cells located in the inner part of the network are called “trunk cells”, which are characterized by the expression of *Nkx6-1/6-2*, *Sox9*, *Tcf2*, *Onecut1*, *Prox1* and *Hes1* and will develop into endocrine and ductal cells (Cano et al. 2013, Schaffer et al. 2013). Within the trunk, some cells temporally express the gene *Neurogenin3* (*Neurog3*), the key regulator of the endocrine cell fate. NEUROG3 is a bHLH transcription factor, whose expression can be first observed at E9.5, peak during secondary transition and then decrease. The timing in *Neurog3* expression is critical to distinguish between the different cell types rising from the trunk (Gradwohl et al. 2000, Schwitzgebel et al. 2000, Johansson et al. 2007). Several studies investigated the role of NEUROG3 during pancreatic development. For instance, *Neurog3* null mice fail to develop endocrine cell types, while the development of the exocrine tissue remains normal (Gradwohl et al. 2000, Magenheimer et al. 2011). Conversely, *Pdx1* driven overexpression of *Neurog3* leads to premature differentiation of MPCs into endocrine cells (Apelqvist et al. 1999). The activation of *Neurog3* is highly regulated by a complex network of TFs including FOXA2, GLIS3, HNF1B, HNF6, PDX1 and SOX9. NEUROG3 itself controls the expression of TFs genes that induce endocrine development, for example *NeuroD1*, *Pax4*, *Insm1*, *Rfx6*, *Nkx2.2* and *Myt1* (Arda et al. 2013). However, the complete mechanism and structure of this network is still not yet resolved. Nevertheless, the NEUROG3 dependent expression of the TFs is critical for endocrine cell type identities. From NEUROG3⁺ precursor cells, five different types of endocrine cell lineages arise, which finally build up the pancreatic islets of Langerhans after E18.5.

2.2.2. Notch signaling in the pancreas

Notch signaling is one of the most important regulating signaling pathways during pancreatic development. Like many other genes the expression of the Notch components is spatiotemporally regulated. NOTCH1 was first detected at E9.5 in the pancreatic epithelium and NOTCH2 was found to be restricted to ductal cells with a peak between E11.5-E15.5. NOTCH3 and NOTCH4 were found to be expressed in the early pancreatic mesenchyme and later in epithelial cells (Lammert et al. 2000). The ligand JAG1 was most abundantly expressed during mid-gestation whereas DLL1 was described to be transiently expressed between E9.5 and E11.5 in the pancreatic duct epithelium (Lammert et al. 2000).

An essential role for Notch signaling lies in preventing the preliminary differentiation of pancreatic progenitors into endocrine or exocrine cell lineage (Apelqvist et al. 1999, Afelik et al. 2012). In pancreatic MPCs, the bHLH TF PTF1A activates the expression of *Dll1*, which then induces the Notch cascade and stabilizes the maintenance of these cells through *Hes1* and *Ptf1a* expression (Ahnfelt-Ronne et al. 2012, O'Dowd et al. 2013). At this step the expression of *Hes1* is critical to maintain the proliferative state of the MPCs for appropriate organ growth. HES1 promotes this cell cycle progression through the direct transcriptional repression of the cell cycle inhibitor *p57 (Cdkn1c)* (Georgia et al. 2006). Loss of Notch signaling and subsequent decreased *Hes1* expression, increases *Cdkn1c* and leads to preliminary cell cycle exit and pancreatic hypoplasia as well as loss of important transcription factors, such as SOX9 and HNF1B (Afelik et al. 2013).

During secondary transition, Notch signaling mediated lateral inhibition is critical for the following cell-fate decisions, which are illustrated in figure 3 (Li et al. 2015).

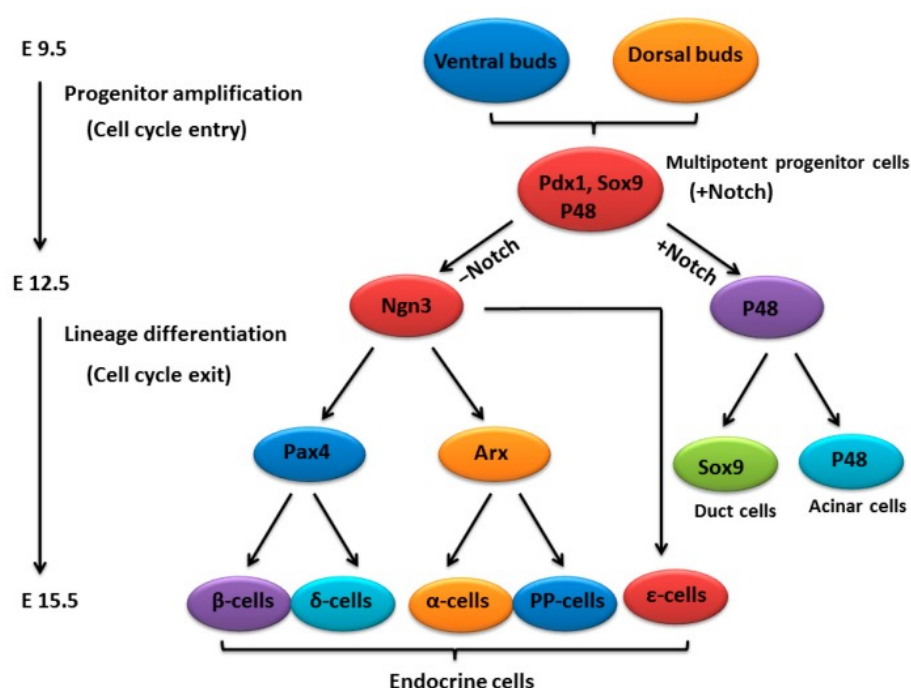


Figure 3: Schematic representation of pancreatic development and the involvement of Notch signaling. Dependent on the activity of Notch, the MPCs develop either into ductal or acinar cells (Notch is active) or undergo endocrine lineage specification (Notch is inactive). The expression of *Pax4* or *Arx* determines further differentiation into the specific endocrine cell types. Illustration was adopted from Li et al. 2015.

When Notch is active, *Hes1* is expressed and inhibits the expression of *Neurog3* and consequently preventing cells from adopting the endocrine fate (Apelqvist et al. 1999, Qu et

al. 2013). Loss of Notch signaling subsequently leads to increased *Neurog3* expression and premature differentiation of the endocrine pancreas (Apelqvist et al. 1999, Nakhai et al. 2008). Mouse models with deficiency for *Dll1* or the intracellular Notch mediator *Rbpjk* have inactive Notch signaling and showed a similar phenotype, the lack of MPC expansion and premature differentiation of *Neurog3* positive cells into endocrine cells (Apelqvist et al. 1999). Contrary, loss of *Jag1* function leads also to a reduced number of NEUROG3⁺ cells and increased expression of Notch transcriptional targets during primary transition, whereas postnatally, *Jag1* loss-of function mice display an increased number of NEUROG3⁺ cells reminiscent to the deletion *Dll1* or *Rbpjk*, suggesting an inhibitory function of JAG1 during pancreatic development (Golson et al. 2009). Since RBPJK directly binds to the promoter of the “pro-trunk” gene *Nkx6.1*, suppression of Notch in MPCs leads to a pro-acinar fate by increased expression of the “pro-tip” gene *Ptf1a* (Afelik et al. 2012). Accordingly, loss of the E3 ubiquitin ligase *Mind bomb 1*, which is essential for Notch ligand endocytosis and pathway activity, causes loss of NKX6.1⁺ but an increased number of PTF1A⁺ cells as well as reduced number of NEUROG3⁺ progenitors (Horn et al. 2012). Furthermore, ectopic expression of NICD in PAX4⁺ endocrine precursor cells causes a switch from the endocrine to the ductal cell fate (Greenwood et al. 2007). Interestingly, it has been suggested that NOTCH1 and NOTCH2 are dispensable for exocrine and endocrine development as long as RBPJK remains active. Therefore, a Notch-independent mechanism of regulating *Rbpjk* has been proposed (Nakhai et al. 2008).

Not much is known about the presence and activity of Notch signaling during adulthood. However, Notch activity has been observed in adult pancreatic islets of mice, rats as well as humans, and a role for Notch signaling in regulating apoptosis of β -cells was proposed (Dror et al. 2007). Moreover, increased expression of HES1 in centroacinar cells was observed during pancreatic tumorigenesis (Miyamoto et al. 2003). As well, a requirement of Notch signaling for pancreatic regeneration of chronic pancreatitis (Jensen et al. 2005) and for the modulation of exocrine cells from adult rats was described (Rooman et al. 2006, Su et al. 2006, Baeyens et al. 2009).

2.2.3. Islets of Langerhans

Pancreatic islets were first described by Paul Langerhans in 1869 as cell clusters with a diameter of about 100-200 μm (Langerhans 1869). These clusters are richly innervated and scattered throughout the exocrine tissue. Islets are strongly vascularized and receive 10-15% of the pancreatic blood flow, while only making up for 1-2% of the pancreatic mass. This enables rapid sensing of plasma glucose levels and consequently an appropriate secretory response of hormones. In average, each adult human possess about 2 million islets, each consisting of 2000-4000 single cells. Five different cell types build up the islets. In general, 70-80% of all islets cells are insulin-producing β -cells. The glucagon-secreting α -cells make up 15-20% of all islet cells. Less than 10% islet mass are represented by somatostatin-producing δ -cells and less than 1% correspond to pancreatic polypeptide-producing PP cells and ghrelin-secreting ϵ -cells (Prado et al. 2004, Brissova et al. 2005). However, the individual content and structure of islets varies between different species (Cabrera et al. 2006). For example, α -cells in human and monkey islets are dispersed throughout the whole islet, while in mice or rodents the α -cells, and δ -cells are located in the periphery and surrounding the centrally located β -cells (Kim et al. 2009). It is suggested, that the individual cellular structure of human islets has advantages for the islet function by improving glucose sensing (Cabrera et al. 2006).

2.2.3.1. Pancreatic β -cells

β -cells are the predominant cell type in pancreatic islets. They secrete the hormone insulin in response to nutrients, hormones and neuronal stimuli and therefore play a primary role in the maintenance of glucose homeostasis. For their development from pancreatic progenitor cells, three main transcription factors are necessary: PAX4, PDX1 and NKX6.1 (Sosa-Pineda et al. 1997, Schaffer et al. 2013). *Pax4* is a direct target gene of NEUROG3 and becomes expressed from E9.5 on transiently. Whereas it is co-expressed with a second NEUROG3 target gene *Arx* (aristaless related homeobox) in the beginning, both start counter regulating each other leading to a restriction of *Pax4* to β - and δ -cell precursors (Smith et al. 2003, Murtaugh 2007). In contrast, *Arx* remains exclusively expressed in α precursor cells. Hence, it has been shown that *Pax4* deficiency resulted in a reduced amount of β - and δ -cells, but an increased number of α -cells (Sosa-Pineda et al. 1997, Collombat et al. 2003).

Parallel with PAX4, the NK-type homeodomain TF NKX2-2 was detected in the pancreatic epithelium and β -cell precursors. During organogenesis, this gene becomes progressively restricted to β -cells and PP cells. Together with *Nkx6-1*, which is thought to be downstream of *Nkx2-2*, it is required for the maturation and expansion of β -cells (Sander et al. 2000, Wang et al. 2004). The disruption of *Nkx2-2* resulted in hyperglycemia and a complete loss of insulin producing β -cells (Sussel et al. 1998). Similar to NKX2-2, NKX6-1 also acts as transcription regulator. It has been suggested that NKX6-1 can repress *glucagon* expression and regulates insulin secretion in adult β -cells (Schisler et al. 2008, Taylor et al. 2013). Moreover, together with PAX4 and NKX2.2, NKX6.1 is associated with the activation of the gene transcription of further crucial genes for β -cell differentiation like *Pax6* and *Islet-1* as well as the increased *Pdx1* expression (Wang et al. 2004). While *Pdx1* is expressed already very early during development, it becomes progressively restricted to β -cells and some δ - as well as PP-cells. After birth, *Pdx1* is exclusively expressed in β -cells and regulates their growth and function (Oliver-Krasinski et al. 2008). For instance in adult β -cells, PDX1 is required for the transcriptional regulation of β -cell specific genes like *insulin*, *Slc2a2* (also known as *Glut2*) and *Nkx6-1* (Cerf 2006). Therefore, adult mice lacking *Pdx1* become hyperglycemic and diabetic with age due to β -cell dysfunction (Ahlgren et al. 1998). Moreover, PDX1 is an often-used reporter and marker for β -cell identity and maturation.

Postnatally, several other genes are required to keep up β -cell identity and function. For instance, it has been shown that the HLH TF Neurogenic differentiation 1 (NEUROD1) regulates the expression of glucokinase and can also bind to the insulin gene promoter. In humans, mutations within *NEUROD1* are associated with the development of diabetes mellitus (Malecki et al. 1999, Moates et al. 2003). Another TF, which can influence insulin gene expression, is the basic leucine zipper MAFA (v-maf musculoaponeurotic fibrosarcoma oncogene family A). MAFA plays an important role in glucose-stimulated insulin secretion *in vivo* and in β -cell identity (Zhang et al. 2005, Nishimura et al. 2015). More detailed information about all β -cell related TFs were reviewed by several publications (Cerf 2006, Oliver-Krasinski et al. 2008).

2.2.3.2. Pancreatic α -cells

The counter players of insulin producing β -cells are the glucagon producing α -cells. Interestingly, in human islets the α -cell population reaches 33-46% of the islet cell mass, suggesting that glucagon plays a major role in humans (Cabrera et al. 2006). However, the focus in research in the last decades was mainly on β -cells and shifted only recently also towards α -cells.

The first GLUCAGON⁺ cells are already evident at E9.5 before secondary transition. However, most of them are created together with other islet-cell types during second transition from NEUROG3⁺ precursor cells after E13.5 (O'Dowd et al. 2013). As mentioned before, here ARX is a critical TF determining the α -cell identity (Collombat et al. 2003). Mice lacking *Arx* expression display reduced α -cell mass along with increased β - and δ -cell mass (Wilcox et al. 2013).

Similar to β -cells, the expression of *Neurod1* is required in α -cells, where it was detected already at E9.5. The loss of *Neurod1* leads parallel to a decrease in the number of β - and δ -cells also to a reduction of α -cells. Moreover, the overexpression of NEUROD1 during embryogenesis leads, similar to the overexpression of *Neurog3*, to premature endocrine differentiation with most of the cells expressing glucagon (Schwitzgebel et al. 2000, Bramswig et al. 2011). Further critical factors for α -cell identity and development are the winged-helix TFs forkhead box A1 and A2 (FOXA1 and FOXA2) (Bramswig et al. 2011). Loss of function of both proteins resulted in severe insulin-dependent hypoglycemia due to a reduced α -cell function and plasma glucagon levels (Heddad Masson et al. 2014). Along with PAX6, both proteins can also bind to the promoter of *preproglucagon* and hence regulate *glucagon* gene transcription (Heddad Masson et al. 2014). PAX6 additionally helps to induce the expression of other TF genes such as *Mafb* and *Neurod1* (Gosmain et al. 2011). While MAFB is present in α - and β -cells during development, it is restricted to α -cells in the adult pancreas. It also triggers the *glucagon* gene expression and maintains α -cell identity (Artner et al. 2006, Hang et al. 2011).

Whereas insulin is acting anabolic on target tissue, glucagon has catabolic effects on muscle, liver and adipose tissue. Glucagon induces gluconeogenesis and glycogenolysis in liver, which results in the release of glucose to the blood stream (Quesada et al. 2008). Glucagon is acting

mainly via binding to the glucagon receptor (GCGR). The GCGR is a single G-protein-coupled receptor expressed mainly in liver but also in brain, kidney, the gastrointestinal tract, adipose tissue and the heart (Campbell et al. 2015). It has been shown that GCGR signaling is required to control fuel homeostasis and body weight and that its pharmacological manipulation might be considered as novel therapy for diabetic or obese patients (Yang J, 2011; van Dongen 2015; Wang M, 2015). Indeed, patients with type 2 diabetes mellitus (T2DM) show often a strong increase in fasting glucagon levels that result in increased hepatic glucose production and hyperglycemia due to the impaired inhibition of glucagon secretion by insulin (Unger 1971, Shah et al. 2000). Details regarding glucagon secretion and α -cell function are reviewed in several publications (Gromada et al. 2007, Campbell et al. 2015).

2.3. Glucose metabolism and insulin secretion

2.3.1. Regulation of glucose metabolism

As mentioned above, β -cells are key players in the regulation of glucose homeostasis. Glucose, or in general carbohydrates, are the main energy source for most organisms. To utilize this energy, a pathway called glycolysis is performed to degrade glucose by producing high-energy compounds. Within the cells, energy obtained from glycolysis (or other metabolic mechanisms) is stored in terms of adenosine triphosphates (ATP). Moreover, one gram of glucose yields about 4 kcal of energy, whereas for example one gram of fat yields about 9 kcal (Bruce Alberts 2002). The degradation of glucose to the end product pyruvate is catalyzed in ten different enzymatic reactions summarized in table 1.

Table 1: Overview of the enzymatic steps during glycolysis

Reaction	Enzyme	catalysed reaction
1	hexokinase	Glucose + ATP \rightarrow Glucose-6-phosphate + ADP
2	phosphoglucose isomerase	Glucose-6-phosphate \rightleftharpoons Fructose-6-phosphate
3	phosphofructokinase 1	Fructose-6-phosphate + ATP \rightarrow Fructose-1,6-bisphosphate + ADP
4	aldolase A	Fructose-1,6-bisphosphate \rightleftharpoons Dihydroxyacetonephosphate + Glyceraldehyde-3-phosphate
5	triosephosphate isomerase	Dihydroxyacetonephosphate \rightleftharpoons Glyceraldehyde-3-phosphate
6	glyceraldehyde phosphate dehydrogenase (GAPDH)	Glyceraldehyde-3-phosphate + Pi + NAD ⁺ \rightleftharpoons 1,3-bisphosphoglycerate + NADH + H ⁺
7	phosphoglycerate kinase	1,3-bisphosphoglycerate + ADP \rightleftharpoons 3-phosphoglycerate + ATP
8	phosphoglycerate mutase	3-phosphoglycerat \rightleftharpoons 2-phosphoglycerate
9	enolase	2-phosphoglycerate \rightleftharpoons phosphoenolpyruvate + H ₂ O
10	pyruvate kinase	phosphoenolpyruvate + ADP \rightarrow pyruvate + ATP

Three of them are irreversible, representing critical points of the pathway (hexokinase, phosphofructokinase1 and pyruvate kinase). During this process, energy in form of phosphate bridges is transferred onto two adenosine diphosphates (ADP), producing two ATP molecules. Furthermore, NAD⁺ gets reduced to NADH (Nicotinamide adenine dinucleotide) (Bruce Alberts 2002, Li et al. 2015). Under aerobic condition, the generated pyruvate molecules get transported to the mitochondria for oxidation. Here, the multi-enzyme complex pyruvate

dehydrogenase catalyzes the decarboxylation into acetyl coenzyme A (acetyl CoA), CO₂ and NADH. Acetyl CoA is also the end product of the fatty acid β-oxidation (Harwood 1988). In the citric cycle or tricarboxylic acid cycle (TCA) (also called Krebs cycle) the oxidized acetyl CoA undergoes complete oxidization to CO₂ with concomitant reduction of the electron transporting coenzymes NADH and flavin adenine dinucleotide (FADH₂) (Kornberg 2000, Bruce Alberts 2002). The TCA cycle involves eight enzymatic steps and produces also the ATP derivate GTP (guanosine triphosphate). However, the highest amount of chemical energy is released in the last step of glucose degradation – the electron-transport chain. In this final step, the electron carriers NADH and FADH₂ transfer electrons into a series of enzyme catalyzed redox reactions, generating a gradient of H⁺ ions at the mitochondrial membrane. This gradient serves as energy source to generate more ATP out of ADP. During oxidative phosphorylation, the electrons get finally transferred to O₂ by producing water and completing the energy metabolism (Bruce Alberts 2002, Sazanov 2015).

In general, the blood-glucose level is determined by intestinal absorption of glucose during fed state and glycogenolysis and gluconeogenesis in the liver during fasted state. To maintain glucose homeostasis, regulatory hormones are secreted. These hormones include insulin, glucagon, amylin, glucagon-like protein1 (GLP-1), glucose-dependent insulinotropic peptide (GIP), epinephrine, cortisol, and growth hormones. Insulin, glucagon as well as amylin are derived from islet cells in the pancreas, whereas GLP1 and GIP origin from intestine cells (Aronoff et al. 2004). Postprandial, secreted insulin leads to an increased glucose uptake in skeletal muscle and adipose tissue and to decreased glyconeogenesis in the liver. During fasting, glucose is constantly removed from circulation by its uptake into peripheral tissues. To keep glucose levels constant, endogenous glucose production is necessary. In this case, glucagon is secreted and stimulates glycogenolysis (within the first 8-12 h of fasting) and gluconeogenesis (after a longer fasting period) in the liver. In general, insulin secretion decreases already at 81 mg/dL blood glucose concentration and stops at levels below 60 mg/dL, whereas glucagon secretion is increased when blood glucose levels drop below a glycemic threshold of 65-70 mg/dL (Schwartz et al. 1987).

2.3.2. Insulin secretion in pancreatic beta cells

By sensing even small fluctuations, β -cells balance the blood glucose level by secreting the hormone insulin. Besides glucose also other factors such as amino acids (arginine, leucine and lysine), GLP1 and GIP as well as parasympathetic stimulation via the vagus nerve are able to stimulate insulin secretion (Krarup et al. 1991, Drucker 2006, Holst 2007). Insulin is a small protein composed of two polypeptide chains containing 51 amino acids. Before insulin is active, it has to be processed from its prohormone proinsulin into its mature form by prohormone convertases (PC1 and PC2) (Turner et al. 2000). The active form is stored within secretory granules in the cytoplasm (Pouli et al. 1998, Fava et al. 2012). The secretion is occurring by exocytosis from the plasma membrane. Secreted insulin functions at the target tissues by binding to specific insulin receptors (Aronoff et al. 2004, Fu et al. 2013).

Following an acute glucose stimulus, the insulin release occurs in two main phases (biphasic insulin secretion). The rapid, but transient first-phase takes place within the first 10-15 min after glucose administration and is followed by the progressively increasing insulin release over the following 1-2 h. This timing of insulin release is critical to keep the blood glucose levels low within the 2 h after glucose administration. For instance, the first phase insulin release is often reduced or even absent in patients with Type 2 diabetes mellitus as a result of the progressive β -cell dysfunction (Grotsky 1989, Jenssen et al. 2015).

In general, the sensing of glucose in β -cells is achieved by the stimulation of glycolysis that results in enhanced mitochondrial ATP synthesis. The increase of the intracellular ATP/ADP ratio leads to the closure of ATP-sensitive K^+ (K_{ATP})-channels and subsequently to a depolarization of the plasma membrane through influx of positively charged ions (Fu et al. 2013, Rutter et al. 2015). This opens voltage-gated Ca^{2+} channels and increases the influx of Ca^{2+} ions, which then induces the exocytosis of insulin-containing granules. The exocytosis is achieved by activation of granule-associated small N-ethylmaleimide-sensitive factor receptor (SNARE) proteins and the fusion of the granules with the plasma membrane. Additionally, Ca^{2+} ions can get released from intracellular organelles, for instance from the endoplasmic reticulum (ER), Golgi or the lysosomes. This is either mediated by the inositol 1,4,5-trisphosphate (IP3) pathway or by the generation of nicotinic acid-adenine dinucleotide phosphate (NAADP) (Masgrau et al. 2003, Gustafsson et al. 2004, Mitchell et al. 2004). The

above-mentioned scenario describes only the essentials of the “canonical” pathway of glucose-stimulated insulin secretion. There are several other mechanism, independent of the K_{ATP} channels that induce the insulin secretion as illustrated in figure 4 (Rutter et al. 2015).

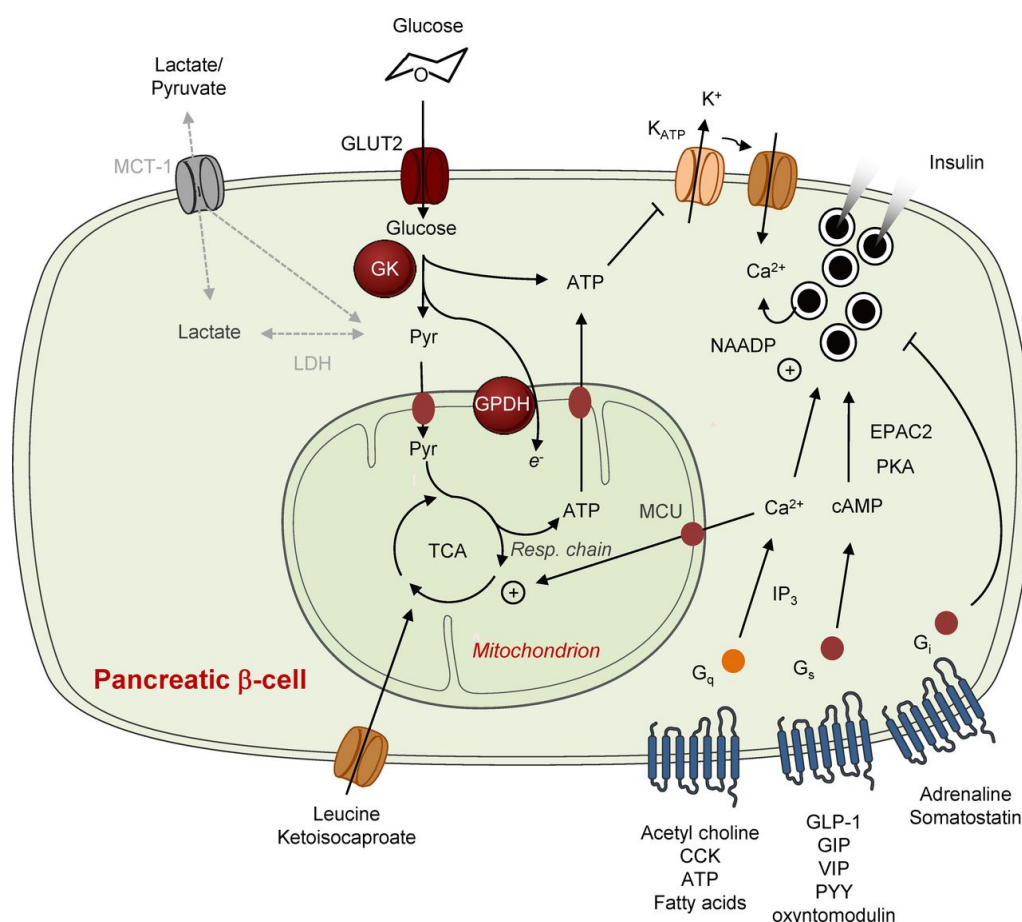


Figure 4: The pathways of insulin secretion.

Insulin secretion gets initiated by glucose-induced ATP production that leads to the closure of K_{ATP} Ca^{2+} channels. Non-glucose molecules can further stimulate insulin secretion via individual pathways often mediated by GPCRs. The illustration is adapted from Rutter et al. 2015.

Importantly, the incretin hormones GLP1 and GIP, both secreted postprandially from the intestine, also have an effect on insulin secretion (Campbell et al. 2013). Incretins act mainly via specific G-protein coupled receptors (GPCR, GLP1R, GIPR), which lead to an increase of intracellular levels of cyclic adenylyl monophosphate (cAMP) by activating the enzyme adenylyl cyclase (AC) (Campbell et al. 2013). The raising cAMP levels activate PKA (activating protein kinase A) (PKA) and EPAC2 (exchange protein activated by cAMP 2) (Seino et al. 2005, Rutter et al. 2015). Both pathways regulate proteins that are involved in insulin exocytosis (Fu et al. 2013). As well, different hormones like vasoactive intestinal peptide, PYY and

oxyntomodulin act via cAMP (Rutter et al. 2015). Factors like ATP, fatty acids or acetylcholine can also enhance insulin secretion through specific GPCRs, which is triggered by increasing cytosolic Ca^{2+} levels (Hillaire-Buys et al. 1994, Itoh et al. 2003, Ruiz de Azua et al. 2011). On the other side, there are several inhibitors of insulin secretion. The most prominent one is somatostatin, which is secreted from δ -cells. Somatostatin acts in part via an inhibitory G protein, adrenaline (epinephrine) and noradrenaline (norepinephrine). For instance, noradrenaline can open K_{ATP} channels and hyperpolarize the cell membrane (Wollheim et al. 1977, Rorsman et al. 1991, Rutter et al. 2015).

2.4. β -cell deficiency in diabetes mellitus

Diabetes mellitus is a metabolic disorder characterized by progressive loss or dysfunction of pancreatic β -cells leading to multiple long-term complications and progressive organ damage (Remedi et al. 2016). Since 1980 the prevalence has been rising from 4.5% of the world population up to 8.8% with 422 Million adult patients worldwide in 2015. The increase is particular strong in middle- and low-income countries (Federation 2015, (NCD-RisC) 2016, WHO 2016). The International diabetes federation estimated the global health spending to treat diabetes and associated complications between 673 billion and 1,197 billion USD in 2015. However, this number is predicted to exceed 1,452 billion USD in 2040 (Federation 2015).

Basically, two main forms of diabetes mellitus – Type 1 and Type 2 - are known (Guariguata et al. 2014). Type 1 diabetes mellitus (T1DM) accounts for 5-10% of all diabetes patients. Pathogenically, T1DM is seen as an autoimmune disease resulting in β -cell dysfunction and destruction via specific autoantibodies. Histological analysis of pancreata from T1D patients often reveals the presence of immunological activity by antibodies and T lymphocytes (Fu et al. 2013). Patients with T1DM are diagnosed often already during childhood and require long-life treatment with insulin. In addition, immune suppressive drugs can help to slow down the progression of β -cell destruction. Several studies implemented also dietary factors like infant feeding, lack of vitamin D or omega 3 polyunsaturated fatty acids as possible risk factors (Virtanen et al. 2003, Wahlberg et al. 2006, Fu et al. 2013, Gregory et al. 2013).

The most common form of diabetes is T2DM as a result of increasing insulin resistance and loss of β -cell mass and function (Fu et al. 2013). T2DM is a multifactorial disease, where

certain life-style aspects (e.g. age, pregnancy, a sedentary life style, energy-dense food consumption, smoking and obesity), sometimes in combination with genetic risk factors (usually multiple gene variations rather than single gene mutations (Ashcroft et al. 2012)), are seen as causative. Basically, T2DM has to be assigned as the disability of the pancreas to respond to hyperglycemia, either due to peripheral insulin intolerance or impaired insulin secretion (Brereton et al. 2016). This is also a vicious cycle since chronic hyperglycemia finally leads to impaired insulin secretion and consequently to further increasing blood glucose levels (Hribal et al. 2003, Brereton et al. 2016). Furthermore, the long-term exposure to high glucose levels has also deleterious effects on β -cells. In detail, high glucose levels lead to an abundant expression of the glucose transporters Glut2 (Slc2a2) and Glut4 (Slc2a4) on β -cells and subsequently excessive glucose concentrations within the cells. This glucotoxicity has not only negative effects on general β -cell specific metabolic pathways, but additionally induces elevated cytosolic Ca^{2+} concentrations finally leading to β -cell destruction (Khaldi et al. 2004, Fu et al. 2013). Moreover, hyperglycemia increases the production of radical oxygen species (ROS) that are implicated in cellular damage and mitochondrial dysfunction (Sakai et al. 2003). A detailed overview on causes of β -cell dysfunction in T2DM is given in Fu et al. 2013 and Brereton et al. 2016. Taken together, many different causes lead to loss of β -cell function and insufficient insulin secretion and, therefore, a further increase in hyperglycemia and insulin resistance.

2.5. Aim of this thesis

Delta-Notch signaling has been shown to be essential for pancreatic development and causes many severe diseases including pancreatic cancer when perturbed (Buchler et al. 2005, Kim et al. 2010, Avila et al. 2013). The presence of Notch components in mature organs also suggested a potential function during adulthood (Su et al. 2006, Dror et al. 2007). In addition, genome wide association studies (GWAS) of human populations identified NOTCH2 and DLL4 as loci robustly associated with T2DM (Morris AP 2012). However, less is known about the presence and function of Delta-Notch signaling in adult pancreatic islets.

In this study, the inducible β -cell specific murine *Cre* deleter line Pdx1-CreERT (Zhang et al. 2005) was used to knock down the Notch ligands *Dll1* and *Dll4* during adulthood. In parallel to the knock-down studies, a gene construct developed by Daniel Gradinger was used to overexpress the intracellular domain of DLL1 (DICD) exclusively in murine β -cells. This mouse model allows the investigation of a still unknown function of the intracellular ligand domain. Homozygous and double homozygous mice, respectively, for the particular genes (*Dll1* and *Dll4*) as well as DICD overexpressing mice were tested for metabolic function *in vivo* and *in vitro* by measuring glucose tolerance and glucose stimulated insulin secretion as well as body weight and basal blood glucose levels. Moreover, the islets were analyzed regarding their morphology and maturation as well as for their hormonal content. In addition, whole genome transcriptome analysis as well as qRT-PCR was performed on isolated islets to reveal affected downstream pathways and target genes.

3. MATERIALS AND METHODS

3.1. Materials

3.1.1. Chemicals

Table 2: List of used chemicals

CHEMICALS	SUPPLIER	CATALOGUE NUMBER
Glucose solution 20%	B. Braun	2356746
Glucagon	VWR	SAFSG2044-5MG
KCl	Sigma Aldrich	P5405-250g
Exendin-4	Sigma Aldrich	E7144
8-Bromo-cAMP	Sigma Aldrich	B5386
Forskolin	Sigma Aldrich	F3917
Norepinephrin	Sigma Aldrich	A7257
H-89	Sigma Aldrich	B1427-5MG
ESI-09	Biozol	SEL-S7499-5MG
BSA	Sigma Aldrich	A3311-100G
FBS	Life Technology	10500064
Ampuwa (ultrapure H ₂ O)	Fresenius Kabi	10333429
Collagenase P	Roche	11 213 857 001
Phire Reaction Buffer (5x)	Biozym Scientific	F-122L
dNTPs (10 mM)	Thermo Scientific Fermentas	10324860
LC Green Dye (10x)	Bioke	BF BCHM-ASY-006

3.1.2. Buffers and solutions

Table 3: List of used buffers, solutions and their preparation

REAGENT	AMOUNT
PBS (10x)	
NaCl	80 g
KCl	2 g
Na ₂ HPO ₄ ·2H ₂ O	17.8 g
KH ₂ PO ₄	2.72 g
dissolved in ddH ₂ O and adjusted to pH 7.3	
ddH ₂ O added to a final volume of 1 L	
PBST (0.1% Tween)	
10x PBS	100 mL
Tween20	100 µL
ddH ₂ O	900 mL

Sucrose

30%	45 g in 150 mL ddH ₂ O
15%	50 mL of 30% + 50 mL ddH ₂ O
9%	9 g in 100 mL

Acid ethanol (0.18M HCl in 71% ethanol)

absolute ethanol	375 mL
ddH ₂ O	117.5 mL
concentrated HCl	7.5 mL

Blocking Serum

1x PBST	50 mL
BSA	2.5 g

2 M GLUCOSE

Glucose	18 g
ddH ₂ O	50 mL
18 g to 40 ml ddH ₂ O, heat to dissolve then make up to 50ml	

G-solution for islet isolation

Hanks' Balanced Salt Solution (Lonza Verviers)	500 mL
antibiotic antimycotic solution	5 mL
BSA	5 g
dissolved and sterile filtered, stored at 4 °C for up to a month	

1 M HEPES

HEPES	26.03 g
ddH ₂ O	100 mL

15% Optiprep®

40% Optiprep®	5 mL
10% RPMI1640 (Lonza Verviers) in HBSS (Lonza Verviers)	3 mL
freshly prepared on the day of use	

40% Optiprep®

60% Optiprep®	20 mL
DBPS (Lonza Verviers)	9.7 mL
1M HEPES (Lonza Verviers)	300 µL
stored at 4 °C for up to a week	

200 mL Stock 10x Modified KRB STOCK (store at 4°C or -20°C)

NaCl	14.0256 g
KCl	0.71568 g
CaCl ₂ •2H ₂ O	0.7351 g
MgCl ₂	0.228528 g

ddH₂O Up to 200 mL

200 mL Stock 1x Modified KRB STOCK (store at 4°C or -20°C)

10x KRB	20 mL
1 M Hepes	1 mL
0.5 M NaHCO ₃	9,6 mL
fill up with ddH ₂ O and adjusted to pH 7.4	
ddH ₂ O added to a final volume of 200 mL	

0.5 M NaHCO₃

NaHCO ₃	4.2 g
ddH ₂ O	100 mL

Paraformaldehyde (20% stock)

stock prepared under a fume hood

PBS	80 mL
PFA	20 g

heat up to 70 °C

add 1 drop of concentrated NaOH until the solution is clear

remove from the heat

add 20 ml PBS, cool to room temperature

adjust pH to 7.2 with HCl

aliquot and store at -20°C, dilute to 4% before use

Tail-buffer

1 M Tris-HCl pH 8.0	50 mL
0.5 M EDTA	5 mL
10% SDS	10 mL
5 M NaCl	20 mL
distilled water	415 mL

3.1.3. Antibodies

Table 4: List of used primary and secondary antibodies

PRIMARY ANTIBODY	HOST (CLONE)	CLONALITY	CATALOGUE NUMBER	COMPANY	DILUTION
Insulin	guinea pig	polyclonal	A0564	Dako	1:200
Glucagon	mouse	monoclonal	G2654	Sigma Aldrich	1:1000- 1:5000
Glucagon	rabbit	polyclonal	ab92517	Abcam	1:200

Somatostatin	rabbit	polyclonal	A0566	Dako	1:200
Somatostatin	goat	polyclonal	sc-7819	Santa Cruz Biotechnology	1:200
Somatostatin	mouse	monoclonal	14-9751-82	Affymetrix eBioscience	1:200
CD31 (PECAM-1)	rabbit	polyclonal	ab28364	Abcam	1:50
CD31 (PECAM-1)	rat	monoclonal	550274	BD Pharmingen	1:200
Dll1 (155-173) extracellular	rabbit	polyclonal	ab10554	Abcam	1:200
Dll3 (M160)	rabbit	polyclonal	sc-67269	Santa Cruz Biotechnology	1:200
Dll4	rabbit	polyclonal	ab7280	Abcam	1:200
Jagged1	rabbit	polyclonal	ab7771	Abcam	1:200
Jagged2	rabbit	polyclonal	sc-5604	Santa Cruz Biotechnology	1:50
Notch1 (complete)	rabbit	polyclonal	ab27526	Abcam	1:200
Notch2 (M-20)	goat	polyclonal	sc-7423	Santa Cruz Biotechnology	1:200
Notch3	rabbit	polyclonal	ab23426	Abcam	1:200
Notch4	rabbit	polyclonal	N5163- 100UG	Sigma Aldrich	1:200
MafA	rabbit	polyclonal	ab26405	abcam	1:200
MafB	rabbit	polyclonal	IHC-00351	biomol	1:200
Ki67	rabbit	monoclonal	RM-9106-S	thermo fisher	1:200
Caspase 3 cleaved	rabbit	polyclonal	9661s	Cell Signaling	1:200
Dll1 intracellular	rat	monoclonal	GSF	Gift from Dr. E. Kremmer	1:5
Pdx1	rabbit	monoclonal	5679	Cell Signaling	1:300
Pdx1	mouse	monoclonal	F6A11-c	DSHB	1:500
Glut-2	rabbit	polyclonal	ab95256	Abcam	1:200
Ghrelin	rat	monoclonal	MAB8200	R&D Systems	1:50
Vegf	rabbit	polyclonal	ab46154	Abcam	1:200
Magi-1	mouse	monoclonal	sc-100326	Santa Cruz	1:100

Magi-2	mouse	monoclonal	sc-517008	Santa Cruz	1:100
Magi-3	mouse	monoclonal		Santa Cruz	1:100
Laminin	rabbit	polyclonal	ab11575	Abcam	1:500
SECONDARY ANTIBODY	HOST (CLONE)	CLONALITY	CATALOGUE NUMBER	COMPANY	DILUTION
Alexa 488 - donkey-anti-goat	donkey-anti-goat	donkey	A11055	Invitrogen	1:500
Alexa 488 - donkey-anti-mouse	donkey-anti-mouse	donkey	A21202	Invitrogen	1:500
Alexa 488 - donkey-anti-rabbit	donkey-anti-rabbit	donkey	A21206	Invitrogen	1:500
Alexa 488 - donkey-anti-rat	donkey-anti-rat	donkey	A21208	Invitrogen	1:500
Alexa 488 - goat-anti-guinea pig	goat-anti-guinea pig	goat	A11073	Invitrogen	1:500
Alexa 594 - donkey-anti-goat	donkey-anti-goat	donkey	A11058	Invitrogen	1:500
Alexa 594 - donkey-anti-rabbit	donkey-anti-rabbit	donkey	A21207	Invitrogen	1:500
Alexa 594 - donkey-anti-mouse	mouse	donkey	A21203	Invitrogen	1:500
Alexa 594 - goat-anti-rat	rat	goat	ab96965	Abcam	1:500
DAPI			D9542	Sigma Aldrich	1:1000

3.1.4. Molecular biology reagents

3.1.5. Oligonucleotide primers

3.1.5.1. Primers for genotyping

Table 5: List of primers used for mouse genotyping

Primer for genotyping

GENE NAME	FORWARD PRIMER 5' -3'	REVERSE PRIMER 5' -3'
DICD lox	GCACTTGCTCTCCCAAAGTC	GATACCGTCGATCCCCACT
DII1lox	CACACCTCCTACTTACCTGA	GAGAGTACTGGATGGAGCAAG

Dll4lox	GTGCTGGGACTGTAGCCACT	TGTTAGGGATGTCGCTCTCC
Pdx1 CreERT	AACCTGGATAGTGAAACAGGGGC	TTCCATGGAGCGAACGACGAGACC

3.1.5.2. Primers for qRT-PCR

Table 6: List of primers used for qRT-PCR

Primer for qPCR (housekeeping genes)

GENE NAME	FORWARD PRIMER 5'-3'	REVERSE PRIMER 5'-3'
YWHAZ	TGCAAAAACAGCTTTTCGATG	TCCGATGTCCACAATGTTAAGT
Rpl13a	TGAAGCCTACCAGAAAGTTTGC	GCCTGTTCCGTAACCTCAA
SDHA	GCAATTTCTACTCAATACCCAGTG	CTCCCTGTGCTGCAACAGTA
B2M	GCTATCCAGAAAACCCCTCA	GGGGTGAATTCAGTGTGAGC
ACTB	GCCACCAGTTCGCCAT	CATCACACCCTGGTGCCTA
GAPDH	TGGAGAAACCTGCCAAGTATG	CATTGTCATAACCAGGAAATGAGC
UBC	AGCCCAGTGTTACCACCAAG	ACCCAAGAACAAGCACAAAG
HMBS	GCTGAAAGGGCTTTTCTGAG	TGCCATCTTTCATCACTGT
Tbp	CCCCACAACCTTCCATTCT	GCAGGAGTGATAGGGGTCAT
Fbxw2	ATGGGTCACCAAGGTGGTT	TCCAATTGGCCAAATCTT
HPRT	CCTAAGATGAGCGCAAGTTGAA	CCACAGGACTAGAACACCTGCTAA
Tuba1a	AAGGAGGATGCTGCCAATAA	GCTGTGGAAAACCAAGAAGC
Zfp91	TTGCAGCACCACATTAATAAC	ATCCCTCTGGTCTGTATGATG
Cyc1	GTTTCGAGCTAGGCATGGTG	CGGGAAAGTAAGGGTTGAAATAG
ATP5B	GGTTTGACCGTTGCTGAATAC	TAAGGCAGACACCTCTGAGC
Pgk1	GAGCCCATAGCTCCATGGT	ACTTTAGCGCCTCCCAAGA

Primer for qPCR (genes of interest)

GENE NAME	FORWARD PRIMER 5'-3'	REVERSE PRIMER 5'-3'
Dll1	TGGCCAGGTACCTTCTCTCT	TCTTTCTGGTTTTCTGTTGC
Dll4	CACAGTGAGAAGCCAGAGTGTC	TCCTGCCTTATACCTCTGTGG
Jagged1	GCCAGACTGCAGGATAAACA	CCCTGAAACTTCATGGCACT
Jagged2	GCCAGGAAGTGGTCATATTCA	ATCCGCACCATACCTTGCTA
Notch1	TCAGGGTGTCTTCCAGATCC	CRACTTGCCTAGGTCATCCA
Notch2	GCAGTGGATGACCATGGAA	GGTGTCTCTTCTTATTGTCCTG
Notch3	TGCACTGGGAATGAAGAACA	CCGGCTCCTCTACCTTCAGT
Notch4	GGATAAAAGGGGAAAAACTGC	CGTCTGTTCCCTACTGTCCTG
Ins1	GCAAGCAGGTCATTGTTTCA	CACTTGTGGGTCCTCCACTT
Ins2	CAGCAAGCAGGAAGCCTATC	GCTCCAGTTGTGCCACTTGT
Glucagon	AGGCTCACAAGGCAGAAAAA	CAATGTTGTTCCGGTTCCTC
MafA	CAGCAGCGGCACATTCTG	GCCCGCCAACTTCTCGTAT
MafB	TAGCGATGGCCGCGGAG	CTTCACGTCGAACTTGAGAAGG
Ucn3	AAGCTGCAACCCTGAACAGT	AGCATCGCTCCCTGTAAGTG
Nkx6.1	CCTGTACCCCATCAAGGAT	GGAACCAGACCTTGACCTGA
Glut2	GGGGACAAACTTGGAAGGAT	TGAGGCCAGCAATCTGACTA

Gcgr	TCTGTTTGAGAATGTTTCAGTGCT	GGCCAGCCGGAACCTTATAG
Glp1r	ACGGTGTCCCTCTCAGAGAC	ATCAAAGGTCCGTTGCAGAA
Neurog3	GTCGGGAGAACTAGGATGGC	GGAGCAGTCCCTAGGTATG
p21	GCAGACCAGCCTGACAGATT	CACACAGAGTGAGGGCTAAGG
p57	CCAATGCGAACGACTTCTT	GCCGTTAGCCTCTAACTAACTCA
Msln	CATCCCAAGGATGTCAAAG	GCAGGCTTTCTGTTCTGCAT
Pdx1 Cre	TGCAACGAGTGATGAGGTTT	GCAAACGGACAGAAGCATT
Ctgf	AGTGTGCACTGCCAAAGATG	TTCCAGTCGGTAGGCAGCTA

3.1.6. Consumables and kits

Table 7: List of used consumables

CONSUMABLE	SUPPLIER
384 well plates (lightcycler)	Roche
6 well tissue-culture plate	Falcon
Cell strainer 70 µm nylon mesh, sterile	BD Bioscience
Corning 100 mm x 20 mm Style dishes	Corning
Corning Filter system 0.22 µm	Corning
Counter blood glucose analyzer	Bayer
Counter sensor strips	Bayer
Disposable centrifuge tubes, sterile, polypropylen, 15 mL/50 mL	Sarstedt
Eppendorf reaction tube	Sarstedt
Gloves	Meditrade
Matrix Liquid Handling Tips 30 µL, 125 µL	Thermo Scientific
Microvette® CB 300 LH	Sarstedt
O.C.T. compound	Thermo Scientific
Omnican F 1.0 mL	B Braun
Omnifix 1 mL, 5 mL, 50 mL	B Braun
Pap Pen	Enzo Life Science
Serological pipets 5, 10, 25 and 50 mL	Greiner Bio One
S-Monovette® 1,2 ml, K3 EDTA	Sarstedt
S-Monovette®-Needle 21Gx1½	Sarstedt
Sterican® Insulin Einmalkanüle für spezielle Indikationen "- G 30 x 1/2"" / Ø 0,30 x 12 mm"	Neolab
Sterile Syringe Filter 0.20 µm	Corning

SuperFrost® Plus slides	VWR
Tips	Sarstedt

Table 8: List of used kits

KITS	SUPPLIER
QIAamp® DNA Mini Kit	Qiagen
RNeasy® Plus Micro Kit	Qiagen
RNeasy® Mini Kit	Qiagen
Mouse Insulin ELISA	Mercodia
Mouse/Rat Proinsulin ELISA	Mercodia
Mouse Glucagon ELISA	Mercodia
Mouse C-Peptide ELISA	Crystal Chem Inc.

3.1.7. Laboratory equipment

Table 9: List of used laboratory equipment

LABORATORY EQUIPMENT	SUPPLIER
Axioplan 2 Fluorescence Microscope	Zeiss
Bio saftey cabine	Schulz Lufttechnik GmbH
Centrifuge Biofuge pico	Heraeus
Freezer -20 °C	Liebherr
Fridge +4 °C	Liebherr
Glassbeaker	Schott
Glassware	Schott
Incubator	Heraeus
Leica CM1850 Cryostat	Leica Microsystems
Leica SP5 Confocal Microscope	Leica
Lightscanner	Idaho Technology
Magnetic Mixer	IKA Labortechnik
Matrixpipette 30 µL, 125 µL	Thermo Scientific
Micro bulldog clamp	Roboz
Multichannel pipette 300 µL	Gilson
Nanodrop ND-1000	NanoDrop Technologies

NanoZoomer 2.0HT	Hamamatsu
Pipetman P10, P20, P200, P1000	Gilson
Rocking Platform	VWR
SpectraMax190 Platereader	Molecular Devices
Stereo Microscope Stemi SV6	Zeiss
Thermomixer 1.5 mL	Eppendorf
Timer	Roth
Universal 32R centrifuge	Hettich Zentrifugen
Vortexer	Neolab
Water bath	Julabo

3.2. Methods

3.2.1. Mouse methods

3.2.1.1. *Animal housing*

Mice were kept in a specific-pathogen-free (SPF) environment in compliance with FELASA (Federation of European Laboratory Animal Science Associations) protocols. Unless otherwise specified, mice received standard rodent nutrition and water *ad libitum*. All animal experiments were performed under the approval of the responsible animal welfare authority.

3.2.1.2. *Generation of β -D1/D4 knock-down mice*

For the knock-down model, mouse lines containing floxed alleles of *Dll1* (Hozumi et al. 2004), *Dll4* (Koch et al. 2008) or both (friendly gift from F. Radtke) were intercrossed with Pdx1-CreERT mice (Zhang et al. 2005). The mice were kept on a mixed Sv/129.C57BL/6 x C57BL/6J x C3HeB/FeJ genetic background.

The Cre dependent recombination was then activated in weaned offspring for 4 weeks by Tamoxifen[®] containing chowder (400 mg/kg). For analyses, only 8-weeks old males were used; all groups including controls expressed Pdx1-CreERT recombinase.

3.2.1.3. *Generation of β -DICD overexpressing mice*

A detailed description of the mouse model overexpressing the intracellular domain of DLL1 (DICD) is given in the doctoral thesis of Daniel Gradinger (in preparation). Briefly, he used gene targeting in the endogenous *Rosa26* locus by recombinase-mediated cassette exchange (RMCE). To specifically induce DICD expression in β -cells of the adult pancreas, Rosa26-DICD and Pdx1-CreERT mice were intercrossed and a breeding colony, including Cre-positive wild-type controls, were generated. The mice were kept on a C3HeB/FeJ genetic background.

3.2.1.4. *Genotyping*

All mice were genotyped using the recently described genotyping method by LightScanner melting curve analysis (Alders et al. 2008, van der Stoep et al. 2009). 14 ng DNA per sample was dried in light protected 96 well plates for at least 2 h at 37 °C. The dried DNA was then mixed with 10 μ l LightScanner master mix, containing the following ingredients:

Table 10: Components and amount for genotyping PCR

COMPONENT	FINAL CONCENTRATION	VOLUME [μ L]
Ampuwa (ultrapure H ₂ O)		6.55
Phire Reaction Buffer (5x)	1x	2
dNTPs (10 mM)	200 μ M	0.2
LC Green Dye (10x)	1x	1
Primer (200 μ M)	0.5 μ M	0.025

All used primers are listed in 3.1.5.1

The mixed solution was then covered with 15 μ L mineral oil, the plate sealed and put into the LightScanner, running the following protocol:

Table 11: PCR conditions

TEMPERATURE [$^{\circ}$ C]	TIME [s]	
98	30	
98	5	40 cycles
58	5	
72	5	
72	60	
98	30-60	Analysis of the melting curves was done with LightScanner
20	forever	Software with Call-IT 2.0.

3.2.1.5. Blood plasma collection

The tail of a mouse was slightly cut with a scissor and massaged gently to enable leakage of blood. Up to 50 μ L were collected in a lithium-heparin coated Microvette[®] CB 300 LH. For higher blood volumes, mice were sacrificed and blood was collected directly from the *vena cava*. The collected blood was then centrifuged at 9,000 rpm and 10 $^{\circ}$ C for two minutes. The plasma supernatant was transferred to a new reaction tube, frozen immediately in liquid nitrogen, and stored at -80 $^{\circ}$ C until usage.

3.2.1.6. Blood glucose evaluation

Blood glucose levels were analyzed in mice fasted for at least six hours or in random fed mice during morning hours. Leakage of a blood drop from the tail was achieved as described in

3.2.1.5. The measurement itself was performed in duplicates with the blood glucose analyzer Contour using supplied sensor strips.

3.2.1.7. *Intraperitoneal and oral glucose tolerance test*

The procedure was performed on conscious mice fasted for 16 h. Mice were weighed before the start of the procedure and fasting glucose levels were obtained via a small tail clip as described in 3.2.1.5. 1 mL/100 g body weight of a 20% glucose solution in sterile saline (corresponding to 2 gramm of glucose per gramm of body weight) was injected intraperitoneally or given by gavage at time point 0. Blood glucose values and plasma samples were obtained as described above after 5, 15, 30, 60, and 120 minutes.

3.2.1.8. *NMR body composition analysis*

Body composition was measured once in 8 weeks old mice. Noninvasive NMR scans were used to measure fat and lean content (Gailus-Durner et al. 2009, Halldorsdottir et al. 2009).

3.2.1.9. *Food consumption analysis*

In advance, mice were separated into single cages with food provided in small bowls. For measurements, the food as well as the animals were weighed two times per day, once in the morning and once in the evening, to evaluate the active and inactive phase of the mice. The individual food intake was measured for three days in a row.

3.2.2. Cell culture methods

3.2.2.1. *Islet isolation and culture*

Islets were isolated as described previously (Carter et al. 2009, Li et al. 2009). In brief, mice were euthanized by cervical dislocation, readily dissected to expose the inner organs, and placed under a dissecting microscope. The gut and the liver were pushed aside with surgical forceps, thereby exposing the common bile duct that was clamped at its junction with the duodenum with a micro bulldog clamp and subsequently cannulated. The pancreas was distended via the injection of 3-5 mL collagenase solution (1 mg/mL), removed from the cadaver, and immediately placed on ice in a 15 mL falcon tube containing further 3-5 mL of the same collagenase solution. When processing more than one animal, organs should not be

stored on ice longer than 60 minutes before proceeding to the next step, allowing for the preparation of approximately 4-6 animals by one experimenter.

Samples were incubated in a 37 °C water bath for 15 minutes and shaken gently once after 7.5 minutes. All remaining steps were performed under a sterile working bench. 10 mL ice-cold G-solution were added to the digested pancreas followed by centrifugation for 2 min at 1620 rpm (all centrifugation steps were performed at room temperature). The supernatant, containing mainly fat tissue that remained attached to the pancreas during removal as well as loose exocrine tissue, was discarded and the pellet resuspended in further 10-12 mL ice-cold G-solution. The suspension was then filtered through a pre-wet small metal mesh (pore size approx. 1 mm) to separate undigested tissue chunks, and collected in a 50 mL falcon tube. Both the 15 mL tube originally containing the pancreatic suspension and the metal mesh were rinsed with additional G-solution to avoid islet loss. The filtrate was then centrifuged again at 1620 rpm for 2 min. The supernatant, made up mostly by acinar cells, was discarded and the pellet resuspended in 5.5 mL of a 15% Optiprep® solution prepared as described and stored at 4 °C until use. This suspension was pipetted carefully onto 2.5 mL of 15% Optiprep® in a new falcon tube, producing two distinct layers of different density. This gradient was then overlaid again with 6 mL G-solution and incubated for 10 min at room temperature followed by 15 minutes centrifugation at 1,750 rpm with the brake turned off to avoid mixing of the gradient during deceleration. The islets, now located at the interface between the first and second layer, were collected with a serological pipette and filtrated through a 70 µm cell strainer to loosen remaining acinar cells. The strainer was turned over a petri dish and rinsed with 12 mL RPMI 1640 to liberate the islets that were hand-picked under a microscope with a 200 µL micropipette to further enhance purity. Islets were plated into non-treated suspension culture dishes to avoid attachment and kept at a maximum density of 50 islets per dish to prevent competition for nutrients and the appearance of hypoxic centers. Culture was carried out in 10 mL 5.5 mM glucose RPMI 1640 supplemented with 10% fetal bovine serum and 1x antibiotic antimycotic solution. Islet dishes were kept in a sterile incubator at 37 °C with 5% CO₂ infusion and humidified air at all times. Unless specified otherwise, islets were cultured overnight and then used.

3.2.2.2. *Glucose-stimulated insulin secretion*

All buffers were warmed to 37 °C and checked for correct pH value (pH 7.4) before the start of the procedure. Islets corresponding to one sample were handpicked under a microscope and collected in a 1.5 mL reaction tube prefilled with 1.4 mL 1.5 mM glucose/mKRB, using a 20 µL micropipette.

After all samples were collected, the islets were allowed to settle to the bottom of the tube for 5 minutes. 1.4 mL of the supernatant was carefully removed using a 1000 µL micropipette and 1 mL 1.5 mM glucose/mKRB was added. After 5 minutes, 1 mL was carefully removed and an additional washing step was performed by adding 1 mL 1.5 mM glucose/mKRB and removed after 5 minutes. Using a 200 µL micropipette, islets were transferred to one well of a 6 well-plate containing 5 mL of 1.5 mM glucose/mKRB and incubated for one hour at 37 °C and 5% CO₂ without the lid. Afterwards, islets were transferred to a new well containing the same buffer and placed in the incubator for a further hour. Islets isolated from the same mouse and treated in the same way were always kept in the same well. During the first of these two incubations, 1.5 mL reaction tubes with the desired treatments were prepared. For a basic GSIS experiment, tubes with each 500 µL of 2.8 mM glucose/mKRB (low glucose) and 16.7 mM glucose/mKRB (high glucose) were pipetted, labeled and placed in the incubator with open lids to allow equilibration with the CO₂ pressure. For advanced GSIS experiments, the solutions were treated additional with different kind of stimulations and inhibitors listed below during high glucose condition.

Table 12: Treatments for GSIS

TREATMENT	FUNCTION	CONCENTRATION
KCl	opens Ca ²⁺ channels	30 mM
Exendin-4	binds to GLP1R	100 nM
8-Bromo-cAMP	cAMP agonist	1 mM
Forskolin	stimulates Adenylyl cyclase and cAMP levels	2.5 µM
Norepinephrin	Adenylyl cyclase inhibitor	10 µM
H-89	PKA inhibitor	10 µM
ESI-09	EPAC inhibitor	10 µM

Upon finishing of the second incubation, 5-10 islets (the same number for each sample within one experiment) were picked with a 20 µL micropipette and pipetted in a tube containing the

designed treatment. Tubes were then placed in the incubators for 1-2 hours (dependent on the purpose) with open lids. If inhibitors were used, the islets were treated with the inhibitor first for 30 min, before the stimulatory treatment was added.

After all incubations were finished, samples were mixed gently with a 200 μ L micropipette and centrifuged for 2 min at 10,000 rpm. 400 μ L supernatant were transferred to a new tube, while 500 μ L of acid ethanol were added to the islets to lyse the cells and mobilize insulin. All samples were stored at -20 $^{\circ}$ C until further use and measured later using a Mouse Insulin ELISA (see 3.2.4.5.1). Insulin secretion was expressed as the amount of secreted insulin per islet and hour.

3.2.3. Isolation and purification methods

3.2.3.1. DNA isolation

To determine the correct genotype of the mice, genomic DNA was isolated. Therefore, a small amount of tissue collected from an ear punch was incubated in 400 μ L Tail-buffer and 4 μ L Proteinase K overnight at 55 $^{\circ}$ C. The digestion was stopped with 20 min incubation at 93 $^{\circ}$ C on the next day and the samples were stored at -20 $^{\circ}$ C until further use.

3.2.3.2. RNA isolation

3.2.3.2.1. Islets

After successful isolation (3.2.2.1) islets were handpicked under a stereomicroscope using a 200 μ L pipette and collected in a 1.5 mL Eppendorf tube kept on ice. For a sufficient amount of RNA, it was necessary to collect at least 50 islets per sample. When all samples were collected, the tissue was harvested by centrifuging 1 min at 12,000 rpm and RT. The supernatant was removed carefully and the islets were lysed immediately by adding 350 μ L RLT buffer containing 10 μ L/mL β -mercaptoethanol and vortexing for at least 30 s. All subsequent steps were performed according to the manufacturer's manual of the RNeasy[®] Plus Micro Kit. The lysed samples were transferred into gDNA eliminator spin columns and centrifuged at 8,000 rpm for 30 s. After addition of 350 μ L 70% ethanol to the flow through, the sample was transferred to an RNeasy MinElute spin column and centrifuged at 8,000 rpm for additional 15 s. To purify the sample, several washing steps with 700 μ L RW1 buffer, 500 μ L RPE buffer and 500 μ L 80% ethanol were performed using centrifugation at 8,000 rpm for 15 s

or 2 min for the ethanol washing step. The pellet was then dried with the lid open in an additional centrifugation step for 5 min at full speed. Afterwards the RNA was eluted with 14 μ L Ampuwa and stored at -80 °C until further usage.

3.2.3.2.2. *Other tissues*

Mice were sacrificed, organs (spleen, liver etc.) removed and snap frozen in liquid nitrogen, immediately. All samples were stored at -80 °C until further usage.

To isolate RNA the frozen tissue was transferred into 4 mL Trizol (Qiagen) and homogenized with a tissue homogenizer (Heidolph DIAX 900) for 60 s. The tube was then rested for 5 min at RT. 1 mL of the solution was transferred into a 1.5 mL Eppendorf tube, 200 μ l chloroform added and mixed vigorously by hand for at least 15 s. After additional 2-3 min incubation at RT, the samples were centrifuged for 15 min at 13,000 rpm at 4°C. From the two-phase solution, the colorless upper aqueous phase was transferred into a new 1.5 mL Eppendorf tube and the same volume of 100% ethanol was added and mixed.

All following steps were done according the manufacturer's instructions for the RNeasy® Mini Kit (QIAGEN). The samples were transferred into RNeasy mini columns and centrifuged for 1 min at 13,000 rpm at RT. After discarding the flow-through, the column was washed with 700 μ L RW1 and 450 μ l RPE. Each washing step was done by centrifugation for 1 min at 13,000 rpm and RT and followed each by the removal of the flow-through. To remove remaining liquid afterwards, the column was transferred into a new collection tube and centrifuged another 2 min at 13,000 rpm and RT. To elute the RNA, 60 μ l RNase-free water was directly pipetted onto the column membrane and incubated for 1 min. By 1 min centrifugation at 13,000 rpm and RT, the elution containing the isolated RNA was then collected into a 1.5 mL Eppendorf tube. The final concentration and quality was determined with Nanodrop.

3.2.4. Molecular methods

3.2.4.1. *Polymerase Chain Reaction*

3.2.4.2. *cDNA synthesis*

cDNA was synthesized from RNA (50-00 ng) using the SuperScript® II reverse transcriptase enzyme and a random primer mix containing both random hexamers and anchored dT23 primers to maximize reaction yields. RNA was mixed with the primers and pre-annealed as follows:

Table 13: Components for the pre-annealing step

COMPONENT	VOLUME
RNA	variable
random primer mix (60 μ M)	2 μ L
dNTPs (10 mM)	1 μ L
Ampuwa	filled to 12 μ L

This preliminary reaction mix was pre-annealed at 65 °C for 5 min and then chilled for 5 min on ice. The reaction mix was completed by adding the following components in the given order to a final volume of 20 μ L.

Table 14: Components for the enzymatic reaction

COMPONENT	VOLUME
First-Strand Buffer (5x)	4 μ L
DTT (0.1 M)	2 μ L
RNaseOUT	1 μ L
SuperScript II	1 μ L

After 10 min pre-incubation at RT, the reverse transcription was performed in a thermal cycler for 60 min at 42°C. Enzyme inactivation, essential for subsequent applications, was achieved by an additional incubation step at 70 °C for 15 min. For further usage, the samples were diluted in Ampuwa to a final concentration of 2.5 ng/ μ L and stored at -20 °C.

3.2.4.3. Quantitative real-time PCR (qRT-PCR)

Quantitative real-time PCR (qRT-PCR) is an umbrella term that summarizes a variety of different experimental procedures and strategies, as has been noted before (Vandesompele et al. 2002).

Here, qRT-PCR was used for the relative quantification of genes in tissue cDNA samples, using the fluorescent cyanine dye SYBR Green I included in the LightCycler®480 DNA SYBR Green I Master. Each sample was measured in four technical replicates to assure measurement quality. For optimal results, the transcribed product should range between 70-300 bp. As reference for sequence information the ensemble genome browser database was used (Yates et al. 2016). For efficient targeting of the genes of interest, all primer sequences were designed manually containing exon/exon junctions to assure the amplification of mRNA only. Therefore, Primer-BLAST (<http://www.ncbi.nlm.nih.gov/tools/primer-blast/>) was used to detect suitable primers dependent on the above-described criteria and to exclude unspecific binding to other gene areas. Primers were ordered from Metabion and tested in a PCR format to assure the amplification of the right product size. Moreover, a melting curve analysis was performed as a part of every qRT-PCR experiment to check that only the specific product was produced.

Given the relative nature of the quantification, normalization against housekeeping genes is possibly the most essential component of the assay and its disregard is a serious problem affecting many experimental results (Gutierrez et al. 2008, Bustin et al. 2009). To avoid this, all experiments described in this study were carried out according to the strategy outlined by Vandesompele et al. (Vandesompele et al. 2002), meaning that for every new experimental setup (e.g. the comparison between islet samples isolated from new genotypes, samples from different tissues or if the culture conditions were different, etc.) a set of 15 candidate housekeeping genes (Table 6) was analyzed with regard to the suitability of said candidates as references. The two most stable housekeeping genes, determined with this method using the geNorm® 3.5 software, were selected for the qRT-PCR experiment.

For each reaction 0.5 ng/μL cDNA were usually amplified. The following reaction mix and conditions were used:

Table 15: Components and amount of the qRT-PCR master mix

COMPONENT	FINAL CONCENTRATION	VOLUME [μ L]
gene-specific primers F+R (3 μ M)	0.3 μ M	2
cDNA	0.5 ng/ μ l	variable X
LightCycler® 480 DNA SYBR Green I Master (2x)	1x	10
Ampuwa		8 - X

Table 16: Reaction conditions

TEMPERATURE [$^{\circ}$ C]	TIME [s]
95	600
94	15
60	60
55-95	dissociation curve

45 cycles

After the reaction was finished, crossing point (Cp) values were obtained by the automatic Cp analysis of the LightCycler®480 software by the second derivative maximum method. All subsequent data analysis was performed in Microsoft Excel. Technical replicates were averaged and their standard deviation was determined to assure data quality. The results were determined using to the $2^{-\Delta\Delta C_p}$ method (Livak et al. 2001).

3.2.4.4. Whole transcriptome microarray analysis

Whole genome transcriptome analysis was kindly performed by Dr. Martin Irmeler according to the following protocol:

3.2.4.4.1. RNA isolation

RNA isolation was performed with the RNeasy® Plus Micro Kit from QIAGEN according to the manufacturer's instructions and described under 3.2.3.2.1

The Agilent 2100 Bioanalyzer in combination with the Agilent RNA 6000 Pico Kit was used to assess RNA quality. Only high quality RNA (RIN>7) was used for further analyses.

3.2.4.4.2. *Expression profiling*

Total RNA (20 ng) was amplified using the Ovation PicoSL WTA System V2 in combination with the Encore Biotin Module (Nugen). Amplified cDNA was hybridized on Affymetrix Mouse Gene ST 2.0 arrays containing about 35,000 probe sets. Staining and scanning (GeneChip Scanner 3000 7G) was done according to the Affymetrix expression protocol including minor modifications as suggested in the Encore Biotin protocol.

3.2.4.4.3. *Statistical transcriptome analysis*

Expression console (v.1.4.0.38, Affymetrix) was used for quality control and to obtain annotated normalized RMA gene-level data (standard settings including median polish and sketch-quantile normalization). Statistical analyses were performed by utilizing the statistical programming environment R (R Development Core Team (Ihaka et al. 1996)) implemented in CARMAweb (Rainer et al. 2006). Genewise testing for differential expression was done employing the limma t-test and Benjamini-Hochberg multiple testing correction (FDR < 10%). Heatmaps were generated with CARMAweb and cluster dendrograms with R scripts (hclust, agnes, diana). Data were analyzed through the use of QIAGEN's Ingenuity® Pathway Analysis (IPA®, QIAGEN Redwood City, www.qiagen.com/ingenuity) (Ihaka et al. 1996, Rainer et al. 2006).

3.2.4.5. **ELISA**

3.2.4.5.1. *Insulin*

Insulin measurements were performed with the Mouse Insulin ELISA kit purchased from Mercodia and were used for measurement of plasma insulin from mice and the assessment of *in vitro* islet samples. The procedure was carried out according to the manufacturer's manual with adjusted dilution for each type of sample. Briefly, the samples were thawed on ice and mixed with calibrator solution (or diabetes sample buffer in case of higher dilution). 10 µL of the mixture (samples were run as duplicates) were added to the pre-coated wells provided in the kit. 100 µL enzyme conjugate were added and the plate incubated for 2 h at RT at 800 rpm. After six manual washing steps with each 350 µL washing buffer, 200 µL TMB substrate were added and the reaction incubated for 15 minutes at room temperature. 50 µL stop solution were used to abort the reaction and the OD₄₅₀ was measured immediately

thereafter in a plate reader (GeniusPRO, Tecan). The standards provided by the kit were used to calculate sample concentrations.

3.2.4.5.2. *Proinsulin*

To measure the proinsulin content in plasma and islets, the Rat/Mouse Proinsulin ELISA kit purchased from Mercodia was used. The procedure was carried out according to the manufacturer's manual with adjusted dilution for each type of sample. Briefly, the samples were thawed on ice and mixed with calibrator solution (or diabetes sample buffer in case of higher dilution). 25 μ L of the mixture (samples were run as duplicates) were added to the pre-coated wells provided in the kit. 50 μ L enzyme conjugate were added and the plate incubated for two hours at room temperature and 800 rpm. After six manual washing steps with each 350 μ L washing buffer, 200 μ L TMB substrate were added and the reaction incubated for 30 min at room temperature. 50 μ L stop solution were used to abort the reaction and the OD₄₅₀ was measured immediately thereafter in a plate reader (GeniusPRO, Tecan). The standards provided by the kit were used to calculate sample concentrations.

3.2.4.5.3. *C-Peptide*

Measurements for Insulin C-Peptide were done with the Mouse C-Peptide ELISA kit supplied by Crystal Chem Inc. according to the manufacturer's instructions. Prior to running the assay, all solutions, standards and sample dilutions were prepared. Then, each well of the provided antibody-coated microplate was filled with 95 μ L sample diluent and 5 μ L sample or standard (assayed in duplicates) and the microplate covered with a plate sealer as well as mixed for 10 s. After 1 h incubation at RT, the well contents were removed and washed six times using 300 μ L washing buffer by inverting and tapping the plate firmly on a clean paper towel. To conjugate the C-Peptide, 100 μ L of anti-C-Peptide Enzyme Conjugate was added into each well and incubated for an additional hour at RT, followed by six more washing steps. After immediate dispensing of 100 μ L per well of enzyme substrate solution, the microplate was covered again and incubated for another 30 min at RT in the dark. The reaction was stopped by adding 100 μ L enzyme reaction stop solution and the absorbance measured within 30 min using a plate reader (GeniusPRO, Tecan) at OD₆₃₀.

3.2.4.5.4. *Glucagon*

Glucagon measurements were performed with the Glucagon ELISA kit purchased from Merckodia according to the manufacturer's manual. On the first day, all reagents including buffers, calibrators and samples were prepared. Therefore, the samples were thawed on ice, diluted in calibrator solution and 10 μ L were transferred in the provided pre-coated wells. After 50 μ L enzyme conjugate was added, the plate was covered with a plate sealer and incubated overnight (18-22 h) at 4 °C and 800 rpm. On the next day, the reaction volume was discarded and the wells were washed six times with each 350 μ L washing buffer. After the wells were filled with 200 μ L TMB substrate, the reaction was incubated for 30 minutes at room temperature; 50 μ L stop solution were used to stop the reaction. The absorbance was measured at OD₄₅₀ immediately thereafter in a plate reader (GeniusPRO, Tecan).

3.2.5. Immunohistochemistry

Adult mice were sacrificed by cervical dislocation and the pancreas was excised and fixed in 4% PFA-PBS for 15 min. The tissue was then washed in PBS, followed by serial incubations in 9% (1 h), 15% (1 h) and 30% (overnight) sucrose solutions and 30% sucrose/OCT (2:1) for another 1 h at 4 °C. Thereafter, the pancreatic tissue was embedded in OCT solution by removing all bubbles and frozen on dry ice. The embedded frozen tissue was cut into 9 μ m thick sections with a Leica CM1850 Cryostat and 3-4 sections each were placed on the SuperFrost® Plus slides and stored at -20 °C for further usage.

For immunostainings, the slides were thawed at RT for 5 min and equilibrated with two washing steps in PBS, one in distilled water and two steps in PBST for 5-10 min each. Then, the slides were blocked with 5% BSA in PBST for at least 2 h at RT and subsequently incubated with appropriate primary antibody overnight at 4 °C. After three more washings steps in PBST, the sections were then incubated in suitable secondary antibody at room temperature for 90 minutes. To remove excessive antibodies, the sections were washed again five times in PBS and were mounted with Vectashield® Mounting Medium afterwards. To avoid drying out of the sections, the slides were covered with coverlids and sealed with nail polish. The stainings were analyzed with an Axioplan 2 epifluorescence microscope (Zeiss) combined to an AxioCam HRC camera (Zeiss) to obtain photographs. Additional confocal images were

taken with a Leica TCS SP5 microscope. Image processing was performed using ImageJ software.

A description of the used antibodies is provided in table 4.

4. RESULTS

4.1. Loss of function studies of *Dll1* and *Dll4* in murine pancreatic β -cells

4.1.1. DLL1 and DLL4 are predominately expressed in pancreatic β -cells

Pancreata from 13-weeks old male C3HeB/FeJ wild-type mice were selected to investigate the presence of DLL1 and DLL4 by immunohistochemistry. The pancreata were prepared as described in chapter 3.2.5.

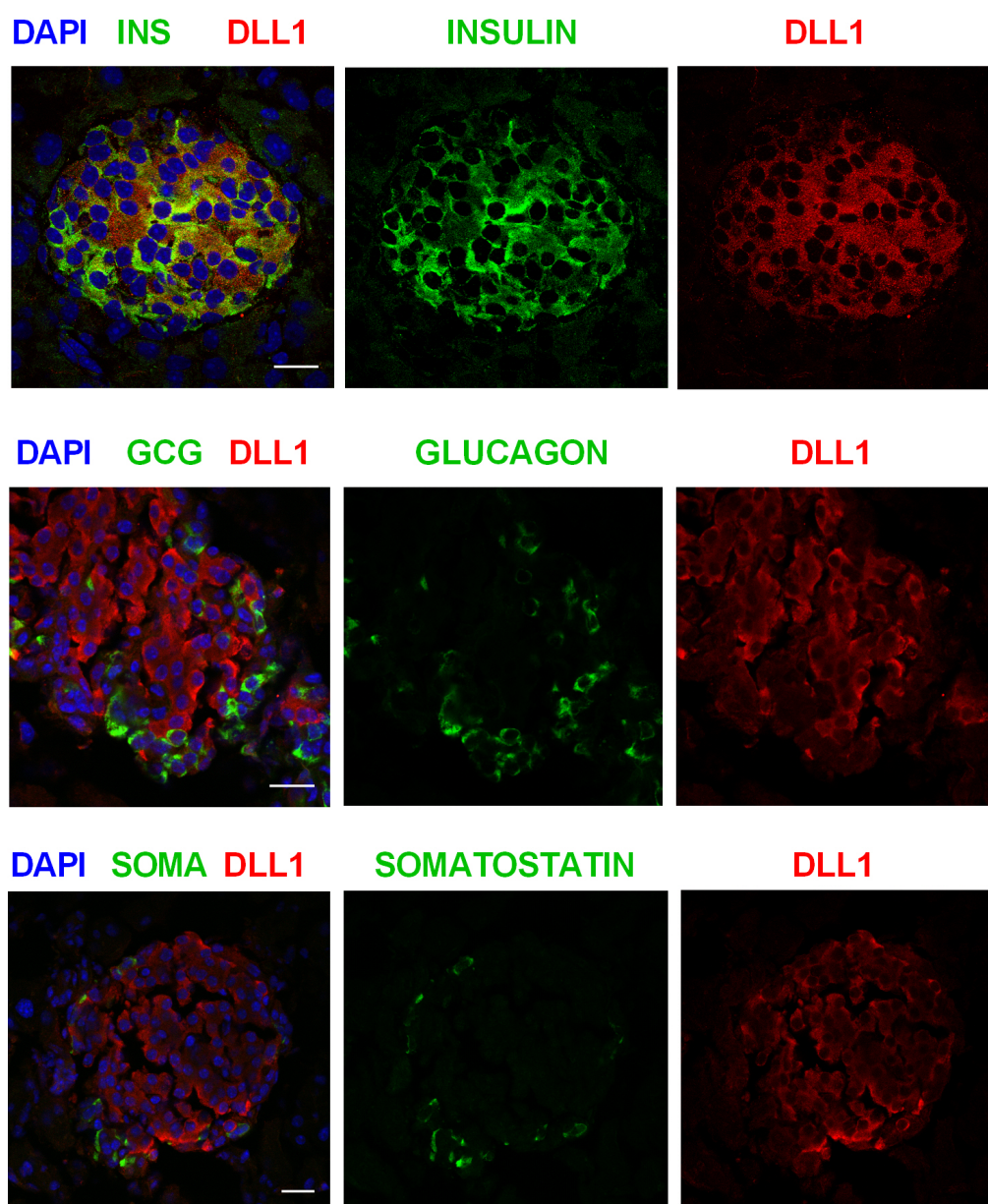


Figure 5: Immunohistochemical analysis of pancreata in 13-weeks old male C3HeB/FeJ mice. Double staining of DLL1 (red) and cell-type specific markers (green) was done on frozen pancreatic sections. INSULIN, GLUCAGON and SOMATOSTATIN were used as marker for β -, α - and δ -cells of islets, respectively. Nuclei were counterstained with DAPI (blue). The scale bar represents 20 μ m.

Both DLL1 and DLL4 could be detected in mouse islets (Figure 5 and Figure 6). To determine the islet cell types they are expressed in, co-immunostainings with islet cell-type specific antibodies (insulin for β -cells, glucagon for α -cells and somatostatin δ -cells) were performed. Using confocal microscopy, a clear overlap of both DLL1 and DLL4 with insulin positive β -cells was detected, whereas none of the ligands showed co-localization with glucagon positive α -cells or somatostatin positive δ -cells.

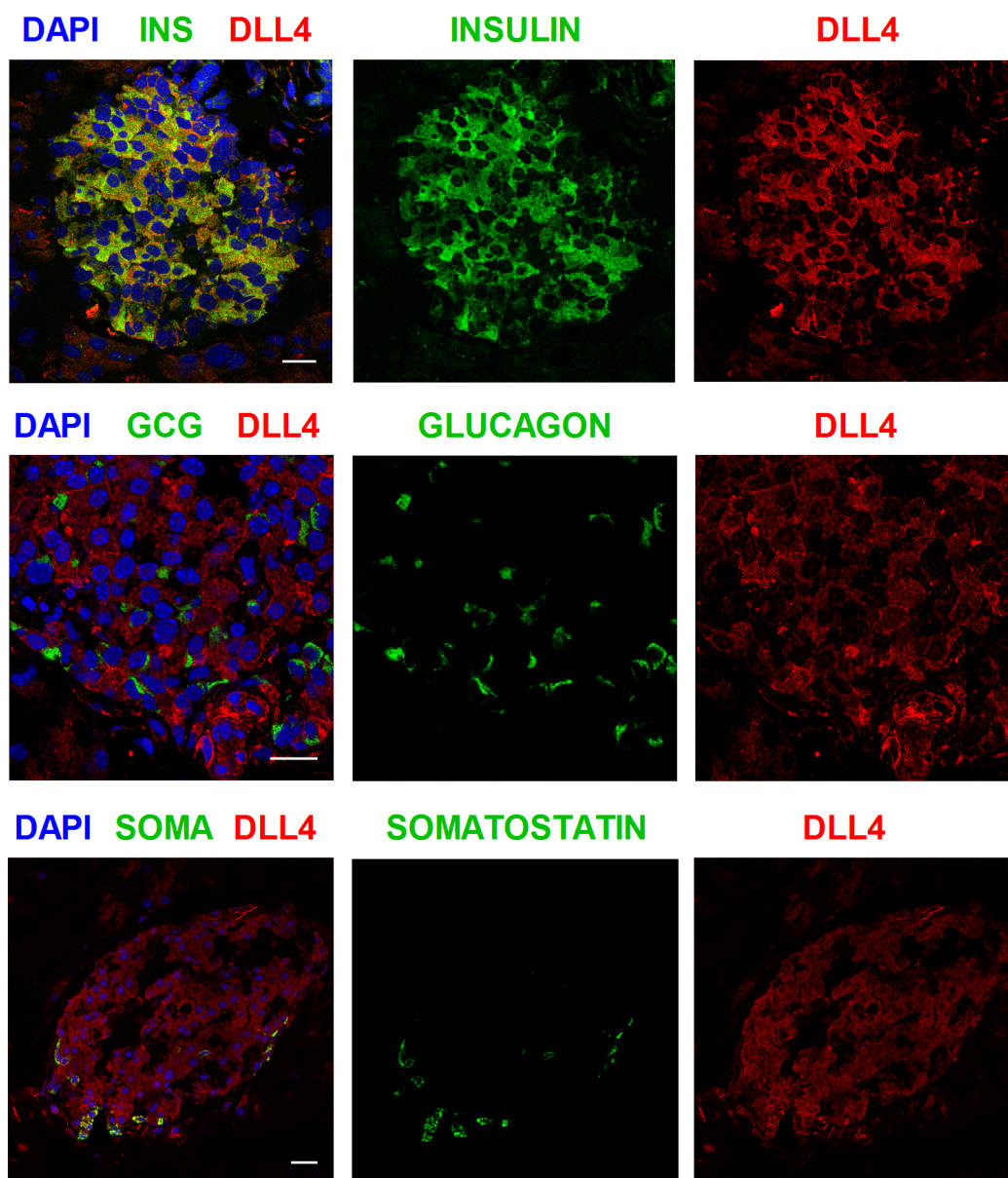


Figure 6: Immunohistochemical analysis of pancreata in 13-weeks old male C3HeB/FeJ mice. Double staining of DLL4 (red) and cell-type specific markers (green) was done on frozen pancreatic sections. INSULIN, GLUCAGON and SOMATOSTATIN were used as markers for β -, α - and δ -cells of islets, respectively. Nuclei were counterstained with DAPI (blue). The scale bar represents 20 μ m.

In addition to DLL1 and DLL4, the other ligands JAGGED1 and JAGGED2 as well as all four NOTCH receptors (NOTCH1-4) were co-stained with islet cell markers, too (Supplementary Figure 1, 2). To highlight here, is the predominately co-localization of JAGGED1 with glucagon positive α -cells and the presence of NOTCH1 in all islet cell nuclei. The other components were randomly expressed within islets and NOTCH3 is not expressed in islets at all.

4.1.2. Mouse models for β -cell specific deletion of *Dll1* and *Dll4*

To analyze potential functions of DLL1 and DLL4 in adult murine β -cells, conditional knockdown mouse models were established by using the tamoxifen-inducible Cre-lox system coupled to the *Pdx1* promoter (Figure 7).

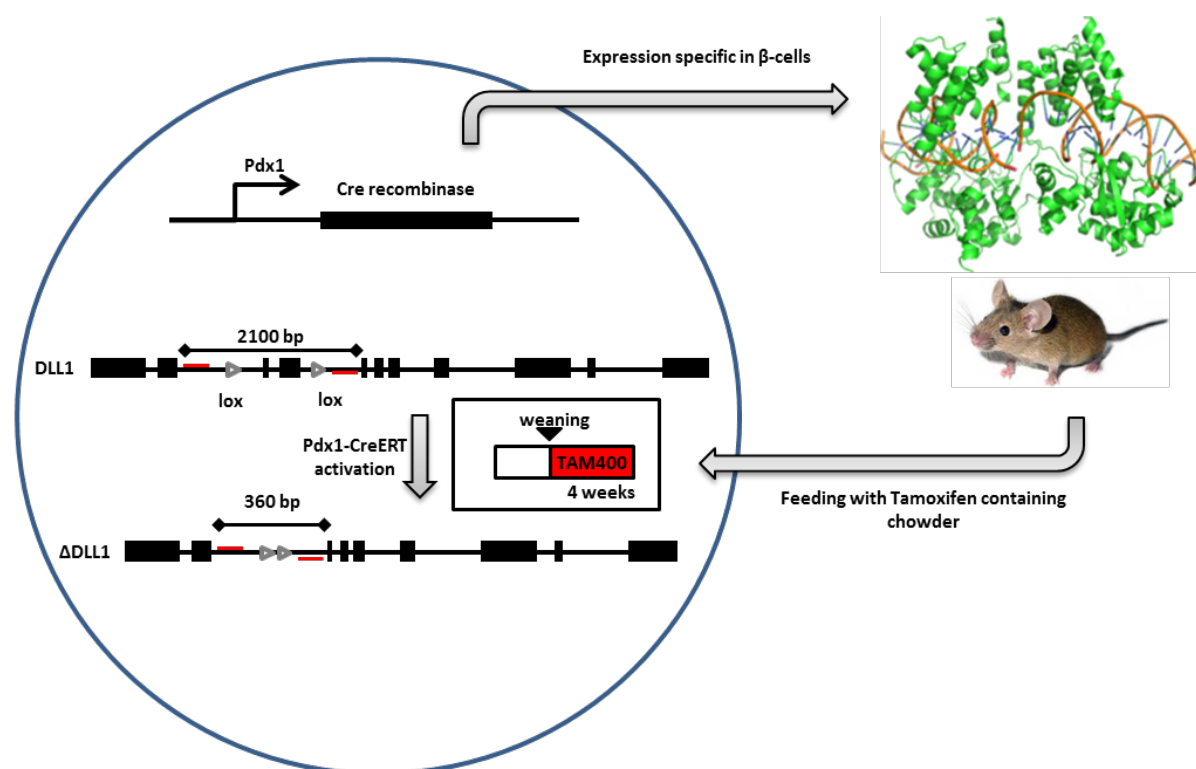


Figure 7: Schematic representation of the *Dll1* locus and its recombination in β -cells of the β -D1 mouse. Upon activation of the *Pdx1*-CreERT recombinase with tamoxifen, exon 3 and 4 are excised and a novel termination codon is generated. The scheme is similar for the *Dll4* locus in β -D4 mice.

In adulthood, the *Pdx1* promoter is only active in β -cells and can thus be used for β -cell specific gene expression (Zhang et al. 2005). Under normal conditions, Cre expression is switched off and no CRE can enter the nucleus. By treating mice with tamoxifen, Cre expression in *Pdx1*-positive cells gets induced and CRE can enter the nucleus to recombine floxed alleles. Here, already established mouse lines with floxed alleles for *Dll1* and *Dll4* were used (Hozumi

et al. 2004, Koch et al. 2008) and intercrossed with the Pdx1-CreERT mouse line (Zhang et al. 2005). Mice homozygous for floxed alleles of *Dll1*, *Dll4* or both and positive for Pdx1-CreERT were fed after weaning for four weeks with tamoxifen-containing chow in order to induce recombination exclusively in β -cells. By using Pdx1-CreERT positive control mice instead of negative but floxed control mice, the reported effects of Cre expression on metabolic function and cellular stress should be reduced (Cavanna 2013). Cavanna hypothesized that Cre positive mice should be more stringently compared to Cre negative animals. The analysis started after the mice reached the age of at least 8-weeks and therefore adulthood. The mouse lines were named according to the deleted genes β -D1, β -D4 and β -D1D4, respectively. To proof for efficient recombination and deletion of the target genes several experiments were performed (Figure 8). For protein levels immunostaining was performed, using antibodies against DLL1 and DLL4 together with a PDX1-specific antibody. In Cre-positive but non-floxed control mice, DLL1 and DLL4 were expressed in all cells with a PDX1 signal in their nuclei. In contrast, in mice with knockdown of either *Dll1* or *Dll4*, and in mice with knockdown of both alleles, the staining in β -cells was drastically reduced (Figure 8A). The expression of Cre as well as *Dll1* and *Dll4* in isolated islets was measured by qRT-PCR. Expression of *Dll1* was reduced by more than 60% in β -D1 but not in β -D4 islets, whereas *Dll4* expression was normal in β -D1 but reduced to about 50% in β -D4 compared to control islets (Figure 8B). As expected, Cre expression could only be detected in islets but not in other control tissues (Figure 8C). Both gene expression and immunofluorescence staining prove for a correct and efficient knockdown of *Dll1* and *Dll4* in pancreatic β -cells only.

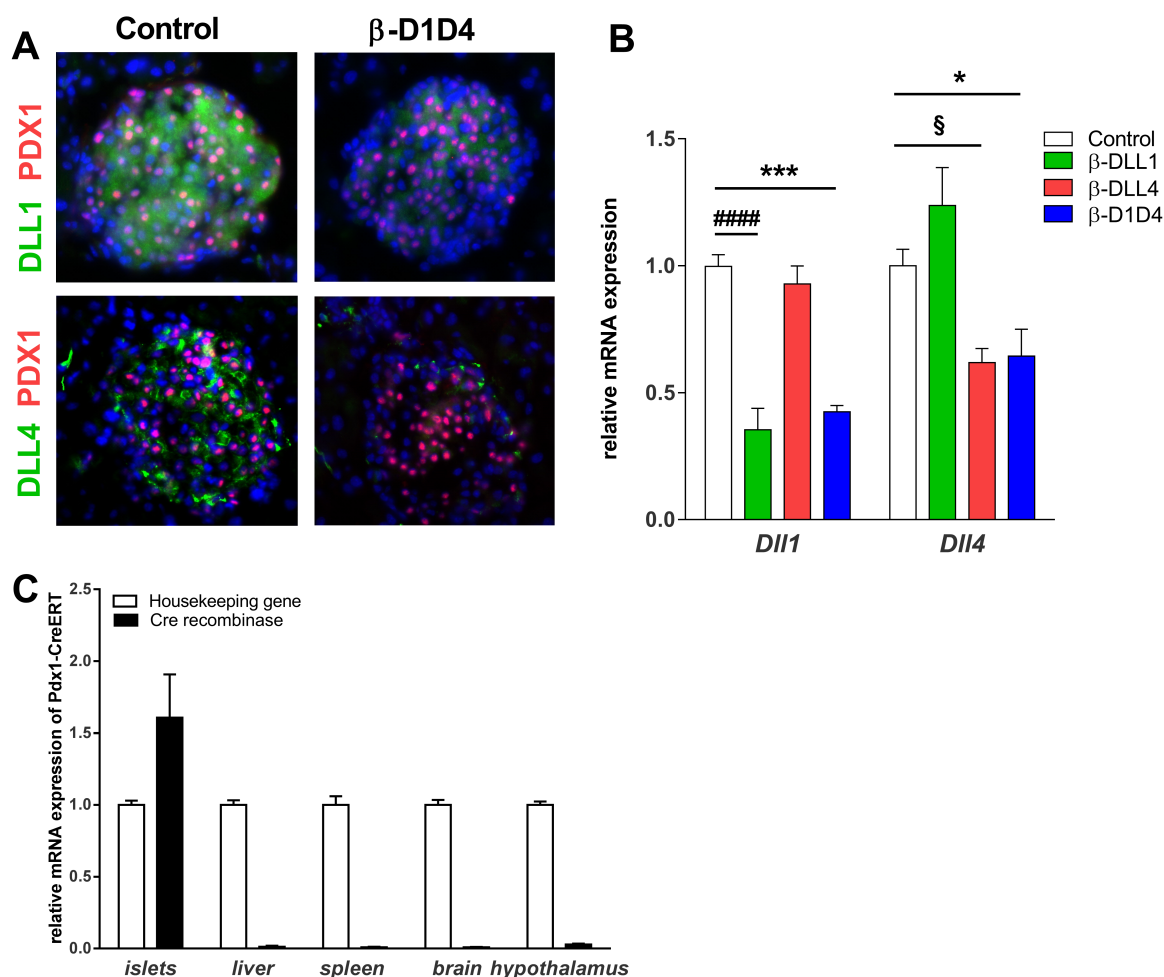


Figure 8: Proof of knock-down efficiency.

(A) Immunohistochemical analysis of pancreata from 8-weeks old male β -D1D4 (n=5) and *Cre*-positive control mice (n=5). Nuclei were counterstained with DAPI (blue). (B) Expression levels of *Dll1* and *Dll4* in isolated islets of β -DLL1, β -DLL4 and β -D1D4 mice compared to *Cre*-positive controls (n=5). (C) *Cre* expression in isolated islets, liver, spleen, whole brain, and hypothalamus from β -D1D4 and *Cre*-positive controls normalized to the housekeeping gene *Hprt* (n=6). Data are shown as mean \pm SEM. Differences were considered statistically significant at * p <0.05, ** p <0.01, *** p <0.001, **** p <0.0001 using a 2-tailed heteroscedastic student's t-test.

4.1.3. Effects of conditional deletion of *Dll1* in adult pancreatic β -cells

The overall islet morphology was analyzed by anti-insulin and anti-glucagon staining in 8-weeks old male β -D1 mice. In normal mouse islets, β -cells are present mainly in the center of the islets and represent with up to 80% the highest amount of islet cells (Figure 9). The α -cells are located in the periphery of the islets around the β -cells (a similar distribution is observed for δ -cells). The β -D1 islets were shaped according to this pattern, although some islets seemed to possess only a few GLUCAGON⁺ α -cells.

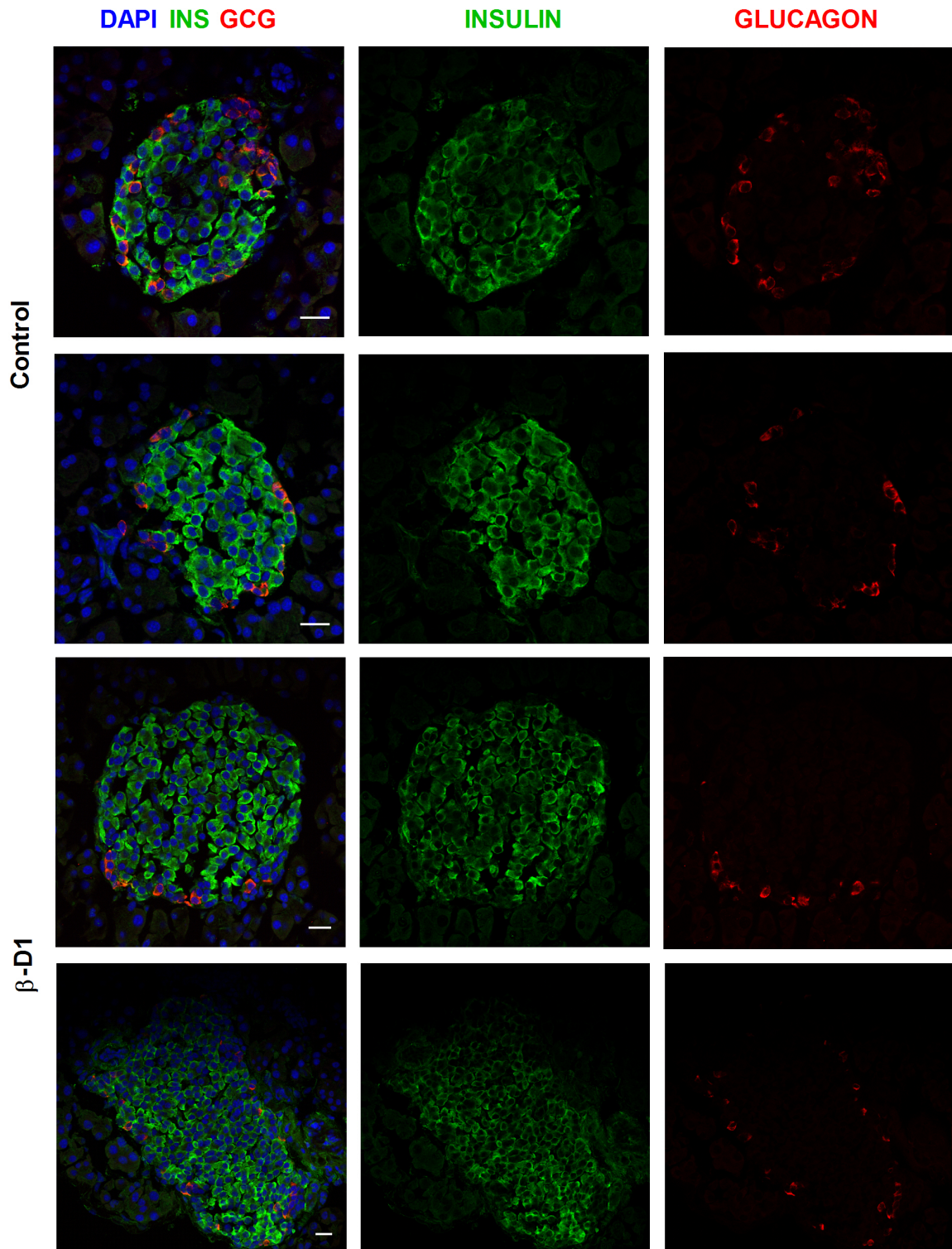


Figure 9: Immunohistochemical analysis of pancreata in 8-weeks old male β -D1 and *Cre*-positive control mice. Double staining of INSULIN (green) and GLUCAGON (red) was done on frozen pancreatic sections from 8-weeks old β -D1 (n=5) and control mice (n=5). Nuclei were counterstained with DAPI (blue). The scale bar represents 20 μ m.

To investigate this further, more than 100 islets from 5 β -D1 and control mice were stained to assess the amount of β - and α -cells per islets (Figure 10A). Indeed, the amount of GLUCAGON⁺ cells in β -D1 mice was found to be reduced to 15% compared to 25% in control mice, with a statistical significance of $p < 0.001$. In contrast, the amount of INSULIN⁺ cells was significantly ($p < 0.001$) increased to 80% compared to 70% in control mice. In addition, to whole islet hormone levels were measured using specific ELISAs for insulin and glucagon (Figure 10B). Interestingly, on the hormone level no significant differences between β -D1 and control mice were detected.

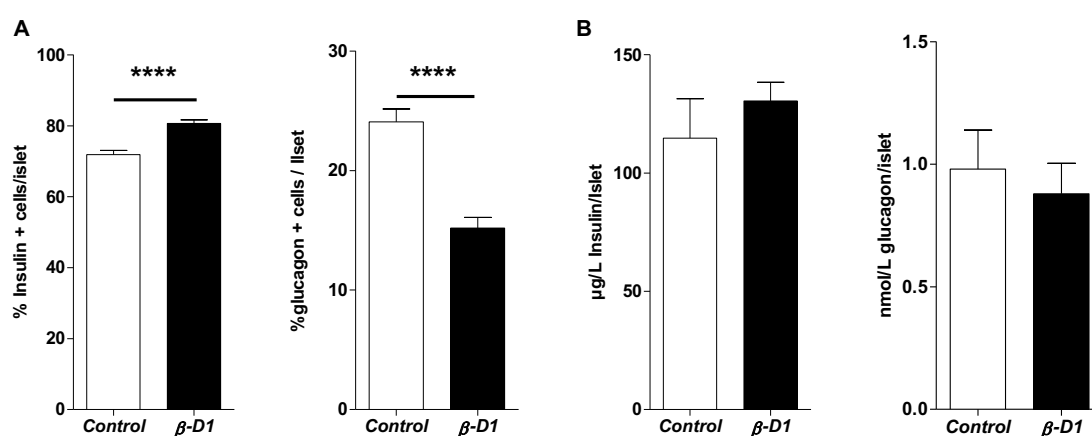


Figure 10: Islet hormone content in 8-weeks old male β -D1 and Cre-positive control mice

(A) Statistical evaluation of the amount of INSULIN⁺ and GLUCAGON⁺ cells per islet ($n=100$ -150 islets per genotype). **(B)** Average hormonal content for insulin and glucagon in isolated islets (Control $n=9$ mice, β -D1 $n=7$ mice). Data are shown as mean \pm SEM. Differences were considered statistically significant at * $p < 0.05$, ** $p < 0.01$, *** $p < 0.001$, **** $p < 0.0001$ using a 2-tailed heteroscedastic student's t-test.

To study the effects of the *Dll1* knockdown in β -cells, the gene expression levels of D/N-pathway components in isolated islets were measured (Figure 11A). As demonstrated above, *Dll1* itself was downregulated whereas the ligand genes *Dll4* as well *Jag1* were tendentially and *Jag2* were significantly upregulated compared to controls. Among the Notch receptors, only *Notch4* was slightly but not significantly upregulated in β -D1 islets. In addition, gene expressions of the insulin genes *Ins1* and *Ins2* as well as for glucagon (*Gcg*) were measured (Figure 11B). While the insulin genes were expressed normally in β -D1 islets, *Gcg* was significantly reduced compared to control islets.

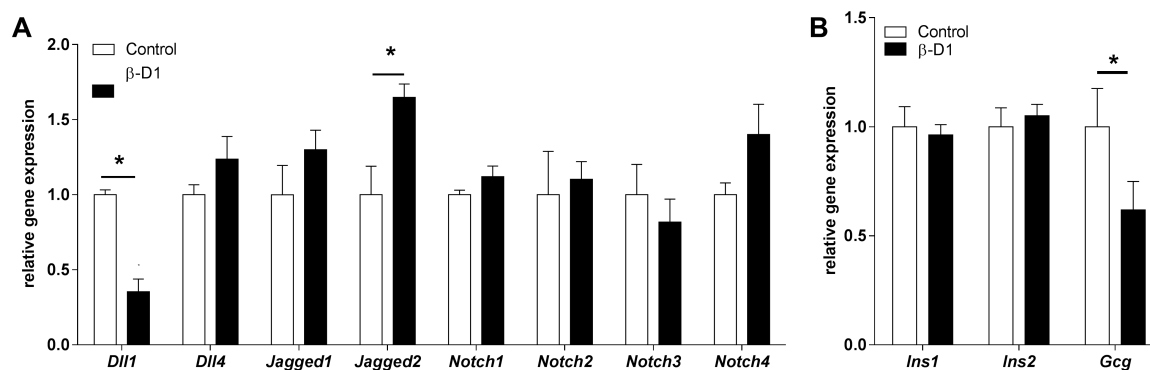


Figure 11: qRT-PCR analysis of mRNA in isolated islets from 8-weeks old male β -D1 and Cre-positive control mice.

Expression levels of (A) Delta-Notch pathway components and (B) *Ins1*, *Ins2* and *Gcg* in isolated islets from β -D1 and Cre-positive controls were assessed by qRT-PCR (n=6). Expression was normalized to the housekeeping genes *Sdha* and *Ubc*. Differences were considered statistically significant at $p < 0.05$ using a heteroscedastic two-tailed Student's t-test. Error bars display the SEM.

Despite slightly altered gene expression and islet morphology β -D1 mice developed normally, which allows to study the metabolic function of β -cells. Therefore, body weight and blood glucose levels were measured on a weekly basis, starting with weaning and feeding with tamoxifen chow for four weeks, until the age of 11 weeks. β -D1 mice developed normal body weight (Figure 12 A) but a mild hyperglycemia compared to control mice (Figure 12B). For example, 8-weeks old male β -D1 mice had averaged blood glucose levels of 160 mg/dL whereas control mice of the same age had only 120 mg/dL. Higher blood glucose levels are usually a sign for altered glucose tolerance. To test for this, mice were challenged in glucose tolerance tests (GTTs) after an overnight fasting period of 16 h (Figure 12 C, D). The mice were either injected intraperitoneally or fed by oral gavage with 2 g glucose per kg body weight. Blood-glucose levels were then measured after 5, 15, 30, 60 and 120 min. Indeed, β -D1 mice perform worse in intraperitoneal (ip) GTT than the control mice. Glucose clearance in β -D1 mice was significantly impaired already during the first phase of insulin secretion after 5 min, whereas the second phase seemed to be functional, because after 2 h the blood glucose levels of β -D1 mice were back to the basal glucose levels did not differ significantly from Cre-positive control mice (Figure 12C). Interestingly, not differences between β -D1 and Cre-positive mice were found during oral GTT (Figure 12D), suggesting a potential effect of the gastrointestinal tract to compensate for the impaired glucose tolerance.

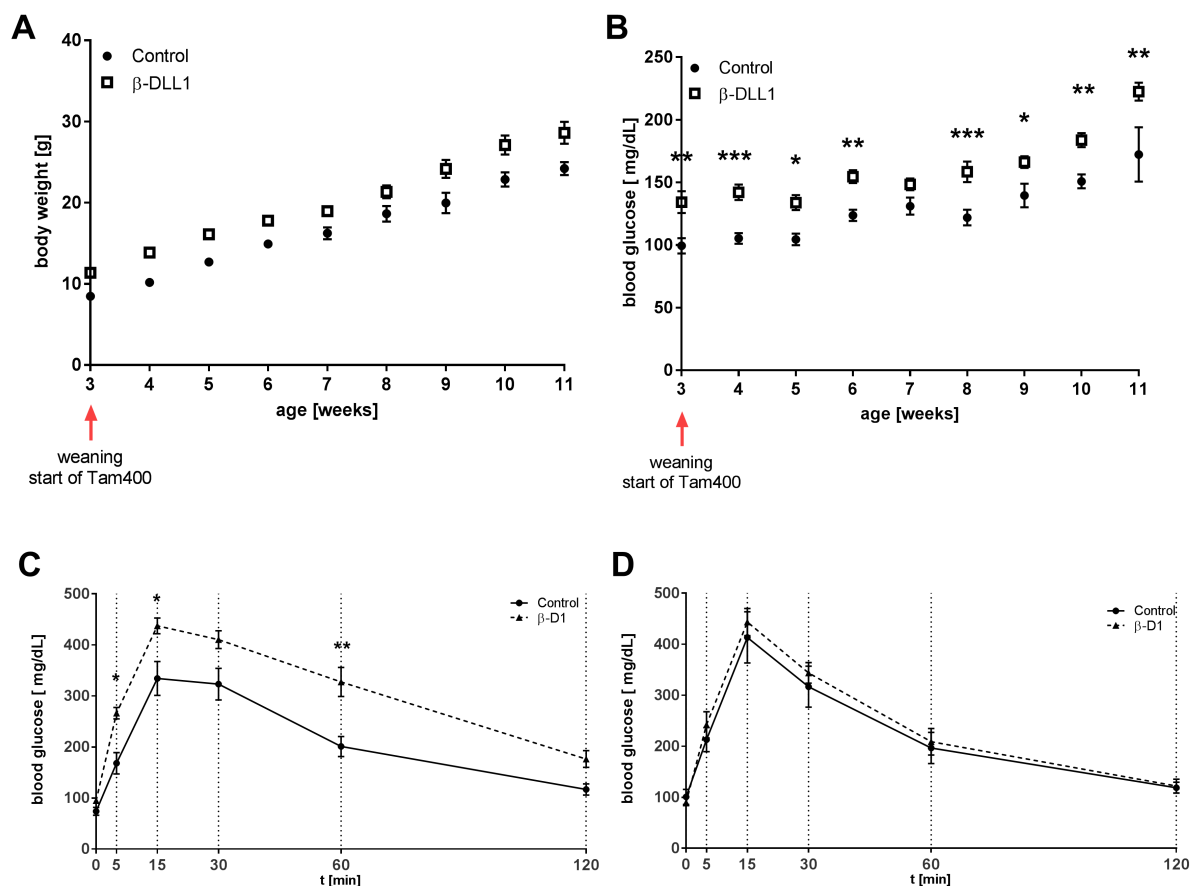


Figure 12: Metabolic phenotype of male β -D1 mice
Development of average body weight (A) and blood glucose levels (B) over time (control n=9, β -D1 n=11); (C) Intraperitoneal glucose tolerance test of 8-10-weeks old male mice (control n=26, β -D1 n=5); (D) Oral glucose tolerance test of 8-10-weeks old male mice (control n=4, β -D1 n=5). Data are shown as mean \pm SEM. Differences were considered statistically significant at * p <0.05, ** p <0.01, * p <0.001, **** p <0.0001 using 2-way ANOVA with Bonferroni's multiple comparison test.**

4.1.4. Effects of conditional deletion of *Dll4* in adult pancreatic β -cells

Likewise, β -D4 mice were analyzed. Although not different by eye (Figure 13), statistical analysis of INSULIN⁺ and GLUCAGON⁺ cells per islet revealed less GLUCAGON⁺ α -cells (20%) in β -D4 compared to *Cre*-positive control mice (Figure 14A). The amount of INSULIN⁺ β -cells was not different. A similar trend, although statistically not different, was measured for islet hormone levels *in vitro* (Figure 14B).

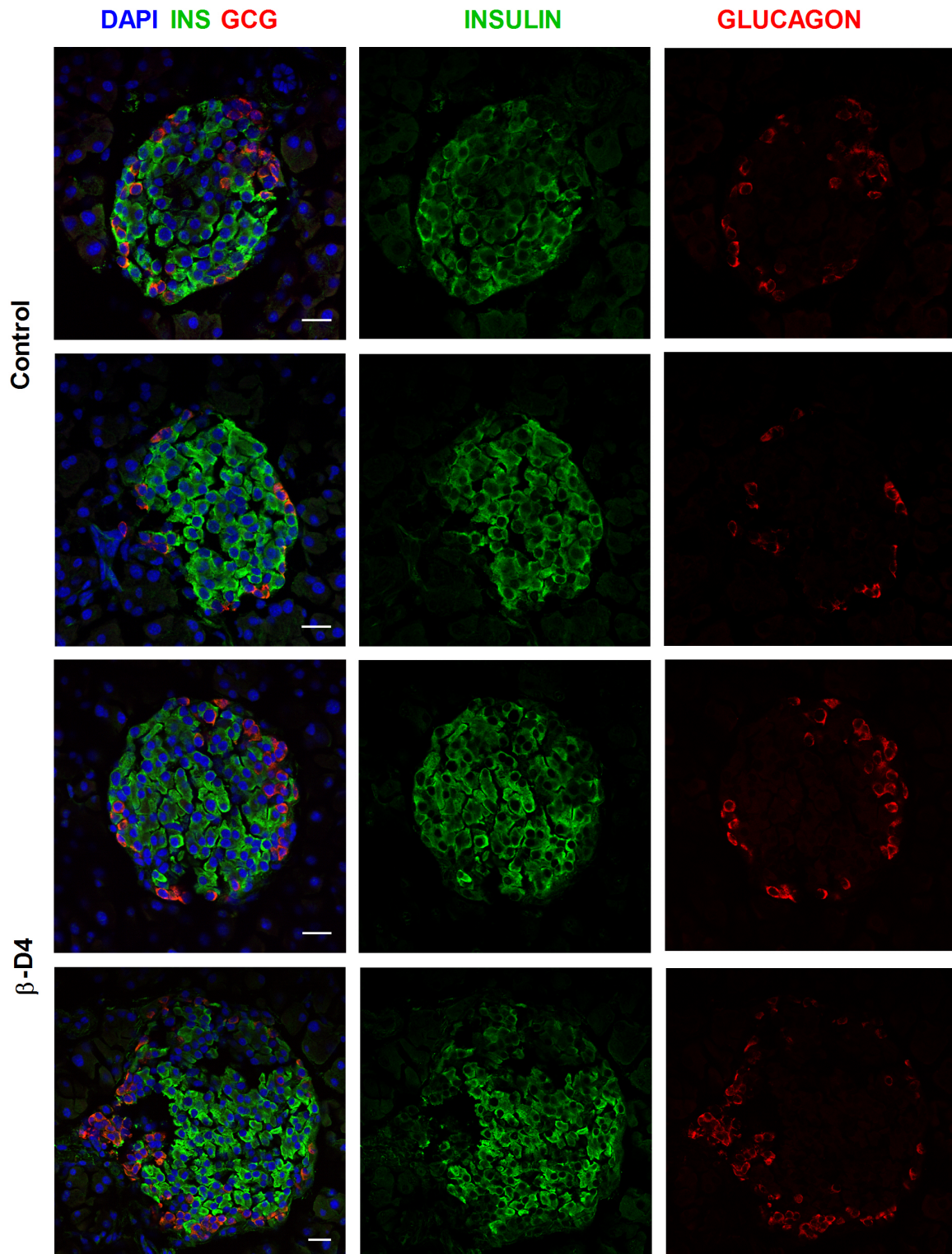


Figure 13: Immunohistochemical analysis of pancreata in 8-weeks old male β -D4 and *Cre*-positive control mice.

Double staining of INSULIN (green) and GLUCAGON (red) was done on frozen pancreatic sections from 8-weeks old β -D4 (n=5) and control mice (n=5). Nuclei were counterstained with DAPI (blue). The scale bars represent 20 μ m.

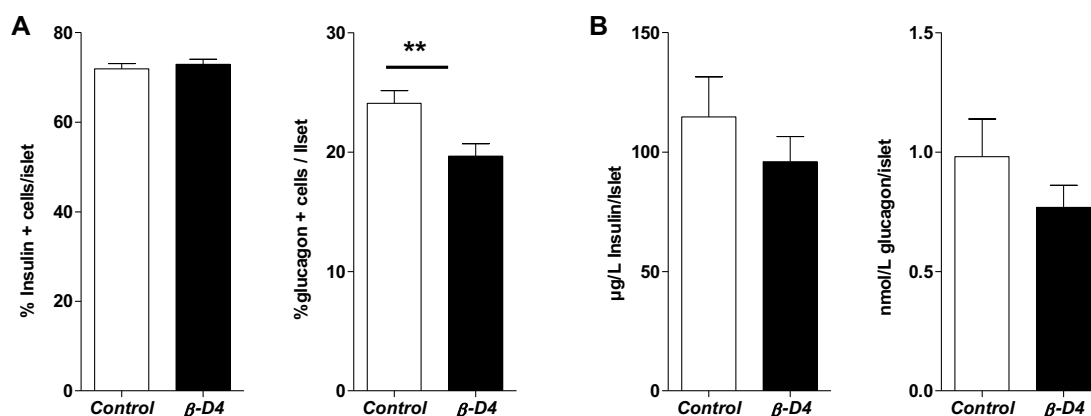


Figure 14: Islet hormone content in 8-weeks old male β -D4 mice

(A) Statistical evaluation of the amount of INSULIN⁺ and GLUCAGON⁺ cells per islet (n=100-150 islets per genotype). (B) Average hormonal content for insulin and glucagon in isolated islets (control n=9, β -D4 n=8). Data are shown as mean \pm SEM. Differences were considered statistically significant at *p<0.05, **p<0.01 using a 2-tailed heteroscedastic student's t-test.

In contrast, on the gene expression level glucagon was increased significantly 3-fold in β -D4 compared to control islets, whereas insulin gene expression was unaltered. No differences on the transcriptional level of Notch signaling components could be observed in any of the genes (except *Dll4* itself) (Figure 15).

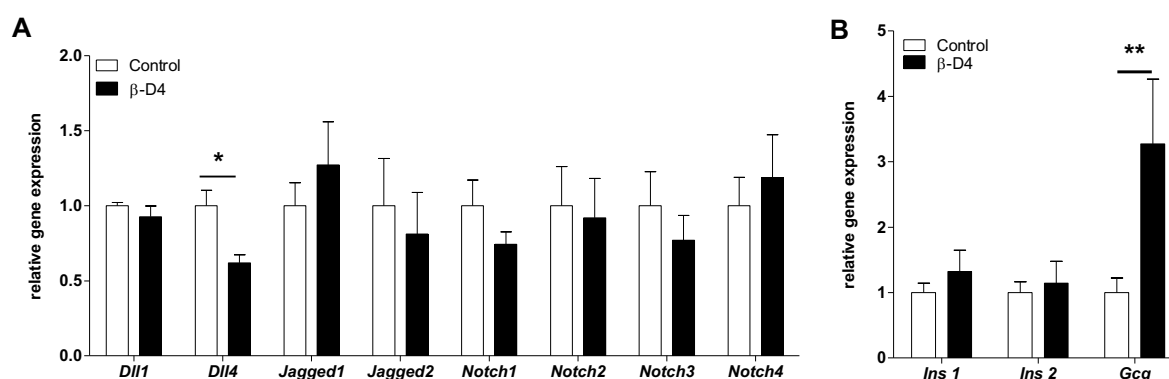


Figure 15: qRT-PCR analysis of isolated islets from 8-weeks old male β -D4 and Cre-positive control mice.

Expression levels of (A) Delta-Notch pathway components and (B) *Ins1*, *Ins2* and *Gcg* in isolated islets from β -D4 and Cre-positive controls were assessed by qRT-PCR (n=6 animals per genotype). Expression was normalized to the housekeeping genes *Sdha* and *Ubc*. Differences were considered statistically significant at p<0.05 using a heteroscedastic two-tailed Student's t-test (*<0.05, **<0.01, ***<0.001). Error bars display the SEM.

On a first sight, the metabolic phenotype of β -D4 mice was unaltered with body weights as well as blood glucose levels similar to control mice (Figure 16A, B). However, glucose challenge during ipGTT and oGTT revealed a much better performance of β -D4 compared to

control mice (Figure 16 C, D). As in β -D1 mice, although in the opposite direction, the first phase of insulin secretion seemed to be affected, since the glucose clearance was improved within 15 minutes after glucose application. Taken together, the data of the single knockdowns of either *Dll1* or *Dll4* suggest an opposed function of the two ligands in adult pancreatic β -cells.

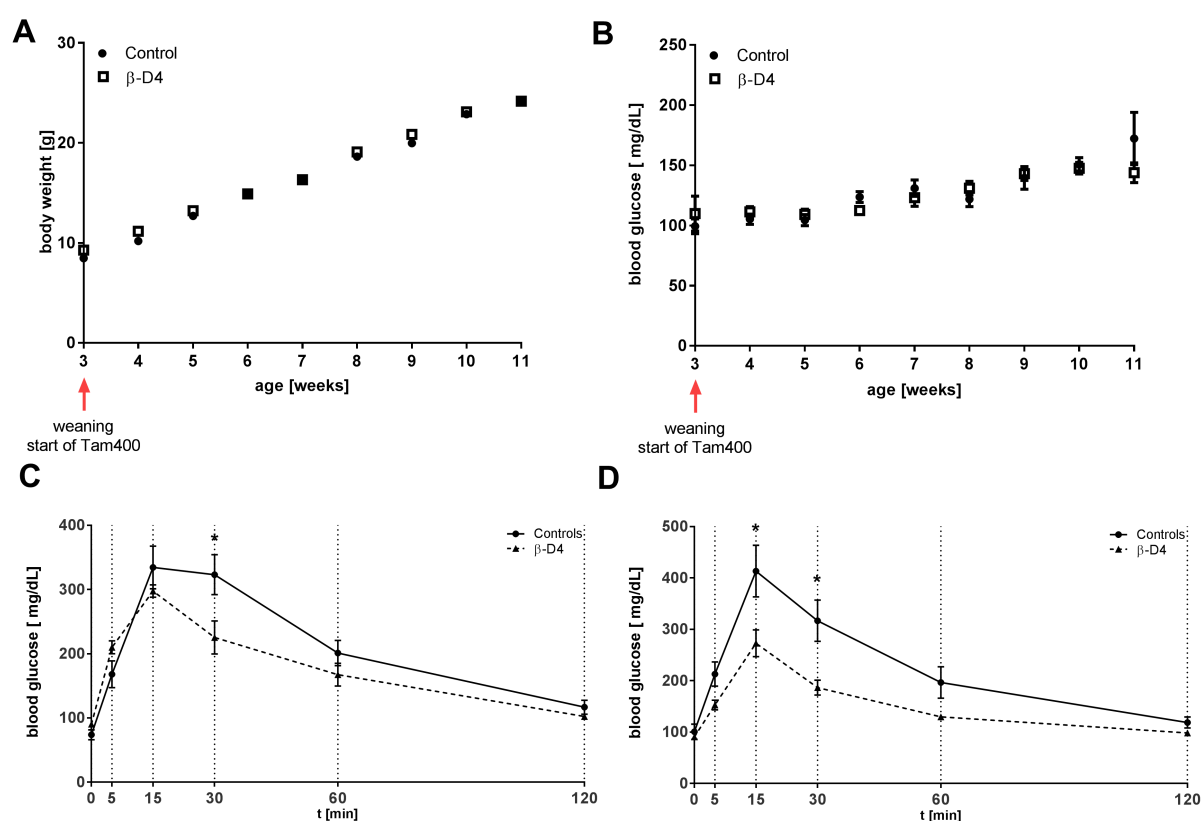


Figure 16: Metabolic phenotype of male β -D4 mice

Development of average body weight (A) and blood glucose levels (B) over time in male mice after weaning and tamoxifen feeding (control n=9, β -D4 n=7). Data were shown as mean \pm SEM. Differences were considered statistically significant at * p <0.05 using a 2-tailed heteroscedastic student's t-test.

(C) Intraperitoneal glucose tolerance test of 8-10-weeks old male mice (control n= 26, β -D4 n=5)

(D) Oral glucose tolerance test of 8-10-weeks old male mice (control n=4, β -D4 n=5)

Data are shown as mean \pm SEM. Differences were considered statistically significant at * p <0.05 using 2-way ANOVA with Bonferroni's multiple comparison test.

4.1.5. Conditional simultaneous deletion of *Dll1* and *Dll4* in adult pancreatic β -cells

There are hints that both genes can compensate each other. While single knock downs of *Dll1* or *Dll4* in intestine tissue did not lead to significant effects, because they are balancing each other, knock down both ligands in parallel resulted in the complete conversion of proliferating progenitors into postmitotic goblet cells (Pellegrinet et al. 2011). Considering these results, a β -cell specific *Dll1-Dll4* double knockdown mouse model (β -D1D4) was established in addition.

4.1.5.1. *Histological analysis of islet morphology*

As the single knockdown models β -D1D4 mice were analyzed for islet morphology (Figure 17). The mutant islets seemed to contain much more α -cells than the control islets, which were proven by statistical analysis (Figure 18). The amount of INSULIN⁺ cells was decreased to 60%, whereas the *in vitro* hormone level of insulin was unaltered. Strikingly, nearly 40% of β -D1D4 islet cell-types, compared to 25% in control islets, were GLUCAGON⁺ suggesting an α -cell identity. In fact, a higher number of α -cells was mirrored in hormone levels of islet extracts with a 2-fold increased glucagon level in β -D1D4 islets (Figure 18A, B).

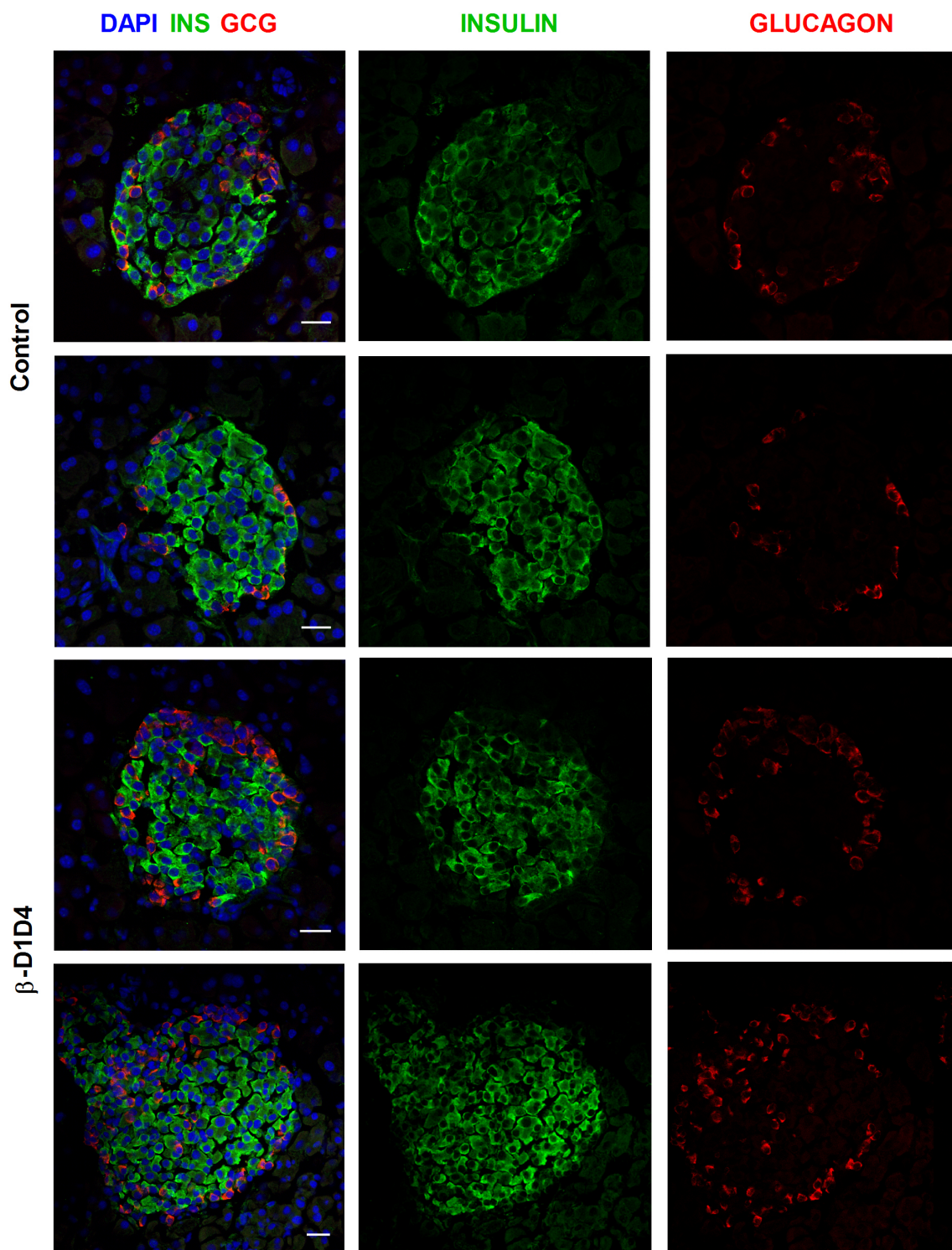


Figure 17: Immunohistochemical analysis of pancreata from 8-weeks old male β -D1D4 and *Cre*-positive control mice.

Double staining of INSULIN (green) and GLUCAGON (red) was done on frozen pancreatic sections from 8-weeks old β -D1D4 (n=5) and control mice (n=5). Nuclei were counterstained with DAPI (blue). The scale bars represent 20 μ m.

To analyze glucagon levels also *in vivo*, blood plasma was collected and the concentration of insulin and glucagon in plasma was measured and therewith the ability to have an effect in target tissues like brain and liver (Figure 18A, B). Consistent with the amount of islet cell types and islet extracts, the plasma levels of β -D1D4 mice showed an almost 2.5-fold increase in glucagon but normal insulin levels.

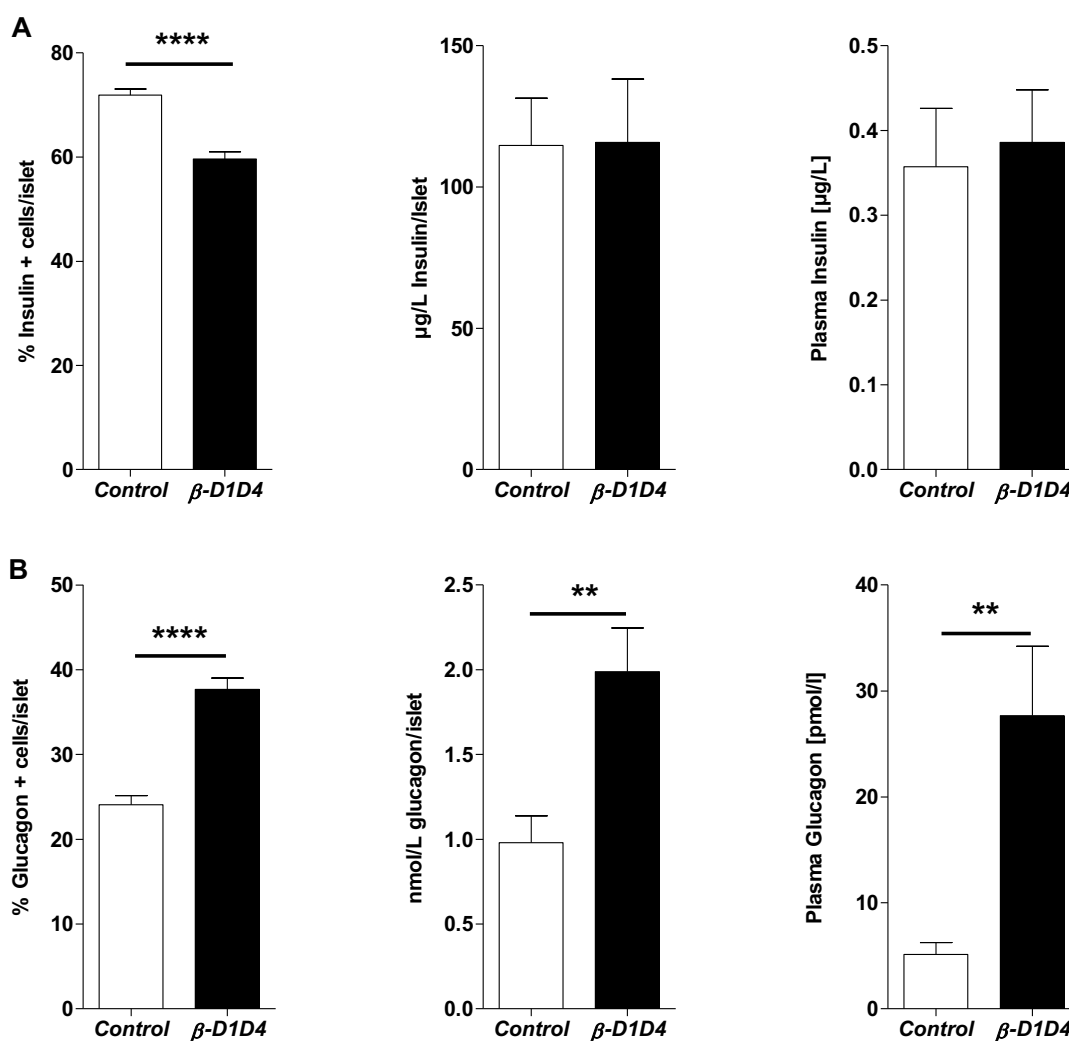


Figure 18: Islet hormone content in 8-weeks old male β -D1D4 and Cre-positive control mice.

Statistical evaluation of the amount of INSULIN+ (A) and GLUCAGON+ (B) cells per islet ($n=100-150$ islets per genotype) and average hormonal content for insulin (A) and glucagon (B) in isolated islets (control $n=9$, β -D1D4 $n=8$) and blood plasma (control $n=10$, β -D1D4 $n=9$). Data are shown as mean \pm SEM. Differences were considered statistically significant at * $p<0.05$, ** $p<0.01$, *** $p<0.001$, **** $p<0.0001$ using a 2-tailed heteroscedastic student's t-test.

The question was now, where the amount of glucagon producing α -cells was coming from. Since both genes were specifically deleted in β -cells, the "new" α -cells might have been

originated directly from original β -cells by transdifferentiation. Moreover, Delta-Notch signaling as a cell-cell communication transducer is known to stimulate neighboring cells through ligand receptor binding. To test these hypotheses, the “new” α -cells were examined for the expression of the β -cell marker PDX1, which triggers the *Cre* dependent deletion. Pancreatic sections were stained for GLUCAGON in green and PDX1 in red and checked for double positive cells with PDX1 in the nucleus and GLUCAGON in the cytoplasm (Figure 19A). However, no double positive cells were detected, but it has to be taken into account that the expression of PDX1 might have been vanished with a possible transdifferentiation process.

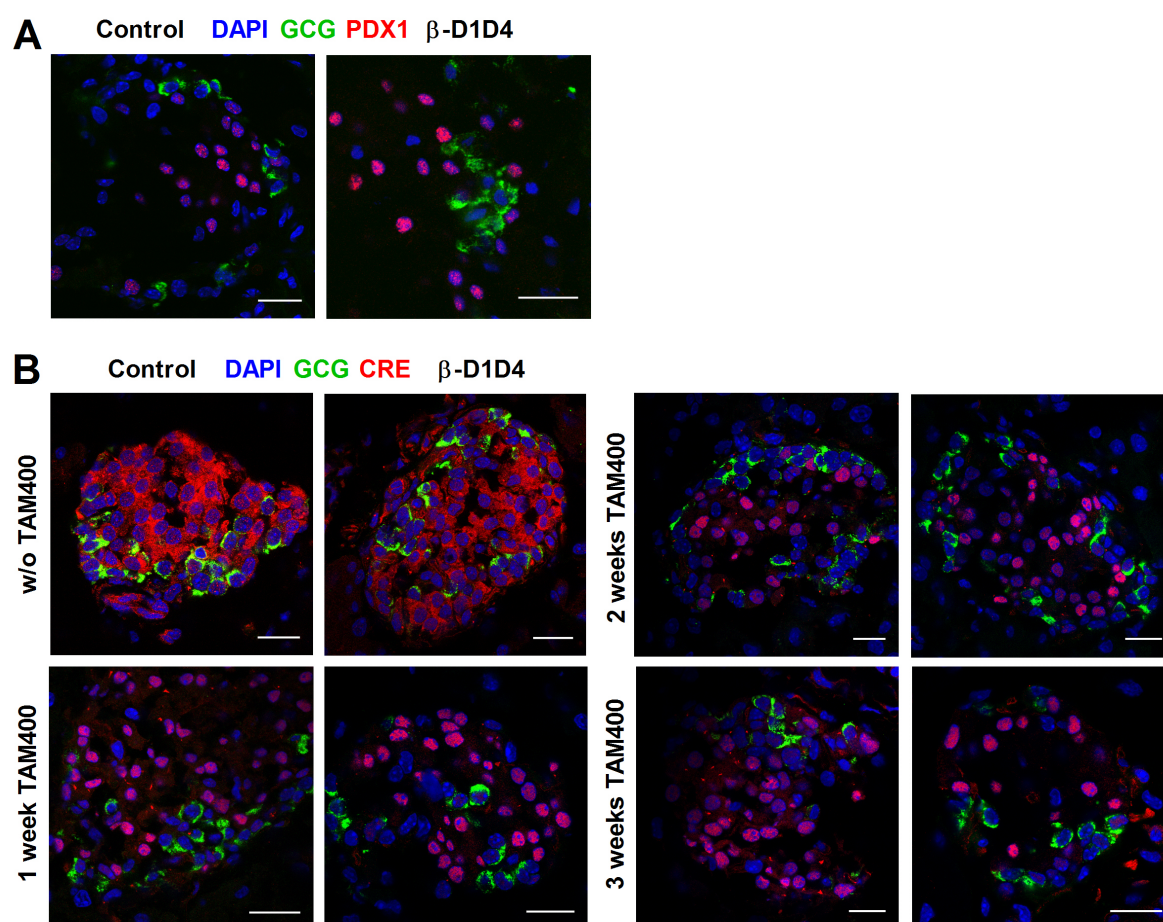


Figure 19: Immunohistochemical analysis for double positive cells in β -D1D4 and *Cre*-positive control islets. (A) Double staining for GLUCAGON (green) and PDX1 (red) was done on frozen pancreatic sections from 8-weeks old male β -D1D4 (n=5) and control mice (n=5). (B) Double staining for GLUCAGON (green) and CRE (red) of frozen pancreatic sections of male mice that were treated without or with tamoxifen for 1,2 and 3 weeks (n=5 each). Nuclei were counterstained with DAPI (blue). The scale bars represent 20 μ m.

Usually, the best way to trace single cells during a differentiation process is the usage of a specific lineage tracer (Kretzschmar et al. 2012). Unfortunately, this mouse line does not include a proper lineage tracer and crossbreeding with an appropriate mouse line would have

taken too long. In order to trace the cells, tissue specific expression of the CRE recombinase was analyzed on pancreatic sections from 3-, 4-, 5- and 6-weeks old mice. In none of the islets double positive cells with obvious CRE (in red) in the nuclei and GLUCAGON (green) in the cytoplasm were detected (Figure 19B).

However, there was still the possibility that the lack of ligands on β -cells affected the behavior of neighboring α -cells since Delta-Notch signaling is quite active on the site of cell cycle regulation (Nosedá et al. 2004, Georgia et al. 2006). Therefore, the glucagon-positive cells were counterstained with the proliferation marker Ki67 (Scholzen et al. 2000). More than 100 islets of β -D1D4 and controls were counted for double positive GLUCAGON⁺Ki67⁺ cells. Statistical analysis revealed that in β -D1D4 mice glucagon-positive cells showed a 3-fold higher proliferation rate than the respective cells in control islets (Figure 20).

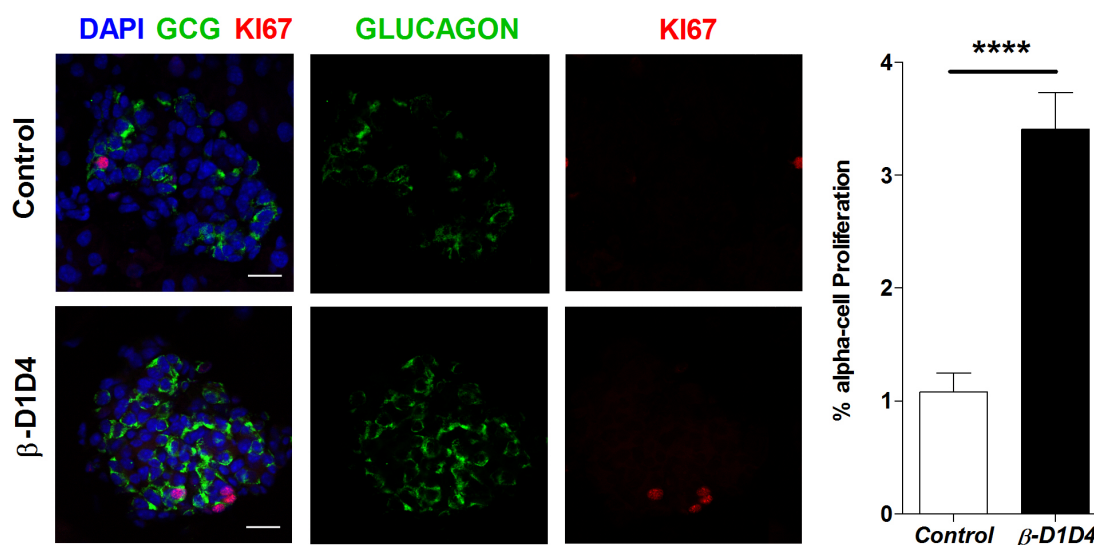


Figure 20: Immunohistochemical analysis for α -cell proliferation in β -D1D4 and Cre-positive control islets. Double staining for GLUCAGON (green) and KI67 (red) was done on pancreatic sections from 8-weeks old male β -D1D4 and control mice. Statistical quantification of GCG⁺/KI67⁺ double-positive cells (islets n=150-200). Data are shown as mean \pm SEM. Differences were considered statistically significant at * p <0.05, ** p <0.01, *** p <0.001, **** p <0.0001 using a 2-tailed heteroscedastic student's t-test. Nuclei were counterstained with DAPI (blue). The scale bars represent 20 μ m.

Therefore, increased proliferation triggered by the lack of DLL1 and DLL4 is more likely to be the reason for the increased α -cell number in β -D1D4 mice. This study showed already that the high amount of glucagon got secreted into the blood. However, this is no proof that the "new" α -cells are also mature. In order to analyze maturity of α -cells in β -D1D4 mice, the expression of MAFA (in β -cells) and MAFB (in α -cells) was analyzed (Artner et al. 2006, Hang

et al. 2011, Nishimura et al. 2015). The co-staining with INSULIN and MAFA (Figure 21A) as well as GLUCAGON and MAFB (Figure 21B) showed no difference in maturation of both β -D1D4 and control islets, suggesting normal maturity.

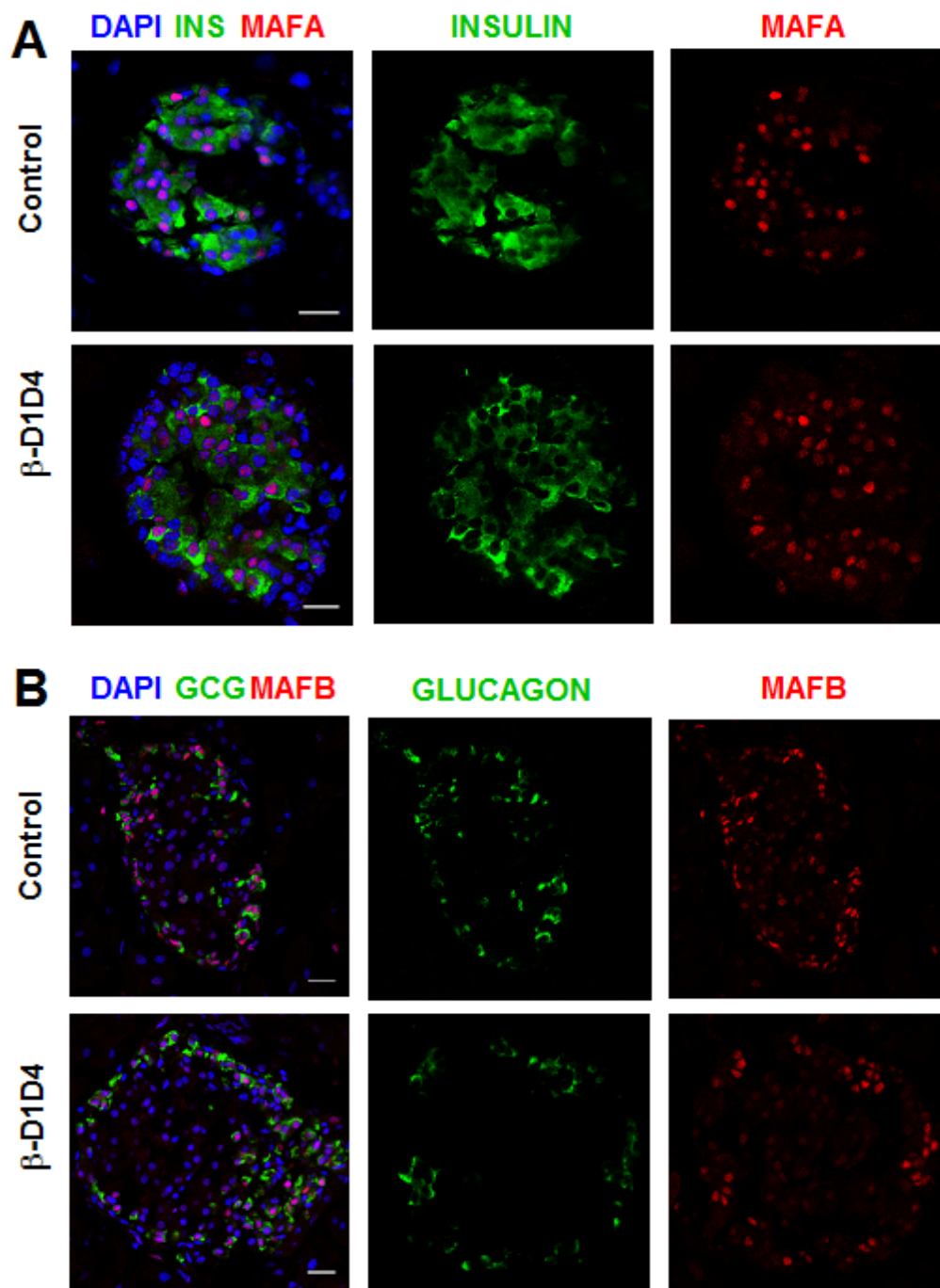


Figure 21: Immunohistochemical analysis of islet maturity in β -D1D4 and *Cre*-positive control mice. Immunostaining for MAFA (A) and MAFB (B) (red) together with INSULIN (A) and GLUCAGON (B) (green) as marker for β - and α -cells was done on pancreatic sections of 8-weeks old male β -D1D4 (n=5) and control mice (n=5). Nuclei were counterstained with DAPI (blue). The scale bars represent 20 μ m.

4.1.5.2. β -D1D4 mice have altered metabolic function *in vivo* and *in vitro*

As already observed in the single knockdowns, loss of Notch ligands in β -cells seemed to affect metabolic function in these mice, even without showing visible effects on islet morphology and gene expression. In β -D1D4, however, the islets showed a different morphology and glucagon levels were increased in islets and in blood plasma. Hyperglucagonemia in general results in hyperglycemia and reduced insulin secretion (Sherwin et al. 1976, Campbell et al. 2015). In contrast, the body weight of male and female β -D1D4 mice did not differ from control mice (Figure 22 A, B, C) and body composition with lean and fat mass was similar in these mice (Figure 22D).

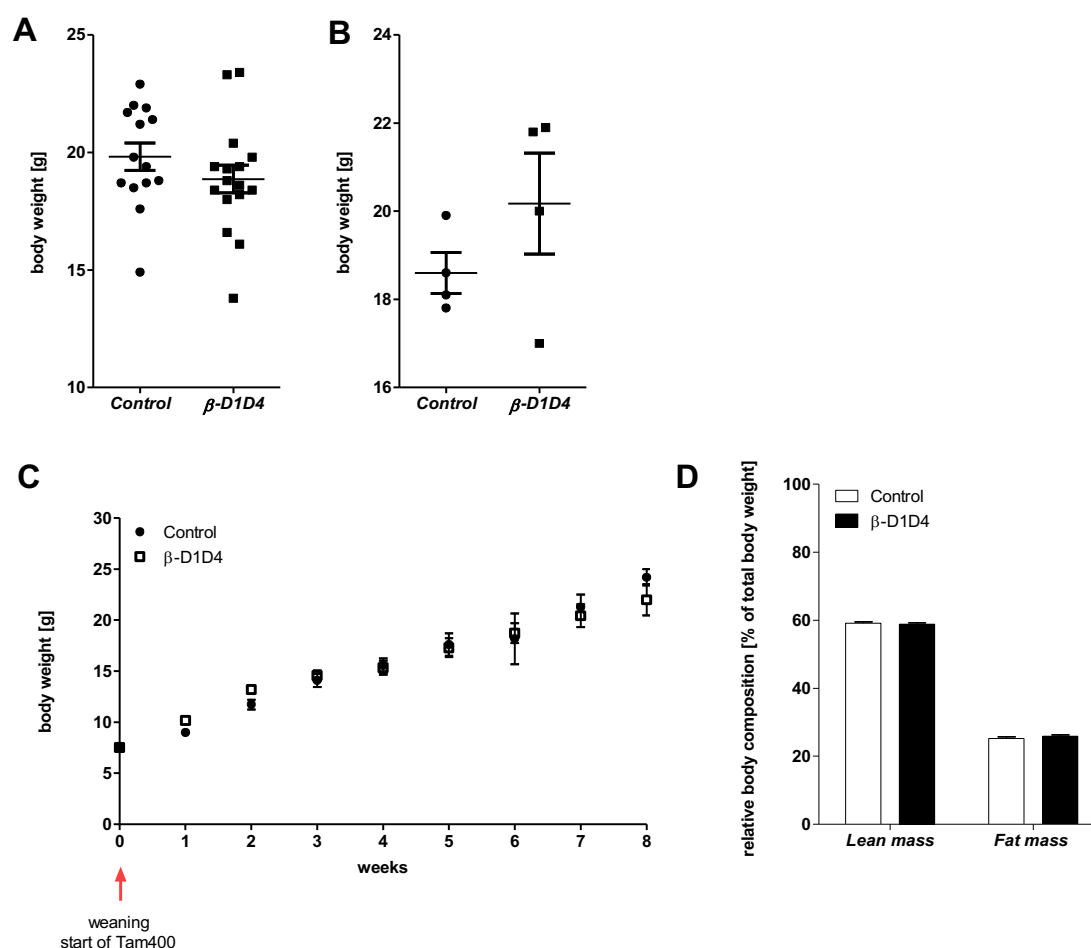


Figure 22: Body weight and composition of male β -D1D4 compared to *Cre*-positive control mice
 Average body weight of 8-weeks old *ad-libitum* fed male (A) and female (B) mice (males: control n=14, β -D1D4 n=16; females: control n=4, β -D1D4 n=4). Data are shown as mean \pm SEM. Differences were considered statistically significant at *p<0.05 using a 2-tailed heteroscedastic student's t-test. (C) Average body weight development of male mice after weaning and tamoxifen feeding (control n=9, β -D1D4 n=11). (D) NMR measurement for body composition of 8-weeks old males (control n=10, β -D1D4 n=11). Data are shown as mean \pm SEM. Differences were considered statistically significant at *p<0.05 using 2-way ANOVA with Bonferroni's multiple comparison test.

Interestingly, despite hyperglucagonemia β -D1D4 mice developed strong hypoglycemia three weeks after weaning and tamoxifen treatment (Figure 23). Some individual mice even displayed blood glucose levels close to 50 mg/dL and therefore might have neurogenic and cognitive impairments (Cryer et al. 2003).

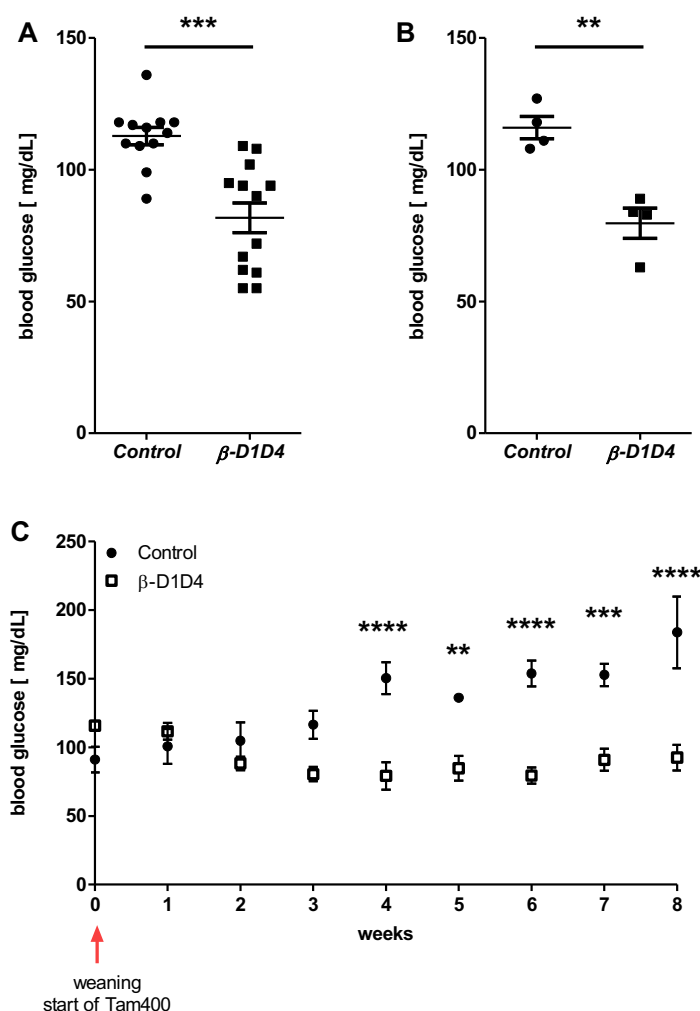


Figure 23: Blood glucose levels of male β -D1D4 compared to *Cre*-positive control mice
 Average blood glucose levels of 8-weeks old *ad-libitum* fed male (A) and female (B) mice (males: control n=14, β -D1D4 n=16; females: control n=4, β -D1D4 n=4). Data are shown as mean \pm SEM. Differences were considered statistically significant at *p<0.05, **p<0.01, ***p<0.001 using a 2-tailed heteroscedastic student's t-test. (C) Average blood glucose levels of *ad-libitum* fed male mice after weaning and tamoxifen feeding (control n=9, β -D1D4 n=11). Data are shown as mean \pm SEM. Differences were considered statistically significant at *p<0.05, **p<0.01, ***p<0.001, ****p<0.0001 using 2-way ANOVA with Bonferroni's multiple comparison test.

To further investigate the metabolic phenotype, an ipGTT and an oGTT were performed (Figure 24A, B).

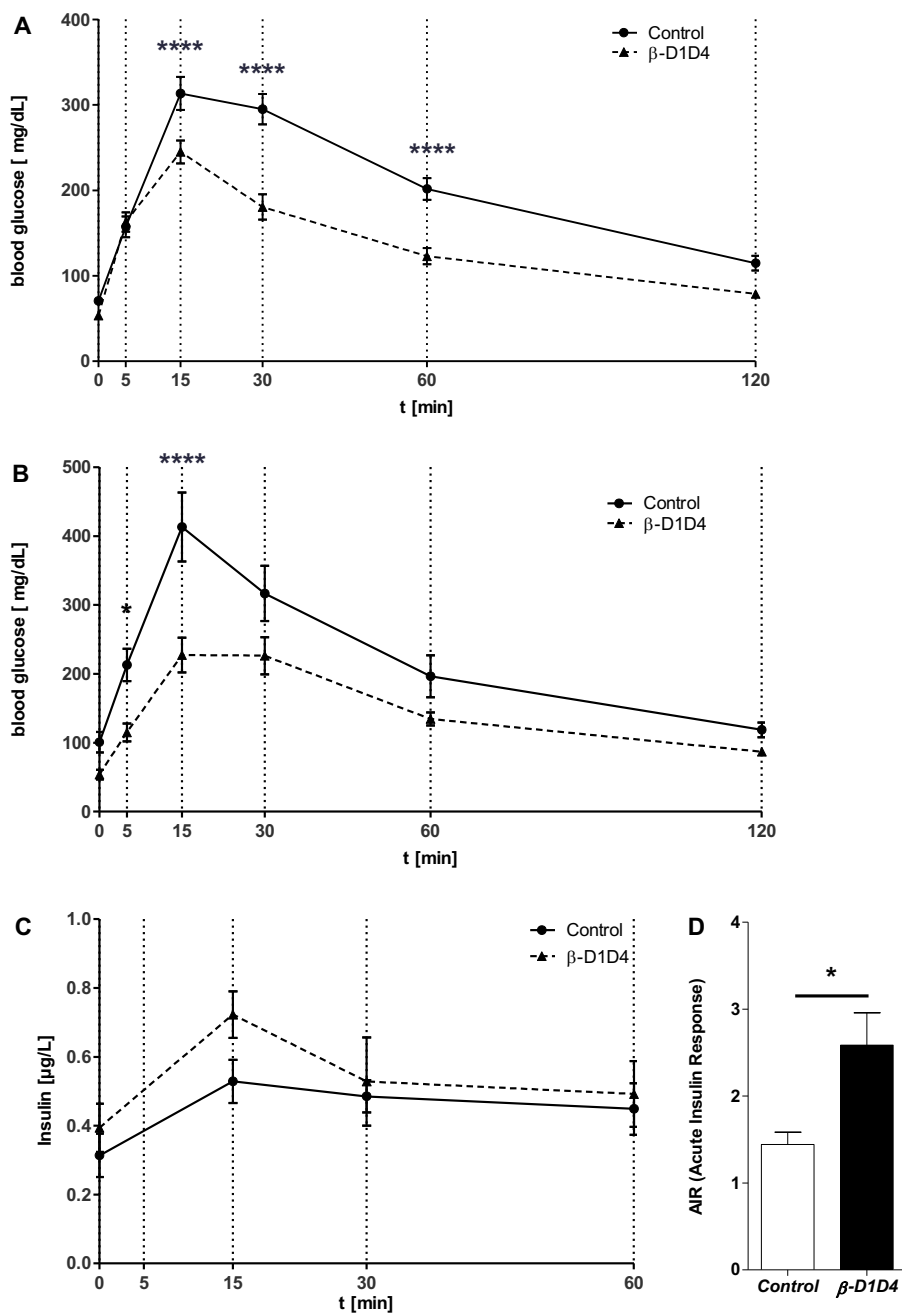


Figure 24: Glucose homeostasis in male β -D1D4 mice

(A) Intra-peritoneal glucose tolerance test of 8-10-weeks old male mice (control n=26, β -D1D4 n=27). (B) Oral glucose tolerance test of 8-10-weeks old male mice (control n=4, β -D1D4 n=6). (C) Blood plasma insulin levels during ipGTT (control n=13, β -D1D4 n=14). Data are shown as mean \pm SEM. Differences were considered statistically significant at * p <0.05, ** p <0.01, *** p <0.001, **** p <0.0001 using 2-way ANOVA with Bonferroni's multiple comparison test. (F) Acute insulin response during ipGTT between t=0 min and t=15 min (control n=5, β -D1D4 n=5; different cohort compared to ipGTT). Data are shown as mean \pm SEM. Differences were considered statistically significant at * p <0.05 using a 2-tailed heteroscedastic student's t-test.

Both tests showed a highly improved glucose clearance for β -D1D4 mice in the first phase. Interestingly, the oGTT showed also a small difference at 5 min. In addition, it seemed that also the second-phase response was slightly impaired compared to the ipGTT, since the slope remained equal between 15 min and 30 min. In control mice, the slope was strongly decreasing during oGTT. To analyze secreted insulin levels using a specific insulin ELISA (see 3.2.4.5.1) plasma samples were collected during ipGTT (Figure 24C). The analysis of non-hemolytic samples showed increased insulin secretion after 15 min in β -D1D4 mice compared to control mice. However, 2-way ANOVA analysis for the whole experiment did not result in statistical significance. Considering the acute insulin response (AIR) between time points 0 min and 15 min, insulin secretion was 2-fold higher and statistical significant using student's t-test and therefore suggesting increased insulin secretion in mutant mice (Figure 24D). As mentioned before, hypoglycemia could lead to impaired brain function (Cryer et al. 2003). In addition, it was reported that weak LacZ expression driven by the Pdx1-CreERT mouse line used in this thesis was detected in hypothalamic regions (Cryer et al. 2003, Wicksteed et al. 2010). Therefore, gene expression of *Pdx1*, *Cre recombinase* as well as *Dll1* and *Dll4* was measured in hypothalamus tissue from β -D1D4 and control mice (Supplementary Figure 3). Even none of these genes were altered, it is still possible that the observed metabolic effects in β -D1D4 mice were influenced by the hypothalamus, which is one of the controlling brain regions for glucose sensing and insulin secretion (Obici et al. 2002, Ogunnowo-Bada et al. 2014). To circumvent such an interference, pancreatic islets were isolated from β -D1D4 and *Cre*-positive control mice and analyzed in a glucose-stimulated insulin secretion (GSIS) assay (see 3.2.2.2.). In addition to low and high glucose concentrations (2.8 mM and 16.7 mM, respectively), Forskolin, a potent adenylyl cyclase stimulant, was used (Wiedenkeller et al. 1983). Consistent with the *in vivo* GTT data, β -D1D4 islets secreted *in vitro* significantly more insulin after stimulation with high glucose and Forskolin (Figure 25).

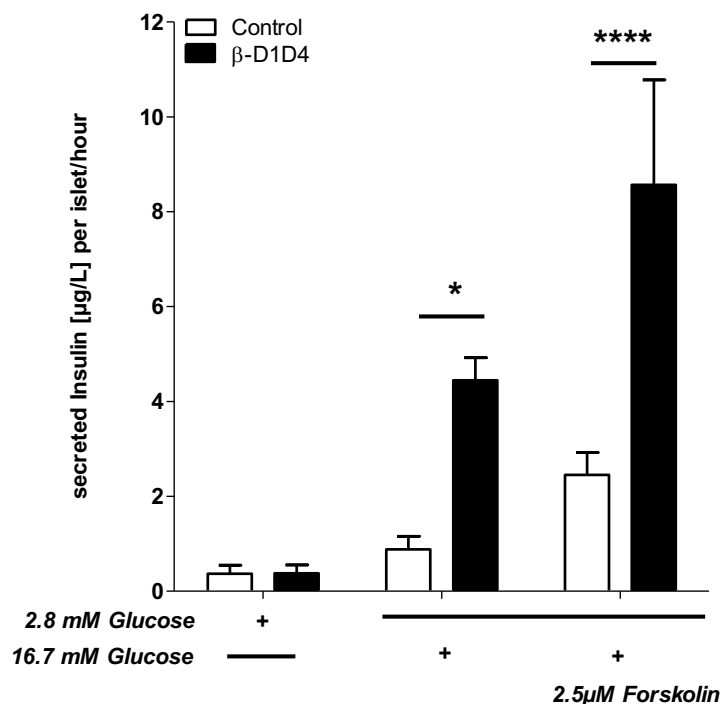


Figure 25: Glucose stimulated insulin secretion of β -D1D4 and *Cre*-positive control islets

Isolated islets from 8-weeks old male β -D1D4 and control mice were incubated with low glucose (2.8 mM) and high glucose (16.7 mM). In addition, islets were stimulated with 2.5 μ M Forskolin under high-glucose condition (β -D1D4 n=4, control n=6). Data are shown as mean \pm SEM. Differences were considered statistically significant at * p <0.05, ** p <0.01, *** p <0.001, **** p <0.0001 using a 2-tailed heteroscedastic student's t-test.

Hypothalamic activity affects not only glucose uptake and insulin secretion, it also controls hunger feeling by binding the hormone leptin to its receptors (Proulx et al. 2002, Sohn 2015). Changes in the hypothalamus can therefore also result in altered appetite and different food intake. Moreover, high glucagon levels also induce appetite and consequently higher food intake (Schulman et al. 1957, Grossman 1986). Therefore, the individual food intake per mouse was measured twice a day after the inactive (8:00-17:00) and active phases (17:00-08:00) in β -D1D4 and *Cre*-positive control mice. Figure 26 shows the food intake for both phases and the total amount per day as raw values (A) and corrected for individual body weight (B) for each mouse. In both cases β -D1D4 mice consumed more food during the active phase than *Cre*-positive control animals. Also, the total food intake per day was higher in β -D1D4 mice, suggesting higher energy consumption but normal circadian rhythm.

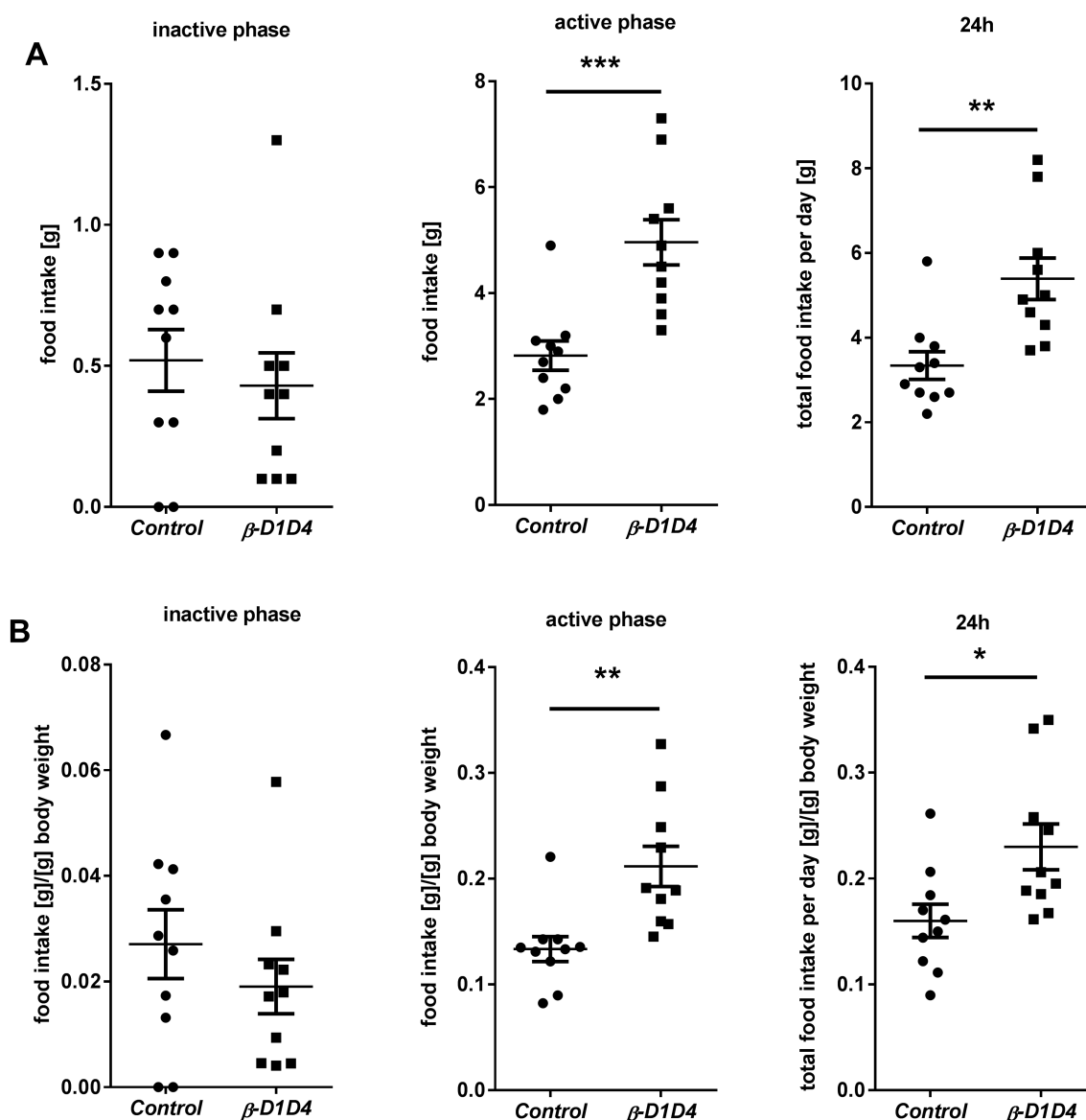


Figure 26: Individual daily food intake of β -D1D4 and Cre-positive control mice

(A) Total food intake and (B) food intake based on the individual body weight during the inactive phase, active phase and 24h of 8-weeks old male mice (control n=10, β -D1D4 n=10). Data are shown as mean \pm SEM. Differences were considered statistically significant at * p <0.05, ** p <0.01, *** p <0.001, **** p <0.0001 using a 2-tailed heteroscedastic student's t-test

4.1.5.3. Expression analysis with whole genome transcriptomics

To investigate the underlying mechanism of the β -D1D4 phenotype in pancreatic islets, gene expression levels of Delta-Notch pathway members were analyzed (Figure 27A). The receptor genes *Notch1*, *Notch2* and *Notch4* were significantly upregulated more than 1.5-fold in β -D1D4 islets. Moreover, *Jagged1* was upregulated almost 1.5-fold. In contrast, *Notch3* and *Jagged2* remained at similar expression levels compared to controls.

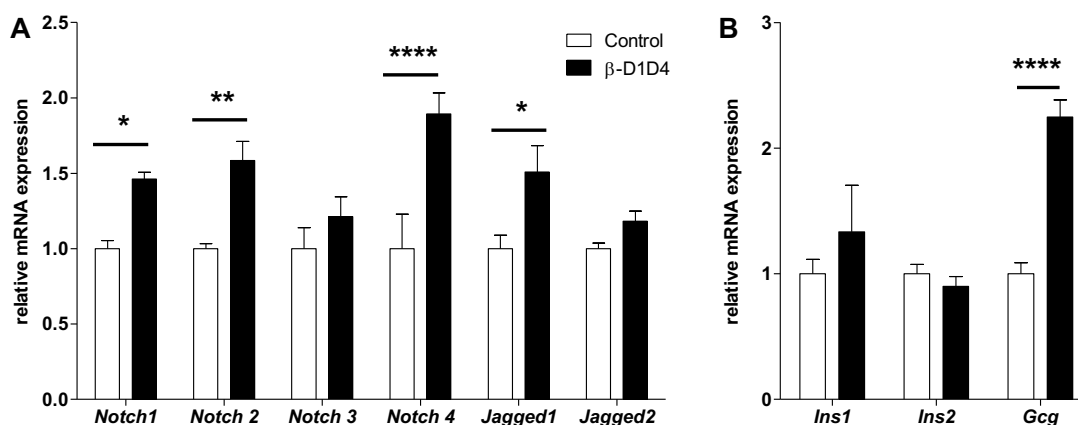


Figure 27: qRT-PCR analysis of isolated islets from 8-weeks old β -D1D4 and *Cre*-positive control mice. Expression levels of (A) Delta-Notch components and (B) *Ins1*, *Ins2* and *Gcg* in isolated islets from β -D1D4 and *Cre*-positive controls were assessed by qRT-PCR (n=6). Expression was normalized to the housekeeping genes *Sdha* and *Ubc*. Differences were considered statistically significant at $p < 0.05$ using a heteroscedastic two-tailed Student's t-test (* <0.05 , ** <0.01 , *** <0.001). Error bars display the SEM.

As expected, the mRNA level of *glucagon* was up to 3-fold increased in β -D1D4 islets (Figure 27B). Interestingly, expression of the insulin genes *Ins1* and *Ins2* remained normal although the insulin secretion was affected physiologically.

To get a broader insight into the changed physiological function of islets and the responsible genes, whole genome transcriptomics was performed by Dr. Martin Irmeler (see 3.2.4.4.). For each genotype, eight different samples of islet RNA were used. Only samples with a high quality and a RIN value above 7 were used. Regulated genes in β -D1D4 islets were filtered for a fold change (FC) of at least 1.3, a false discover range (FDR) of $<10\%$ and a p-value less than $p < 0.01$ compared to *Cre*-positive control samples. In total, 257 genes fulfilled these requirements, from which 107 genes were up- and 150 genes were downregulated in β -D1D4 compared to control islets (Supplementary Table 1). The altered genes were sorted and evaluated regarding overrepresented diseases and signaling pathways by GeneRanker analysis.

Consistent with the obtained *in vivo* and *in vitro* data, downregulated genes were overrepresented for diseases and related symptoms such as hyperglycemia, diabetic nephropathy, noninsulin dependent diabetes mellitus, metabolic diseases, obesity and impaired glucose tolerance (Table 17). Especially interesting were genes like *Ucn3*, *Slc2a2* (*Glut2*), *Gcgr* and *Glp1r*, since they all are known to be associated with altered insulin

secretion and islet function (Gelling et al. 2003, Li et al. 2007, Gelling et al. 2009, Meloni et al. 2013, Thorens 2015). The differential regulation of some of these genes was confirmed by qRT-PCR (Figure 28A).

Table 17: Overrepresented downregulated diseases

Disease	P-value	List of observed genes
HYPERGLYCEMIA	1,48E-04	<i>Slco2a1, Ucn3, Mlxipl, Cpb2, Gcgr, Fn3k, Glo1, Glp1r</i>
DIABETIC NEPHROPATHY	3,09E-04	<i>Mlxipl, Cpb2, Fn3k, Adora2b, Col8a1, Npnt, Glo1, Glp1r</i>
NONINSULIN DEPENDENT DIABETES MELLITUS	7,10E-04	<i>Negr1, Insig1, Mlxipl, Cpb2, Gcgr, Kcnk16, Pdk2, Grk5, Glo1, Glp1r</i>
METABOLIC DISEASES	2,99E-03	<i>Mlxipl, Cers6, Bckdhb, Dll4, Gstk1, Pomgnt2, Glp1r</i>
OBESITY	6,77E-03	<i>Negr1, Insig1, Ucn3, Mlxipl, Gcgr, Cers6, Epm2aip1, Gstk1, Glp1r</i>
IMPAIRED GLUCOSE TOLERANCE	8,64E-03	<i>Mlxipl, Cpb2, Gcgr, Cers6, Glp1r</i>

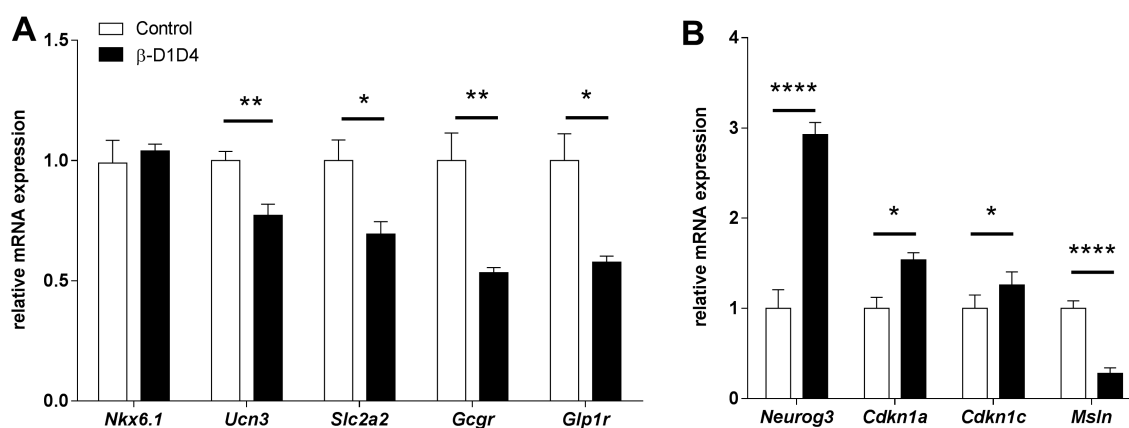


Figure 28: qRT-PCR analysis of insulin-secretion and cell-cycle marker genes in isolated islets from 8-weeks old male β -D1D4 and *Cre*-positive control mice.

Expression levels of (A) *Nkx6.1*, *Ucn3*, *Glut2*, *Gcgr* and *Glp1r* and (B) *Neurog3*, *Cdkn1a*, *Cdkn1c* and *Msln* in isolated islets from β -D1D4 and *Cre*-positive controls were assessed by qRT-PCR (n=6). Expression was normalized to the housekeeping genes *Sdha* and *Ubc*. Differences were considered statistically significant at $p < 0.05$ using a heteroscedastic two-tailed student's t-test (* <0.05 , ** <0.01 , *** <0.001 , **** <0.0001). Error bars display SEM.

On the other hand, genes upregulated in β -D1D4 islets are known to be involved in pancreatic cancer, impaired glucose tolerance, growth arrest and atypical hyperplasia (Table 18). The latter fits with the increased α -cell hyperplasia and proliferation rate of these cells.

Table 18: Overrepresented up regulated diseases

Disease	P-value	List of observed genes
PANCREATIC DUCTAL ADENOCARCINOMA	9,82E-05	<i>Gdf15, Ube2c, Cd24a, Dclk1, Spp1, Lmo4, Ezh</i>
IMPAIRED GLUCOSE TOLERANCE	1,77E-03	<i>Trib3, Cox6a2, Nnt, Gm6484, Neurog3</i>
GROWTH ARREST	2,74E-03	<i>Ddit3, Dclk1, Ppp1r15a, Gadd45b, Mfge8, Elk3, Plp2</i>
RESECTABLE PANCREATIC CANCER	5,20E-03	<i>Gdf15, Cd24a</i>
ATYPICAL HYPERPLASIA	5,34E-03	<i>Ube2c, Efemp1, Ezh</i>

Aside from GeneRanker analysis, significantly higher gene expression levels in β -D1D4 islets were proved for the cell-cycle inhibitor genes *Cdkn1a* and *Cdkn1c* (Figure 28B). Furthermore, the gene with the strongest down regulation in β -D1D4 islets was the tumor marker *Mesothelin (Msln)*.

Emphasis was also given to the upregulation of *Neurog3*, which was confirmed by qRT-PCR (Figure 28B). During embryonic development NEUROG3 is expressed downstream of Delta-Notch signaling in endocrine precursor cells (Gradwohl et al. 2000, Dror et al. 2007). However, on the protein level NEUROG3 could not be detected due to the lack of a working antibody.

GeneRanker analysis was additionally used to detect overrepresented signaling pathways (Table 19). Most significantly regulated was protein kinase A (PKA), followed by Nf κ B, matrix metalloprotease, parathyroid hormone, nuclear receptor subfamily 4, eTIF2 and the advanced glycosylation end product specific receptor.

Table 19: Overrepresented signaling pathways up & down

Pathway	P-value	List of observed genes
PROTEIN KINASE A	6,96E-04	<i>Slco2a1, Ezh, Fbp2, Pdyn, Adora2b, Ropn1, Scara3, Ptger3, Aqp4, Kcnj12, Tnnc1, Th, Gcgr, Nr4a2, Mtr, Clec2d, Adm2, Fkbp1b, Camk1, Sox9, Prkar2b, Glp1r, Mgst1</i>
NF KAPPA B	1,13E-03	<i>Cd24a, Esm1, Nod1, Tnfrsf12a, Nme4, Cttnal1, Tnf, Trim9, Spp1, Ifih1, Trib3, Nmb, Rgn, Adm2, S100a8, Pigr, Adgre1, Eda2r, Npnt, Glo1, Pebp1, Gadd45b</i>

MATRIX METALLOPROTEINASE	2,06E-03	<i>Cnn2, Jam2, Msln, Fbln5, Tnf, Adora2b, Mmp14, Efemp1, Aqp4, Spp1, Anpep, Nmb, Mmp24, Lgi1</i>
PARATHYROID HORMONE	6,04E-03	<i>Ezr, Nfil3, Mmp14, Rgn, Nr4a2, Glp1r</i>
NUCLEAR RECEPTOR SUBFAMILY 4, GROUP A, MEMBER 2	8,97E-03	<i>Nfil3, Ret, Th, Nr4a2</i>
EUKARYOTIC TRANSLATION INITIATION FACTOR 2 ALPHA KINASE 3, (PRKR LIKE ENDOPLASMIC RETICULUM KINASE)	9,78E-03	<i>Ppp1r15a, Insig1, Slc2a2, Ddit3</i>
ADVANCED GLYCOSYLATION END PRODUCT SPECIFIC RECEPTOR (AGER)	9,78E-03	<i>Mmp14, Spp1, S100a8, Glo1</i>

4.2. Overexpression of DLL1ICD in pancreatic β -cells

The double knockdown of *Dll1* and *Dll4* in adult β -cells induced strong effects in particular regarding insulin secretion. This is interesting and might hint to an intracellular function of the ligands but also to a role in cell-cell communication between β -cells. To get a deeper insight, a mouse model (generated by former PhD student Daniel Grading) was analyzed that overexpresses the intracellular domain of Delta-like 1 (DICD) in an inducible manner specifically in adult β -cells under the control of Pdx1-CreERT. Using this model should enable to study intracellular effects of the DLL1 ligand without influencing directly extracellular cell-cell communication.

4.2.1. Metabolic physiology

Adult male β -DICD mice at the age of eight weeks significantly displayed lower body weight and increased blood glucose levels (Figure 29), whereas female mice showed normal blood glucose levels compared to *Cre*-positive controls. This finding suggested also for the β -DICD mouse model an altered metabolic function, which was confirmed by ipGTT and oGTT measurements (Figure 30 A, C).

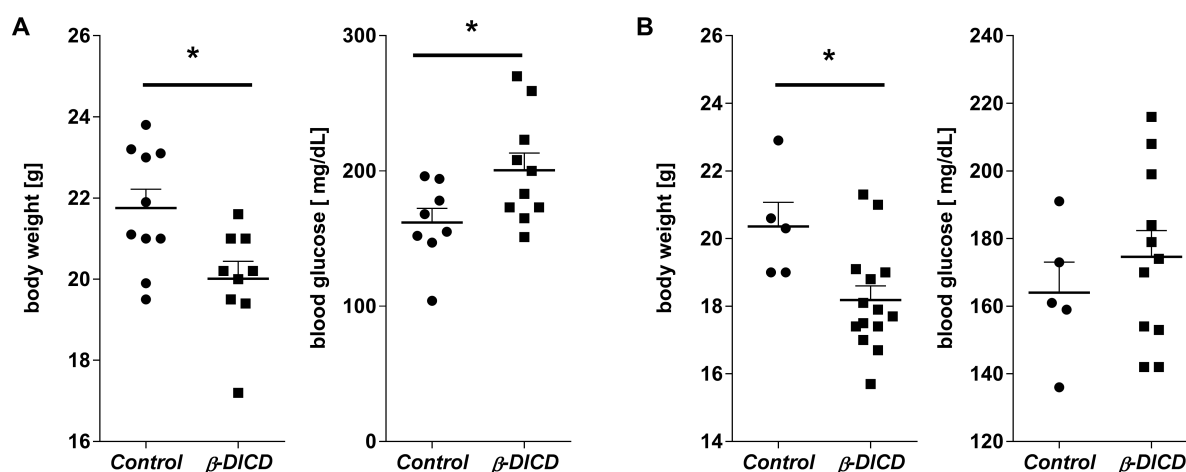


Figure 29: Body weight and blood glucose levels of β -DICD mice

Average body weight and blood glucose levels of 8-weeks old male (A) and female (B) β -DICD and *Cre*-positive control mice (males: control n=10, β -DICD n=9; females: control n=5, β -DICD n=11). Data are shown as mean \pm SEM. Differences were considered statistically significant at * $p < 0.05$ using a 2-tailed heteroscedastic student's t-test

Male β -DICD mice showed an impaired glucose tolerance *in vivo* and analysis of plasma insulin levels detected a decreased insulin secretion in the first phase of insulin response compared

to control mice (Figure 30B, D). However, the performance in the oGTT was slightly better, suggesting a compensatory effect by the gastrointestinal mechanism.

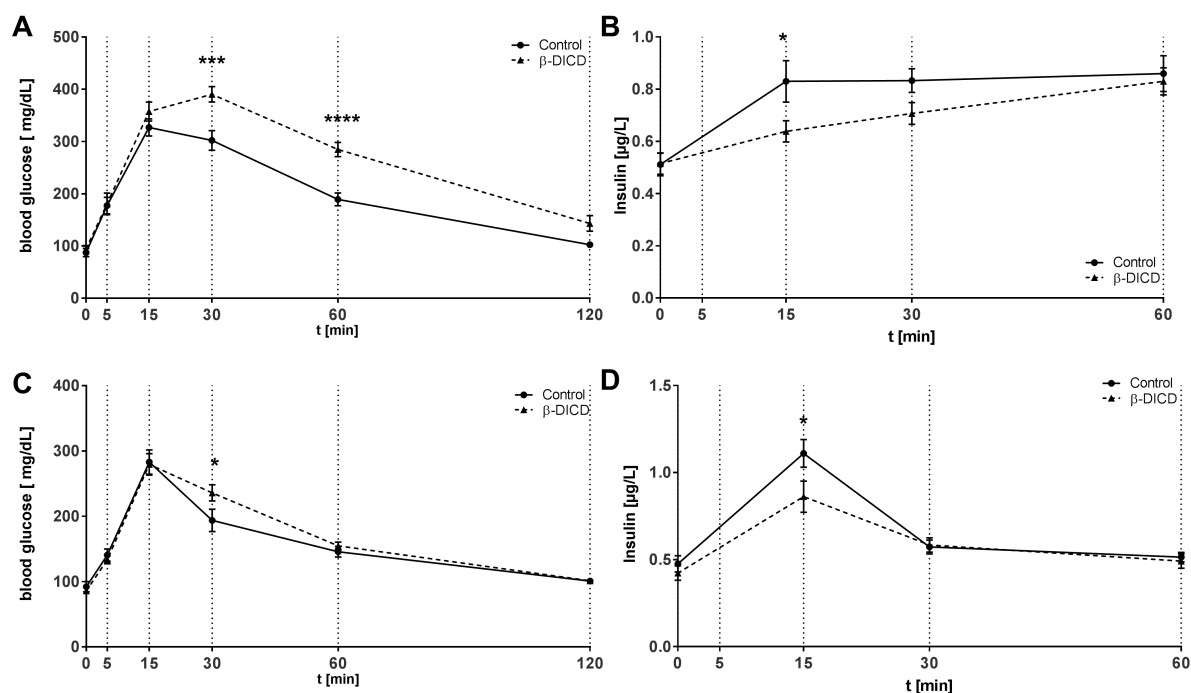


Figure 30: Glucose homeostasis in male β -DICD mice compared to Cre-positive control animals. Intraperitoneal glucose tolerance test (A) of 8-10-weeks old male mice (control n=8, β -DICD n=9). (B) Blood plasma Insulin levels during ipGTT (control n=9, β -DICD n=10). (C) Oral glucose tolerance test of 8-10-weeks old male mice (control n=8, β -DICD n=9). (D) Blood plasma Insulin levels during oGTT (control n=9, β -DICD n=10). Data are shown as mean \pm SEM. Differences were considered statistically significant at * p <0.05, ** p <0.01, *** p <0.001, **** p <0.0001 using 2-way ANOVA with Bonferroni's multiple comparison test.

To exclude a possible Pdx1-CreERT dependent hypothalamic influence on the β -DICD model, islets were isolated and stimulated *in vitro* with glucose and the insulin secretagogues KCL, Exendin-4 and Forskolin (Figure 31). A decreased insulin secretion in β -DICD islets under high-glucose condition was not statistical significant, however, stimulation with all additional stimulants showed a clear defect in insulin secretion in these islets.

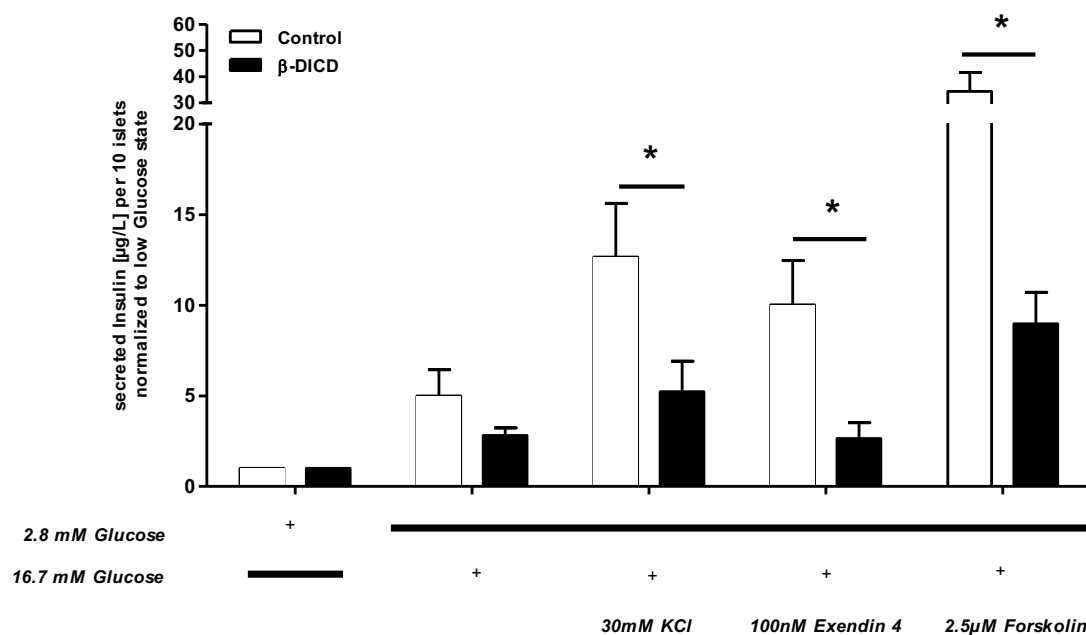


Figure 31: Glucose stimulated insulin secretion of β -DICD islets

Isolated islets from 8-weeks old male β -DICD and *Cre*-positive control mice were isolated and incubated with low glucose (2.8 mM) and high glucose (16.7 mM). In addition, islets were stimulated with 30 mM KCl, 100 nM Exendin-4 or 2.5 μ M Forskolin under high-glucose condition (β -D1D4 n=5, control n=5). Data are shown as mean \pm SEM. Differences were considered statistically significant at * p <0.05 using a 2-tailed heteroscedastic student's t-test.

The total insulin and glucagon levels in islets were not significantly different and insulin plasma levels were only slightly but not significantly decreased (Figure 32).

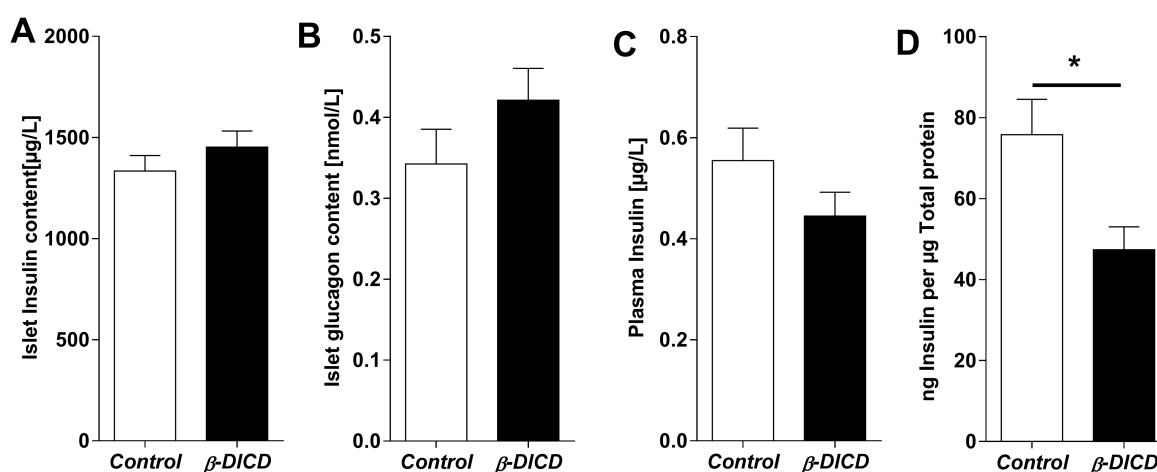


Figure 32: Hormonal content in islets and plasma of male β -DICD mice

Average hormonal content for insulin (A, C, D) and glucagon (B) in isolated islets (A, B; control n= 7, β -DICD n=7), blood plasma (C; control n=12, β -DICD n=11) and whole pancreatic insulin content compared to whole pancreatic protein content (D; control n=5, β -DICD n=5) from 8-weeks old male β -DICD and *Cre*-positive control mice. Data are shown as mean \pm SEM. Differences were considered statistically significant at * p <0.05 using a 2-tailed heteroscedastic student's t-test.

However, measurements of the whole pancreatic insulin content in relation to the total protein amount revealed a significant decrease in insulin. It is therefore possible that β -D1CD mice possessed less islets in total compared to the control mice.

4.2.2. Molecular phenotyping

To analyze the islet morphology, insulin and glucagon stainings were performed (Figure 33). The β -D1CD islets showed a normal morphology with β -cells in the center and α -cells in the periphery.

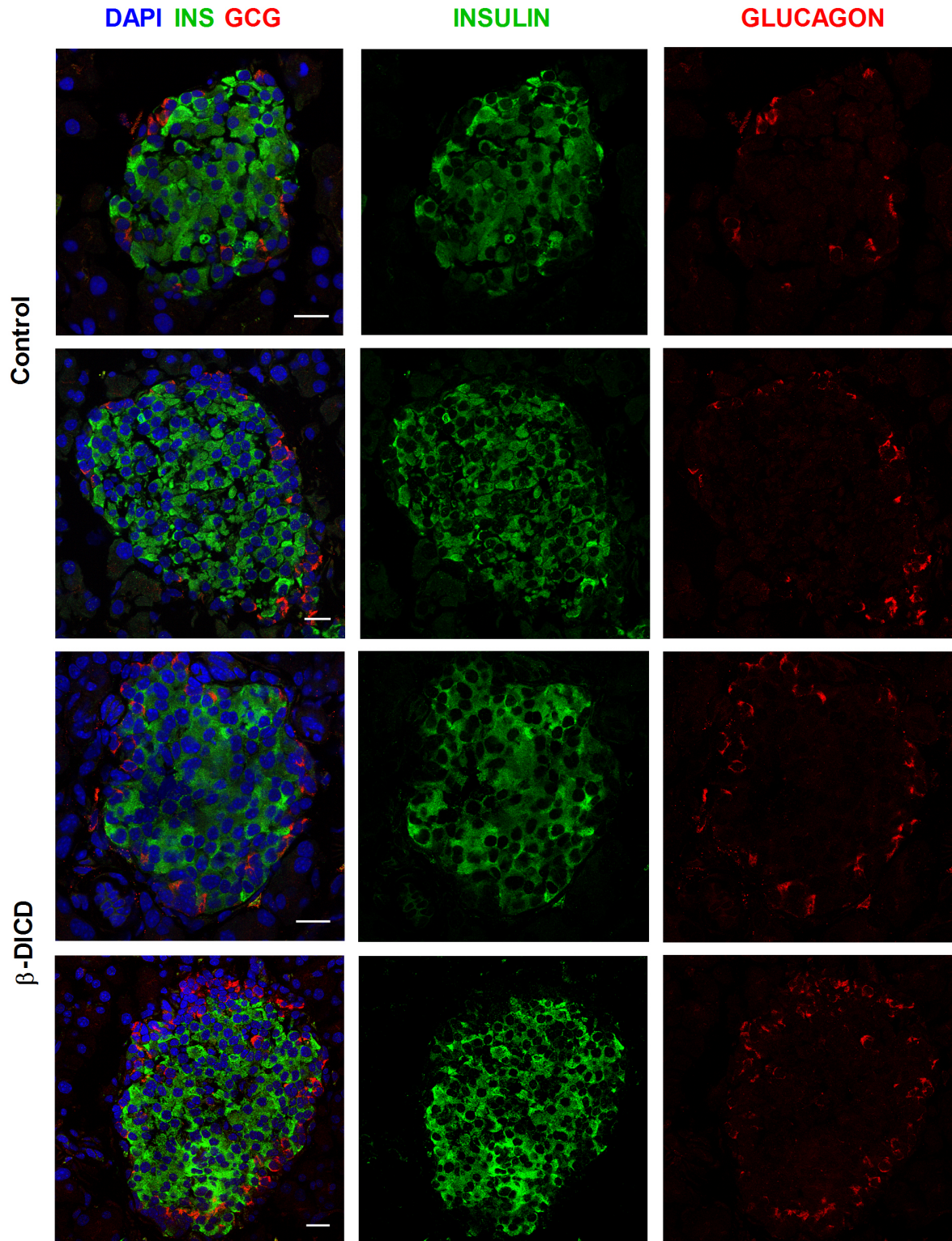


Figure 33: Immunohistochemical analysis of pancreata from 8-weeks old male β -DICD and *Cre*-positive control mice

Double staining against INSULIN (green) and GLUCAGON (red) was done on frozen pancreatic sections from 8-weeks old β -DICD (n=5) and control mice (n=5). Nuclei were counterstained with DAPI (blue). The scale bars represent 20 μ m.

4.2.3. Gene expression analysis

To reveal the underlying mechanism of DICD, gene expression levels in isolated islets were measured by qRT-PCR in isolated islets from β -DICD and control mice. To proof the overexpression of DICD only, the mRNA expression of *Dll1* exon 4 (extracellular domain) and exon 9 (intracellular domain) were measured (Figure 34B). Correspondingly, the expression of *exon 9* is more than 300-fold higher than *exon 4* and *exon 9* in control islet. Among the Delta-Notch components, none of the genes showed altered gene expression in β -DICD islets (Figure 34A). Likewise, *Ins1*, *Ins2* and *Gcg* expression was similar in β -DICD and control islets (Figure 34C).

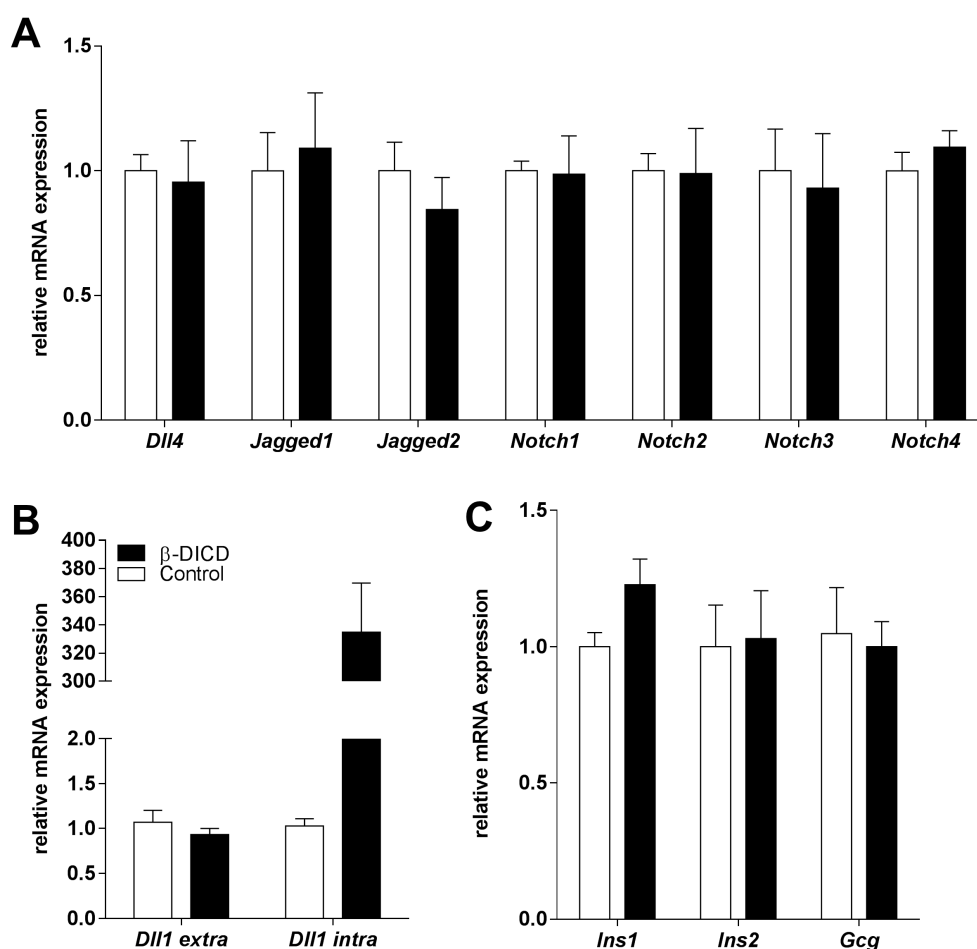


Figure 34: qRT-PCR analysis of isolated islets from 8-weeks old male β -DICD and *Cre*-positive control mice Expression levels of (A) Delta-Notch pathway components, (B) *Dll1* exon 4 (extracellular) and *Dll1* exon 9 (intracellular) and (C) *Ins1*, *Ins2* and *Gcg* were assessed by qRT-PCR (n=6). Expression was normalized to the housekeeping genes *Sdha* and *Ubc*. Differences were considered statistically significant at $p < 0.05$ using a heteroscedastic two-tailed Student's t-test. Data are shown as mean \pm SEM.

To get a broader insight, whole genome transcriptomics on isolated islets was kindly performed by Dr. Martin Irmeler with islet RNA samples from 9 β -DICD and 7 *Cre*-positive control male mice of 8 weeks of age. Only RNA samples with a RIN value higher than 8 were

used. Out of all tested genes, only the gene *Pianp* (PILR alpha associated neural protein) had a fold change (FC) higher than 2 (-5.54) and a false discovery rate (FDR) of <10% and was therefore the most significantly regulated gene in β -D1CD islets. Without considering the FDR and having in mind that islet gene expression is often only slightly regulated (personal correspondence with M. Irmeler), the gene expression analysis showed 162 differentially regulated genes that had a FC > 1.2 and were statistically highly significant ($p < 0.01$) (Supplementary Table 2). Additionally, 306 genes were statistically significant with $p < 0.05$ and FC > 1.2 (data not shown). The comparison between the regulated genes in β -D1D4 and β -D1CD islets gave only 7 different genes (*Efemp1*, *Slc26a1*, *Slco2a1*, *Sult1d1*, *Zfp386*, *2410021H03Rik* and *Cib3*, Supplementary Table 3), most of them connected to extracellular matrix and transporter systems. To find links between regulated genes and potential functions in the β -D1CD data set, GeneRanker analysis regarding overrepresented diseases and signaling pathways of all 162 significantly regulated genes ($p < 0.01$, AV > 20, FC > 1.2) was performed (Table 20, 21).

Diseases that were overrepresented in the downregulated gene set are mostly involved in vascularization and angiogenesis, suggesting effects on intra-islet blood vessels (Table 20).

Table 20: Overrepresented downregulated diseases

Disease	P-value	List of observed genes
TUMOR ANGIOGENESIS	1,16E-06	<i>Slco2a1</i> , <i>Epas1</i> , <i>Spp1</i> , <i>Cd34</i> , <i>Tek</i> , <i>Rgs5</i> , <i>Slit2</i> , <i>Fbln5</i>
PATHOLOGIC NEOVASCULARIZATION	4,05E-06	<i>Slco2a1</i> , <i>Epas1</i> , <i>Spp1</i> , <i>Cd34</i> , <i>Prrx1</i> , <i>Tek</i> , <i>Rgs5</i> , <i>Slit2</i>
TUMOR ASSOCIATED VASCULATURE	3,96E-05	<i>Cd34</i> , <i>Sele</i> , <i>Tek</i> , <i>Rgs5</i>
PANCREAS INFECTION	9,03E-05	<i>Tlr4</i> , <i>Lbp</i>
DIABETIC FOOT ULCER	2,60E-03	<i>Slco2a1</i> , <i>Tlr4</i>

Diseases that were overrepresented in the upregulated gene set comprise hypoglycemia, glycogen storage disease, diabetes mellitus and noninsulin dependent diabetes mellitus 2 (Table 21). Especially *Ghrelin* and *Hnf1 α* are correlating strongly with diabetes and glucose tolerance (Yang et al. 2002, Tong et al. 2010, Brial et al. 2015).

Table 21: Overrepresented upregulated diseases

Disease	P-value	List of observed genes
HYPOGLYCEMIA	1,35E-03	<i>Hnf1a, Acadl, Ghrl</i>
GLYCOGEN STORAGE DISEASE	4,06E-03	<i>Acadl, Idua</i>
DIABETES MELLITUS	5,23E-03	<i>Hnf1a, Vwf, Ghrl</i>
NONINSULIN DEPENDENT DIABETES MELLITUS 2	8,25E-03	<i>Hnf1a</i>

The most downregulated pathways associated with the β -D1CD mouse model are related to the cardiovascular system, in particular the VEGF (vascular endothelial growth factor) pathway. Interestingly, pathways that seemed to be affected in the β -D1D4 model such as the Nf κ B-, Notch- and matrix-metalloproteinase related pathways (Table 19) were downregulated in β -D1CD islets (Table 22).

Table 22: Down regulated signaling pathways

Pathway	P-value	List of observed genes
VASCULAR ENDOTHELIAL GROWTH FACTOR RECEPTOR	7,20E-06	<i>Epas1, Spp1, Cd34, Efemp1, Sele, Tek, Slit2, Fbln5</i>
NF KAPPA B	1,87E-04	<i>Plekhg5, Tnfrsf21, Tlr4, Pycard, Spp1, Nmb, Sele, Lbp, Ppap2a</i>
PLATELET DERIVED GROWTH FACTOR	4,09E-04	<i>Tcf21, Eno2, Rgs5, Ppap2a, Ddx5</i>
NOTCH	8,92E-04	<i>Cd34, Efemp1, Gt(ROSA)26Sor, Prrx1, Notch3, Zeb1, Ddx5</i>
CADHERIN 5, TYPE 2 (VASCULAR ENDOTHELIUM)	2,68E-03	<i>Epas1, Tek, Rgs5</i>
SNAIL FAMILY ZINC FINGER 1	3,80E-03	<i>Slit2, Zeb1, Ddx5</i>
MATRIX METALLOPROTEINASE	5,29E-03	<i>Spp1, Efemp1, Nmb, Zeb1, Fbln5</i>
ARYL HYDROCARBON RECEPTOR NUCLEAR TRANSLOCATOR	8,29E-03	<i>Epas1, Ahr</i>
INTEGRIN	9,03E-03	<i>Spp1, Cd34, Sele, Acer2</i>

The only upregulated signaling pathway was associated with *Ghrelin* (Table 23).

Table 23: Upregulated signaling pathways

Pathway	P-value	List of observed genes
GHRELIN/OBESTATIN	5,98E-03	<i>Scnn1a, Ghrl</i>

4.2.3.1. The cardiovascular system in β -DICD islets

Further analysis of the above-mentioned pathways with Ingenuity software revealed that signaling around VEGF (Vascular Endothelial Growth Factor) was remarkably affected. These regulated genes are represented in a heatmap in Figure 35B.

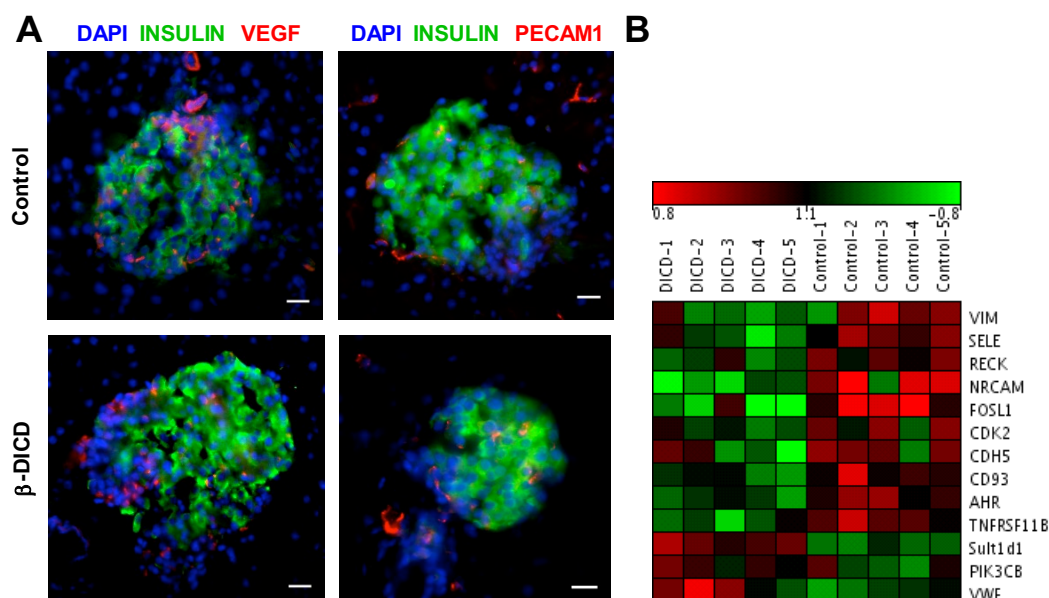


Figure 35: The vascular system in 8-weeks old male β -DICD and *Cre*-positive control mice

(A) Immunohistochemical analysis of VEGF (red) and PECAM1 (red) expression in islets, counterstained with INSULIN (green). Nuclei were counterstained with DAPI (blue). The scale bars represent 20 μ m. **(B)** Heatmap of the transcriptomics data associated with the VEGF network.

However, VEGF expression itself was not affected. VEGF has been shown to be necessary for islet vascularization and therefore essential for glucose sensing and islet function (Lammert et al. 2003, Brissova et al. 2006, Jabs et al. 2008). Interestingly, also Delta-Notch components including DLL1 play crucial roles in vascularization (Scehnet et al. 2007, Sørensen et al. 2009, Lobov et al. 2011). Therefore, β -DICD islets were checked for their vascularization by staining against VEGF and PECAM1 (Platelet endothelial cell adhesion molecule) (Figure 35A).

Although it was not possible to image whole islets in z-stacks, the 9 μm slices did not show any differences between β -DICD and control islets. In both groups, the islets were randomly infused with blood vessels.

4.2.3.2. Genes associated with islet function and diabetes

Besides the GeneRanker and Ingenuity pathway analysis, some single genes that were differentially regulated in β -DICD islets looked promising in particular *Glut2* (*Slc2a2*; +1.35-fold), *Kl* (*Klotho*; +2.05-fold) and *Gal* (*Galanin*; -2.21-fold), which are associated with β -cell function and insulin secretion (Lindskog et al. 1987, Lin et al. 2012, Thorens 2015). As already mentioned, *ghrelin*, which is expressed by ϵ -cells, was 3.28-fold up regulated in β -DICD islets and confirmed by qRT-PCR (Figure 36A). However, *Ghrelin* gene expression alone is no proof for the active hormone or the presence of ϵ -cells (Date et al. 2002, Ghelardoni et al. 2006). Moreover, GHRELIN⁺ cells are hard to detect in pancreatic sections, since they account only for 1% of islets cells. It was therefore not unexpected that staining with a GHRELIN specific antibody showed almost no ϵ -cells and no double positive cells were GHRELIN was co-expressed with the DICD-coupled GFP marker (Figure 36B).

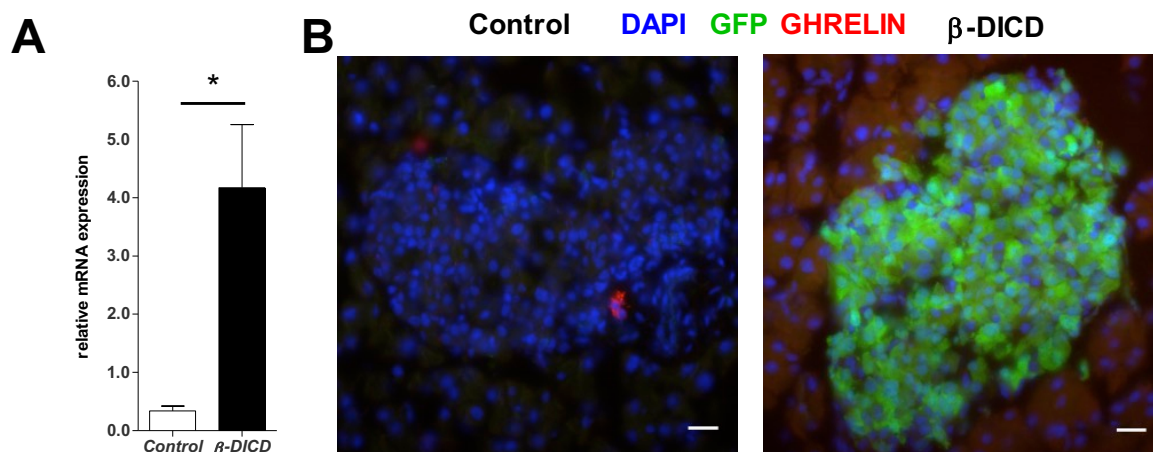


Figure 36: Ghrelin expression in islets from 8-weeks old male β -DICD and *Cre*-positive control mice. (A) mRNA expression levels of *Ghrelin* in isolated islets from β -DICD and *Cre*-positive controls were assessed by qRT-PCR (n=6). Expression was normalized to the housekeeping genes *Hprt* and *Ubc*. Differences were considered statistically significant at $p < 0.05$ using a heteroscedastic two-tailed Student's t-test. Error bars display SEM. (B) Immunohistochemical analysis of GHRELIN (red) expression in islets, counterstained with GFP (green), which is only present in the VENUS vector of β -DICD mice. Nuclei were counterstained with DAPI (blue). The scale bars represent 20 μm .

4.2.3.3. β -DICD islets express less CTGF

One gene that did not show up in the transcriptomics data but might be relevant in this mouse model because of its described association with DICD (Bordonaro et al. 2011) is *Ctgf* (connective tissue growth factor). qRT-PCR quantification of *Ctgf* expression in isolated islets of β -DICD mice revealed a downregulation of more than 50%. Other genes that were reported to be associated with DICD such as *Smad2*, *Smad7* and *Mtor* were not changed in their expression (Figure 37) (Bordonaro et al. 2011).

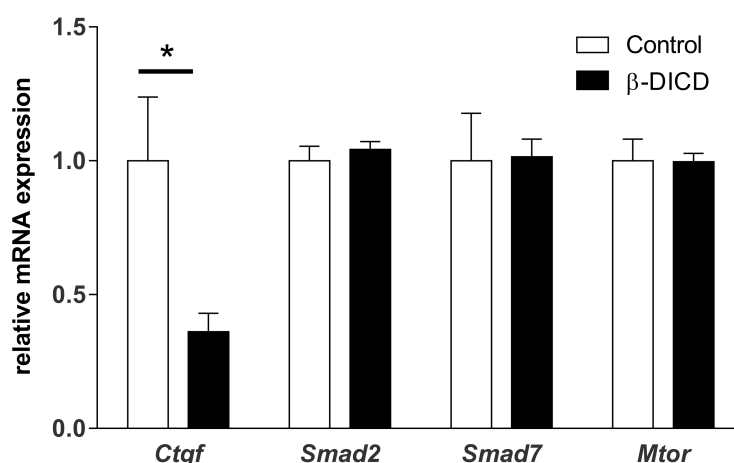


Figure 37: qRT-PCR analysis of Tgf β components in isolated islets from 8-weeks old male β -DICD and *Cre*-positive control mice.

Expression levels of *Ctgf*, *Smad2*, *Smad7* and *Mtor* in isolated islets from β -DICD and *Cre*-positive controls were assessed by qRT-PCR (n=6). Expression was normalized to the housekeeping genes *Hprt* and *Ubc*. Differences were considered statistically significant at $P < 0.05$ using a heteroscedastic two-tailed Student's t-test (* $p < 0.05$, ** $p < 0.01$, *** $p < 0.001$). Error bars display the SEM.

Ctgf has been shown to be very important for the β -cell survival, proliferation as well as maturation (Crawford et al. 2009, Riley et al. 2014). Based on this, β -DICD islets were tested for their grade of maturation and proliferation by immunostainings (Figure 38). To investigate the number of mature β -cells, MAFA and INSULIN double positive cells were compared to only INSULIN positive cells and counted. Both, β -DICD islets and controls, showed about 70% mature β -cells per islets (Figure 38A), which was within normal range. Additionally, proliferation was measured with the KI67 antibody, which is specific for mitotic cells, and the number of INSULIN⁺ KI67⁺ double positive cells was determined. 2-3% of all β -cells were proliferating in β -DICD and control mice (Figure 38B). Taken together, β -DICD islets did not show any conspicuity regarding β -cell maturation and proliferative potential.

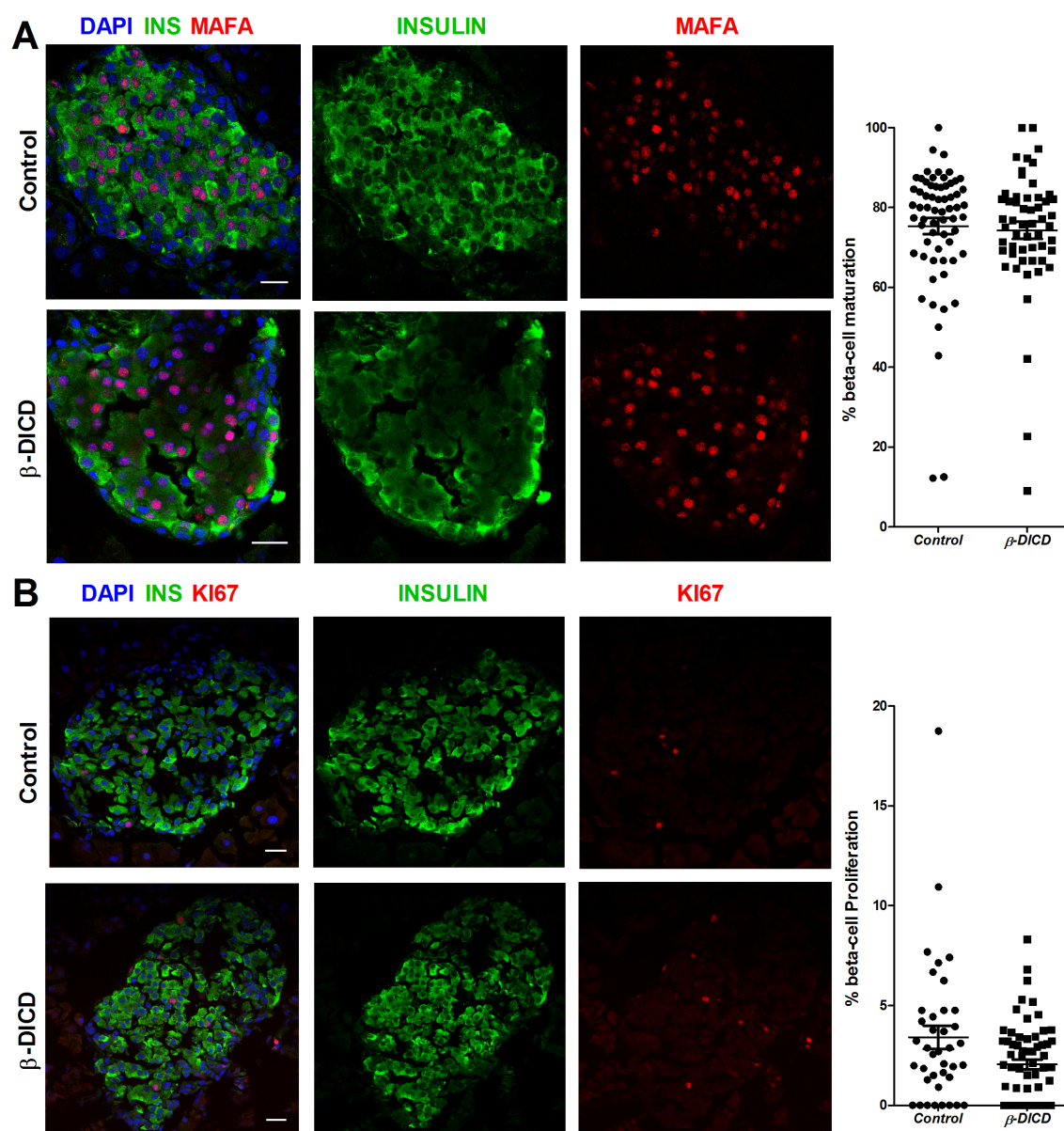


Figure 38: Immunohistochemical analysis of pancreata in 8-weeks old male β -DICD and *Cre*-positive control mice.

Double staining for INSULIN (green) and MAFA (A) or KI67 (B) (red) were done on frozen pancreatic sections from 8-weeks old β -DICD and control mice (n=5). Stainings were statistically quantified by calculating the percentage of INSULIN⁺MAFA⁺ or INSULIN⁺KI67⁺ double positive cells. Nuclei were counterstained with DAPI (blue). The scale bars represent 20 μ m. Differences were considered statistically significant at *p<0.05 using a 2-tailed heteroscedastic student's t-test.

5. DISCUSSION

5.1. DLL1- and DLL4 mediated signaling in pancreatic β -cells

The Delta-Notch signaling pathway is found in many tissues and is widespread in the animal kingdom (Ehebauer et al. 2006). While its major roles during embryogenesis have been shown several times (Wolter 2013), studies for relevant function during adulthood remain sparse or deal mainly with neuronal stem-cell differentiation processes and different kinds of cancers, in particular pancreatic cancer, which in most cases proves to be lethal (Stump et al. 2002, Chapouton et al. 2010, Avila et al. 2013). Notch components have been shown to act mainly as an oncogene, because their loss reduces tumor progression, but in some cases they have been shown to function as tumor suppressors (Avila et al. 2013). However, under normal physiological conditions most studies suggest that the expression and activation of Notch receptors is downregulated (Miyamoto et al. 2003, Jensen et al. 2005). Interestingly, about 80% of pancreatic cancer patients show additionally diabetes dependent glucose intolerance, which led to the broad suggestion that both diseases correlate with each other. However, it remains unclear how they are connected, induced or influence each other (Wang et al. 2003). Malfunction of pancreatic β -cells is critical for the development of diabetes (Oliver-Krasinski et al. 2008). Pancreatic β -cells share plenty of properties with neuroendocrine cells (Eberhard 2013). Both use membrane depolarization to secrete message molecules to the blood stream such as insulin and share a common set of expressed genes (Arntfield et al. 2011, Martens et al. 2011). Considering the role of Delta-Notch signaling in both pancreatic cancer and neurons, a function of the pathway in pancreatic islets seems likely. Indeed, the presence of NOTCH1 as well as NEUROG3 has been demonstrated in adult pancreatic islets (Dror et al. 2007). However, it remains unknown whether DLL1 and DLL4 are active in adult islets. Therefore, this study represents, so far as known, the first description of DLL1 and DLL4 in adult pancreatic islets. Moreover, an expression of DLL1 and DLL4 predominantly in β -cells has been proven. This is relevant because other components of the pathway, especially on the side of the receptors, are not exclusively expressed in certain cellular populations but are rather randomly distributed within the islets (i.e. NOTCH1, 2, 4). The importance of ligands within the islets is further substantiated by the exclusive expression of JAGGED1 in α -cells.

5.1.1. DLL1 and DLL4 are necessary for islet function, but not islet morphology

To assess a potential function of these ligands in β -cells, *Pdx1*-Cre dependent mouse models were established and induced with tamoxifen starting post-weaning. Mice with a downregulation of *Dll1* showed impaired glucose tolerance and a mild hyperglycemia, while the islets showed normal morphology. These data are in accordance with a previous study performed by former PhD student Dr. Davide Cavanna, who used the same floxed *Dll1* mouse line but the *Tg(Ins2-cre/ERT)1Dam/J* Cre-driver line to knockdown *Dll1* in adult β -cells (Dor et al. 2004, Cavanna 2013). Both studies showed hyperglycemia and an impaired glucose tolerance under normal chow diet. However, the *Pdx1*-dependent loss of *Dll1* showed stronger and more consistent effects on both hyperglycemia and glucose tolerance. Cavanna interpreted the high variation in his data with the impact of the used *Cre* line. The *Tg(Ins2-cre/ERT)1Dam/J* Cre-driver line has been shown to have noteworthy impact on metabolic function (Liu et al. 2010) and most of Cavanna's data were collected without a *Cre*-positive control. Nevertheless, considering the comparable data of this study, which uses a different *Cre* line together with *Cre*-positive control animals, the metabolic data collected by Cavanna are esteemed to be reliable and not dependent on *Cre* expression. Interestingly, Cavanna's phenotype seems to be abolished under high-fat diet challenge. However, the experimental design was not optimal because only four animals were used for a *Cre*-positive control group under high fat diet but no *Cre*-positive control animals under normal chow diet. Under the *Pdx1* promoter, the impact of a high-fat diet was not investigated, since the phenotype was already significant on normal chow. Moreover, it is questionable whether high-fat diet would really attenuate the observed glucose intolerance, when it is generally known that high-fat diet induces hyperglycemia and glucose intolerance (Winzell et al. 2004). Furthermore, β -D1 islets did not exhibit less α -cells and *glucagon* gene expression. The whole islet protein content of glucagon is normal, and therefore not suggested to impact the overall phenotype. Both studies also performed gene expression analysis with qRT-PCR. In general, remarkable changes in Notch receptor genes were not observed. However, in β -D1 islets *Jagged2* was marginally upregulated, whereas the expression of *Dll4* was contradictory. While Cavanna showed a 1.5-fold increase in *Dll4* expression, no significant changes were measured in β -D1 islets. Based on Cavanna's observations, the present thesis additionally describes the analysis of the *Dll4* knockdown model. Cavanna suggested a possible counterbalancing of *Dll4*

in the absence of *Dll1*, which has also been shown for intestinal progenitor cells (Pellegrinet et al. 2011). However, parts of the results obtained in the present thesis speak against this hypothesis, because β -D4 mice displayed with normal blood glucose levels and an improved glucose tolerance characteristics opposite to β -D1 mice. Additionally, β -D4 showed a modest loss of α -cell mass but in contrast higher *glucagon* gene expression, while the hormone content itself remained normal as in β -D1. Gene expression analysis of Notch pathway components by qRT-PCR data did not show any significant changes in β -D4 islets. If *Dll4* would counterbalance *Dll1*, one would have expected that the downregulation of *Dll4* in islets would have led to a similar phenotype as the downregulation of *Dll1* in β -D1 mice. Indeed, opposing effects of *Dll4* have already been observed before in connection with *Jagged1* during angiogenesis (Benedito et al. 2009). Moreover, *Dll1* and *Jagged1* show opposing effects also during development of the inner ear (Brooker et al. 2006). Furthermore, while DLL4 enhance proliferation and expression of the early activation markers CD69 and CD25 in T cells, DLL1 can induce partial and JAGGED1 nearly complete inhibition of T cell activation (Rutz et al. 2005).

However, since the starting point of the present thesis based on Cavanna's suggestion that DLL4 can at least in part compensate for the loss of DLL1, the focus was on the simultaneous deletion of *Dll1* and *Dll4* in adult β -cells.

5.1.2. Simultaneous deletion of *Dll1* and *Dll4* in pancreatic β -cells leads to hypoglycemia and hyperglucagonemia through increased insulin secretion

Based on the gene expression of both *Dll1* and *Dll4* in isolated islets, the newly generated β -D1D4 mouse line showed a knockdown efficiency of about 50-60% compared to *Cre*-positive control animals. On a first view, this seems to be relatively low. However, taking into account that whole islet RNA extracts include also material from non β -cells such as blood vessel cells, which are known to express *Dll4* and *Dll1* as well (Scehnet et al. 2007, Sørensen et al. 2009, Lobov et al. 2011), the obtained downregulation was considered as acceptable. In addition, the observed phenotype was found to be robust and strong. Surprisingly, β -D1D4 mice became hypoglycemic after tamoxifen treatment, a phenotype that was not observed for the single knockdowns. In certain individuals, the blood glucose levels dropped down even below 50 mg/dl, which is considered as severe hypoglycemia (Cryer et al. 2003).

Hypoglycemia mostly occurs as result of hyperinsulinemia or incorrect insulin administration as medication for diabetes. The β -D1D4 mice neither showed increased insulin levels in plasma nor on the gene expression level or in whole islet hormone levels. In contrast, β -D1D4 mice developed hyperglucagonemia, which was in accordance to increased *glucagon* mRNA expression and protein level in the islets and plasma. However, this observation seems to be contradictory, since hyperglucagonemia usually leads to hyperglycemia in consequence of increased endogenous glucose production in liver as well as inhibition of insulin secretion (Sherwin et al. 1976, Schwartz et al. 1987). Instead, β -D1D4 mice performed much better during glucose tolerance tests than the control mice. Furthermore, the obtained measurements of insulin secretion after glucose stimulation *in vivo* and *in vitro* leads to the suggestion that these mice secrete more insulin without affecting basal insulin levels. The β -D1D4 mice displayed a phenotype more similar to β -D4 mice rather than β -D1 mice. This suggests that DLL4 could be more important than DLL1 in β -cells and that *Dll4* expression is not counterbalanced by *Dll1*. Whether DLL4 has simply a higher capacity to activate Notch signaling than DLL1 remains to be investigated. Interestingly, a similar effect was observed during T-cell differentiation (Mohtashami et al. 2010).

Where does the prevalent hyperglucagonemia in β -D1D4 mice come from? Immunofluorescence staining showed an increased α -cell population in β -D1D4 compared to control islets, although the overall islet size remained equal. Interestingly, the induced downregulation should exclusively affect β -cells and α -cells not at all. One possible explanation would be that these new α -cells could develop out of former β -cells, which would represent some novel form of transdifferentiation. On the other hand, it cannot be excluded that the used Pdx1-CreERT line is completely specific to β -cells (Zhang et al. 2005, Lu et al. 2014, Ye et al. 2015). Moreover, it has been shown, for instance for the RIP-Cre line, that *Cre* is expressed and can enter the nucleus to a certain degree even in absence of tamoxifen, making it possible that recombination can occur before the actual age or even during development (Liu et al. 2010). If this would be the case for the Pdx1-CreERT line, it is thinkable that the loss of ligands affects the endocrine lineage decision during secondary transition of pancreas development. To assess this, pancreata were stained for PDX1 and CRE, as alternative to a lineage tracer, together with GLUCAGON. This experiment was carried out not

only with 8-weeks old mice, i.e post tamoxifen treatment, but also during the weekly tamoxifen administration. In no cases, double positive cells for either PDX1 or CRE were detected in any of the islets. Moreover, based on this finding, a potential leakiness of *Cre* could be excluded, because without tamoxifen treatment, CRE expression was observed only within the cytoplasm, and entered the nucleus only in β -cells after tamoxifen treatment. Taken together, a potential trans-differentiation of the β -cells to α -cells in β -D1D4 mice can be excluded.

Considering the expression pattern of Notch receptors in islets, it is also possible that loss of ligands and consequently their binding to the receptors have effects on the α -cells. For instance, DLL1 and DLL4 have been shown to bind to NOTCH1, which is present among all kind of islet cell types, including α -cells (Andrawes et al. 2013). Inefficient Notch signaling can lead to failure in lineage commitment, neurogenesis or result in cancer. The relevance of Delta-Notch especially in cell-cycle regulation and survival has been described in various studies (Weng et al. 2004, Purow et al. 2005, Georgia et al. 2006, Dror et al. 2007, Pellegrinet et al. 2011). Indeed, the α -cells in β -D1D4 islets showed a 3-fold higher proliferative rate than in control islets, suggesting a possible role of Delta-Notch signaling in balancing α - and β -cell turnover. However, a clear proof of this hypothesis is still missing.

A third and maybe the most promising reason for the hyperglucagonemia, is the increased insulin secretion itself and its physiological consequences. Extreme insulin increment leads to hypoglycemia and in the β -D1D4 mice to a severe form. The high amount of glucagon could be crucial to counterbalance a prevailing hypoglycemia, which can, when unopposed, result in coma, seizures, or even death (Cryer 1999, Cryer 2002). In general, glucagon secretion in humans is increased when blood glucose levels fall below a glycemic threshold of 65-70mg/dL, whereas insulin secretion should decline upon reaching 81 mg/dL (Schwartz et al. 1987). This could also explain why the plasma insulin levels were not increased. Consequently, β -D1D4 mice produce and secrete more glucagon for survival, and the need for glucagon stimulated the additional production of α -cells through proliferation (Liu et al. 2011). The high amount of glucagon and increased hypoglycemia might also be the driver of the increased food intake during the active phase of β -D1D4 mice. Hypoglycemia in non-diabetic patients leads to increased hunger, hyperglucagonemia and increased energy

expenditure (Nair 1987, Sprague et al. 2011), which could also explain why β -D1D4 mice did not gain weight even with higher calorie uptake.

5.1.3. Gene expression analysis

Whether the observed effects are the response to an altered Delta-Notch pathway, was analyzed by gene expression analysis. In β -D1D4 islets, the ligand gene *Jagged1* and all Notch receptors except *Notch3* were significantly upregulated. NOTCH3 is known to inhibit the function of NOTCH1 by repressing the upregulation of the *Hes* target genes (Beatus et al. 1999). So, it is thinkable here that NOTCH3 has a similar repressing function and does not following the trend of the other Notch receptors, whose upregulation can be explained with the loss of cis-inhibitory function through DLL1 and DLL4. Usually, the presence of ligands reduces the expression of the receptors on the very same cell or the other way around (Sprinzak et al. 2010). To proof this, a simple staining could be done, to check whether the protein expression of the Notch receptors is increased in β -cells where normally the ligands should be expressed. Alternatively, the loss of Delta-Notch signaling induces a feedback loop by increasing the receptors to enhance signaling.

Aside from the receptors, only the ligand *Jagged1* was found to be upregulated. It is possible that *Jagged1* is counterbalancing the lack of *Dll1* and *Dll4* in β -cells. However, protein expression analysis in islets showed that JAGGED1 was exclusively expressed in α -cells. Therefore, it is more likely that the increase in *Jagged1* gene expression was due to the increased α -cell mass rather than a counterbalancing mechanism in β -cells.

5.1.3.1. *Delta-Notch regulates the cell cycle arrest in pancreatic β -cells*

Interestingly, analyzing downstream targets of the Notch pathway, an upregulation of *Neurog3* was observed. Under normal conditions, Notch activity represses the activity of *Neurog3* during pancreatic development (Kopinke et al. 2011, Magenheim et al. 2011). Recently, *Neurog3* has shown to be active in mature islets, where it seems to be present mainly in α -cells but also to a certain extent in β -cells (Dror et al. 2007). *Neurog3* is further important for the proliferation of pre-existing and newly formed β -cells and reprogramming of non- β -cells. This is critical for *in vivo* β -cell expansion in the injured pancreas of adult mice (Van de Casteele et al. 2013), especially because the regulation of *Neurog3* gene expression

is suggested to be posttranscriptional and not part of an upstream signaling pathway (Van de Castele et al. 2013), which would explain the apparent contradictory higher expression of Notch receptors. It is therefore possible that in β -D1D4 mice, *Neurog3* upregulation is due to reprogramming or expansion of the β -cell mass. However, presence of NEUROG3 protein on frozen tissue sections could not be detected. *Neurog3* expression on the mRNA level has been reported several times before, but the presence of the protein is rather difficult (Dror et al. 2007, Brereton et al. 2014). There is a lack of a working antibody against NEUROG3 and probably the technical procedure during tissue and slide preparation is affecting the protein structure of NEUROG3. Most studies demonstrating NEUROG3 protein presence used NEUROG3 coupled to reporter proteins or in-house antibodies (Xu et al. 2008, Taylor et al. 2013, Van de Castele et al. 2013, Baeyens et al. 2014), which were not available. Nevertheless, the presence of *Neurog3* mRNA in β -D1D4 points towards an altered cell cycle in β -D1D4. As shown before, the α -cells are highly proliferative, but it remains unclear whether *Neurog3* expression can also induce α -cell proliferation. Further, other cell cycle factors that are associated with *Hes1* or *Neurog3* expression were also differently expressed in β -D1D4 islets. For example, the cell-cycle inhibitors *Cdkn1c* and *Cdkn1a* (Cozar-Castellano et al. 2006, Georgia et al. 2006) were both significantly upregulated in β -D1D4 islets. This speaks more against a proliferative activity and for a cell-cycle arrest in β -D1D4 islets. However, both factors could be independent from each other, if *Neurog3* activity is considered to be independent of Notch activity and specified to α -cells. Instead, the upregulation of *Cdkn1c* and *Cdkn1a* could be a direct effect of reduced Notch activity in β -D1D4 islets. For instance, *Cdkn1c* has been shown to be upregulated in the absence of Notch signaling in pancreatic progenitors (Georgia et al. 2006) and Notch activation can repress *Cdkn1a* in endothelial cells (Nosedá et al. 2004). Moreover, as cell-cycle dependent function of Delta-Notch signaling in islets can be seen the dramatic downregulation of *Mesothelin* (*Msln*), which is the most strongly regulated gene in the β -D1D4 data set. *Msln* promotes proliferation and inhibits apoptosis in pancreatic cancer cells and is therefore an important target for pancreatic cancer therapy (Zheng et al. 2012, Yin et al. 2014). Thus, the downregulation of *Msln* in β -D1D4 islets indicates cell-cycle arrest and apoptosis. Moreover, Notch was suggested to suppress apoptosis or cell-cycle arrest in islet cells (Dror et al. 2007). Loss of Notch signaling might consequently result in increased cell-cycle arrest and cell death,

which was observed in parts in this study. However, the presence of typical cell-death markers like Caspase-3 could not be demonstrated, because all used Caspase3 antibodies showed unspecific staining in α -cells of mutant and control mice. Therefore, apoptosis assays should be performed in future.

5.1.3.2. Genes associated with insulin secretion

Aside from apparent cell-cycle changes in β -D1D4 islets, the collected data revealed that β -D1D4 mice secreted more insulin than required for glucose homeostasis. As discussed before, β -D1D4 mice were probably struggling with a lethal hypoglycemia. The overall insulin content was not affected, proving that insulin was produced and present in islets in a normal manner. However, insulin secretion seems to be the main reason for hypoglycemia and improved glucose tolerance in β -D1D4 mice. Whole genome transcriptomics on isolated islets revealed several differentially regulated genes that are associated with insulin secretion. For example *Ucn3*, which is a typical marker for β -cell maturation and improves the capacity for GSIS (Blum et al. 2012), was found to be downregulated. Loss of *Ucn3* in murine pancreatic β -cells protects animals from high-fat diet induced hyperglycemia, hyperinsulinemia and glucose intolerance. In general, such animals can handle glucose loads better than the control mice (Li et al. 2007).

Similar effects have been shown for glucagon-receptor (*Gcgr*) null mice. Several studies were performed on such knockouts and all of them showed lower blood glucose levels, increased α -cell mass and hyperglucagonemia as well as improved glucose tolerance *in vivo* (Gelling et al. 2003, Gelling et al. 2009). However, the improved glucose tolerance was suggested to be due to a compensatory mechanism by increased GLP1 levels and not by increased insulin secretion (Sørensen et al. 2006). Moreover, the hyperglucagonemia in *Gcgr* $-/-$ mice is probably to compensate inefficient glucagon sensing in target tissues like liver (Gelling et al. 2003). With increasing age, mice and also humans lacking *Gcgr* tend to develop pancreatic neuroendocrine tumors (Yu et al. 2011). This is interesting, because in β -D1D4 islets *Gcgr* was found to be downregulated and GeneRanker analysis also suggested an increased risk for pancreatic carcinomas. In this study, β -D1D4 mice did not show any tumor development, but most of the tissue analysis was carried out with mice in the age of 8-10 weeks. However, Yu et al. showed that tumor development was not observed before the age of 10 months in

Gcgr^{-/-} mice. Hence, a further study elevating the potential for tumor development in older β -D1D4 mice could be worthwhile, because Delta-Notch signaling is a common target gene for several types of cancer including pancreatic cancer (Miyamoto et al. 2003, Weng et al. 2004, Buchler et al. 2005, Avila et al. 2013).

In addition to *Ucn3* and *Gcgr*, also *Glp1r* was found to be downregulated in β -D1D4 islets. Under normal physiological conditions, the binding of GLP1 to its receptor GLP1R enhances insulin secretion by inhibiting K_{ATP} channels and consequently further membrane depolarization. GLP1R agonists are used broadly in diabetes therapy to improve glycemic control and to reduce blood glucose levels (Meloni et al. 2013). Moreover, *Glp1r* null mice showed impaired glucose tolerance and insulin secretion, but normal basal glucose metabolism (Scrocchi et al. 1996, Baggio et al. 2000). Interestingly, loss of *Glp1r* was found to be beneficial under high-fat diet challenge, where it reduced insulin resistance and hyperglycemia (Ayala et al. 2010). In this study, the data showed an improved glucose tolerance while *Glp1r* was downregulated. However, loss of *Glp1r* in β -cells does not affect insulin-secretory response to glucose, suggesting that GLP1R is either not essential for efficient insulin secretion or its effects can be compensated (Flamez et al. 1999). It has also been suggested but not yet demonstrated that loss of *Glp1r* might be able to increase glucagon levels, because GLP1R suppresses glucagon secretion (de Heer et al. 2008, Ayala et al. 2010). It is therefore possible that *Glp1r* downregulation in β -D1D4 islets improves and enables additional glucagon secretion to oppose the increased insulin secretion. It would be interesting to analyze the GLP1 content in blood and islets, to investigate whether these mice have also a decreased incretin secretion. Supportive for this hypothesis is the result of the oral GTT, where glucose tolerance was overall remarkably improved in β -D1D4 mice, but unchanged between 15 min and 30 min, whereas in control mice the blood levels drop steeply during this time. This points towards impaired incretin-based stimulation of insulin secretion in β -D1D4 mice either because of the reduced presence of GLP1R or secreted GLP1.

Like *Glp1r*, *Slc2a2* (*Glut2*) was surprisingly downregulated in β -D1D4 islets. GLUT2 as glucose transporter is expressed not only in β -cells but also in liver, intestine, kidney and the central nervous system (Thorens 2015). Via GLUT2 glucose enters the cell, where it is further metabolized and consequently promotes insulin secretion through ATP production. Thus, the

presence of GLUT2 is required for maintaining normal glucose homeostasis and the proper function of the endocrine pancreas (Guillam et al. 1997). Loss of *Glut2* leads to impaired GSIS due to glucose-unresponsiveness and symptoms typically for non-insulin-dependent diabetes mellitus (Guillam et al. 1997). However, it has been demonstrated, that already 20% of the normal *Glut2* mRNA expression is sufficient to normalize GSIS (Thorens 2015). In β -D1D4 islets, *Glut2* mRNA was to be reduced to 80% compared to control islets, suggesting only minor effects due to *Glut2* downregulation. It is therefore thinkable that *Glut2* was downregulated to reduce the glucose equilibration into the cell to further minimize insulin secretion as a compensatory mechanism.

5.1.3.3. Mitochondrial dysfunction in β -D1D4 mice

As mentioned before, β -D1D4 mice consumed more food probably due to increased energy expenditure. This hypothesis is accompanied with several differentially regulated genes in β -D1D4 islets that are associated with mitochondrial function. The mitochondria in β -cells are the powerhouse of a cell, producing ATP during the TCA cycle and inducing insulin secretion by closing the K_{ATP} channels in the β -cell (Wollheim et al. 2002). Mitochondrial dysfunction can therefore result in impaired GSIS, which is also a key factor for T2DM development (Lowell et al. 2005, Wiederkehr et al. 2006). In β -D1D4 islets, *Pdk1* and *Pdk2* (Pyruvate Dehydrogenase Kinase) were found to downregulated in whole-genome transcriptomics analysis. PDKs are kinases that are inactivating the pyruvate dehydrogenase by ATP dependent phosphorylation. The pyruvate dehydrogenase catalyzes the oxidation of pyruvate to acetyl-CoA for further downstream metabolic pathways (Sugden et al. 2006). Reduced levels of PDKs consequently lead to diminished inactivation of the pyruvate dehydrogenase and increased pyruvate oxidation and energy production. Interestingly, studies investigating β -cell specific loss-of-function models for *Pdk1* showed progressive hyperglycemia and loss of islet mass (Hashimoto et al. 2006). PDK1 was further suggested to be a crucial regulator of the pancreatic growth during embryogenesis and mature pancreatic cell types (Westmoreland et al. 2009). In addition, altered expression of *Pdk2* or *Pdk4* in skeletal muscle was associated with T2DM (Kulkarni et al. 2012). On the other hand, stimulation of islets with prolactin results in enhanced GSIS by downregulating *Pdk2* and *Pdk4* mRNA and increasing pyruvate

dehydrogenase activity (Arumugam et al. 2010). However, *Pdk4* gene expression was not altered in β -D1D4 islets.

Further supportive for the hypothesis of altered energy expenditure was the upregulation of genes associated with the electron transport chain in mitochondria. For instance, *Cox6a2* (cytochrome C oxidase), which encodes for the last enzyme of the electron transport chain, was 1.5-fold upregulated. *Cox6a* deficiency has been shown to protect from high-fat diet induced obesity, insulin resistance and glucose intolerance. Moreover, these animals developed enhanced thermogenesis and increased whole-body energy metabolism (Quintens et al. 2013). But in β -D1D4 mice, *Cox6a2* was up- and not downregulated. However, Quintens et al. investigated the function of COX6A2 was only in whole-body mutants with a focus on cardiac function and muscle. Whether the loss of *Cox6a2* in only β -cells would show a similar metabolic phenotype remains unclear. Even less is known about the function of *Ndufa12*, which was also upregulated 1.52-fold in β -D1D4 islets. *Ndufa12* encodes for a subunit of the mitochondria NADH dehydrogenase complex I, likewise part of the electron transport chain. This complex transfers electrons from NADH to ubiquinone which establishes a proton gradient for the generation of ATP (Mimaki et al. 2012). Deficiency in this complex is reported to be the most common respiratory chain defect in human disorders like Parkinson or Leigh syndrome (Schapira et al. 1989, Ostergaard et al. 2011, Mimaki et al. 2012). Hence, increased activity of this complex might lead to increased energy turnover as well as reduced and, hence, beneficial production of superoxide radicals (Pitkanen et al. 1996).

5.1.4. General remarks (Limitations of the project) and future perspective

The analysis of β -D1D4 mice revealed certain unexpected problems. For example, that these mice developed hyperglucagonemia and showed an increased α -cell mass was highly unanticipated. Ideally, molecular tracers like a GFP signal would help a lot to proof or exclude a potential trans-differentiation mechanism from original β -cells. Moreover, it would be an advantage in further experiments to include single cell sorting. The whole-genome transcriptomics data set is hard to analyze, since the genes can origin from β - as well as from α -cells. It remains further unknown which genes were associated with the loss of the Delta ligands rather than with the observed α -cell hyperplasia. In future, it could be more efficient to perform single-cell transcriptome analysis (Segerstolpe et al. 2016). This technique enables

the separation of differentially regulated genes in β - and α -cells and therefore makes it possible to reveal distinct transcriptional profiles. Particularly, it could help to investigate the cell type specific activity of Delta-Notch components on cell cycle regulation and cell turnover. Additionally, cell-culture experiments could support the analysis. β -cell cell lines, for example Min6 cells, that lack *Dll1* and *Dll4* could be treated with stimulants and checked for insulin secretion. Furthermore, rescue experiments could be interesting and additional *in vivo* experiments are also conceivable. For example, it would be helpful to test whether β -D1D4 mice have altered insulin or glucagon sensitivity that makes the higher secretion of these hormones necessary. Moreover, the observed increase in food consumption could be completed by calorimetric TSE measurements to get a better insight into the energy expenditure of β -D1D4 mice. In this context, seahorse analysis of isolated islets could be performed to investigate the mitochondrial function. Considering additional data from this study, showing exclusive expression of *Jagged1* in α -cells, a mouse model with an α -cell specific *Jagged1* knockdown could be interesting and provide further insight. Based on the hypothesis that loss of DLL1 and DLL4 on β -cells induces α -cell proliferation, it is possible that loss of JAG1 in α -cell leads to certain paracrine effects on β -cells.

Another problem might be the reported expression of *Pdx1* in the hypothalamus. It has been shown recently that the in this work used Pdx1-CreERT mouse line shows ectopic, although weak, *Cre* expression in neurons expressing hypocretin and in neurons activated by leptin (Wicksteed et al. 2010, Mitchell et al. 2017). These neurons maintain body energy balance by sensing the energy status and regulate food intake, blood glucose levels and energy expenditure by inducing appetite (González et al. 2008). It is therefore possible that the observed altered blood glucose levels and the increased food intake of β -D1D4 mice occurred because of a hypothalamic dysregulation. We cannot completely exclude a potential *Cre* expression and consequently altered gene expression within these cells in β -D1D4 mice. However, overall hypothalamic *Cre* expression was much lower as compared to the expression in islets. Moreover, the human protein atlas (<http://www.proteinatlas.org/>) did not show any expression of *Dll1* or *Dll4* in these cells either. Additionally, the increased insulin secretion was also observed *in vitro* independent of any hypothalamic signals, suggesting that most of the observed metabolic phenotype is due to loss of *Dll1* and *Dll4* in β -cells and not

because of altered hypothalamic function. To get a better understanding of a potential hypothalamic effect, it might be advisable to perform additional *in vitro* studies and staining for CRE, DLL1 and DLL4 expression on hypothalamus sections. The usage of a different *Cre*-driver line, for instance MIP-CreERT^{1L^{phii}s}, would be also an option (Wicksteed et al. 2010, Tamarina et al. 2014). But even that *Cre*-driver line is not free from *Cre*-dependent effects, making it necessary to include enough controls that carry the *Cre* gene and were treated with tamoxifen in the same way as the mutant mouse lines, which was part of this project's experimental design (Oropeza et al. 2015).

5.2. What is happening inside the β -cell – the DLL1 intracellular domain

5.2.1. The DLL1 intracellular domain inhabits a function in β -cells

The potential bi-directional signaling of the Delta-Notch pathway is of particular interest and has gained interest over the past few years (Bland et al. 2003, Pintar et al. 2007). However, no clear function and mechanism, *in vivo* or *in vitro* has been shown. A summary of all known functions and appearance of ligand ICDs was provided in the introduction. As mentioned, none of them showed a distinct mechanism or relevance of ICDs. The ubiquitous expression of D1CD in ES cells and mouse embryos did not show blocked proliferation or stimulated neuronal differentiation (Redeker et al. 2013) which is consistent with the observation made in our group using the Ella-Cre promoter (doctoral study from Daniel Gradinger). In both studies the embryos as well as adult mice were viable, fertile and showed no obvious phenotypic alterations, arguing against a signaling function of D1CD (Redeker et al. 2013). A recent publication showed the first physiological role *in vivo* (Furukawa et al. 2016). In mice lacking *Dll1*, the number of CD4⁺ T cells was reduced and the mice exhibited lower clinical scores of experimental autoimmune encephalitis than control mice. This loss of the *Dll1* gene was rescued by retro viral transfection of D1CD in isolated CD4⁺ T cells, which improved the survival rate of these cells (Furukawa et al. 2016). The group described their results as the first *in vivo* function of D1CD, however, these experiments based on isolated and cultured CD4⁺ T cells. Consequently, the cells in the experiment should preferably be called as *ex vivo*. So far, our β -D1CD model is the first real *in vivo* model, where a functional impact of the D1CD is shown. After tamoxifen treatment, all β -D1CD mice were healthy and showed a normal life span. However, as the knockdown mouse models (β -D1, β -D4, and β -D1D4), they revealed an

altered glucose metabolism. Interestingly, β -DICD mice showed opposite metabolic parameters (hyperglycemia, impaired glucose tolerance and impaired insulin secretion) compared to β -D1D4 mice. This further supports the theory that DLL1 and DLL4 are needed for correct insulin secretion and glucose homeostasis. It is assumed, that β -DICD mice allow normal extracellular DLL1 signal transduction, but increased DICD availability within the cell. This model should therefore exclude any extracellular effects on neighboring cells, as seen in the β -D1D4 model on α -cells. Again, altered insulin secretion and glucose homeostasis can be seen as evidence for a β -cell specific requirement of at least DLL1 but perhaps also DLL4. Moreover, this study clearly showed the impact and requirement of the DICD in β -cells. However, the generation of a loss-of-function model for DICD would be very interesting and probably should then show similar metabolic alterations than β -D1D4 mice. However, the development of such a mouse model seems to be rather challenging. In fact, our group tried to establish such a DICD knockdown model, but these mice did not survive and died before birth, most probably due to an unspecific recombination event within the DNA (Christina Hofer, unpublished results), which had crucial effects on embryonic development.

5.2.2. Gene expression analysis

In contrast to the β -D1D4 mice, we can consider that all the observed alterations on the mRNA level were due to changes within the β -cells, because extracellular stimulation can be excluded *per se*. The gene expression of main Delta-Notch components in β -DICD islets was not altered. This is consistent with the observation made by Furukawa et al., who also did not observe altered Notch target gene expression and suggested a mechanism independent of Notch cis-signaling (Furukawa et al. 2016). Similar results were observed in study by Hiratochi et al 2006 using neuronal stem cells, which share some properties with β -cells (Hiratochi et al. 2007, Martens et al. 2011, Eberhard 2013). Moreover, they showed an association of DICD with the TGF- β /Activin pathway through binding SMAD proteins. They also suggested a link between this pathway and the PDZ-domain containing protein MAGI2 (Acvrinp1), which has been shown to bind strongly to the C-terminal PDZ-binding motif of DICD (Pfister et al. 2003). For that reason, it is more likely that DICD acts through an assembling signaling molecule or by protein-protein binding rather than translocation into the nucleus and inducing gene expression directly. This theory is highly attractive, since several PDZ proteins are present in

pancreatic islets or even β -cells (Ort et al. 2000, Wente et al. 2005, Suen et al. 2008). In fact, three MAGI proteins MAGI1, 2 and 3 are expressed in murine pancreatic islets and especially in the laminin expressing basal membrane (Supplementary Figure 4), making them promising potential DICD binding partners in β -cells.

The whole-genome transcriptomics data revealed only very few differentially regulated genes in β -DICD islets, which are associated with the observed phenotype. The most regulated gene was *Pianp* (*PILR alpha associated neural protein*), a gene which is not well understood and mainly expressed in brain (Kogure et al. 2011). It has not yet discovered to be connected to either β -cell function or Delta-Notch signaling. Therefore, this gene should be kept in mind but cannot be associated with a potential function in this mouse model yet.

Ghrelin was the gene that was next most regulated in β -DICD islets compared to controls. *Ghrelin* is present in pancreatic ϵ -cells of humans and rats. Additionally, GHRELIN is secreted to regulate GSIS. Knockout mice for *Ghrelin* show improved glucose tolerance as well as increased insulin secretion and are prevented from high-fat diet induced glucose intolerance (Dezaki et al. 2006). It has been suggested that GHRELIN gets secreted by ϵ -cells to directly inhibit GSIS from β -cells (Egido et al. 2002, Wierup et al. 2004). Similar effects were observed in a human study, where healthy patients were treated with exogenous ghrelin. These patients showed reduced GSIS and glucose clearance. This leads to the suggestion that endogenous GHRELIN regulates insulin secretion from β -cells and antagonizing ghrelin could improve β -cell function and insulin secretion and could therefore be a potential target for diabetes therapy (Meyer 2010, Tong et al. 2010, Brial et al. 2015). The observed higher *Ghrelin* expression would explain the metabolic phenotype of β -DICD mice. However, we could not detect altered levels of endogenous GHRELIN in plasma nor in islets, and immunostaining also did not show an increased amount of GHRELIN⁺ cells. It is therefore thinkable that the increased *Ghrelin* gene expression was an artifact or that we were not able to measure the GHRELIN protein content due to sample degradation. Secondly, on the molecular level we have no clear explanation how DICD overexpression in β -cells can induce *Ghrelin* expression. Up to now, there is no known connection between DICD and *Ghrelin* as well no evidence for transdifferentiation of adult and mature β -cells into new ϵ -cells, which has only been observed during pancreatic development (Prado et al. 2004). Such a transdifferentiation

event is also unlikely, because on the one hand the β -cell mass was not altered in β -D1CD compared to control mice and, on the other hand, we would have detected more GHRELIN⁺ cells by immunohistochemistry, which was not the case.

Another, differentially regulated gene in β -D1CD islet was adenylyl cyclase 5 (*Adcy5*), which is able to influence Ca²⁺ concentrations. ADCY5 was found in islet exon-eQTL studies and to be associated with T2DM (Dupuis et al. 2010, van de Bunt et al. 2015). In human islets, silencing of *Adcy5* lead to impaired glucose tolerance as result of a reduced cAMP production. It was suggested that ADCY5 is activated by glucose rather than by the incretin GLP1, which is primarily connected to the cAMP-signaling pathway during insulin secretion (Hodson et al. 2014). Instead, ADCY5 is required to increase intracellular Ca²⁺ for insulin granule exocytosis after glucose stimulation (Hodson et al. 2014). This could explain why we observed impaired GSIS even after stimulation with Forskolin and Exendin-4. ADCY5 is active downstream of both stimulants and in case of Forskolin dependent on the adenylyl cyclase (Laurenza et al. 1989, Göke et al. 1993). In β -D1CD islets, ADCY5 is downregulated and therefore not available for cAMP production.

5.2.2.1. Genes that state for a compensatory effect

In addition, several genes that are associated with altered glucose homeostasis and insulin secretion were differentially regulated in β -D1CD. For instance, hepatocyte nuclear factor-1alpha (*Hnf1a*), which encodes for a transcription factor controlling β -cell function and is the most common gene locus for genetic modifications in maturity onset diabetes of the young (MODY3) (Servitja et al. 2009). Patients with MODY3 progressively develop a severe hyperglycemia and have attenuated early phase insulin secretion due to pancreatic β -cell dysfunction (Ekholm et al. 2012). Mice heterozygous for a *Hnf1a* mutation displayed β -cell dysfunction and develop monogenic diabetes (Servitja et al. 2009). Moreover, suppression of *Hnf1a* in transgenic mice leads to diabetes, impaired glucose tolerance and reduced GSIS at a juvenile age of 6 weeks. The insulin content in these animals is decreased whereas the glucagon content is increased (Hagenfeldt-Johansson et al. 2001). β -D1CD islets showed a 1.3-fold higher *Hnf1a* gene expression than control islets, pointing more towards the opposite mechanism or a compensatory pathway. Additionally, the HNF1 α downstream target *Slc2a2* (Cha et al. 2000) was upregulated, proving a functional aspect of HNF1 α in these islets. As

mentioned earlier for the β -D1D4 model, GLUT2 is the main glucose transporter in pancreatic β -cells (Thorens 2015) and an upregulation should improve glucose uptake and metabolism, which was not observed in β -D1CD mice. Also for β -D1CD mice, a compensatory mechanism to prevent further hyperglycemia or even the development of a diabetic state is likely. However, it has been shown that during a hyperglycemic clamp *Slc2a2* mRNA increases in rat islets to prevent early glucotoxicity (Chen et al. 1990), which might be also the case in β -D1CD mice. Interestingly, GLUT2 is not the only glucose transporter that showed an altered gene expression level in β -D1CD islets. *Glut1* (*Slc2a1*) was found to be 1.5-fold downregulated, which could have led to decreased glucose homeostasis. Nevertheless, GLUT1 does not seem to be more important for glucose sensing in mouse islets than GLUT2 and both cannot compensate each other (De Vos et al. 1995, Guillam et al. 2000, Hosokawa et al. 2001).

Another gene which showed a 2-fold upregulation in β -D1CD islets is the antiaging gene *Klotho*, which is further linked to control of blood pressure, regulation of cholesterol and bone mineral density as well as glucose metabolism and T2DM (Razzaque 2012). The gene is expressed in islets and has shown to be required for the pancreatic hormone content. Mice lacking *Klotho* show decreased insulin production, but improved glucose tolerance due to increased insulin sensitivity (Utsugi et al. 2000). In contrast, *Klotho* overexpression enhances GSIS by increasing the intracellular Ca^{2+} influx in Min6 cells. In our study, it is more likely that *Klotho* possess a counter regulatory function in β -D1CD β -cells, similar to the study in Min6 cells. The *Klotho* knockout mice are whole-body knockouts and the observed metabolic alterations were suggested to be associated with decreased white adipose tissue and increased insulin sensitivity in adipocytes due to adipocyte differentiation and maturation (Utsugi et al. 2000, Razzaque 2012). Interestingly, the antiaging function of KLOTHO was suggested to be dependent on Wnt signaling. Ectopic *Klotho* expression can antagonize Wnt signaling and *Klotho* knockout mice show increased Wnt signaling (Liu et al. 2007). The Wnt pathway could be the missing link between *Klotho* and D1CD, because the Wnt pathway is not only required during pancreatic development, but is also one of the few pathways (Tgf β , PDZ proteins, Wnt) associated with D1CD (Murtaugh 2008, Bordonaro et al. 2011).

Of note, the gene *Galanin* (*Gal*) was more than 2-fold downregulated in β -D1CD islets. *Galanin* has been shown to inhibit basal and stimulated insulin secretion and stimulate glucagon

secretion in mice and dogs. Consequently, *Galanin* mutant animals became hyperglycemic (McDonald et al. 1985, Lindskog et al. 1987). Galanin hyperpolarized and reduces spontaneous electrical activity by activating a population of K_{ATP} channels. Glibenclamide, a drug for diabetes treatment, can block galanin-activated K_{ATP} channels (de Weille et al. 1988, Balsells et al. 2015). Nevertheless, remains the connection to DICD unknown, but as *Klotho*, *Galanin* has impact on the membrane depolarization and Ca^{2+} concentration.

5.2.3. What is the mechanism behind Delta in islets?

The explicit mechanism underlying the Notch ligands and DICD in β -cells still remains unclear. However, based on literature research and on the results of the gene expression analysis as well as the collected experimental data in this thesis, some pathways are more likely than others.

In this context, a first hint for a possible mechanism is the detected downregulation of *Ctgf*, which encodes for transcription factor that is among the few proteins that have been associated with DICD (Bordonaro et al. 2011). In the study by Bordonaro et al. with colon cancer cells DICD showed two activities. On the one side, DICD enhanced the Wnt/ β -catenin transcriptional activity and, on the other side, was able to bind to and increase the activity of the *Ctgf* promoter (Bordonaro et al. 2011). Contradictory to these results, in our study the overexpression of DICD in β -cells showed a downregulation of *Ctgf* compared to control islets. Nevertheless, CTGF could have divergent functions in different tissues and cell states (cancer vs. normal). In islets, CTGF has been shown to be expressed and required for the β -cell maturity and proliferation (Crawford et al. 2009, Riley et al. 2014). In β -DICD mice both maturity and proliferation seem to be not affected. However, one has to note that the study by Riley et al. was performed after partial β -cell destruction. Under non-stimulatory conditions, they did not observed changes in both functions, either. An additional study with damaged β -cells (i.e. streptozocin treatment) in β -DICD mice could provide further insight about the relevance and function of CTGF in this model. More recently, CTGF has been shown to have an impact on β -cell function especially during pregnancy. Pregnant female mice lacking *Ctgf* in endocrine cells, showed gestational diabetes, hyperglycemia and glucose intolerance due to impaired insulin secretion and not due to reduced maternal β -cell proliferation (Pasek et al. 2016). Thus, a potential connection between the downregulation of

Ctgf and the observed phenotype in β -D1CD mice could be conceivable. This hypothesis could be scrutinized by performing a chromatin-immunoprecipitation to test whether D1CD binds to the *Ctgf* promoter as seen in colon cancer cells. Moreover, an *in vitro* rescue experiment with exogenous *Ctgf* could be worthwhile.

Of further interest was the Ingenuity analysis based on the whole-genome transcriptome analysis. Here, especially proteins correlated to the VEGF network were found to be differentially regulated. VEGF is required for proper vascularization of the pancreatic islets (Lammert et al. 2003), is essential to sense glucose levels and to secrete hormones directly into the blood stream (Brissova et al. 2006). The relevance of Delta-Notch signaling for the vascular system has been described many times before (Gridley 2007, Roca et al. 2007, Thurston et al. 2008, Gridley 2010). Most of the studies regarding islet vascularization detected VEGF as critical factor. In β -D1CD islets, *Vegf* mRNA was normally expressed, however, several to VEGF associated genes were differentially expressed. On the other hand, the analysis of the vascular system within β -D1CD islets was inconspicuous. However, it has to be considered that this analysis was performed only on 9 μ m thick tissue slides and whole islets were not imaged for vascular integrity. To exclude a defect within the vascular system, whole islets need to be analyzed under confocal microscopy using z-stacks to receive complete 3D images (Brissova et al. 2005, El-Gohary et al. 2012). However, an insufficient vascularization in β -D1CD islets might explain the observed phenotype. Mice with reduced VEGF expression have normal pancreatic islet insulin contents and β -cell mass, but impaired GSIS due to a reduced blood flow (Brissova et al. 2006).

Also revealed by whole genome transcriptomics of β -D1CD and control islets was a conspicuous accumulation differentially regulated genes related to the SLIT-ROBO pathway. This pathway has been associated originally with neuronal axon guidance but also in many types of cancer and the reproductive system, which was reviewed by Brose et al., Gara et al. and Dickinson et al., (Brose et al. 2000, Dickinson et al. 2010, Gara et al. 2015). Recently, the presence and relevance of SLIT-ROBO signaling in islets has been discovered, which was demonstrated to be required for beta-cell survival. Furthermore, SLIT-ROBO potentiates insulin secretion by controlling the release of Ca^{2+} from the ER and actin remodeling (Yang et al. 2013). A graphical overview of SLIT-ROBO in islets is displayed in Figure 39.

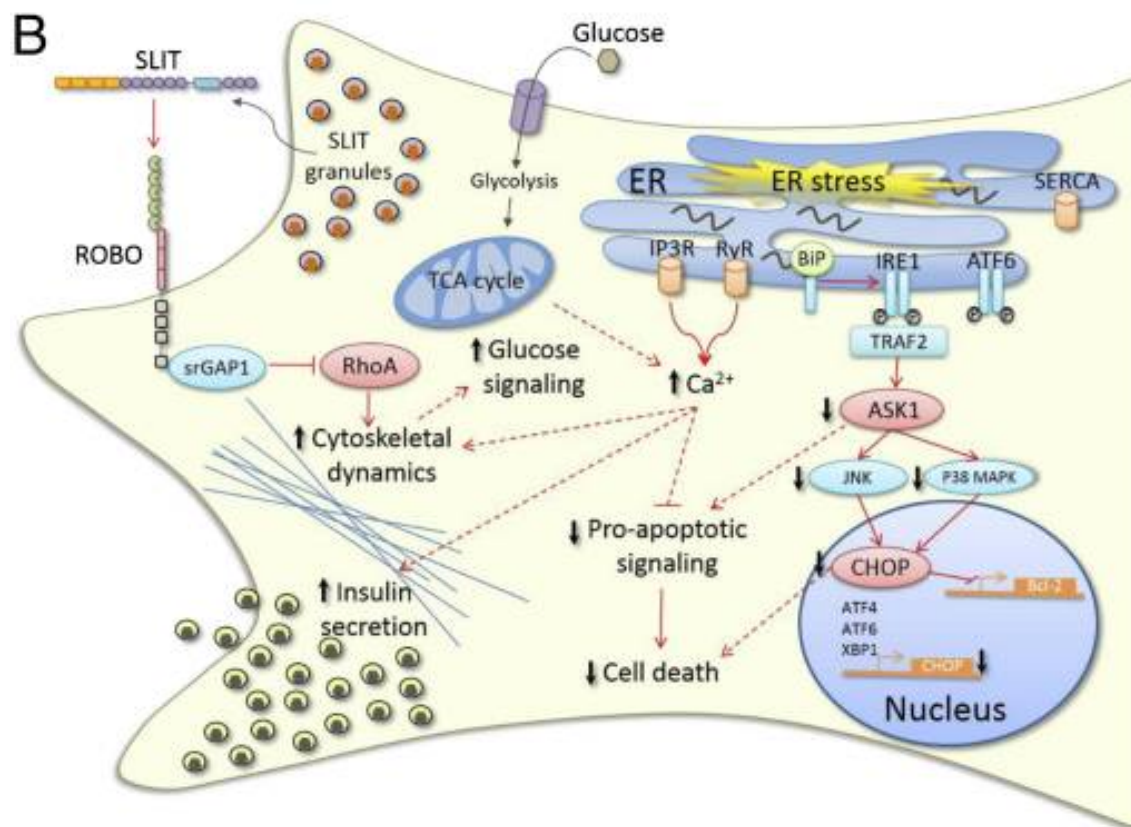


Figure 39: Model of Slit–Robo signaling in pancreatic beta cells
 Secreted SLIT proteins bind to ROBO receptors and activate srGAPs. This leads to changes in the cytoskeleton and also influences ER stress and apoptosis. Illustration is adapted from Yang et al. 2013.

Moreover, SLIT proteins do not affect *Ins1* and *Ins2* gene transcription but acting mechanistically downstream of adenylyl cyclase, which would explain why observed impaired insulin secretion in β -DICD islets even after Forskolin treatment. In β -DICD islets, the genes *Slit2*, *Slit3*, *Srgap1* and *Srgap3* as well as genes associated with the cytoskeleton (*Tubb1*, *Myh11* and *Actg2*) were all downregulated indicating a clear involvement of this pathway in β -DICD mice. The loss of these genes in β -DICD could lead to reduced ROBO and srGAP activation on β -cells and cellular migrations, which in turn leads to ER stress, reduced Ca^{2+} influx and subsequently reduced insulin secretion. Delta-Notch signaling has been shown to regulate cell-cell adhesion molecules and cytoskeletal components and to be connected to the SLIT-ROBO pathway (Bayless et al. 2011, Bonini et al. 2013). For instance, mice lacking *Robo* show cardiac defects by down regulating Notch signaling (Mommersteeg et al. 2015). Additionally, ROBO receptors maintain cortical progenitor balance during neurogenesis

through interaction with the Notch pathway by controlling *Hes1* transcription (Borrell et al. 2012).

Considering all suggested pathways and the underlying differentially regulated genes in both β -D1D4 and β -DICD islets, the correlation of the Delta-Notch with the adenylyl cyclase and Ca^{2+} dependent pathways of insulin secretion might be the affected mechanism causal to the observed phenotypes. What still remains unknown is how and whether Delta-Notch can directly influence insulin secretion. The β -DICD model supports the conclusion that the intracellular domains of Notch ligands are critical in β -cells. It is questionable whether DICD enters the nucleus and regulates gene expression directly, because most of the differentially regulated genes are not directly associated with impaired insulin secretion but with associated pathways. However, it cannot be excluded completely, since known target genes of DICD like *Ctgf* were found to be differentially regulated. Another, possibly more likely mechanism underlying the observed phenotypes is mediated through protein-protein interactions. As mentioned before, PDZ proteins are the most likely proteins that are directly associated with DICD (Pfister et al. 2003). Recently, our group established binding studies with DICD and a selection of PDZ proteins. These analyses revealed that DICD is able to bind with high affinity to PDZD2 (Diller et al. unpublished), a protein which was found to be exclusively expressed in β -cells (Ma et al. 2006). Interestingly, PDZD2 is the only PDZ protein that bind DICD and is known to have crucial effects on insulin secretion *in vivo* and *in vitro* (Tsang et al. 2010). PDZD2 depletion leads to increased insulin secretion by changing the activity of K_{ATP} channels and consequently opening of the Ca^{2+} channels. The overexpression of DICD leads to an opposite effect, suggesting DICD in a functional cooperation with PDZD2. In addition, PDZ proteins can regulate the traffic and function of GPCR, which has further impact on the downstream signaling including adenylyl cyclase activity and PKA or EPAC2 signaling (Romero et al. 2011). For instance, the DICD binding and PDZ protein MAGI1 (Diller et al. unpublished) has been shown to interact with EPAC2 in vascular endothelial cells (Sakurai et al. 2006) pointing towards a potential role also in EPAC2 associated insulin secretion.

5.2.4. Conclusion and future perspectives

Based on previous studies on ligand ICDs, it was on a first view surprising that the β -DICD mouse model developed such a robust phenotype. It is the first adult *in vivo* model, where

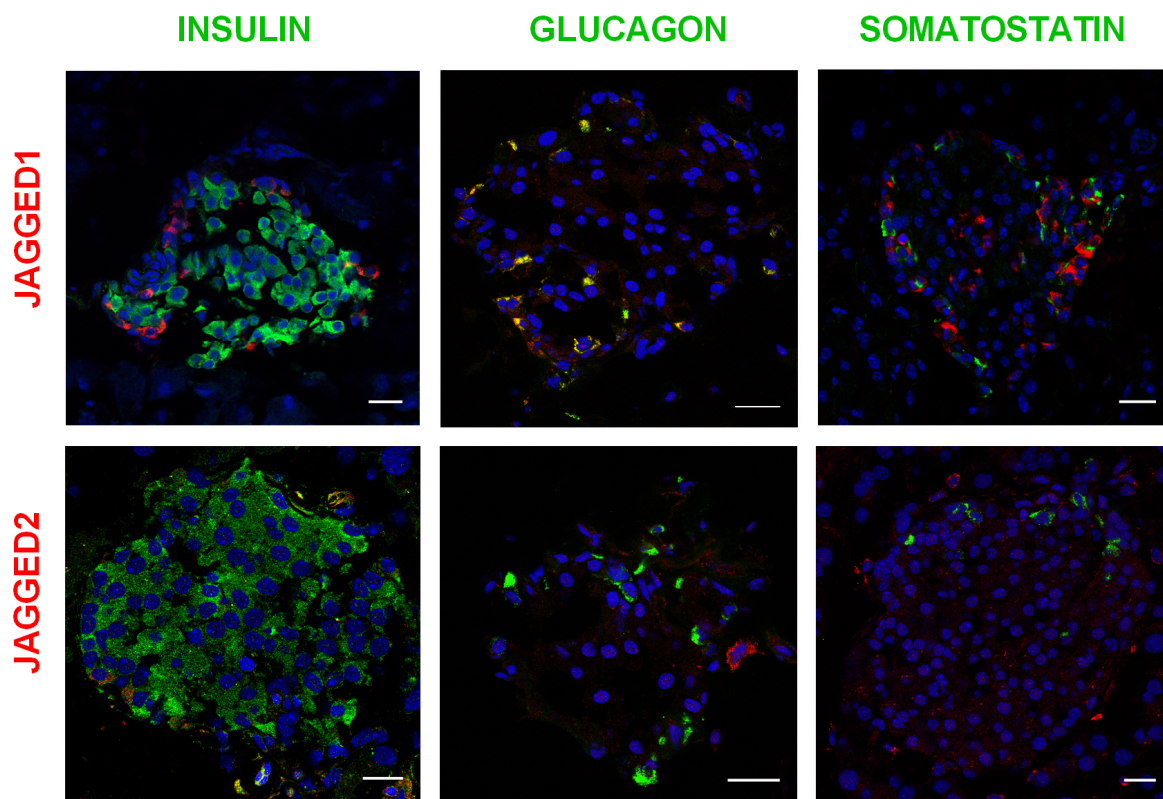
DICD could be assigned to a tissue-specific function. According to our findings for the ligand knockdown models, it could be even more interesting to analyze the ICD of DLL4. This study provided several potential pathways that might be relevant for the observed phenotypes, but none of them could be clarified. It is therefore critical to perform further experiments regarding these pathways. For instance, to prove the action on the Ca^{2+} influx and cAMP content, islet lysates could be checked for both factors using specific ELISAs. In addition, chromatin-immunoprecipitations could provide insight into possible transcription factor activities of DICD and downstream targets. Furthermore, extended protein-binding studies could reveal the known and even unknown binding partners of DICD in β -cells. Taken together, such experiments would possibly provide a complete picture about the function of DICD in β -cells and its connection to the observed insulin secretion defect. Also, interestingly would be the combination of the β -D1D4 and β -DICD mouse models by using two different inducible β -cell specific *Cre* lines. For example, by using one *Cre*-line being active upon tetracycline treatment and the other one being active upon tamoxifen treatment, it would be possible to delete first the ligand genes *Dll1* and *Dll4* to induce a hypoglycemic state, and then to induce DICD overexpression. Said study would clarify whether the ligand ICD alone is sufficient to recover from hypoglycemia and improve glucose tolerance by increasing insulin secretion.

5.3. Closing remarks

The results obtained within this study confirmed a role for DLL1 and DLL4 not only during pancreatic development but also in adult islets of Langerhans. While the knockdown of only one ligand gene each in pancreatic β -cells led to opposing phenotypes regarding glucose homeostasis, the simultaneous knockdown of both *Dll1* and *Dll4* in β -cells results in severe hypoglycemia and improved glucose tolerance, because of a significantly increased insulin secretion. An influence of Delta-Notch on insulin secretion was additionally confirmed by the β -cell specific overexpression of the D1CD only. Taken together, this thesis provides the first description on the function of Delta-Notch ligands in the adult pancreas. Moreover, the work provides the first *in vivo* mouse model, where the intracellular domain of the Delta ligand is ascribed to an important function. In conclusion, studies analyzing the role of ligand ICDs are more promising than previously assumed. Finally, Delta-Notch signaling could be a potential target for diabetes therapy.

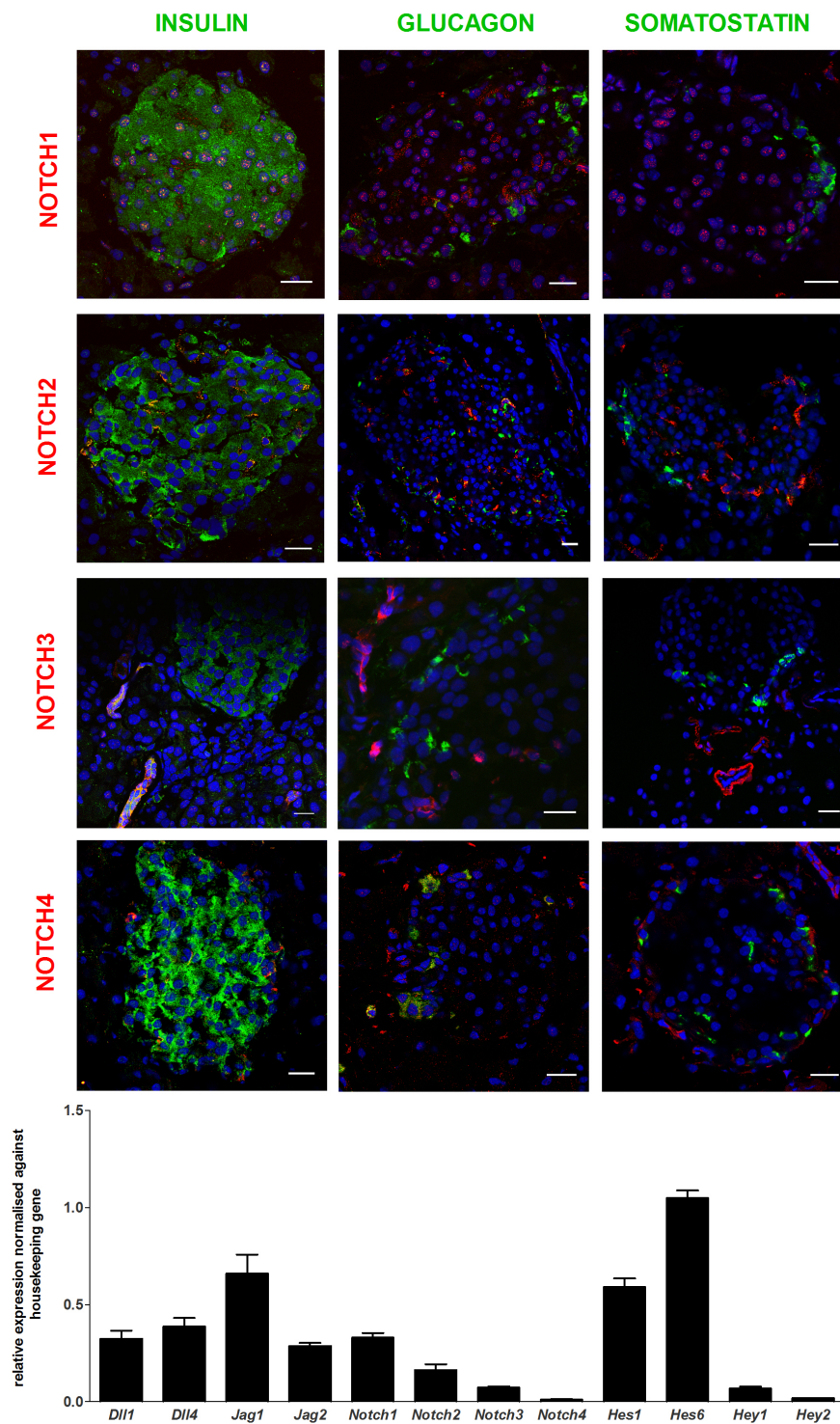
6. APPENDIX

6.1. Supplementary figures



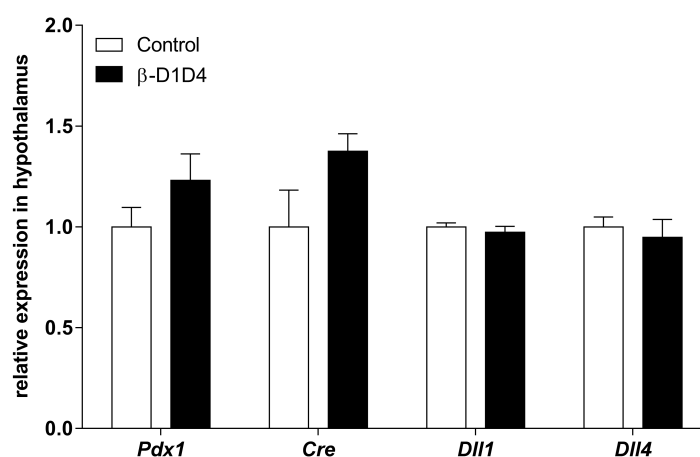
Supplementary Figure 1: Protein expression of Notch ligands

Co-immunostaining of ligands JAGGED1 and JAGGED2 with β - (insulin), α - (glucagon) and δ -cell (somatostatin) specific markers on pancreatic sections from 13-weeks old male C3HeB/FeJ (n= 3-5). Nuclei were counterstained with DAPI (blue). The scale bar represents 20 μ m.



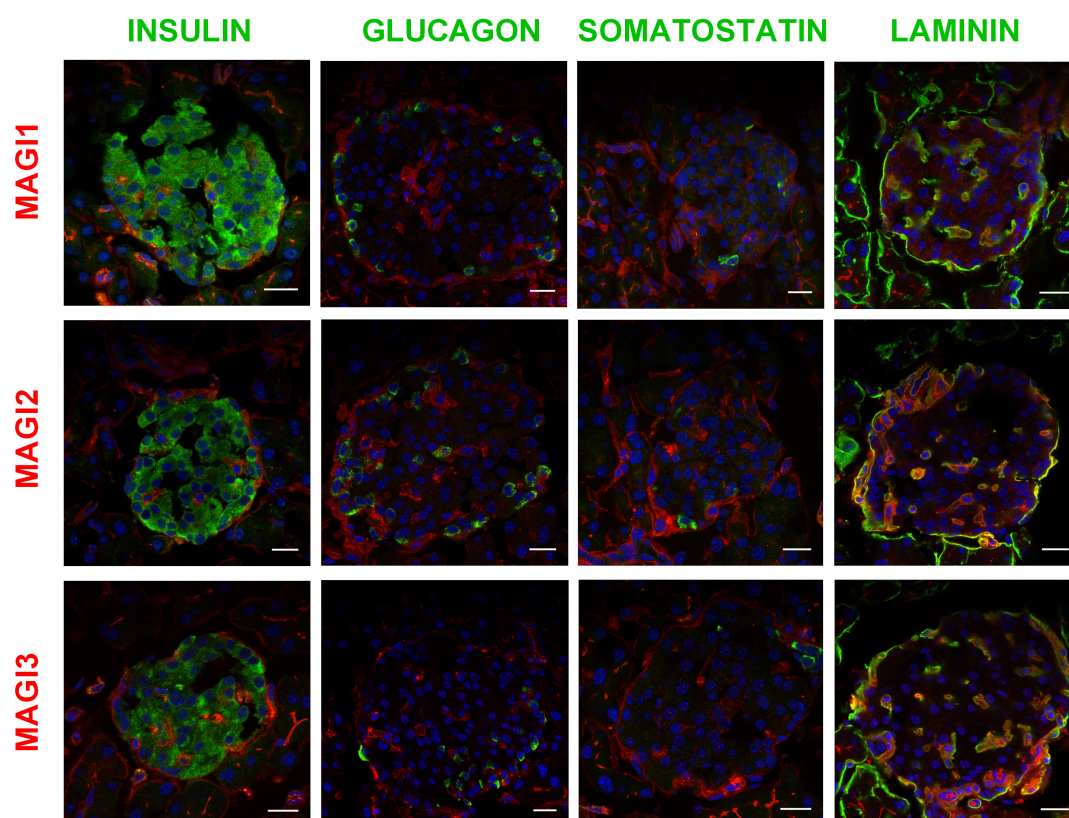
Supplementary Figure 2: Protein expression of Notch receptors

CO-immunostaining of Notch receptors NOTCH1, NOTCH2, NOTCH3 and NOTCH4 with β - (insulin), α - (glucagon) and δ -cell (somatostatin) specific markers on pancreatic sections from 13-weeks old male C3HeB/FeJ mice (n= 3-5). Nuclei were counterstained with DAPI (blue). The scale bar represents 20 μ m. qRT-PCR analysis for gene expression levels of D/N components in isolated islets from 8-weeks old male C3HeB/FeJ I mice (n=5) compared to the housekeeping gene *Hprt*.



Supplementary Figure 3: qRT-PCR analysis of the hypothalamus from 8-weeks old male β -DICD and Cre-positive control mice.

Expression levels of *Pdx1*, *Cre recombinase*, *Dll1* and *Dll4* were assessed by qRT-PCR (n=6). Expression was normalized to the housekeeping genes *Sdha* and *Ubc*. Differences were considered statistically significant at $p < 0.05$ using a heteroscedastic two-tailed Student's t-test. Data are shown as mean \pm SEM.



Supplementary Figure 4: Protein expression of MAGI proteins.

CO-immunostaining of Notch receptors MAGI1, MAGI2 and MAGI3 with β - (insulin), α - (glucagon), δ -cell (somatostatin) and extracellular matrix (laminin) specific markers on pancreatic sections from 13-weeks old male C3HeB/FeJ mice (n= 3-5). Nuclei were counterstained with DAPI (blue). The scale bar represents 20 μ m.

6.2. Supplementary tables

Supplementary Table 1: Differentially expressed genes in isolated islets from 8-weeks old male β -D1D4 and Cre-positive control mice (4.1.5.3) filtered for a fold change of at least 1.3, FDR <10% and p<0.01

Gene Symbol	Gene Name	β -D1D4/Control
<i>Msln</i>	mesothelin	-4,23
4833420G17Rik	RIKEN cDNA 4833420G17 gene /// RIKEN cDNA 4833420G17 gene	-4,12
<i>Hist3h2ba</i>	histone cluster 3, H2ba /// histone cluster 3, H2bb, pseudogene	-4,09
<i>Bambi-ps1</i>	BMP and activin membrane-bound inhibitor, pseudogene (<i>Xenopus laevis</i>)	-3,42
<i>Tmsb15b1</i>	thymosin beta 15b1 /// thymosin beta 15b like /// thymosin beta 15b2	-3,21
<i>H2-Ea-ps</i>	histocompatibility 2, class II antigen E alpha, pseudogene /// histocompatibility 2, class II antigen E alpha, pseudogene	-3,14
<i>Rhox3f</i>	reproductive homeobox 3F /// reproductive homeobox 3E /// reproductive homeobox 3C /// reproductive homeobox 3A /// reproductive homeobox 3G /// reproductive homeobox 3H /// reproductive homeobox 2B /// predicted gene, 21085 /// reproductive homeobox 3, pseudogene /// reproductive homeobox 3B	-2,70
<i>Gm9855</i>	thymine DNA glycosylase pseudogene /// thymine DNA glycosylase /// predicted pseudogene 9855	-2,63
<i>Slc26a1</i>	solute carrier family 26 (sulfate transporter), member 1	-2,39
<i>Gm17767</i>	predicted gene, 17767	-2,30
<i>Tmem255a</i>	transmembrane protein 255A	-2,26
<i>Rhox3f</i>	reproductive homeobox 3F /// reproductive homeobox 3E /// reproductive homeobox 3C /// reproductive homeobox 3A /// reproductive homeobox 3G /// reproductive homeobox 3H /// reproductive homeobox 2B /// predicted gene, 21085 /// reproductive homeobox 3, pseudogene /// reproductive homeobox 3B	-2,10
<i>Aqp4</i>	aquaporin 4	-2,09
<i>Krt80</i>	keratin 80 /// keratin 80	-2,09
<i>Jmjd7-pla2g4b</i>	Jmjd7-Pla2g4b readthrough /// jumonji domain containing 7 /// phospholipase A2, group IVB (cytosolic)	-2,08
1700020I14Rik	RIKEN cDNA 1700020I14 gene /// RIKEN cDNA 1700020I14 gene	-2,03
<i>Pttg1</i>	pituitary tumor-transforming gene 1 /// pituitary tumor-transforming gene 1	-1,97

Gm14403	predicted gene 14403	-1,89
Col8a1	collagen, type VIII, alpha 1	-1,88
Insrr	insulin receptor-related receptor	-1,86
Rap1gapos	RAP1 GTPase activating protein, opposite strand /// RIKEN cDNA 1810058N05 gene	-1,85
Rab38	RAB38, member RAS oncogene family	-1,85
Upp2	uridine phosphorylase 2	-1,83
Gstk1	glutathione S-transferase kappa 1	-1,82
Cib3	calcium and integrin binding family member 3	-1,81
Gm20448	predicted gene 20448	-1,81
Prss23os	protease, serine 23, opposite strand /// RIKEN cDNA 1700019G06 gene	-1,73
17547971		-1,73
Adora2b	adenosine A2b receptor	-1,71
2410021H03Rik	RIKEN cDNA 2410021H03 gene	-1,69
Pax6os1	paired box 6 opposite strand 1 /// paired box 6 opposite strand 1	-1,69
Rhox3f	reproductive homeobox 3F /// reproductive homeobox 3E /// reproductive homeobox 3C /// reproductive homeobox 3A /// reproductive homeobox 3G /// reproductive homeobox 3H /// reproductive homeobox 2B /// predicted gene, 21085 /// reproductive homeobox 3, pseudogene /// reproductive homeobox 3B	-1,69
Vil1	villin 1	-1,68
Cdhr1	cadherin-related family member 1	-1,65
Sult1d1	sulfotransferase family 1D, member 1	-1,64
ND3	NADH dehydrogenase subunit 3	-1,64
Anpep	alanyl (membrane) aminopeptidase	-1,63
1700028I16Rik	RIKEN cDNA 1700028I16 gene /// RIKEN cDNA 1700028I16 gene	-1,63
3110070M22Rik	RIKEN cDNA 3110070M22 gene /// RIKEN cDNA 3110070M22 gene	-1,63
Fkbp1b	FK506 binding protein 1b	-1,62
Itgb8	integrin beta 8 /// integrin beta 8	-1,62
Glp1r	glucagon-like peptide 1 receptor	-1,62
Met	met proto-oncogene	-1,61
Mlxipl	MLX interacting protein-like	-1,60
Amph	amphiphysin /// amphiphysin /// amphiphysin	-1,60
Chmp4c	charged multivesicular body protein 4C	-1,60
Lypd8	LY6/PLAUR domain containing 8	-1,60
Mreg	melanoregulin	-1,59
Nell1	NEL-like 1	-1,59
Cer1	cerberus 1 homolog (<i>Xenopus laevis</i>)	-1,59
Grk5	G protein-coupled receptor kinase 5	-1,58
ND3	NADH dehydrogenase subunit 3	-1,58

Zkscan16	zinc finger with KRAB and SCAN domains 16	-1,58
Pcyt1b	phosphate cytidylyltransferase 1, choline, beta isoform	-1,58
Gm11789	predicted gene 11789 /// predicted gene 11789	-1,58
Ikzf2	IKAROS family zinc finger 2	-1,57
Hist1h3f	histone cluster 1, H3f /// histone cluster 2, H3b /// histone cluster 1, H3e /// histone cluster 1, H3b /// histone cluster 1, H3d /// histone cluster 1, H3c /// histone cluster 2, H3c2 /// histone cluster 2, H3c1	-1,57
Olfm3	olfactomedin 3	-1,57
Ank2	ankyrin 2, brain	-1,57
Ap1s2	adaptor-related protein complex 1, sigma 2 subunit	-1,57
Ust	uronyl-2-sulfotransferase	-1,56
T2	brachyury 2 /// brachyury 2 /// brachyury 2	-1,56
Fn3k	fructosamine 3 kinase /// fructosamine 3 kinase	-1,56
Efhc1	EF-hand domain (C-terminal) containing 1	-1,56
Lgi1	leucine-rich repeat LGI family, member 1 /// leucine-rich repeat LGI family, member 1	-1,55
Gm9958	predicted gene 9958 /// predicted gene 9958	-1,54
Galnt13	UDP-N-acetyl-alpha-D-galactosamine:polypeptide N-acetylgalactosaminyltransferase 13	-1,54
Tsga10	testis specific 10 /// testis specific 10	-1,54
17213578		-1,53
4933432K03Rik	RIKEN cDNA 4933432K03 gene	-1,53
Nfix	nuclear factor I/X	-1,52
Gm4924	predicted gene 4924 /// predicted gene 4924	-1,52
Cabp7	calcium binding protein 7	-1,52
Hist3h2a	histone cluster 3, H2a	-1,52
Pigr	polymeric immunoglobulin receptor	-1,52
Dll4	delta-like 4 (Drosophila)	-1,51
Atp1b2	ATPase, Na ⁺ /K ⁺ transporting, beta 2 polypeptide /// ATPase, Na ⁺ /K ⁺ transporting, beta 2 polypeptide	-1,51
4933406P04Rik	RIKEN cDNA 4933406P04 gene /// RIKEN cDNA 4933406P04 gene	-1,51
Gpr165	G protein-coupled receptor 165	-1,51
Ocel1	occludin/ELL domain containing 1	-1,51
Cped1	cadherin-like and PC-esterase domain containing 1	-1,50
Zfyve21	zinc finger, FYVE domain containing 21	-1,49
Hepacam2	HEPACAM family member 2	-1,49
Ucn3	urocortin 3	-1,47
Glo1	glyoxalase 1 /// predicted gene 13443	-1,47
Slco2a1	solute carrier organic anion transporter family, member 2a1	-1,47
Synj2	synaptojanin 2	-1,47
NONMMUT002671		-1,46

<i>Naip2</i>	NLR family, apoptosis inhibitory protein 2	-1,45
<i>Lgr4</i>	leucine-rich repeat-containing G protein-coupled receptor 4	-1,45
<i>Kcnk16</i>	potassium channel, subfamily K, member 16	-1,44
<i>Mansc1</i>	MANSC domain containing 1	-1,44
<i>Itfg3</i>	integrin alpha FG-GAP repeat containing 3	-1,44
<i>Sirt5</i>	sirtuin 5 /// sirtuin 5	-1,44
<i>Zfp113</i>	zinc finger protein 113	-1,44
<i>Me3</i>	malic enzyme 3, NADP(+)-dependent, mitochondrial	-1,44
<i>Edem2</i>	ER degradation enhancer, mannosidase alpha-like 2	-1,44
<i>Ppp1r10</i>	protein phosphatase 1, regulatory subunit 10	-1,44
<i>17495673</i>		-1,44
<i>Rcan2</i>	regulator of calcineurin 2 /// regulator of calcineurin 2	-1,43
<i>Sqrdl</i>	sulfide quinone reductase-like (yeast)	-1,43
<i>Dcdc2a</i>	doublecortin domain containing 2a /// doublecortin domain containing 2a	-1,43
<i>9230110C19Rik</i>	RIKEN cDNA 9230110C19 gene	-1,43
<i>Cdh7</i>	cadherin 7, type 2	-1,42
<i>Dcaf12l1</i>	DDB1 and CUL4 associated factor 12-like 1	-1,42
<i>Kcnj12</i>	potassium inwardly-rectifying channel, subfamily J, member 12 /// potassium inwardly-rectifying channel, subfamily J, member 12	-1,42
<i>Itpkb</i>	inositol 1,4,5-trisphosphate 3-kinase B	-1,42
<i>Efhc2</i>	EF-hand domain (C-terminal) containing 2	-1,42
<i>Bckdhb</i>	branched chain ketoacid dehydrogenase E1, beta polypeptide	-1,41
<i>LOC102641857</i>	uncharacterized LOC102641857 /// RIKEN cDNA D630024D03 gene	-1,41
<i>Epm2aip1</i>	EPM2A (laforin) interacting protein 1	-1,41
<i>Cers6</i>	ceramide synthase 6	-1,40
<i>Pomgnt2</i>	protein O-linked mannose beta 1,4-N-acetylglucosaminyltransferase 2	-1,40
<i>Fert2</i>	fer (fms/fps related) protein kinase, testis specific 2 /// fer (fms/fps related) protein kinase, testis specific 2	-1,40
<i>Npnt</i>	nephronectin	-1,40
<i>2810468N07Rik</i>	RIKEN cDNA 2810468N07 gene /// RIKEN cDNA 2810468N07 gene	-1,39
<i>2310034G01Rik</i>	RIKEN cDNA 2310034G01 gene	-1,39
<i>X61497</i>		-1,38
<i>Rnf138rt1</i>	ring finger protein 138, retrogene 1	-1,38
<i>Prune2</i>	prune homolog 2 (Drosophila) /// prune homolog 2 (Drosophila)	-1,37
<i>Ush2a</i>	Usher syndrome 2A (autosomal recessive, mild)	-1,37

Engase	endo-beta-N-acetylglucosaminidase	-1,37
Cdx4	caudal type homeobox 4	-1,37
Dcaf8	DDB1 and CUL4 associated factor 8 /// DDB1 and CUL4 associated factor 8	-1,37
17515340		-1,37
Negr1	neuronal growth regulator 1	-1,37
Gcgr	glucagon receptor	-1,37
Ropn1l	ropporin 1-like	-1,36
Ckmt1	creatine kinase, mitochondrial 1, ubiquitous	-1,36
Pdk2	pyruvate dehydrogenase kinase, isoenzyme 2 /// pyruvate dehydrogenase kinase, isoenzyme 2	-1,36
Scnn1b	sodium channel, nonvoltage-gated 1 beta	-1,36
Pdzk1ip1	PDZK1 interacting protein 1	-1,36
Ccrl2	chemokine (C-C motif) receptor-like 2	-1,36
Rspo4	R-spondin family, member 4	-1,35
Insig1	insulin induced gene 1	-1,35
Zfp386	zinc finger protein 386 (Kruppel-like) /// zinc finger protein 386 (Kruppel-like)	-1,35
Kcnmb2	potassium large conductance calcium-activated channel, subfamily M, beta member 2	-1,34
Trmt2b	TRM2 tRNA methyltransferase 2B	-1,34
Atp2a3	ATPase, Ca++ transporting, ubiquitous	-1,34
Spock2	sparc/osteonectin, cwcv and kazal-like domains proteoglycan 2	-1,33
Cpb2	carboxypeptidase B2 (plasma)	-1,33
Cntfr	ciliary neurotrophic factor receptor	-1,33
1810021B22Rik	RIKEN cDNA 1810021B22 gene /// RIKEN cDNA 1810021B22 gene /// RIKEN cDNA 1810021B22 gene	-1,32
Ddx31	DEAD/H (Asp-Glu-Ala-Asp/His) box polypeptide 31	-1,32
Ret	ret proto-oncogene	-1,32
17485586		-1,31
Bphl	biphenyl hydrolase-like (serine hydrolase, breast epithelial mucin-associated antigen) /// biphenyl hydrolase-like (serine hydrolase, breast epithelial mucin-associated antigen)	-1,31
Gm572	predicted gene 572	-1,31
Cxx1c	CAAX box 1C	-1,31
9530077C05Rik	RIKEN cDNA 9530077C05 gene	-1,31
Fam135a	family with sequence similarity 135, member A /// family with sequence similarity 135, member A	1,31
Angptl6	angiopoietin-like 6	1,31
Gm13669	predicted gene 13669 /// proteolipid protein 2 /// predicted gene 13669	1,31
Ezr	ezrin	1,31
Rnf41	ring finger protein 41 /// ring finger protein 41	1,32

<i>Pacsin2</i>	protein kinase C and casein kinase substrate in neurons 2	1,32
<i>Elk3</i>	ELK3, member of ETS oncogene family /// ELK3, member of ETS oncogene family	1,33
<i>Thg1l</i>	tRNA-histidine guanylyltransferase 1-like (<i>S. cerevisiae</i>) /// tRNA-histidine guanylyltransferase 1-like (<i>S. cerevisiae</i>)	1,33
<i>6030458C11Rik</i>	RIKEN cDNA 6030458C11 gene /// RIKEN cDNA 6030458C11 gene	1,34
<i>Ifrd1</i>	interferon-related developmental regulator 1 /// interferon-related developmental regulator 1	1,35
<i>Asap3</i>	ArfGAP with SH3 domain, ankyrin repeat and PH domain 3	1,35
<i>Plp2</i>	proteolipid protein 2	1,35
<i>Prickle3</i>	prickle homolog 3 (<i>Drosophila</i>)	1,36
<i>Elp6</i>	elongator acetyltransferase complex subunit 6	1,36
<i>Stk35</i>	serine/threonine kinase 35	1,36
<i>Xpot</i>	exportin, tRNA (nuclear export receptor for tRNAs)	1,37
<i>Mir674</i>	microRNA 674 /// microRNA 674	1,37
<i>Smarca1</i>	SWI/SNF related, matrix associated, actin dependent regulator of chromatin, subfamily a, member 1	1,37
<i>Cd24a</i>	CD24a antigen	1,37
<i>Snhg1</i>	small nucleolar RNA host gene 1 /// small nucleolar RNA host gene (non-protein coding) 1	1,37
<i>Flt3l</i>	FMS-like tyrosine kinase 3 ligand /// ribosomal protein L13A	1,38
<i>Sftpd</i>	surfactant associated protein D /// surfactant associated protein D	1,38
<i>17386421</i>		1,38
<i>Efemp1</i>	epidermal growth factor-containing fibulin-like extracellular matrix protein 1 /// epidermal growth factor-containing fibulin-like extracellular matrix protein 1	1,39
<i>Tmem221</i>	transmembrane protein 221	1,39
<i>Cav2</i>	caveolin 2	1,39
<i>Pxdc1</i>	PX domain containing 1	1,40
<i>Nup93</i>	nucleoporin 93	1,41
<i>Ifih1</i>	interferon induced with helicase C domain 1	1,41
<i>2310001K24Rik</i>	RIKEN cDNA 2310001K24 gene /// RIKEN cDNA 2310001K24 gene	1,42
<i>17286496</i>		1,43
<i>Snhg1</i>	small nucleolar RNA host gene 1 /// small nucleolar RNA host gene (non-protein coding) 1	1,43
<i>Hsd3b7</i>	hydroxy-delta-5-steroid dehydrogenase, 3 beta- and steroid delta-isomerase 7	1,43
<i>Crip1</i>	cysteine-rich protein 1 (intestinal)	1,44
<i>Gdf15</i>	growth differentiation factor 15	1,44

<i>Gadd45b</i>	growth arrest and DNA-damage-inducible 45 beta	1,44
<i>2410006H16Rik</i>	RIKEN cDNA 2410006H16 gene /// RIKEN cDNA 2410006H16 gene	1,44
<i>Tmem212</i>	transmembrane protein 212	1,46
<i>Gm25099</i>	predicted gene, 25099	1,47
<i>Psph</i>	phosphoserine phosphatase	1,48
<i>Etv5</i>	ets variant 5	1,48
<i>Snhg9</i>	small nucleolar RNA host gene 9 /// small nucleolar RNA host gene (non-protein coding) 9	1,48
<i>Gm6484</i>	predicted gene 6484	1,48
<i>Kdelr3</i>	KDEL (Lys-Asp-Glu-Leu) endoplasmic reticulum protein retention receptor 3	1,48
<i>17550456</i>		1,49
<i>Kcni3</i>	Kv channel interacting protein 3, calsenilin	1,50
<i>Mest</i>	mesoderm specific transcript	1,50
<i>Cox6a2</i>	cytochrome c oxidase subunit VIa polypeptide 2	1,50
<i>Tcf24</i>	transcription factor 24 /// predicted gene 10567	1,50
<i>Eif3j2</i>	eukaryotic translation initiation factor 3, subunit J2	1,51
<i>Adm2</i>	adrenomedullin 2	1,51
<i>Ndufa12</i>	NADH dehydrogenase (ubiquinone) 1 alpha subcomplex, 12	1,52
<i>Cttnal1</i>	catenin (cadherin associated protein), alpha-like 1	1,53
<i>Cyb5r1</i>	cytochrome b5 reductase 1 /// cytochrome b5 reductase 1	1,53
<i>Ddit3</i>	DNA-damage inducible transcript 3 /// DNA-damage inducible transcript 3	1,54
<i>Gm11360</i>	predicted gene 11360	1,57
<i>Neurog3</i>	neurogenin 3	1,59
<i>Zfp97</i>	zinc finger protein 97 /// predicted gene 6712	1,60
<i>A730063M14Rik</i>	RIKEN cDNA A730063M14 gene	1,60
<i>Trib3</i>	tribbles homolog 3 (Drosophila)	1,63
<i>Nostrin</i>	nitric oxide synthase trafficker	1,64
<i>Tnnc1</i>	troponin C, cardiac/slow skeletal /// troponin C, cardiac/slow skeletal	1,64
<i>Lgi2</i>	leucine-rich repeat LGI family, member 2	1,64
<i>Dgkg</i>	diacylglycerol kinase, gamma /// diacylglycerol kinase, gamma	1,65
<i>Tcte3</i>	t-complex-associated testis expressed 3 /// predicted gene 3448 /// predicted gene 3417 /// t-complex-associated testis expressed 3 /// predicted gene 3417 /// predicted gene 3448	1,65
<i>Areg</i>	amphiregulin	1,66
<i>Nr4a2</i>	nuclear receptor subfamily 4, group A, member 2	1,66
<i>Lgmn</i>	legumain /// legumain	1,68
<i>Gm11974</i>	predicted gene 11974 /// predicted gene 11974 /// predicted gene 11974 /// predicted gene 11974	1,68

<i>Ube2c</i>	ubiquitin-conjugating enzyme E2C	1,71
BC021614	cDNA sequence BC021614	1,71
17547554		1,71
<i>Nnt</i>	nicotinamide nucleotide transhydrogenase /// nicotinamide nucleotide transhydrogenase /// nicotinamide nucleotide transhydrogenase	1,73
<i>Tcte3</i>	t-complex-associated testis expressed 3 /// predicted gene 3448 /// predicted gene 3417	1,74
<i>Lmo4</i>	LIM domain only 4	1,74
<i>Dclk1</i>	doublecortin-like kinase 1	1,74
<i>Tmem59l</i>	transmembrane protein 59-like	1,75
<i>Ppp1r15a</i>	protein phosphatase 1, regulatory (inhibitor) subunit 15A	1,76
LOC102641603	cyclin-dependent kinases regulatory subunit 2-like /// CDC28 protein kinase regulatory subunit 2 /// predicted gene 15452 /// cyclin-dependent kinases regulatory subunit 2-like	1,76
<i>Snhg5</i>	small nucleolar RNA host gene 5 /// small nucleolar RNA host gene 5	1,76
Gm11974	predicted gene 11974 /// predicted gene 11974 /// predicted gene 11974	1,77
NONMMUT029510		1,77
<i>Fbp2</i>	fructose biphosphatase 2	1,79
<i>Steap1</i>	six transmembrane epithelial antigen of the prostate 1	1,79
5430416N02Rik	RIKEN cDNA 5430416N02 gene /// RIKEN cDNA 5430416N02 gene	1,79
<i>Snhg6</i>	small nucleolar RNA host gene 6 /// small nucleolar RNA host gene 6	1,80
<i>Plet1</i>	placenta expressed transcript 1	1,84
<i>Oit1</i>	oncoprotein induced transcript 1 /// oncoprotein induced transcript 1	1,84
<i>Mfge8</i>	milk fat globule-EGF factor 8 protein	1,85
5430416N02Rik	RIKEN cDNA 5430416N02 gene /// RIKEN cDNA 5430416N02 gene	1,86
<i>Slc7a3</i>	solute carrier family 7 (cationic amino acid transporter, y+ system), member 3	1,87
<i>Dusp4</i>	dual specificity phosphatase 4	1,92
<i>Syt12</i>	synaptotagmin-like 2	1,94
<i>Vgf</i>	VGF nerve growth factor inducible	1,94
Gm7241	predicted pseudogene 7241 /// predicted pseudogene 7241	1,95
<i>Tmem181b-ps</i>	transmembrane protein 181B, pseudogene	1,96
9030025P20Rik	RIKEN cDNA 9030025P20 gene /// predicted gene 3435 /// RIKEN cDNA 9030025P20 gene /// ER membrane associated RNA degradation /// predicted gene 3435	1,97

LOC102638562	uncharacterized LOC102638562 /// uncharacterized LOC102638889 /// predicted gene 3255	2,03
Stom	stomatin	2,08
Vwde	von Willebrand factor D and EGF domains	2,28
Ttyh1	tweety homolog 1 (Drosophila)	2,29
9030025P20Rik	RIKEN cDNA 9030025P20 gene /// RIKEN cDNA 9030025P20 gene	2,46
Slc38a5	solute carrier family 38, member 5	2,51
Guca2a	guanylate cyclase activator 2a (guanylin)	2,57
Spp1	secreted phosphoprotein 1 /// secreted phosphoprotein 1	2,79
Hbb-bt	hemoglobin, beta adult t chain /// hemoglobin, beta adult s chain /// hemoglobin, beta adult minor chain /// hemoglobin, beta adult major chain	3,11
BC048594	cDNA sequence BC048594 /// doublecortin domain containing 5	6,40

Supplementary Table 2: Differentially expressed genes in isolated islets from 8-weeks old male β -D1CD and Control mice (4.2.2.1) filtered for a fold change of at least 1.2 and $p < 0.01$

Gene Symbol	Gene Name	β-D1CD /Control
Pianp	PILR alpha associated neural protein	-5.54
Trim12a	tripartite motif-containing 12A	-2.60
Trim34a	tripartite motif-containing 34A	-2.36
Efemp1	epidermal growth factor-containing fibulin-like extracellular matrix protein 1	-2.14
Ifi205	interferon activated gene 205	-1.96
Gm15135	predicted gene 15135	-1.96
Spp1	secreted phosphoprotein 1 /// secreted phosphoprotein 1	-1.88
Med13	mediator complex subunit 13	-1.83
Mir467e	microRNA 467e /// microRNA 467e	-1.79
Abi3bp	ABI gene family, member 3 (NESH) binding protein	-1.78
Darc	Duffy blood group, chemokine receptor	-1.73
4931430N09Rik	RIKEN cDNA 4931430N09 gene	-1.69
Gt(ROSA)26Sor	gene trap ROSA 26, Philippe Soriano /// gene trap ROSA 26, Philippe Soriano	-1.68
n271712		-1.64
ENSMUST00000177901		-1.64
Gm13833	predicted gene 13833	-1.63
Gdap10	ganglioside-induced differentiation-associated-protein 10 /// ganglioside-induced differentiation-associated- protein 10	-1.62

2810047C21Rik1	RIKEN cDNA 2810047C21 gene 1 /// predicted gene 3912 /// predicted gene 3912 /// predicted gene 20482 /// predicted gene, 18191	-1.62
Nrcam	neuron-glia-CAM-related cell adhesion molecule	-1.57
Slc26a1	solute carrier family 26 (sulfate transporter), member 1	-1.57
Tubb1	tubulin, beta 1 class VI	-1.56
Gm15758	predicted gene 15758	-1.56
Phxr4	per-hexamer repeat gene 4 /// per-hexamer repeat gene 4	-1.52
LOC100503146	uncharacterized LOC100503146 /// uncharacterized LOC100503146	-1.48
ENSMUST00000157638		-1.48
ENSMUST00000158433		-1.46
Coq2	coenzyme Q2 homolog, prenyltransferase (yeast)	-1.45
Gm15760	mitochondrial ribosomal protein S18B pseudogene /// adaptor-related protein complex 2, mu 1 subunit /// mitochondrial ribosomal protein S18B pseudogene	-1.45
Gm9968	predicted gene 9968 /// predicted gene 9968	-1.44
ENSMUST00000083083		-1.43
Rgs5	regulator of G-protein signaling 5	-1.42
Slco2a1	solute carrier organic anion transporter family, member 2a1	-1.42
Lbp	lipopolysaccharide binding protein	-1.42
Tbrg3	transforming growth factor beta regulated gene 3	-1.41
Rbpms2	RNA binding protein with multiple splicing 2 /// predicted gene 3470	-1.40
Tek	endothelial-specific receptor tyrosine kinase	-1.40
Tcf21	transcription factor 21	-1.39
GENSCAN00000036122		-1.39
Itfg2	integrin alpha FG-GAP repeat containing 2 /// integrin alpha FG-GAP repeat containing 2	-1.39
ENSMUST00000083115		-1.38
ENSMUST00000175216		-1.38
Ephx4	epoxide hydrolase 4	-1.38
Prrx1	paired related homeobox 1	-1.37
Ddx5	DEAD (Asp-Glu-Ala-Asp) box polypeptide 5	-1.37
Rgs5	regulator of G-protein signaling 5	-1.37
Tlr4	toll-like receptor 4	-1.37
Sele	selectin, endothelial cell	-1.37
Sema5a	sema domain, seven thrombospondin repeats (type 1 and type 1-like), transmembrane domain (TM) and short cytoplasmic domain, (semaphorin) 5A	-1.36
Gm9936	predicted gene 9936 /// predicted gene 9936	-1.36
Nmb	neuromedin B	-1.36

Ahr	aryl-hydrocarbon receptor /// aryl-hydrocarbon receptor	-1.35
Tspan9	tetraspanin 9	-1.34
Tenm4	teneurin transmembrane protein 4	-1.34
Pygl	liver glycogen phosphorylase	-1.33
AI506816	expressed sequence AI506816	-1.33
Myo7a	myosin VIIA	-1.33
Fbln5	fibulin 5	-1.33
Eno2	enolase 2, gamma neuronal	-1.33
Zeb1	zinc finger E-box binding homeobox 1	-1.32
Srgap1	SLIT-ROBO Rho GTPase activating protein 1	-1.31
Cd34	CD34 antigen	-1.31
3110057012Rik	RIKEN cDNA 3110057012 gene	-1.31
ENSMUST00000104238		-1.30
Plekhh5	pleckstrin homology domain containing, family G (with RhoGef domain) member 5	-1.30
Ttc9	tetratricopeptide repeat domain 9	-1.30
Gm14178	predicted gene 14178	-1.30
Gpr116	G protein-coupled receptor 116	-1.29
Gm11209	predicted gene 11209	-1.29
Pkd2	polycystic kidney disease 2	-1.29
Enpp3	ectonucleotide pyrophosphatase/phosphodiesterase 3	-1.28
Malat1	metastasis associated lung adenocarcinoma transcript 1 (non-coding RNA) /// metastasis associated lung adenocarcinoma transcript 1 (non-coding RNA)	-1.28
Edem1	ER degradation enhancer, mannosidase alpha-like 1	-1.28
Hand1	heart and neural crest derivatives expressed transcript 1	-1.27
Edem1	ER degradation enhancer, mannosidase alpha-like 1	-1.26
Sync	syncoilin	-1.26
Pag1	phosphoprotein associated with glycosphingolipid microdomains 1	-1.26
Slit2	slit homolog 2 (Drosophila)	-1.26
Slc22a15	solute carrier family 22 (organic anion/cation transporter), member 15	-1.26
Pycard	PYD and CARD domain containing	-1.25
Epas1	endothelial PAS domain protein 1	-1.25
Ppap2a	phosphatidic acid phosphatase type 2A /// superkiller viralicidic activity 2-like 2 (S. cerevisiae)	-1.25
Cpne8	copine VIII	-1.24
LOC552890	uncharacterized LOC552890	-1.24
Cers1	ceramide synthase 1 /// growth differentiation factor 1	-1.24
Notch3	notch 3	-1.24
Ung	uracil DNA glycosylase	-1.24
Dbn1	drebrin 1	-1.23

<i>n288754</i>		-1.22
<i>Fam109b</i>	family with sequence similarity 109, member B	-1.22
<i>Tnfrsf21</i>	tumor necrosis factor receptor superfamily, member 21	-1.21
<i>Hoxb5</i>	homeobox B5	-1.21
<i>Acer2</i>	alkaline ceramidase 2 /// alkaline ceramidase 2	-1.21
<i>GENSCAN00000007907</i>		-1.21
<i>Tnnc2</i>	troponin C2, fast	-1.21
<i>Vps52</i>	vacuolar protein sorting 52 (yeast) /// vacuolar protein sorting-associated protein 52 homolog	1.21
<i>0610011F06Rik</i>	RIKEN cDNA 0610011F06 gene	1.21
<i>Ankrd42</i>	ankyrin repeat domain 42	1.21
<i>Abca7</i>	ATP-binding cassette, sub-family A (ABC1), member 7	1.21
<i>Hps4</i>	Hermansky-Pudlak syndrome 4 homolog (human)	1.21
<i>C1qtnf4</i>	C1q and tumor necrosis factor related protein 4	1.21
<i>Ccdc17</i>	coiled-coil domain containing 17	1.22
<i>Pacrg</i>	PARK2 co-regulated	1.22
<i>Galnt10</i>	UDP-N-acetyl-alpha-D-galactosamine:polypeptide N-acetylgalactosaminyltransferase 10	1.23
<i>Tmem175</i>	transmembrane protein 175	1.23
<i>Zfp7</i>	zinc finger protein 7	1.23
<i>Ttl10</i>	tubulin tyrosine ligase-like family, member 10	1.24
<i>Slc18a1</i>	solute carrier family 18 (vesicular monoamine), member 1	1.24
<i>Cetn4</i>	centrin 4 /// centrin-1-like	1.25
<i>Mblac1</i>	metallo-beta-lactamase domain containing 1	1.25
<i>Homez</i>	homeodomain leucine zipper-encoding gene	1.25
<i>Tbc1d9</i>	TBC1 domain family, member 9	1.25
<i>4930547M16Rik</i>	RIKEN cDNA 4930547M16 gene	1.25
<i>Ift27</i>	intraflagellar transport 27	1.26
<i>Gm10566</i>	predicted gene 10566	1.26
<i>Plekhg6</i>	pleckstrin homology domain containing, family G (with RhoGef domain) member 6	1.26
<i>Sult1d1</i>	sulfotransferase family 1D, member 1	1.27
<i>2510002D24Rik</i>	RIKEN cDNA 2510002D24 gene	1.27
<i>Gm10358</i>	predicted gene 10358	1.27
<i>Hnf1a</i>	HNF1 homeobox A	1.28
<i>Zfp931</i>	zinc finger protein 931	1.29
<i>Tnfrsf1a</i>	tumor necrosis factor receptor superfamily, member 1a	1.29
<i>Gm13824</i>	predicted gene 13824 /// predicted gene 13825	1.29
<i>Tnni2</i>	troponin I, skeletal, fast 2	1.30
<i>17359855</i>		1.31
<i>Asic1</i>	acid-sensing (proton-gated) ion channel 1	1.31
<i>Gm10033</i>	predicted gene 10033	1.31

<i>Ncapd2</i>	non-SMC condensin I complex, subunit D2	1.31
<i>Fah</i>	fumarylacetoacetate hydrolase	1.31
<i>Idua</i>	iduronidase, alpha-L-	1.31
<i>Hapln4</i>	hyaluronan and proteoglycan link protein 4	1.31
<i>Acadl</i>	acyl-Coenzyme A dehydrogenase, long-chain	1.32
<i>Cnbd2</i>	cyclic nucleotide binding domain containing 2	1.32
<i>Pms1</i>	postmeiotic segregation increased 1 (<i>S. cerevisiae</i>) /// postmeiotic segregation increased 1 (<i>S. cerevisiae</i>)	1.33
<i>lft27</i>	intraflagellar transport 27	1.33
<i>Rbm11</i>	RNA binding motif protein 11	1.34
<i>Zbtb7c</i>	zinc finger and BTB domain containing 7C	1.34
GENSCAN00000020829		1.35
<i>Cgrrf1</i>	cell growth regulator with ring finger domain 1	1.36
<i>Zfp386</i>	zinc finger protein 386 (Kruppel-like)	1.36
GENSCAN00000049628		1.37
<i>Gm16295</i>	predicted gene 16295	1.40
<i>Tmem71</i>	transmembrane protein 71	1.41
<i>H2-Q5</i>	histocompatibility 2, Q region locus 5	1.41
<i>Rps4y2</i>	ribosomal protein S4, Y-linked 2 /// ribosomal protein S4, Y-linked 2	1.42
<i>2900076A07Rik</i>	RIKEN cDNA 2900076A07 gene /// mmu-mir-1839	1.44
<i>2310015A10Rik</i>	RIKEN cDNA 2310015A10 gene /// RIKEN cDNA 2310015A10 gene	1.45
<i>Mettl21d</i>	methyltransferase like 21D /// methyltransferase-like protein 21D-like	1.46
<i>Magohb</i>	mago-nashi homolog B (<i>Drosophila</i>)	1.47
<i>2510049J12Rik</i>	RIKEN cDNA 2510049J12 gene	1.48
<i>Scnn1a</i>	sodium channel, nonvoltage-gated 1 alpha	1.56
<i>Vmn1r127</i>	vomer nasal 1 receptor 127	1.59
<i>2410021H03Rik</i>	RIKEN cDNA 2410021H03 gene	1.63
ENSMUST00000082922		1.67
<i>Vwf</i>	Von Willebrand factor homolog	1.71
<i>Cib3</i>	calcium and integrin binding family member 3	1.73
<i>Gbp11</i>	guanylate binding protein 11	1.74
<i>Gm10069</i>	predicted gene 10069 /// predicted gene 10069	1.79
GENSCAN00000039853		1.82
<i>Kl</i>	klotho	2.05
<i>Gm16567</i>	predicted gene 16567	2.32
<i>Rps13</i>	ribosomal protein S13 /// predicted gene 15483 /// ribosomal protein S13, pseudogene 4	2.98
<i>Ghrl</i>	ghrelin /// ghrelin	3.28

Supplementary Table 3: Genes that are differentially expressed in both (β -D1D4 and β -DICD) data sets

<i>Gene Symbol</i>	<i>β-D1D4</i>	<i>β-DICD</i>
<i>Efemp1</i>	1,39	-2,14
<i>Slc26a1</i>	-2,39	-1,57
<i>Slco2a1</i>	-1,47	-1,42
<i>Sult1d1</i>	-1,64	1,27
<i>Zfp386</i>	-1,35	1,36
<i>2410021H03Rik</i>	-1,69	1,63
<i>Cib3</i>	-1,81	1,73

7. REFERENCES

- (NCD-RisC), N. R. F. C. (2016). "Worldwide trends in diabetes since 1980: a pooled analysis of 751 population-based studies with 4.4 million participants." Lancet **387**(10027): 1513-1530.
- Afelik, S. and J. Jensen (2013). "Notch signaling in the pancreas: patterning and cell fate specification." Wiley Interdiscip Rev Dev Biol **2**(4): 531-544.
- Afelik, S., X. Qu, E. Hasrouni, M. A. Bukys, T. Deering, S. Nieuwoudt, W. Rogers, R. J. Macdonald and J. Jensen (2012). "Notch-mediated patterning and cell fate allocation of pancreatic progenitor cells." Development **139**(10): 1744-1753.
- Ahlgren, U., J. Jonsson, L. Jonsson, K. Simu and H. Edlund (1998). "beta-cell-specific inactivation of the mouse *Ipf1/Pdx1* gene results in loss of the beta-cell phenotype and maturity onset diabetes." Genes Dev **12**(12): 1763-1768.
- Ahnfelt-Ronne, J., M. C. Jorgensen, R. Klinck, J. N. Jensen, E. M. Fuchtbauer, T. Deering, R. J. MacDonald, C. V. Wright, O. D. Madsen and P. Serup (2012). "Ptf1a-mediated control of *Dll1* reveals an alternative to the lateral inhibition mechanism." Development **139**(1): 33-45.
- Alders, M., J. Bliiek, K. vd Lip, R. vd Bogaard and M. Mannens (2008). "Determination of *KCNQ10T1* and *H19* methylation levels in BWS and SRS patients using methylation-sensitive high-resolution melting analysis." Eur J Hum Genet **17**(4): 467-473.
- Andrawes, M. B., X. Xu, H. Liu, S. B. Ficarro, J. A. Marto, J. C. Aster and S. C. Blacklow (2013). "Intrinsic selectivity of Notch 1 for Delta-like 4 over Delta-like 1." J Biol Chem **288**(35): 25477-25489.
- Apelqvist, A., H. Li, L. Sommer, P. Beatus, D. J. Anderson, T. Honjo, M. Hrabe de Angelis, U. Lendahl and H. Edlund (1999). "Notch signalling controls pancreatic cell differentiation." Nature **400**(6747): 877-881.
- Arda, H. E., Cecil M. Benitez and Seung K. Kim (2013). "Gene Regulatory Networks Governing Pancreas Development." Developmental Cell **25**(1): 5-13.
- Arntfield, M. E. and D. van der Kooy (2011). "beta-Cell evolution: How the pancreas borrowed from the brain: The shared toolbox of genes expressed by neural and pancreatic endocrine cells may reflect their evolutionary relationship." Bioessays **33**(8): 582-587.
- Aronoff, S. L., K. Berkowitz, B. Shreiner and L. Want (2004). "Glucose Metabolism and Regulation: Beyond Insulin and Glucagon." Diabetes Spectrum **17**(3): 183-190.
- Artner, I., J. Le Lay, Y. Hang, L. Elghazi, J. C. Schisler, E. Henderson, B. Sosa-Pineda and R. Stein (2006). "MafB: an activator of the glucagon gene expressed in developing islet alpha- and beta-cells." Diabetes **55**(2): 297-304.
- Arumugam, R., E. Horowitz, R. C. Noland, D. Lu, D. Fleenor and M. Freemark (2010). "Regulation of Islet β -Cell Pyruvate Metabolism: Interactions of Prolactin, Glucose, and Dexamethasone." Endocrinology **151**(7): 3074-3083.
- Ashcroft, Frances M. and P. Rorsman (2012). "Diabetes Mellitus and the β Cell: The Last Ten Years." Cell **148**(6): 1160-1171.

-
- Atouf, F., P. Czernichow and R. Scharfmann (1997). "Expression of neuronal traits in pancreatic beta cells. Implication of neuron-restrictive silencing factor/repressor element silencing transcription factor, a neuron-restrictive silencer." J Biol Chem **272**(3): 1929-1934.
- Avila, J. L. and J. L. Kissil (2013). "Notch signaling in pancreatic cancer: oncogene or tumor suppressor?" Trends in Molecular Medicine **19**(5): 320-327.
- Axelrod, J. D. (2010). "Delivering the Lateral Inhibition Punchline: It's All About the Timing." Science Signaling **3**(145): pe38-pe38.
- Ayala, J. E., D. P. Bracy, F. D. James, M. A. Burmeister, D. H. Wasserman and D. J. Drucker (2010). "Glucagon-like peptide-1 receptor knockout mice are protected from high-fat diet-induced insulin resistance." Endocrinology **151**(10): 4678-4687.
- Baeyens, L., S. Bonne, T. Bos, I. Rooman, C. Peleman, T. Lahoutte, M. German, H. Heimberg and L. Bouwens (2009). "Notch signaling as gatekeeper of rat acinar-to-beta-cell conversion in vitro." Gastroenterology **136**(5): 1750-1760.e1713.
- Baeyens, L., M. Lemper, G. Leuckx, S. De Groef, P. Bonfanti, G. Stange, R. Shemer, C. Nord, D. W. Scheel, F. C. Pan, U. Ahlgren, G. Gu, D. A. Stoffers, Y. Dor, J. Ferrer, G. Gradwohl, C. V. E. Wright, M. Van de Casteele, M. S. German, L. Bouwens and H. Heimberg (2014). "Transient cytokine treatment induces acinar cell reprogramming and regenerates functional beta cell mass in diabetic mice." Nat Biotech **32**(1): 76-83.
- Baggio, L., T. J. Kieffer and D. J. Drucker (2000). "Glucagon-like peptide-1, but not glucose-dependent insulinotropic peptide, regulates fasting glycemia and nonenteral glucose clearance in mice." Endocrinology **141**(10): 3703-3709.
- Balsells, M., A. García-Patterson, I. Solà, M. Roqué, I. Gich and R. Corcoy (2015). "Glibenclamide, metformin, and insulin for the treatment of gestational diabetes: a systematic review and meta-analysis." BMJ : British Medical Journal **350**.
- Bayless, K. J. and G. A. Johnson (2011). "Role of the Cytoskeleton in Formation and Maintenance of Angiogenic Sprouts." Journal of Vascular Research **48**(5): 369-385.
- Beatus, P., J. Lundkvist, C. Oberg and U. Lendahl (1999). "The notch 3 intracellular domain represses notch 1-mediated activation through Hairy/Enhancer of split (HES) promoters." Development **126**(17): 3925-3935.
- Benedito, R., C. Roca, I. Sørensen, S. Adams, A. Gossler, M. Fruttiger and R. H. Adams (2009). "The Notch Ligands Dll4 and Jagged1 Have Opposing Effects on Angiogenesis." Cell **137**(6): 1124-1135.
- Bettenhausen, B., M. Hrabe de Angelis, D. Simon, J. L. Guenet and A. Gossler (1995). "Transient and restricted expression during mouse embryogenesis of Dll1, a murine gene closely related to Drosophila Delta." Development **121**(8): 2407-2418.
- Bhushan, A., N. Itoh, S. Kato, J. P. Thiery, P. Czernichow, S. Bellusci and R. Scharfmann (2001). "Fgf10 is essential for maintaining the proliferative capacity of epithelial progenitor cells during early pancreatic organogenesis." Development **128**(24): 5109-5117.
- Bland, C. E., P. Kimberly and M. D. Rand (2003). "Notch-induced proteolysis and nuclear localization of the Delta ligand." J Biol Chem **278**(16): 13607-13610.

- Blaumueller, C. M., H. Qi, P. Zagouras and S. Artavanis-Tsakonas (1997). "Intracellular Cleavage of Notch Leads to a Heterodimeric Receptor on the Plasma Membrane." Cell **90**(2): 281-291.
- Blum, B., S. Hrvatin, C. Schuetz, C. Bonal, A. Rezania and D. A. Melton (2012). "Functional beta-cell maturation is marked by an increased glucose threshold and by expression of urocortin 3." Nat Biotech **30**(3): 261-264.
- Bonini, S. A., G. Ferrari-Toninelli, M. Montinaro and M. Memo (2013). "Notch signalling in adult neurons: a potential target for microtubule stabilization." Therapeutic Advances in Neurological Disorders **6**(6): 375-385.
- Bordonaro, M., S. Tewari, W. Atamna and D. L. Lazarova (2011). "The Notch ligand Delta-like 1 integrates inputs from TGFbeta/Activin and Wnt pathways." Exp Cell Res **317**(10): 1368-1381.
- Borrell, V., A. Cárdenas, G. Ciceri, J. Galcerán, N. Flames, R. Pla, S. Nóbrega-Pereira, C. García-Frigola, S. Peregrín, Z. Zhao, L. Ma, M. Tessier-Lavigne and O. Marín (2012). "Slit/Robo Signaling Modulates the Proliferation of Central Nervous System Progenitors." Neuron **76**(2): 338-352.
- Bramswig, N. C. and K. H. Kaestner (2011). "Transcriptional regulation of alpha-cell differentiation." Diabetes Obes Metab **13 Suppl 1**: 13-20.
- Bray, S. J. (2006). "Notch signalling: a simple pathway becomes complex." Nat Rev Mol Cell Biol **7**(9): 678-689.
- Brereton, M. F., M. Iberl, K. Shimomura, Q. Zhang, A. E. Adriaenssens, P. Proks, I. I. Spiliotis, W. Dace, K. K. Mattis, R. Ramracheya, F. M. Gribble, F. Reimann, A. Clark, P. Rorsman and F. M. Ashcroft (2014). "Reversible changes in pancreatic islet structure and function produced by elevated blood glucose." Nature Communications **5**: 4639.
- Brereton, M. F., M. Rohm and F. M. Ashcroft (2016). "β-Cell dysfunction in diabetes: a crisis of identity?" Diabetes, Obesity and Metabolism **18**: 102-109.
- Brial, F., C. R. Lussier, K. Belleville, P. Sarret and F. Boudreau (2015). "Ghrelin inhibition restores glucose homeostasis in hepatocyte nuclear factor-1alpha (MODY3) deficient mice." Diabetes.
- Brissova, M., M. J. Fowler, W. E. Nicholson, A. Chu, B. Hirshberg, D. M. Harlan and A. C. Powers (2005). "Assessment of Human Pancreatic Islet Architecture and Composition by Laser Scanning Confocal Microscopy." Journal of Histochemistry & Cytochemistry **53**(9): 1087-1097.
- Brissova, M., A. Shostak, M. Shiota, P. O. Wiebe, G. Poffenberger, J. Kantz, Z. Chen, C. Carr, W. G. Jerome, J. Chen, H. S. Baldwin, W. Nicholson, D. M. Bader, T. Jetton, M. Gannon and A. C. Powers (2006). "Pancreatic islet production of vascular endothelial growth factor--a is essential for islet vascularization, revascularization, and function." Diabetes **55**(11): 2974-2985.
- Brooker, R., K. Hozumi and J. Lewis (2006). "Notch ligands with contrasting functions: Jagged1 and Delta1 in the mouse inner ear." Development **133**(7): 1277-1286.
- Brose, K. and M. Tessier-Lavigne (2000). "Slit proteins: key regulators of axon guidance, axonal branching, and cell migration." Current Opinion in Neurobiology **10**(1): 95-102.
- Brou, C., F. Logeat, N. Gupta, C. Bessia, O. LeBail, J. R. Doedens, A. Cumano, P. Roux, R. A. Black and A. Israel (2000). "A novel proteolytic cleavage involved in Notch signaling: the role of the disintegrin-metalloprotease TACE." Mol Cell **5**(2): 207-216.

- Bruce Alberts, A. J., Julian Lewis, Martin Raff, Keith Roberts, and Peter Walter (2002). "Molecular Biology of the Cell, 4th edition."
- Buchler, P., A. Gazdhar, M. Schubert, N. Giese, H. A. Reber, O. J. Hines, T. Giese, G. O. Ceyhan, M. Muller, M. W. Buchler and H. Friess (2005). "The Notch signaling pathway is related to neurovascular progression of pancreatic cancer." Ann Surg **242**(6): 791-800, discussion 800-791.
- Bustin, S. A., V. Benes, J. A. Garson, J. Hellems, J. Huggett, M. Kubista, R. Mueller, T. Nolan, M. W. Pfaffl, G. L. Shipley, J. Vandesompele and C. T. Wittwer (2009). "The MIQE guidelines: minimum information for publication of quantitative real-time PCR experiments." Clin Chem **55**(4): 611-622.
- Cabrera, O., D. M. Berman, N. S. Kenyon, C. Ricordi, P. O. Berggren and A. Caicedo (2006). "The unique cytoarchitecture of human pancreatic islets has implications for islet cell function." Proc Natl Acad Sci U S A **103**(7): 2334-2339.
- Campbell, Jonathan E. and Daniel J. Drucker (2013). "Pharmacology, Physiology, and Mechanisms of Incretin Hormone Action." Cell Metabolism **17**(6): 819-837.
- Campbell, J. E. and D. J. Drucker (2015). "Islet [alpha] cells and glucagon[mdash]critical regulators of energy homeostasis." Nat Rev Endocrinol **11**(6): 329-338.
- Cano, D., B. Soria, F. Martín and A. Rojas (2013). "Transcriptional control of mammalian pancreas organogenesis." Cellular and Molecular Life Sciences: 1-20.
- Carter, J. D., S. B. Dula, K. L. Corbin, R. Wu and C. S. Nunemaker (2009). "A practical guide to rodent islet isolation and assessment." Biol Proced Online **11**: 3-31.
- Cavanna, D. (2013). "In vivo and in vitro analysis of Dll1 and Pax6 function in the adult mouse pancreas."
- Cerf, M. E. (2006). "Transcription factors regulating beta-cell function." Eur J Endocrinol **155**(5): 671-679.
- Cha, J. Y., H. Kim, K. S. Kim, M. W. Hur and Y. Ahn (2000). "Identification of transacting factors responsible for the tissue-specific expression of human glucose transporter type 2 isoform gene. Cooperative role of hepatocyte nuclear factors 1alpha and 3beta." J Biol Chem **275**(24): 18358-18365.
- Chapouton, P., P. Skupien, B. Hesl, M. Coolen, J. C. Moore, R. Madelaine, E. Kremmer, T. Faus-Kessler, P. Blader, N. D. Lawson and L. Bally-Cuif (2010). "Notch activity levels control the balance between quiescence and recruitment of adult neural stem cells." J Neurosci **30**(23): 7961-7974.
- Chen, L., T. Alam, J. H. Johnson, S. Hughes, C. B. Newgard and R. H. Unger (1990). "Regulation of beta-cell glucose transporter gene expression." Proceedings of the National Academy of Sciences of the United States of America **87**(11): 4088-4092.
- Collombat, P., A. Mansouri, J. Hecksher-Sørensen, P. Serup, J. Krull, G. Gradwohl and P. Gruss (2003). "Opposing actions of Arx and Pax4 in endocrine pancreas development." Genes & Development **17**(20): 2591-2603.
- Cordle, J., C. Redfieldz, M. Stacey, P. A. van der Merwe, A. C. Willis, B. R. Champion, S. Hambleton and P. A. Handford (2008). "Localization of the delta-like-1-binding site in human Notch-1 and its modulation by calcium affinity." J Biol Chem **283**(17): 11785-11793.

- Cozar-Castellano, I., M. Haught and A. F. Stewart (2006). "The cell cycle inhibitory protein p21cip is not essential for maintaining beta-cell cycle arrest or beta-cell function in vivo." *Diabetes* **55**(12): 3271-3278.
- Crawford, L. A., M. A. Guney, Y. A. Oh, R. A. Deyoung, D. M. Valenzuela, A. J. Murphy, G. D. Yancopoulos, K. M. Lyons, D. R. Brigstock, A. Economides and M. Gannon (2009). "Connective tissue growth factor (CTGF) inactivation leads to defects in islet cell lineage allocation and beta-cell proliferation during embryogenesis." *Mol Endocrinol* **23**(3): 324-336.
- Cryer, P. E. (1999). "Hypoglycemia is the limiting factor in the management of diabetes." *Diabetes Metab Res Rev* **15**(1): 42-46.
- Cryer, P. E. (2002). "Hypoglycaemia: the limiting factor in the glycaemic management of Type I and Type II diabetes." *Diabetologia* **45**(7): 937-948.
- Cryer, P. E., S. N. Davis and H. Shamoan (2003). "Hypoglycemia in Diabetes." *Diabetes Care* **26**(6): 1902-1912.
- Date, Y., M. Nakazato, S. Hashiguchi, K. Dezaki, M. S. Mondal, H. Hosoda, M. Kojima, K. Kangawa, T. Arima, H. Matsuo, T. Yada and S. Matsukura (2002). "Ghrelin Is Present in Pancreatic α -Cells of Humans and Rats and Stimulates Insulin Secretion." *Diabetes* **51**(1): 124-129.
- de Heer, J., C. Rasmussen, D. H. Coy and J. J. Holst (2008). "Glucagon-like peptide-1, but not glucose-dependent insulintropic peptide, inhibits glucagon secretion via somatostatin (receptor subtype 2) in the perfused rat pancreas." *Diabetologia* **51**(12): 2263-2270.
- De Vos, A., H. Heimberg, E. Quartier, P. Huypens, L. Bouwens, D. Pipeleers and F. Schuit (1995). "Human and rat beta cells differ in glucose transporter but not in glucokinase gene expression." *Journal of Clinical Investigation* **96**(5): 2489-2495.
- de Welle, J., H. Schmid-Antomarchi, M. Fosset and M. Lazdunski (1988). "ATP-sensitive K⁺ channels that are blocked by hypoglycemia-inducing sulfonylureas in insulin-secreting cells are activated by galanin, a hyperglycemia-inducing hormone." *Proc Natl Acad Sci U S A* **85**(4): 1312-1316.
- del Alamo, D., H. Rouault and F. Schweisguth (2011). "Mechanism and significance of cis-inhibition in Notch signalling." *Curr Biol* **21**(1): R40-47.
- Dexter, J. S. (1914). "The Analysis of a Case of Continuous Variation in *Drosophila* by a Study of Its Linkage Relations." *The American Naturalist* **48**(576): 712-758.
- Dezaki, K., H. Sone, M. Koizumi, M. Nakata, M. Kakei, H. Nagai, H. Hosoda, K. Kangawa and T. Yada (2006). "Blockade of Pancreatic Islet-Derived Ghrelin Enhances Insulin Secretion to Prevent High-Fat Diet-Induced Glucose Intolerance." *Diabetes* **55**(12): 3486-3493.
- Dickinson, R. E. and W. C. Duncan (2010). "The SLIT/ROBO pathway: a regulator of cell function with implications for the reproductive system." *Reproduction (Cambridge, England)* **139**(4): 697-704.
- Dor, Y., J. Brown, O. I. Martinez and D. A. Melton (2004). "Adult pancreatic beta-cells are formed by self-duplication rather than stem-cell differentiation." *Nature* **429**(6987): 41-46.
- Dror, V., V. Nguyen, P. Walia, T. B. Kalynyak, J. A. Hill and J. D. Johnson (2007). "Notch signalling suppresses apoptosis in adult human and mouse pancreatic islet cells." *Diabetologia* **50**(12): 2504-2515.

Drucker, D. J. (2006). "The biology of incretin hormones." *Cell Metab* **3**(3): 153-165.

Dupuis, J., C. Langenberg, I. Prokopenko, R. Saxena, N. Soranzo, A. U. Jackson, E. Wheeler, N. L. Glazer, N. Bouatia-Naji, A. L. Gloyn, C. M. Lindgren, R. Magi, A. P. Morris, J. Randall, T. Johnson, P. Elliott, D. Rybin, G. Thorleifsson, V. Steinthorsdottir, P. Henneman, H. Grallert, A. Dehghan, J. J. Hottenga, C. S. Franklin, P. Navarro, K. Song, A. Goel, J. R. Perry, J. M. Egan, T. Lajunen, N. Grarup, T. Sparso, A. Doney, B. F. Voight, H. M. Stringham, M. Li, S. Kanoni, P. Shrader, C. Cavalcanti-Proenca, M. Kumari, L. Qi, N. J. Timpson, C. Gieger, C. Zabena, G. Rocheleau, E. Ingelsson, P. An, J. O'Connell, J. Luan, A. Elliott, S. A. McCarroll, F. Payne, R. M. Roccascocca, F. Pattou, P. Sethupathy, K. Ardlie, Y. Ariyurek, B. Balkau, P. Barter, J. P. Beilby, Y. Ben-Shlomo, R. Benediktsson, A. J. Bennett, S. Bergmann, M. Bochud, E. Boerwinkle, A. Bonnefond, L. L. Bonnycastle, K. Borch-Johnsen, Y. Bottcher, E. Brunner, S. J. Bumpstead, G. Charpentier, Y. D. Chen, P. Chines, R. Clarke, L. J. Coin, M. N. Cooper, M. Cornelis, G. Crawford, L. Crisponi, I. N. Day, E. J. de Geus, J. Delplanque, C. Dina, M. R. Erdos, A. C. Fedson, A. Fischer-Rosinsky, N. G. Forouhi, C. S. Fox, R. Frants, M. G. Franzosi, P. Galan, M. O. Goodarzi, J. Graessler, C. J. Groves, S. Grundy, R. Gwilliam, U. Gyllensten, S. Hadjadj, G. Hallmans, N. Hammond, X. Han, A. L. Hartikainen, N. Hassanali, C. Hayward, S. C. Heath, S. Hercberg, C. Herder, A. A. Hicks, D. R. Hillman, A. D. Hingorani, A. Hofman, J. Hui, J. Hung, B. Isomaa, P. R. Johnson, T. Jorgensen, A. Jula, M. Kaakinen, J. Kaprio, Y. A. Kesaniemi, M. Kivimaki, B. Knight, S. Koskinen, P. Kovacs, K. O. Kyvik, G. M. Lathrop, D. A. Lawlor, O. Le Bacquer, C. Lecoeur, Y. Li, V. Lyssenko, R. Mahley, M. Mangino, A. K. Manning, M. T. Martinez-Larrad, J. B. McAtaer, L. J. McCulloch, R. McPherson, C. Meisinger, D. Melzer, D. Meyre, B. D. Mitchell, M. A. Morken, S. Mukherjee, S. Naitza, N. Narisu, M. J. Neville, B. A. Oostra, M. Orru, R. Pakyz, C. N. Palmer, G. Paolisso, C. Pattaro, D. Pearson, J. F. Peden, N. L. Pedersen, M. Perola, A. F. Pfeiffer, I. Pichler, O. Polasek, D. Posthuma, S. C. Potter, A. Pouta, M. A. Province, B. M. Psaty, W. Rathmann, N. W. Rayner, K. Rice, S. Ripatti, F. Rivadeneira, M. Roden, O. Rolandsson, A. Sandbaek, M. Sandhu, S. Sanna, A. A. Sayer, P. Scheet, L. J. Scott, U. Seedorf, S. J. Sharp, B. Shields, G. Sigurdsson, E. J. Sijbrands, A. Silveira, L. Simpson, A. Singleton, N. L. Smith, U. Sovio, A. Swift, H. Syddall, A. C. Syvanen, T. Tanaka, B. Thorand, J. Tichet, A. Tonjes, T. Tuomi, A. G. Uitterlinden, K. W. van Dijk, M. van Hoek, D. Varma, S. Visvikis-Siest, V. Vitart, N. Vogelzangs, G. Waeber, P. J. Wagner, A. Walley, G. B. Walters, K. L. Ward, H. Watkins, M. N. Weedon, S. H. Wild, G. Willemsen, J. C. Witteman, J. W. Yarnell, E. Zeggini, D. Zelenika, B. Zethelius, G. Zhai, J. H. Zhao, M. C. Zillikens, I. B. Borecki, R. J. Loos, P. Meneton, P. K. Magnusson, D. M. Nathan, G. H. Williams, A. T. Hattersley, K. Silander, V. Salomaa, G. D. Smith, S. R. Bornstein, P. Schwarz, J. Spranger, F. Karpe, A. R. Shuldiner, C. Cooper, G. V. Dedoussis, M. Serrano-Rios, A. D. Morris, L. Lind, L. J. Palmer, F. B. Hu, P. W. Franks, S. Ebrahim, M. Marmot, W. H. Kao, J. S. Pankow, M. J. Sampson, J. Kuusisto, M. Laakso, T. Hansen, O. Pedersen, P. P. Pramstaller, H. E. Wichmann, T. Illig, I. Rudan, A. F. Wright, M. Stumvoll, H. Campbell, J. F. Wilson, R. N. Bergman, T. A. Buchanan, F. S. Collins, K. L. Mohlke, J. Tuomilehto, T. T. Valle, D. Altshuler, J. I. Rotter, D. S. Siscovick, B. W. Penninx, D. I. Boomsma, P. Deloukas, T. D. Spector, T. M. Frayling, L. Ferrucci, A. Kong, U. Thorsteinsdottir, K. Stefansson, C. M. van Duijn, Y. S. Aulchenko, A. Cao, A. Scuteri, D. Schlessinger, M. Uda, A. Ruukonen, M. R. Jarvelin, D. M. Waterworth, P. Vollenweider, L. Peltonen, V. Mooser, G. R. Abecasis, N. J. Wareham, R. Sladek, P. Froguel, R. M. Watanabe, J. B. Meigs, L. Groop, M. Boehnke, M. I. McCarthy, J. C. Florez and I. Barroso (2010). "New genetic loci implicated in fasting glucose homeostasis and their impact on type 2 diabetes risk." *Nat Genet* **42**(2): 105-116.

Dyczynska, E., D. Sun, H. Yi, A. Sehara-Fujisawa, C. P. Blobel and A. Zolkiewska (2007). "Proteolytic processing of delta-like 1 by ADAM proteases." *J Biol Chem* **282**(1): 436-444.

Eberhard, D. (2013). "Neuron and beta-cell evolution: Learning about neurons is learning about beta-cells." *BioEssays* **35**(7): 584-584.

Egido, E. M., J. Rodriguez-Gallardo, R. A. Silvestre and J. Marco (2002). "Inhibitory effect of ghrelin on insulin and pancreatic somatostatin secretion." *Eur J Endocrinol* **146**(2): 241-244.

- Ehebauer, M., P. Hayward and A. Martinez-Arias (2006). "Notch Signaling Pathway." Science's STKE **2006**(364): cm7-cm7.
- Ekhholm, E., N. Shaat and J. J. Holst (2012). "Characterization of beta cell and incretin function in patients with MODY1 (HNF4A MODY) and MODY3 (HNF1A MODY) in a Swedish patient collection." Acta Diabetol **49**(5): 349-354.
- El-Gohary, Y., S. Sims-Lucas, N. Lath, S. Tulachan, P. Guo, X. Xiao, C. Welsh, J. Paredes, J. Wiersch, K. Prasad, C. Shiota and G. K. Gittes (2012). "Three-Dimensional Analysis of the Islet Vasculature." The Anatomical Record: Advances in Integrative Anatomy and Evolutionary Biology **295**(9): 1473-1481.
- Fava, E., J. Dehghany, J. Ouwendijk, A. Muller, A. Niederlein, P. Verkade, M. Meyer-Hermann and M. Solimena (2012). "Novel standards in the measurement of rat insulin granules combining electron microscopy, high-content image analysis and in silico modelling." Diabetologia **55**(4): 1013-1023.
- Federation, I. D. (2015). "IDF diabetes atlas 2015- 7th edition." <http://www.diabetesatlas.org/>.
- Flamez, D., P. Gilon, K. Moens, A. Van Breusegem, D. Delmeire, L. A. Scrocchi, J. C. Henquin, D. J. Drucker and F. Schuit (1999). "Altered cAMP and Ca²⁺ signaling in mouse pancreatic islets with glucagon-like peptide-1 receptor null phenotype." Diabetes **48**(10): 1979-1986.
- Fortini, M. E. (2002). "Gamma-secretase-mediated proteolysis in cell-surface-receptor signalling." Nat Rev Mol Cell Biol **3**(9): 673-684.
- Fryer, C. J., E. Lamar, I. Turbachova, C. Kintner and K. A. Jones (2002). "Mastermind mediates chromatin-specific transcription and turnover of the Notch enhancer complex." Genes Dev **16**.
- Fryer, C. J., J. B. White and K. A. Jones (2004). "Mastermind recruits CycC:CDK8 to phosphorylate the Notch ICD and coordinate activation with turnover." Mol Cell **16**(4): 509-520.
- Fu, Z., E. R. Gilbert and D. Liu (2013). "Regulation of Insulin Synthesis and Secretion and Pancreatic Beta-Cell Dysfunction in Diabetes." Current diabetes reviews **9**(1): 25-53.
- Furukawa, T., C. Ishifune, S.-i. Tsukumo, K. Hozumi, Y. Maekawa, N. Matsui, R. Kaji and K. Yasutomo (2016). "Transmission of survival signals through Delta-like 1 on activated CD4⁺ T cells." Scientific Reports **6**: 33692.
- Gailus-Durner, V., H. Fuchs, T. Adler, A. Aguilar Pimentel, L. Becker, I. Bolle, J. Calzada-Wack, C. Dalke, N. Ehrhardt, B. Ferwagner, W. Hans, S. M. Hölter, G. Hölzlwimmer, M. Horsch, A. Javaheri, M. Kallnik, E. Kling, C. Lengger, C. Mörth, I. Mossbrugger, B. Naton, C. Prehn, O. Puk, B. Rathkolb, J. Rozman, A. Schrewe, F. Thiele, J. Adamski, B. Aigner, H. Behrendt, D. H. Busch, J. Favor, J. Graw, G. Heldmaier, B. Ivandic, H. Katus, M. Klingenspor, T. K. Elisabeth Kremmer, M. Ollert, L. Quintanilla-Martinez, H. Schulz, E. Wolf, W. Wurst and M. H. de Angelis (2009). Systemic First-Line Phenotyping. Gene Knockout Protocols: Second Edition. W. Wurst and R. Kühn. Totowa, NJ, Humana Press: 463-509.
- Gara, R. K., S. Kumari, A. Ganju, M. M. Yallapu, M. Jaggi and S. C. Chauhan (2015). "Slit/Robo pathway: a promising therapeutic target for cancer." Drug Discov Today **20**(1): 156-164.
- Gelling, R. W., X. Q. Du, D. S. Dichmann, J. Romer, H. Huang, L. Cui, S. Obici, B. Tang, J. J. Holst, C. Fledelius, P. B. Johansen, L. Rossetti, L. A. Jelicks, P. Serup, E. Nishimura and M. J. Charron (2003). "Lower blood glucose, hyperglucagonemia, and pancreatic alpha cell hyperplasia in glucagon receptor knockout mice." Proc Natl Acad Sci U S A **100**(3): 1438-1443.

- Gelling, R. W., P. M. Vuguin, X. Q. Du, L. Cui, J. Rømer, R. A. Pederson, M. Leiser, H. Sørensen, J. J. Holst, C. Fledelius, P. B. Johansen, N. Fleischer, C. H. S. McIntosh, E. Nishimura and M. J. Charron (2009). "Pancreatic β -cell overexpression of the glucagon receptor gene results in enhanced β -cell function and mass." *American Journal of Physiology - Endocrinology and Metabolism* **297**(3): E695-E707.
- Georgia, S., R. Soliz, M. Li, P. Zhang and A. Bhushan (2006). "p57 and Hes1 coordinate cell cycle exit with self-renewal of pancreatic progenitors." *Dev Biol* **298**(1): 22-31.
- Ghelardoni, S., V. Carnicelli, S. Frascarelli, S. Ronca-Testoni and R. Zucchi (2006). "Ghrelin tissue distribution: comparison between gene and protein expression." *J Endocrinol Invest* **29**(2): 115-121.
- Göke, R., H. C. Fehmann, T. Linn, H. Schmidt, M. Krause, J. Eng and B. Göke (1993). "Exendin-4 is a high potency agonist and truncated exendin-(9-39)-amide an antagonist at the glucagon-like peptide 1-(7-36)-amide receptor of insulin-secreting beta-cells." *Journal of Biological Chemistry* **268**(26): 19650-19655.
- Golson, M. L., J. Le Lay, N. Gao, N. Brämwig, K. M. Loomes, R. Oakey, C. L. May, P. White and K. H. Kaestner (2009). "Jagged1 is a competitive inhibitor of Notch signaling in the embryonic pancreas." *Mechanisms of development* **126**(8-9): 687-699.
- González, J. A., L. T. Jensen, L. Fugger and D. Burdakov (2008). "Metabolism-Independent Sugar Sensing in Central Orexin Neurons." *Diabetes* **57**(10): 2569-2576.
- Gosmain, Y., C. Cheyssac, M. Heddad Masson, C. Dibner and J. Philippe (2011). "Glucagon gene expression in the endocrine pancreas: the role of the transcription factor Pax6 in alpha-cell differentiation, glucagon biosynthesis and secretion." *Diabetes Obes Metab* **13 Suppl 1**: 31-38.
- Grabher, C., H. von Boehmer and A. T. Look (2006). "Notch 1 activation in the molecular pathogenesis of T-cell acute lymphoblastic leukaemia." *Nat Rev Cancer* **6**(5): 347-359.
- Gradwohl, G., A. Dierich, M. LeMeur and F. Guillemot (2000). "neurogenin3 is required for the development of the four endocrine cell lineages of the pancreas." *Proc Natl Acad Sci U S A* **97**(4): 1607-1611.
- Greenwood, A. L., S. Li, K. Jones and D. A. Melton (2007). "Notch signaling reveals developmental plasticity of Pax4+ pancreatic endocrine progenitors and shunts them to a duct fate." *Mechanisms of Development* **124**(2): 97-107.
- Gregory, J. M., D. J. Moore and J. H. Simmons (2013). "Type 1 Diabetes Mellitus." *Pediatrics in Review* **34**(5): 203-215.
- Gridley, T. (2007). "Notch signaling in vascular development and physiology." *Development* **134**(15): 2709-2718.
- Gridley, T. (2010). "Notch signaling in the vasculature." *Curr Top Dev Biol* **92**: 277-309.
- Grodsky, G. M. (1989). "A new phase of insulin secretion. How will it contribute to our understanding of beta-cell function?" *Diabetes* **38**(6): 673-678.
- Gromada, J., I. Franklin and C. B. Wollheim (2007). "Alpha-cells of the endocrine pancreas: 35 years of research but the enigma remains." *Endocr Rev* **28**(1): 84-116.
- Grossman, S. P. (1986). "The role of glucose, insulin and glucagon in the regulation of food intake and body weight." *Neurosci Biobehav Rev* **10**(3): 295-315.

- Gu, G., J. Dubauskaite and D. A. Melton (2002). "Direct evidence for the pancreatic lineage: NGN3+ cells are islet progenitors and are distinct from duct progenitors." Development **129**(10): 2447-2457.
- Guariguata, L., D. R. Whiting, I. Hambleton, J. Beagley, U. Linnenkamp and J. E. Shaw (2014). "Global estimates of diabetes prevalence for 2013 and projections for 2035." Diabetes Research and Clinical Practice **103**(2): 137-149.
- Guillam, M.-T., E. Hummler, E. Schaerer, J. Y. Wu, M. J. Birnbaum, F. Beermann, A. Schmidt, N. Deriaz and B. Thorens (1997). "Early diabetes and abnormal postnatal pancreatic islet development in mice lacking Glut-2." Nat Genet **17**(3): 327-330.
- Guillam, M. T., P. Dupraz and B. Thorens (2000). "Glucose uptake, utilization, and signaling in GLUT2-null islets." Diabetes **49**(9): 1485-1491.
- Guruharsha, K. G., M. W. Kankel and S. Artavanis-Tsakonas (2012). "The Notch signalling system: recent insights into the complexity of a conserved pathway." Nat Rev Genet **13**(9): 654-666.
- Gustafsson, A. J., H. Ingelman-Sundberg, M. Dzabic, J. Awasum, N. K. Hoa, C.-G. Östenson, C. Pierro, P. Tedeschi, O. Woolcott, S. Chiouan, P.-E. Lund, O. Larsson and M. S. Islam (2004). "Ryanodine receptor-operated activation of TRP-like channels can trigger critical Ca²⁺ signaling events in pancreatic β -cells." The FASEB Journal.
- Gutierrez, L., M. Mauriat, S. Guenin, J. Pelloux, J. F. Lefebvre, R. Louvet, C. Rusterucci, T. Moritz, F. Guerineau, C. Bellini and O. Van Wuytswinkel (2008). "The lack of a systematic validation of reference genes: a serious pitfall undervalued in reverse transcription-polymerase chain reaction (RT-PCR) analysis in plants." Plant Biotechnol J **6**(6): 609-618.
- Hagenfeldt-Johansson, K. A., P. L. Herrera, H. Wang, A. Gjinovci, H. Ishihara and C. B. Wollheim (2001). "Beta-cell-targeted expression of a dominant-negative hepatocyte nuclear factor-1 alpha induces a maturity-onset diabetes of the young (MODY)3-like phenotype in transgenic mice." Endocrinology **142**(12): 5311-5320.
- Haines, N. and K. D. Irvine (2003). "Glycosylation regulates Notch signalling." Nat Rev Mol Cell Biol **4**(10): 786-797.
- Halldorsdottir, S., J. Carmody, C. N. Boozer, C. A. Leduc and R. L. Leibel (2009). "Reproducibility and accuracy of body composition assessments in mice by dual energy x-ray absorptiometry and time domain nuclear magnetic resonance." International journal of body composition research **7**(4): 147-154.
- Hang, Y. and R. Stein (2011). "MafA and MafB activity in pancreatic β cells." Trends in endocrinology and metabolism: TEM **22**(9): 364-373.
- Harwood, J. L. (1988). "Fatty acid metabolism." Annual Review of Plant Physiology and Plant Molecular Biology **39**(1): 101-138.
- Hashimoto, N., Y. Kido, T. Uchida, S. Asahara, Y. Shigeyama, T. Matsuda, A. Takeda, D. Tsuchihashi, A. Nishizawa, W. Ogawa, Y. Fujimoto, H. Okamura, K. C. Arden, P. L. Herrera, T. Noda and M. Kasuga (2006). "Ablation of PDK1 in pancreatic beta cells induces diabetes as a result of loss of beta cell mass." Nat Genet **38**(5): 589-593.

- Heddad Masson, M., C. Poisson, A. Guerardel, A. Mamin, J. Philippe and Y. Gosmain (2014). "Foxa1 and Foxa2 regulate alpha-cell differentiation, glucagon biosynthesis, and secretion." Endocrinology **155**(10): 3781-3792.
- Hillaire-Buys, D., J. Chapal, G. Bertrand, P. Petit and M. M. Loubatieres-Mariani (1994). "Purinergic receptors on insulin-secreting cells." Fundam Clin Pharmacol **8**(2): 117-127.
- Hiratochi, M., H. Nagase, Y. Kuramochi, C.-S. Koh, T. Ohkawara and K. Nakayama (2007). "The Delta intracellular domain mediates TGF- β /Activin signaling through binding to Smads and has an important bi-directional function in the Notch-Delta signaling pathway." Nucleic Acids Research **35**(3): 912-922.
- Hodson, D. J., R. K. Mitchell, L. Marselli, T. J. Pullen, S. Gimeno Brias, F. Semplici, K. L. Everett, D. M. F. Cooper, M. Bugliani, P. Marchetti, V. Lavallard, D. Bosco, L. Piemonti, P. R. Johnson, S. J. Hughes, D. Li, W.-H. Li, A. M. J. Shapiro and G. A. Rutter (2014). "ADCY5 Couples Glucose to Insulin Secretion in Human Islets." Diabetes **63**(9): 3009-3021.
- Holst, J. J. (2007). "The physiology of glucagon-like peptide 1." Physiol Rev **87**(4): 1409-1439.
- Horn, S., S. Kobberup, M. C. Jorgensen, M. Kalisz, T. Klein, R. Kageyama, M. Gegg, H. Lickert, J. Lindner, M. A. Magnuson, Y. Y. Kong, P. Serup, J. Ahnfelt-Ronne and J. N. Jensen (2012). "Mind bomb 1 is required for pancreatic beta-cell formation." Proc Natl Acad Sci U S A **109**(19): 7356-7361.
- Hosokawa, M., W. Dolci and B. Thorens (2001). "Differential sensitivity of GLUT1- and GLUT2-expressing beta cells to streptozotocin." Biochem Biophys Res Commun **289**(5): 1114-1117.
- Hozumi, K., N. Negishi, D. Suzuki, N. Abe, Y. Sotomaru, N. Tamaoki, C. Mailhos, D. Ish-Horowicz, S. Habu and M. J. Owen (2004). "Delta-like 1 is necessary for the generation of marginal zone B cells but not T cells in vivo." Nat Immunol **5**(6): 638-644.
- Hrabe de Angelis, M., J. McIntyre, 2nd and A. Gossler (1997). "Maintenance of somite borders in mice requires the Delta homologue Dll1." Nature **386**(6626): 717-721.
- Hribal, M. L., L. Perego, S. Lovari, F. Andreozzi, R. Menghini, C. Perego, G. Finzi, L. Usellini, C. Placidi, C. Capella, V. Guzzi, D. Lauro, F. Bertuzzi, A. Davalli, G. Pozza, A. Pontiroli, M. Federici, R. Lauro, A. Brunetti, F. Folli and G. Sesti (2003). "Chronic hyperglycemia impairs insulin secretion by affecting insulin receptor expression, splicing, and signaling in RIN beta cell line and human islets of Langerhans." Faseb j **17**(10): 1340-1342.
- Ihaka, R. and R. Gentleman (1996). "R: A Language for Data Analysis and Graphics." Journal of Computational and Graphical Statistics **5**(3): 299-314.
- Itoh, Y., Y. Kawamata, M. Harada, M. Kobayashi, R. Fujii, S. Fukusumi, K. Ogi, M. Hosoya, Y. Tanaka, H. Uejima, H. Tanaka, M. Maruyama, R. Satoh, S. Okubo, H. Kizawa, H. Komatsu, F. Matsumura, Y. Noguchi, T. Shinohara, S. Hinuma, Y. Fujisawa and M. Fujino (2003). "Free fatty acids regulate insulin secretion from pancreatic beta cells through GPR40." Nature **422**(6928): 173-176.
- Jabs, N., I. Franklin, M. B. Brenner, J. Gromada, N. Ferrara, C. B. Wollheim and E. Lammert (2008). "Reduced insulin secretion and content in VEGF-a deficient mouse pancreatic islets." Exp Clin Endocrinol Diabetes **116 Suppl 1**: S46-49.
- Jarriault, S. and I. Greenwald (2005). "Evidence for functional redundancy between C. elegans ADAM proteins SUP-17/Kuzbanian and ADM-4/TACE." Dev Biol **287**(1): 1-10.

- Jensen, J. N., E. Cameron, M. V. Garay, T. W. Starkey, R. Gianani and J. Jensen (2005). "Recapitulation of elements of embryonic development in adult mouse pancreatic regeneration." Gastroenterology **128**(3): 728-741.
- Jensen, T. and A. Hartmann (2015). "Emerging treatments for post-transplantation diabetes mellitus." Nat Rev Nephrol **11**(8): 465-477.
- Johansson, K. A., U. Dursun, N. Jordan, G. Gu, F. Beermann, G. Gradwohl and A. Grapin-Botton (2007). "Temporal control of neurogenin3 activity in pancreas progenitors reveals competence windows for the generation of different endocrine cell types." Dev Cell **12**(3): 457-465.
- Jung, J., J.-S. Mo, M.-Y. Kim, E.-J. Ann, J.-H. Yoon and H.-S. Park (2011). "Regulation of Notch1 signaling by delta-like ligand 1 intracellular domain through physical interaction." Molecules and Cells **32**(2): 161-165.
- Khalidi, M. Z., Y. Guiot, P. Gilon, J. C. Henquin and J. C. Jonas (2004). "Increased glucose sensitivity of both triggering and amplifying pathways of insulin secretion in rat islets cultured for 1 wk in high glucose." Am J Physiol Endocrinol Metab **287**(2): E207-217.
- Kim, A., K. Miller, J. Jo, G. Kilimnik, P. Wojcik and M. Hara (2009). "Islet architecture: A comparative study." Islets **1**(2): 129-136.
- Kim, W., Y. K. Shin, B. J. Kim and J. M. Egan (2010). "Notch signaling in pancreatic endocrine cell and diabetes." Biochem Biophys Res Commun **392**(3): 247-251.
- Koch, U., E. Fiorini, R. Benedito, V. Besseyrias, K. Schuster-Gossler, M. Pierres, N. R. Manley, A. Duarte, H. R. Macdonald and F. Radtke (2008). "Delta-like 4 is the essential, nonredundant ligand for Notch1 during thymic T cell lineage commitment." J Exp Med **205**(11): 2515-2523.
- Kogure, A., I. Shiratori, J. Wang, L. L. Lanier and H. Arase (2011). "PANP is a novel O-glycosylated PILRalpha ligand expressed in neural tissues." Biochem Biophys Res Commun **405**(3): 428-433.
- Kolev, V., D. Kacer, R. Trifonova, D. Small, M. Duarte, R. Soldi, I. Graziani, O. Sideleva, B. Larman, T. Maciag and I. Prudovsky (2005). "The intracellular domain of Notch ligand Delta1 induces cell growth arrest." FEBS Lett **579**(25): 5798-5802.
- Kopan, R. and M. X. G. Ilagan (2009). "The Canonical Notch Signaling Pathway: Unfolding the Activation Mechanism." Cell **137**(2): 216-233.
- Kopinke, D., M. Brailsford, J. E. Shea, R. Leavitt, C. L. Scaife and L. C. Murtaugh (2011). "Lineage tracing reveals the dynamic contribution of Hes1+ cells to the developing and adult pancreas." Development **138**(3): 431-441.
- Kornberg, H. (2000). "Krebs and his trinity of cycles." Nat Rev Mol Cell Biol **1**(3): 225-228.
- Krarup, T. and P. H. Groop (1991). "Physiology and pathophysiology of GIP: A review." Scandinavian Journal of Clinical and Laboratory Investigation **51**(7): 571-579.
- Kretzschmar, K. and Fiona M. Watt (2012). "Lineage Tracing." Cell **148**(1): 33-45.
- Kulkarni, S. S., F. Salehzadeh, T. Fritz, J. R. Zierath, A. Krook and M. E. Osler (2012). "Mitochondrial regulators of fatty acid metabolism reflect metabolic dysfunction in type 2 diabetes mellitus." Metabolism **61**(2): 175-185.

-
- Kurooka, H., K. Kuroda and T. Honjo (1998). "Roles of the ankyrin repeats and C-terminal region of the mouse notch1 intracellular region." Nucleic Acids Res **26**(23): 5448-5455.
- Lammert, E., J. Brown and D. A. Melton (2000). "Notch gene expression during pancreatic organogenesis." Mechanisms of Development **94**(1–2): 199-203.
- Lammert, E., G. Gu, M. McLaughlin, D. Brown, R. Brekken, L. C. Murtaugh, H. P. Gerber, N. Ferrara and D. A. Melton (2003). "Role of VEGF-A in vascularization of pancreatic islets." Curr Biol **13**(12): 1070-1074.
- Langerhans, P. (1869). "Beiträge zur mikroskopischen anatomie der bauchspeicheldrüse." Dissertation.
- Laurenza, A., E. M. Sutkowski and K. B. Seamon (1989). "Forskolin: a specific stimulator of adenylyl cyclase or a diterpene with multiple sites of action?" Trends in Pharmacological Sciences **10**(11): 442-447.
- Le Borgne, R. (2006). "Regulation of Notch signalling by endocytosis and endosomal sorting." Curr Opin Cell Biol **18**(2): 213-222.
- Li, C., P. Chen, J. Vaughan, K. F. Lee and W. Vale (2007). "Urocortin 3 regulates glucose-stimulated insulin secretion and energy homeostasis." Proc Natl Acad Sci U S A **104**(10): 4206-4211.
- Li, D. S., Y. H. Yuan, H. J. Tu, Q. L. Liang and L. J. Dai (2009). "A protocol for islet isolation from mouse pancreas." Nat Protoc **4**(11): 1649-1652.
- Li, X.-b., J.-d. Gu and Q.-h. Zhou (2015). "Review of aerobic glycolysis and its key enzymes – new targets for lung cancer therapy." Thoracic Cancer **6**(1): 17-24.
- Li, X. Y., W. J. Zhai and C. B. Teng (2015). "Notch Signaling in Pancreatic Development." Int J Mol Sci **17**(1).
- Lin, Y. and Z. Sun (2012). "Antiaging gene Klotho enhances glucose-induced insulin secretion by up-regulating plasma membrane levels of TRPV2 in MIN6 beta-cells." Endocrinology **153**(7): 3029-3039.
- Lindskog, S. and B. Ahrén (1987). "Galanin: effects on basal and stimulated insulin and glucagon secretion in the mouse." Acta Physiologica Scandinavica **129**(3): 305-309.
- Liu, H., M. M. Fergusson, R. M. Castilho, J. Liu, L. Cao, J. Chen, D. Malide, I. I. Rovira, D. Schimel, C. J. Kuo, J. S. Gutkind, P. M. Hwang and T. Finkel (2007). "Augmented Wnt Signaling in a Mammalian Model of Accelerated Aging." Science **317**(5839): 803-806.
- Liu, Y., J. Suckale, J. Masjkur, M. G. Magro, A. Steffen, K. Anastassiadis and M. Solimena (2010). "Tamoxifen-Independent Recombination in the *RIP-CreER* Mouse." PLoS ONE **5**(10): e13533.
- Liu, Z., W. Kim, Z. Chen, Y.-K. Shin, O. D. Carlson, J. L. Fiori, L. Xin, J. K. Napora, R. Short, J. O. Odetunde, Q. Lao and J. M. Egan (2011). "Insulin and Glucagon Regulate Pancreatic α -Cell Proliferation." PLoS ONE **6**(1): e16096.
- Livak, K. J. and T. D. Schmittgen (2001). "Analysis of relative gene expression data using real-time quantitative PCR and the $2^{-\Delta\Delta C(T)}$ Method." Methods **25**(4): 402-408.

- Lobov, I. B., E. Cheung, R. Wudali, J. Cao, G. Halasz, Y. Wei, A. Economides, H. C. Lin, N. Papadopoulos, G. D. Yancopoulos and S. J. Wiegand (2011). "The Dll4/Notch pathway controls postangiogenic blood vessel remodeling and regression by modulating vasoconstriction and blood flow." *Blood* **117**(24): 6728-6737.
- Logeat, F., C. Bessia, C. Brou, O. LeBail, S. Jarriault, N. G. Seidah and A. Israel (1998). "The Notch1 receptor is cleaved constitutively by a furin-like convertase." *Proc Natl Acad Sci U S A* **95**(14): 8108-8112.
- Lowell, B. B. and G. I. Shulman (2005). "Mitochondrial dysfunction and type 2 diabetes." *Science* **307**(5708): 384-387.
- Lu, J., R. Jaafer, R. Bonnavion, P. Bertolino and C.-X. Zhang (2014). "Transdifferentiation of pancreatic α -cells into insulin-secreting cells: From experimental models to underlying mechanisms." *World Journal of Diabetes* **5**(6): 847-853.
- Ma, R. Y., T. S. Tam, A. P. Suen, P. M. Yeung, S. W. Tsang, S. K. Chung, M. K. Thomas, P. S. Leung and K. M. Yao (2006). "Secreted PDZD2 exerts concentration-dependent effects on the proliferation of INS-1E cells." *Int J Biochem Cell Biol* **38**(5-6): 1015-1022.
- Magenheim, J., A. M. Klein, B. Z. Stanger, R. Ashery-Padan, B. Sosa-Pineda, G. Gu and Y. Dor (2011). "Ngn3(+) endocrine progenitor cells control the fate and morphogenesis of pancreatic ductal epithelium." *Developmental biology* **359**(1): 26-36.
- Malecki, M. T., U. S. Jhala, A. Antonellis, L. Fields, A. Doria, T. Orban, M. Saad, J. H. Warram, M. Montminy and A. S. Krolewski (1999). "Mutations in NEUROD1 are associated with the development of type 2 diabetes mellitus." *Nat Genet* **23**(3): 323-328.
- Martens, G. A., L. Jiang, K. H. Hellemans, G. Stange, H. Heimberg, F. C. Nielsen, O. Sand, J. Van Helden, L. Van Lommel, F. Schuit, F. K. Gorus and D. G. Pipeleers (2011). "Clusters of conserved beta cell marker genes for assessment of beta cell phenotype." *PLoS One* **6**(9): e24134.
- Masgrau, R., G. C. Churchill, A. J. Morgan, S. J. Ashcroft and A. Galione (2003). "NAADP: a new second messenger for glucose-induced Ca²⁺ responses in clonal pancreatic beta cells." *Curr Biol* **13**(3): 247-251.
- McDonald, T. J., J. Dupre, K. Tatemoto, G. R. Greenberg, J. Radziuk and V. Mutt (1985). "Galanin Inhibits Insulin Secretion and Induces Hyperglycemia in Dogs." *Diabetes* **34**(2): 192-196.
- Meloni, A. R., M. B. DeYoung, C. Lowe and D. G. Parkes (2013). "GLP-1 receptor activated insulin secretion from pancreatic β -cells: mechanism and glucose dependence." *Diabetes, Obesity & Metabolism* **15**(1): 15-27.
- Meyer, C. (2010). "Final Answer: Ghrelin Can Suppress Insulin Secretion in Humans, but Is It Clinically Relevant?" *Diabetes* **59**(11): 2726-2728.
- Mimaki, M., X. Wang, M. McKenzie, D. R. Thorburn and M. T. Ryan (2012). "Understanding mitochondrial complex I assembly in health and disease." *Biochimica et Biophysica Acta (BBA) - Bioenergetics* **1817**(6): 851-862.
- Mitchell, K. J., T. Tsuboi and G. A. Rutter (2004). "Role for Plasma Membrane-Related Ca²⁺ATPase-1 (ATP2C1) in Pancreatic β -Cell Ca²⁺ Homeostasis Revealed by RNA Silencing." *Diabetes* **53**(2): 393-400.

- Mitchell, R. K., M.-S. Nguyen-Tu, P. Chabosseau, R. M. Callingham, T. J. Pullen, R. Cheung, I. Leclerc, D. J. Hodson and G. A. Rutter (2017). "The transcription factor Pax6 is required for pancreatic β cell identity, glucose-regulated ATP synthesis and Ca^{2+} dynamics in adult mice." Journal of Biological Chemistry.
- Miyamoto, Y., A. Maitra, B. Ghosh, U. Zechner, P. Argani, C. A. Iacobuzio-Donahue, V. Sriuranpong, T. Iso, I. M. Meszoely, M. S. Wolfe, R. H. Hruban, D. W. Ball, R. M. Schmid and S. D. Leach (2003). "Notch mediates TGF α -induced changes in epithelial differentiation during pancreatic tumorigenesis." Cancer Cell **3**(6): 565-576.
- Moates, J. M., S. Nanda, M. A. Cissell, M. J. Tsai and R. Stein (2003). "BETA2 activates transcription from the upstream glucokinase gene promoter in islet beta-cells and gut endocrine cells." Diabetes **52**(2): 403-408.
- Mohtashami, M., D. K. Shah, H. Nakase, K. Kianizad, H. T. Petrie and J. C. Zúñiga-Pflücker (2010). "Direct Comparison of Dll1- and Dll4-Mediated Notch Activation Levels Shows Differential Lymphomyeloid Lineage Commitment Outcomes." The Journal of Immunology **185**(2): 867-876.
- Mommersteeg, M. T., M. L. Yeh, J. G. Parnavelas and W. D. Andrews (2015). "Disrupted Slit-Robo signalling results in membranous ventricular septum defects and bicuspid aortic valves." Cardiovasc Res **106**(1): 55-66.
- Morris AP, V. B., Teslovich TM, Ferreira T, Segrè AV, Steinthorsdottir V, Strawbridge RJ, Khan H, Grallert H, Mahajan A, Prokopenko I, Kang HM, Dina C, Esko T, Fraser RM, Kanoni S, Kumar A, Lagou V, Langenberg C, Luan J, Lindgren CM, Müller-Nurasyid M, Pechlivanis S, Rayner NW, Scott LJ, Wiltshire S, Yengo L, Kinnunen L, Rossin EJ, Raychaudhuri S, Johnson AD, Dimas AS, Loos RJ, Vedantam S, Chen H, Florez JC, Fox C, Liu CT, Rybin D, Couper DJ, Kao WH, Li M, Cornelis MC, Kraft P, Sun Q, van Dam RM, Stringham HM, Chines PS, Fischer K, Fontanillas P, Holmen OL, Hunt SE, Jackson AU, Kong A, Lawrence R, Meyer J, Perry JR, Platou CG, Potter S, Rehnberg E, Robertson N, Sivapalaratnam S, Stančáková A, Stirrups K, Thorleifsson G, Tikkanen E, Wood AR, Almgren P, Atalay M, Benediktsson R, Bonnycastle LL, Burt N, Carey J, Charpentier G, Crenshaw AT, Doney AS, Dorkhan M, Edkins S, Emilsson V, Eury E, Forsen T, Gertow K, Gigante B, Grant GB, Groves CJ, Guiducci C, Herder C, Hreidarsson AB, Hui J, James A, Jonsson A, Rathmann W, Klopp N, Kravic J, Krjutškov K, Langford C, Leander K, Lindholm E, Lobbens S, Männistö S, Mirza G, Mühleisen TW, Musk B, Parkin M, Rallidis L, Saramies J, Sennblad B, Shah S, Sigurðsson G, Silveira A, Steinbach G, Thorand B, Trakalo J, Veglia F, Wennauer R, Winckler W, Zabaneh D, Campbell H, van Duijn C, Uitterlinden AG, Hofman A, Sijbrands E, Abecasis GR, Owen KR, Zeggini E, Trip MD, Forouhi NG, Syvänen AC, Eriksson JG, Peltonen L, Nöthen MM, Balkau B, Palmer CN, Lyssenko V, Tuomi T, Isomaa B, Hunter DJ, Qi L; Wellcome Trust Case Control Consortium; Meta-Analyses of Glucose and Insulin-related traits Consortium (MAGIC) Investigators; Genetic Investigation of ANthropometric Traits (GIANT) Consortium; Asian Genetic Epidemiology Network–Type 2 Diabetes (AGEN-T2D) Consortium; South Asian Type 2 Diabetes (SAT2D) Consortium, Shuldiner AR, Roden M, Barroso I, Wilsgaard T, Beilby J, Hovingh K, Price JF, Wilson JF, Rauramaa R, Lakka TA, Lind L, Dedoussis G, Njølstad I, Pedersen NL, Khaw KT, Wareham NJ, Keinanen-Kiukaanniemi SM, Saaristo TE, Korpi-Hyövälti E, Saltevo J, Laakso M, Kuusisto J, Metspalu A, Collins FS, Mohlke KL, Bergman RN, Tuomilehto J, Boehm BO, Gieger C, Hveem K, Cauchi S, Froguel P, Baldassarre D, Tremoli E, Humphries SE, Saleheen D, Danesh J, Ingelsson E, Ripatti S, Salomaa V, Erbel R, Jöckel KH, Moebus S, Peters A, Illig T, de Faire U, Hamsten A, Morris AD, Donnelly PJ, Frayling TM, Hattersley AT, Boerwinkle E, Melander O, Kathiresan S, Nilsson PM, Deloukas P, Thorsteinsdottir U, Groop LC, Stefansson K, Hu F, Pankow JS, Dupuis J, Meigs JB, Altshuler D, Boehnke M, McCarthy MI; DIAbetes Genetics Replication And Meta-analysis (DIAGRAM) Consortium. (2012). "Large-scale

- association analysis provides insights into the genetic architecture and pathophysiology of type 2 diabetes." *Nat Genet* **44**(9): 981-990.
- Mumm, J. S., E. H. Schroeter, M. T. Saxena, A. Griesemer, X. Tian, D. J. Pan, W. J. Ray and R. Kopan (2000). "A ligand-induced extracellular cleavage regulates gamma-secretase-like proteolytic activation of Notch1." *Mol Cell* **5**(2): 197-206.
- Murtaugh, L. C. (2007). "Pancreas and beta-cell development: from the actual to the possible." *Development* **134**(3): 427-438.
- Murtaugh, L. C. (2008). "The what, where, when and how of Wnt/ β -catenin signaling in pancreas development." *Organogenesis* **4**(2): 81-86.
- Murtaugh, L. C. and D. A. Melton (2003). "Genes, signals, and lineages in pancreas development." *Annu Rev Cell Dev Biol* **19**: 71-89.
- Nair, K. S. (1987). "Hyperglucagonemia Increases Resting Metabolic Rate In Man During Insulin Deficiency." *The Journal of Clinical Endocrinology & Metabolism* **64**(5): 896-901.
- Nakhai, H., J. T. Siveke, B. Klein, L. Mendoza-Torres, P. K. Mazur, H. Algul, F. Radtke, L. Strobl, U. Zimmer-Strobl and R. M. Schmid (2008). "Conditional ablation of Notch signaling in pancreatic development." *Development* **135**(16): 2757-2765.
- Nam, Y., P. Sliz, L. Song, J. C. Aster and S. C. Blacklow (2006). "Structural basis for cooperativity in recruitment of MAML coactivators to Notch transcription complexes." *Cell* **124**(5): 973-983.
- Nishimura, W., S. Takahashi and K. Yasuda (2015). "MafA is critical for maintenance of the mature beta cell phenotype in mice." *Diabetologia* **58**(3): 566-574.
- Norgaard, G. A., J. N. Jensen and J. Jensen (2003). "FGF10 signaling maintains the pancreatic progenitor cell state revealing a novel role of Notch in organ development." *Developmental Biology* **264**(2): 323-338.
- Nosedá, M., L. Chang, G. McLean, J. E. Grim, B. E. Clurman, L. L. Smith and A. Karsan (2004). "Notch Activation Induces Endothelial Cell Cycle Arrest and Participates in Contact Inhibition: Role of p21(Cip1) Repression." *Molecular and Cellular Biology* **24**(20): 8813-8822.
- O'Dowd, J. and C. Stocker (2013). "Endocrine pancreatic development: impact of obesity and diet." *Frontiers in Physiology* **4**(170).
- Obici, S., B. B. Zhang, G. Karkanas and L. Rossetti (2002). "Hypothalamic insulin signaling is required for inhibition of glucose production." *Nat Med* **8**(12): 1376-1382.
- Ogunnowo-Bada, E. O., N. Heeley, L. Brochard and M. L. Evans (2014). "Brain glucose sensing, glucokinase and neural control of metabolism and islet function." *Diabetes Obes Metab* **16 Suppl 1**: 26-32.
- Oliver-Krasinski, J. M. and D. A. Stoffers (2008). "On the origin of the beta cell." *Genes Dev* **22**(15): 1998-2021.
- Oropeza, D., N. Jouvét, L. Budry, J. E. Campbell, K. Bouyakdan, J. Lacombe, G. Perron, V. Bergeron, J. C. Neuman, H. K. Brar, R. J. Fenske, C. Meunier, S. Szelecki, M. E. Kimple, D. J. Drucker, R. A. Screaton, V. Poutout, M. Ferron, T. Alquier and J. L. Estall (2015). "Phenotypic Characterization of MIP-

- CreERT(1Lphi) Mice With Transgene-Driven Islet Expression of Human Growth Hormone." Diabetes **64**(11): 3798-3807.
- Ort, T., E. Maksimova, R. Dirx, A. M. Kachinsky, S. Berghs, S. C. Froehner and M. Solimena (2000). "The receptor tyrosine phosphatase-like protein ICA512 binds the PDZ domains of beta2-syntrophin and nNOS in pancreatic beta-cells." Eur J Cell Biol **79**(9): 621-630.
- Ostergaard, E., R. J. Rodenburg, M. van den Brand, L. L. Thomsen, M. Duno, M. Batbayli, F. Wibrand and L. Nijtmans (2011). "Respiratory chain complex I deficiency due to NDUFA12 mutations as a new cause of Leigh syndrome." Journal of Medical Genetics **48**(11): 737-740.
- Parks, A. L., J. R. Stout, S. B. Shepard, K. M. Klueg, A. A. Dos Santos, T. R. Parody, M. Vaskova and M. A. T. Muskavitch (2006). "Structure-Function Analysis of Delta Trafficking, Receptor Binding and Signaling in Drosophila." Genetics **174**(4): 1947-1961.
- Pasek, R. C., J. C. Dunn, J. M. Elsagr, M. Aramandla, A. R. Matta and M. Gannon (2016). "Connective tissue growth factor is critical for proper beta-cell function and pregnancy-induced beta-cell hyperplasia in adult mice." Am J Physiol Endocrinol Metab **311**(3): E564-574.
- Pellegrinet, L., V. Rodilla, Z. Liu, S. Chen, U. Koch, L. Espinosa, K. H. Kaestner, R. Kopan, J. Lewis and F. Radtke (2011). "Dll1- and dll4-mediated notch signaling are required for homeostasis of intestinal stem cells." Gastroenterology **140**(4): 1230-1240 e1231-1237.
- Petcherski, A. G. and J. Kimble (2000). "Mastermind is a putative activator for Notch." Curr Biol **10**(13): R471-473.
- Pfister, S., G. K. Przemeck, J. K. Gerber, J. Beckers, J. Adamski and M. Hrabe de Angelis (2003). "Interaction of the MAGUK family member Acvrinp1 and the cytoplasmic domain of the Notch ligand Delta1." J Mol Biol **333**(2): 229-235.
- Pictet, R. L., W. R. Clark, R. H. Williams and W. J. Rutter (1972). "An ultrastructural analysis of the developing embryonic pancreas." Dev Biol **29**(4): 436-467.
- Pintar, A., A. De Biasio, M. Popovic, N. Ivanova and S. Pongor (2007). "The intracellular region of Notch ligands: does the tail make the difference?" Biol Direct **2**: 19.
- Piper, K., S. G. Ball, L. W. Turnpenny, S. Brickwood, D. I. Wilson and N. A. Hanley (2002). "Beta-cell differentiation during human development does not rely on nestin-positive precursors: implications for stem cell-derived replacement therapy." Diabetologia **45**(7): 1045-1047.
- Pitkanen, S. and B. H. Robinson (1996). "Mitochondrial complex I deficiency leads to increased production of superoxide radicals and induction of superoxide dismutase." Journal of Clinical Investigation **98**(2): 345-351.
- Pouli, A. E., E. Emmanouilidou, C. Zhao, C. Wasmeier, J. C. Hutton and G. A. Rutter (1998). "Secretory-granule dynamics visualized in vivo with a phogrin-green fluorescent protein chimera." Biochem J **333 (Pt 1)**: 193-199.
- Poulson, D. F. (1940). "The effects of certain X-chromosome deficiencies on the embryonic development of Drosophila melanogaster." Journal of Experimental Zoology **83**(2): 271-325.
- Prado, C. L., A. E. Pugh-Bernard, L. Elghazi, B. Sosa-Pineda and L. Sussel (2004). "Ghrelin cells replace insulin-producing beta cells in two mouse models of pancreas development." Proc Natl Acad Sci U S A **101**(9): 2924-2929.

-
- Proulx, K., D. Richard and C. D. Walker (2002). "Leptin regulates appetite-related neuropeptides in the hypothalamus of developing rats without affecting food intake." *Endocrinology* **143**(12): 4683-4692.
- Przemeck, G. K., U. Heinzmann, J. Beckers and M. Hrabe de Angelis (2003). "Node and midline defects are associated with left-right development in Delta1 mutant embryos." *Development* **130**(1): 3-13.
- Purow, B. W., R. M. Haque, M. W. Noel, Q. Su, M. J. Burdick, J. Lee, T. Sundaresan, S. Pastorino, J. K. Park, I. Mikolaenko, D. Maric, C. G. Eberhart and H. A. Fine (2005). "Expression of Notch-1 and its ligands, Delta-like-1 and Jagged-1, is critical for glioma cell survival and proliferation." *Cancer Res* **65**(6): 2353-2363.
- Qu, X., S. Afelik, J. N. Jensen, M. A. Bukys, S. Kobberup, M. Schmerr, F. Xiao, P. Nyeng, M. Veronica Albertoni, A. Grapin-Botton and J. Jensen (2013). "Notch-mediated post-translational control of Ngn3 protein stability regulates pancreatic patterning and cell fate commitment." *Developmental Biology* **376**(1): 1-12.
- Quesada, I., E. Tudurí, C. Ripoll and Á. Nadal (2008). "Physiology of the pancreatic α -cell and glucagon secretion: role in glucose homeostasis and diabetes." *Journal of Endocrinology* **199**(1): 5-19.
- Quintens, R., S. Singh, K. Lemaire, K. De Bock, M. Granvik, A. Schraenen, I. O. C. M. Vroegrijk, V. Costa, P. Van Noten, D. Lambrechts, S. Lehnert, L. Van Lommel, L. Thorrez, G. De Faudeur, J. A. Romijn, J. M. Shelton, L. Scorrano, H. R. Lijnen, P. J. Voshol, P. Carmeliet, P. P. A. Mammen and F. Schuit (2013). "Mice Deficient in the Respiratory Chain Gene *Cox6a2* Are Protected against High-Fat Diet-Induced Obesity and Insulin Resistance." *PLoS ONE* **8**(2): e56719.
- Radtke, F. and K. Raj (2003). "The role of Notch in tumorigenesis: oncogene or tumour suppressor?" *Nat Rev Cancer* **3**(10): 756-767.
- Rainer, J., F. Sanchez-Cabo, G. Stocker, A. Sturn and Z. Trajanoski (2006). "CARMAweb: comprehensive R- and bioconductor-based web service for microarray data analysis." *Nucleic Acids Res* **34**(Web Server issue): W498-503.
- Razzaque, M. S. (2012). "The role of Klotho in energy metabolism." *Nat Rev Endocrinol* **8**(10): 579-587.
- Rebay, I., R. J. Fleming, R. G. Fehon, L. Cherbas, P. Cherbas and S. Artavanis-Tsakonas (1991). "Specific EGF repeats of Notch mediate interactions with Delta and Serrate: implications for Notch as a multifunctional receptor." *Cell* **67**(4): 687-699.
- Redeker, C., K. Schuster-Gossler, E. Kremmer and A. Gossler (2013). "Normal Development in Mice Over-Expressing the Intracellular Domain of DLL1 Argues against Reverse Signaling by DLL1 In Vivo." *PLoS One* **8**(10): e79050.
- Remedi, M. S. and C. Emfinger (2016). "Pancreatic β -cell identity in diabetes." *Diabetes, Obesity and Metabolism* **18**: 110-116.
- Riley, K. G., R. C. Pasek, M. F. Maulis, J. Peek, F. Thorel, D. R. Brigstock, P. L. Herrera and M. Gannon (2014). "CTGF modulates adult beta-cell maturity and proliferation to promote beta-cell regeneration in mice." *Diabetes*.
- Roca, C. and R. H. Adams (2007). "Regulation of vascular morphogenesis by Notch signaling." *Genes Dev* **21**(20): 2511-2524.

-
- Romero, G., M. von Zastrow and P. A. Friedman (2011). "Role of PDZ Proteins in Regulating Trafficking, Signaling, and Function of GPCRs: Means, Motif, and Opportunity." Advances in pharmacology (San Diego, Calif.) **62**: 279-314.
- Rooman, I., N. De Medts, L. Baeyens, J. Lardon, S. De Breuck, H. Heimberg and L. Bouwens (2006). "Expression of the Notch Signaling Pathway and Effect on Exocrine Cell Proliferation in Adult Rat Pancreas." The American Journal of Pathology **169**(4): 1206-1214.
- Rorsman, P., K. Bokvist, C. Ammala, P. Arkhammar, P. O. Berggren, O. Larsson and K. Wahlander (1991). "Activation by adrenaline of a low-conductance G protein-dependent K⁺ channel in mouse pancreatic B cells." Nature **349**(6304): 77-79.
- Ruiz de Azua, I., D. Gautam, J. M. Guettier and J. Wess (2011). "Novel insights into the function of beta-cell M3 muscarinic acetylcholine receptors: therapeutic implications." Trends Endocrinol Metab **22**(2): 74-80.
- Rutter, Guy A., Timothy J. Pullen, David J. Hodson and A. Martinez-Sanchez (2015). "Pancreatic β -cell identity, glucose sensing and the control of insulin secretion." Biochemical Journal **466**(2): 203-218.
- Rutz, S., B. Mordmuller, S. Sakano and A. Scheffold (2005). "Notch ligands Delta-like1, Delta-like4 and Jagged1 differentially regulate activation of peripheral T helper cells." Eur J Immunol **35**(8): 2443-2451.
- Sakai, K., K. Matsumoto, T. Nishikawa, M. Suefuji, K. Nakamaru, Y. Hirashima, J. Kawashima, T. Shirotani, K. Ichinose, M. Brownlee and E. Araki (2003). "Mitochondrial reactive oxygen species reduce insulin secretion by pancreatic beta-cells." Biochem Biophys Res Commun **300**(1): 216-222.
- Sakurai, A., S. Fukuhara, A. Yamagishi, K. Sako, Y. Kamioka, M. Masuda, Y. Nakaoka and N. Mochizuki (2006). "MAGI-1 Is Required for Rap1 Activation upon Cell-Cell Contact and for Enhancement of Vascular Endothelial Cadherin-mediated Cell Adhesion." Molecular Biology of the Cell **17**(2): 966-976.
- Sander, M., L. Sussel, J. Connors, D. Scheel, J. Kalamaras, F. Dela Cruz, V. Schwitzgebel, A. Hayes-Jordan and M. German (2000). "Homeobox gene Nkx6.1 lies downstream of Nkx2.2 in the major pathway of beta-cell formation in the pancreas." Development **127**(24): 5533-5540.
- Sazanov, L. A. (2015). "A giant molecular proton pump: structure and mechanism of respiratory complex I." Nat Rev Mol Cell Biol **16**(6): 375-388.
- Scehnet, J. S., W. Jiang, S. Ram Kumar, V. Krasnoperov, A. Trindade, R. Benedito, D. Djokovic, C. Borges, E. J. Ley, A. Duarte and P. S. Gill (2007). "Inhibition of Dll4-mediated signaling induces proliferation of immature vessels and results in poor tissue perfusion." Blood **109**(11): 4753-4760.
- Schaffer, A. E., B. L. Taylor, J. R. Benthuisen, J. Liu, F. Thorel, W. Yuan, Y. Jiao, K. H. Kaestner, P. L. Herrera, M. A. Magnuson, C. L. May and M. Sander (2013). "Nkx6.1 controls a gene regulatory network required for establishing and maintaining pancreatic Beta cell identity." PLoS Genet **9**(1): e1003274.
- Schapira, A., J. Cooper, D. Dexter, P. Jenner, J. Clark and C. Marsden (1989). "Mitochondrial complex I deficiency in Parkinson's disease." The Lancet **333**(8649): 1269.
- Schisler, J. C., P. T. Fueger, D. A. Babu, H. E. Hohmeier, J. S. Tessem, D. Lu, T. C. Becker, B. Naziruddin, M. Levy, R. G. Mirmira and C. B. Newgard (2008). "Stimulation of human and rat islet beta-cell proliferation with retention of function by the homeodomain transcription factor Nkx6.1." Mol Cell Biol **28**(10): 3465-3476.

- Scholzen, T. and J. Gerdes (2000). "The Ki-67 protein: from the known and the unknown." J Cell Physiol **182**(3): 311-322.
- Schulman, J. L., J. L. Carleton, G. Whitney and J. C. Whitehorn (1957). "<http://www.w3.org/1999/xhtml>>Effect of Glucagon on Food Intake and Body Weight in Man</div>." Journal of Applied Physiology **11**(3): 419-421.
- Schwartz, N. S., W. E. Clutter, S. D. Shah and P. E. Cryer (1987). "Glycemic thresholds for activation of glucose counterregulatory systems are higher than the threshold for symptoms." Journal of Clinical Investigation **79**(3): 777-781.
- Schwitzgebel, V. M., D. W. Scheel, J. R. Conners, J. Kalamaras, J. E. Lee, D. J. Anderson, L. Sussel, J. D. Johnson and M. S. German (2000). "Expression of neurogenin3 reveals an islet cell precursor population in the pancreas." Development **127**(16): 3533-3542.
- Scrocchi, L. A., T. J. Brown, N. MaClusky, P. L. Brubaker, A. B. Auerbach, A. L. Joyner and D. J. Drucker (1996). "Glucose intolerance but normal satiety in mice with a null mutation in the glucagon-like peptide 1 receptor gene." Nat Med **2**(11): 1254-1258.
- Segerstolpe, Å., A. Palasantza, P. Eliasson, E.-M. Andersson, A.-C. Andréasson, X. Sun, S. Picelli, A. Sabirsh, M. Clausen, M. K. Bjursell, David M. Smith, M. Kasper, C. Ämmälä and R. Sandberg (2016). "Single-Cell Transcriptome Profiling of Human Pancreatic Islets in Health and Type 2 Diabetes." Cell Metabolism **24**(4): 593-607.
- Seino, S. and T. Shibasaki (2005). "PKA-Dependent and PKA-Independent Pathways for cAMP-Regulated Exocytosis." Physiological Reviews **85**(4): 1303-1342.
- Servitja, J. M., M. Pignatelli, M. A. Maestro, C. Cardalda, S. F. Boj, J. Lozano, E. Blanco, A. Lafuente, M. I. McCarthy, L. Sumoy, R. Guigo and J. Ferrer (2009). "Hnf1alpha (MODY3) controls tissue-specific transcriptional programs and exerts opposed effects on cell growth in pancreatic islets and liver." Mol Cell Biol **29**(11): 2945-2959.
- Shah, P., A. Vella, A. Basu, R. Basu, W. F. Schwenk and R. A. Rizza (2000). "Lack of suppression of glucagon contributes to postprandial hyperglycemia in subjects with type 2 diabetes mellitus." J Clin Endocrinol Metab **85**(11): 4053-4059.
- Sherwin, R. S., M. Fisher, R. Hendler and P. Felig (1976). "Hyperglucagonemia and Blood Glucose Regulation in Normal, Obese and Diabetic Subjects." New England Journal of Medicine **294**(9): 455-461.
- Shih, H. P., A. Wang and M. Sander (2013). "Pancreas organogenesis: from lineage determination to morphogenesis." Annu Rev Cell Dev Biol **29**: 81-105.
- Smith, S. B., R. Gasa, H. Watada, J. Wang, S. C. Griffen and M. S. German (2003). "Neurogenin3 and Hepatic Nuclear Factor 1 Cooperate in Activating Pancreatic Expression of Pax4." Journal of Biological Chemistry **278**(40): 38254-38259.
- Sohn, J.-W. (2015). "Network of hypothalamic neurons that control appetite." BMB Reports **48**(4): 229-233.
- Solnica-Krezel, L. and D. S. Sepich (2012). "Gastrulation: making and shaping germ layers." Annu Rev Cell Dev Biol **28**: 687-717.

-
- Sørensen, H., M. S. Winzell, C. L. Brand, K. Fosgerau, R. W. Gelling, E. Nishimura and B. Ahren (2006). "Glucagon Receptor Knockout Mice Display Increased Insulin Sensitivity and Impaired β -Cell Function." Diabetes **55**(12): 3463-3469.
- Sørensen, I., R. H. Adams and A. Gossler (2009). "DLL1-mediated Notch activation regulates endothelial identity in mouse fetal arteries." Blood **113**(22): 5680-5688.
- Sosa-Pineda, B., K. Chowdhury, M. Torres, G. Oliver and P. Gruss (1997). "The Pax4 gene is essential for differentiation of insulin-producing beta cells in the mammalian pancreas." Nature **386**(6623): 399-402.
- Sprague, J. E. and A. M. Arbeláez (2011). "Glucose Counterregulatory Responses to Hypoglycemia." Pediatric endocrinology reviews : PER **9**(1): 463-475.
- Sprinzak, D., A. Lakhanpal, L. Lebon, L. A. Santat, M. E. Fontes, G. A. Anderson, J. Garcia-Ojalvo and M. B. Elowitz (2010). "Cis-interactions between Notch and Delta generate mutually exclusive signalling states." Nature **465**(7294): 86-90.
- Stump, G., A. Durrer, A.-L. Klein, S. Lütolf, U. Suter and V. Taylor (2002). "Notch1 and its ligands Delta-like and Jagged are expressed and active in distinct cell populations in the postnatal mouse brain." Mechanisms of Development **114**(1-2): 153-159.
- Su, Y., P. Buchler, A. Gazdhar, N. Giese, H. A. Reber, O. J. Hines, T. Giese, M. W. Buchler and H. Friess (2006). "Pancreatic regeneration in chronic pancreatitis requires activation of the notch signaling pathway." J Gastrointest Surg **10**(9): 1230-1241; discussion 1242.
- Suen, P. M., C. Zou, Y. A. Zhang, T. K. Lau, J. Chan, K. M. Yao and P. S. Leung (2008). "PDZ-domain containing-2 (PDZD2) is a novel factor that affects the growth and differentiation of human fetal pancreatic progenitor cells." The International Journal of Biochemistry & Cell Biology **40**(4): 789-803.
- Sugden, M. C. and M. J. Holness (2006). "Mechanisms underlying regulation of the expression and activities of the mammalian pyruvate dehydrogenase kinases." Archives of Physiology and Biochemistry **112**(3): 139-149.
- Sussel, L., J. Kalamaras, D. J. Hartigan-O'Connor, J. J. Meneses, R. A. Pedersen, J. L. Rubenstein and M. S. German (1998). "Mice lacking the homeodomain transcription factor Nkx2.2 have diabetes due to arrested differentiation of pancreatic beta cells." Development **125**(12): 2213-2221.
- Tamarina, N. A., M. W. Roe and L. Philipson (2014). "Characterization of mice expressing Ins1 gene promoter driven CreERT recombinase for conditional gene deletion in pancreatic beta-cells." Islets **6**(1): e27685.
- Taylor, Brandon L., F.-F. Liu and M. Sander (2013). "Nkx6.1 Is Essential for Maintaining the Functional State of Pancreatic Beta Cells." Cell Reports **4**(6): 1262-1275.
- Thorens, B. (2015). "GLUT2, glucose sensing and glucose homeostasis." Diabetologia **58**(2): 221-232.
- Thorens, B. (2015). "GLUT2, glucose sensing and glucose homeostasis." Diabetologia **58**(2): 221-232.
- Thurston, G. and J. Kitajewski (2008). "VEGF and Delta-Notch: interacting signalling pathways in tumour angiogenesis." Br J Cancer **99**(8): 1204-1209.

-
- Tong, J., R. L. Prigeon, H. W. Davis, M. Bidlingmaier, S. E. Kahn, D. E. Cummings, M. H. Tschop and D. D'Alessio (2010). "Ghrelin suppresses glucose-stimulated insulin secretion and deteriorates glucose tolerance in healthy humans." Diabetes **59**(9): 2145-2151.
- Tsang, S. W., D. Shao, K. S. E. Cheah, K. Okuse, P. S. Leung and K. M. Yao (2010). "Increased basal insulin secretion in Pdzd2-deficient mice." Molecular and Cellular Endocrinology **315**(1–2): 263-270.
- Turner, M. D. and P. Arvan (2000). "Protein Traffic from the Secretory Pathway to the Endosomal System in Pancreatic β -Cells." Journal of Biological Chemistry **275**(19): 14025-14030.
- Unger, R. H. (1971). "Glucagon Physiology and Pathophysiology." New England Journal of Medicine **285**(8): 443-449.
- Utsugi, T., T. Ohno, Y. Ohyama, T. Uchiyama, Y. Saito, Y. Matsumura, H. Aizawa, H. Itoh, M. Kurabayashi, S. Kawazu, S. Tomono, Y. Oka, T. Suga, M. Kuro-o, Y. Nabeshima and R. Nagai (2000). "Decreased insulin production and increased insulin sensitivity in the klotho mutant mouse, a novel animal model for human aging." Metabolism **49**(9): 1118-1123.
- van de Bunt, M., J. E. Manning Fox, X. Dai, A. Barrett, C. Grey, L. Li, A. J. Bennett, P. R. Johnson, R. V. Rajotte, K. J. Gaulton, E. T. Dermitzakis, P. E. MacDonald, M. I. McCarthy and A. L. Gloyn (2015). "Transcript Expression Data from Human Islets Links Regulatory Signals from Genome-Wide Association Studies for Type 2 Diabetes and Glycemic Traits to Their Downstream Effectors." PLoS Genet **11**(12): e1005694.
- Van de Castele, M., G. Leuckx, L. Baeyens, Y. Cai, Y. Yuchi, V. Coppens, S. De Groef, M. Eriksson, C. Svensson, U. Ahlgren, J. Ahnfelt-Ronne, O. D. Madsen, A. Waisman, Y. Dor, J. N. Jensen and H. Heimberg (2013). "Neurogenin 3+ cells contribute to beta-cell neogenesis and proliferation in injured adult mouse pancreas." Cell Death Dis **4**: e523.
- van der Stoep, N., C. D. van Paridon, T. Janssens, P. Krenkova, A. Stambergova, M. Macek, G. Matthijs and E. Bakker (2009). "Diagnostic guidelines for high-resolution melting curve (HRM) analysis: an interlaboratory validation of BRCA1 mutation scanning using the 96-well LightScanner." Hum Mutat **30**(6): 899-909.
- Vandesompele, J., K. De Preter, F. Pattyn, B. Poppe, N. Van Roy, A. De Paepe and F. Speleman (2002). "Accurate normalization of real-time quantitative RT-PCR data by geometric averaging of multiple internal control genes." Genome Biol **3**(7): Research0034.
- Virtanen, S. M. and M. Knip (2003). "Nutritional risk predictors of β cell autoimmunity and type 1 diabetes at a young age." The American Journal of Clinical Nutrition **78**(6): 1053-1067.
- Wahlberg, J., O. Vaarala and J. Ludvigsson (2006). "Dietary risk factors for the emergence of type 1 diabetes-related autoantibodies in 21/2 year-old Swedish children." Br J Nutr **95**(3): 603-608.
- Wallberg, A. E., K. Pedersen, U. Lendahl and R. G. Roeder (2002). "p300 and PCAF act cooperatively to mediate transcriptional activation from chromatin templates by notch intracellular domains in vitro." Mol Cell Biol **22**(22): 7812-7819.
- Wang, F., M. Herrington, J. Larsson and J. Permert (2003). "The relationship between diabetes and pancreatic cancer." Molecular Cancer **2**(1): 1-5.

- Wang, J., L. Elghazi, S. E. Parker, H. Kizilocak, M. Asano, L. Sussel and B. Sosa-Pineda (2004). "The concerted activities of Pax4 and Nkx2.2 are essential to initiate pancreatic β -cell differentiation." Developmental Biology **266**(1): 178-189.
- Watt, F. M., S. Estrach and C. A. Ambler (2008). "Epidermal Notch signalling: differentiation, cancer and adhesion." Curr Opin Cell Biol **20**(2): 171-179.
- Weng, A. P., A. A. Ferrando, W. Lee, J. P. t. Morris, L. B. Silverman, C. Sanchez-Irizarry, S. C. Blacklow, A. T. Look and J. C. Aster (2004). "Activating mutations of NOTCH1 in human T cell acute lymphoblastic leukemia." Science **306**(5694): 269-271.
- Wente, W., A. M. Efanov, I. Treinies, H. Zitzer, J. Gromada, D. Richter and H.-J. Kreienkamp (2005). "The PDZ/coiled-coil domain containing protein PIST modulates insulin secretion in MIN6 insulinoma cells by interacting with somatostatin receptor subtype 5." FEBS Letters **579**(28): 6305-6310.
- Westmoreland, J. J., Q. Wang, M. Bouzaffour, S. J. Baker and B. Sosa-Pineda (2009). "Pdk1 activity controls proliferation, survival, and growth of developing pancreatic cells." Developmental biology **334**(1): 285-298.
- WHO (2016). "Global report on diabetes." <http://www.who.int/mediacentre/factsheets/fs312/en/>.
- Wicksteed, B., M. Brissova, W. Yan, D. M. Opland, J. L. Plank, R. B. Reinert, L. M. Dickson, N. A. Tamarina, L. H. Philipson, A. Shostak, E. Bernal-Mizrachi, L. Elghazi, M. W. Roe, P. A. Labosky, M. G. Myers, Jr., M. Gannon, A. C. Powers and P. J. Dempsey (2010). "Conditional gene targeting in mouse pancreatic β -cells: analysis of ectopic Cre transgene expression in the brain." Diabetes **59**(12): 3090-3098.
- Wiedenkeller, D. E. and G. W. Sharp (1983). "Effects of forskolin on insulin release and cyclic AMP content in rat pancreatic islets." Endocrinology **113**(6): 2311-2313.
- Wiederkehr, A. and C. B. Wollheim (2006). "Minireview: Implication of Mitochondria in Insulin Secretion and Action." Endocrinology **147**(6): 2643-2649.
- Wierup, N., S. Yang, R. J. McEvelly, H. Mulder and F. Sundler (2004). "Ghrelin is expressed in a novel endocrine cell type in developing rat islets and inhibits insulin secretion from INS-1 (832/13) cells." J Histochem Cytochem **52**(3): 301-310.
- Wilcox, C. L., N. A. Terry, E. R. Walp, R. A. Lee and C. L. May (2013). "Pancreatic α -Cell Specific Deletion of Mouse Arx Leads to α -Cell Identity Loss." PLoS ONE **8**(6): e66214.
- Wilson, J. J. and R. A. Kovall (2006). "Crystal structure of the CSL-Notch-Mastermind ternary complex bound to DNA." Cell **124**(5): 985-996.
- Winzell, M. S. and B. Ahrén (2004). "The High-Fat Diet–Fed Mouse." A Model for Studying Mechanisms and Treatment of Impaired Glucose Tolerance and Type 2 Diabetes **53**(suppl 3): S215-S219.
- Wollheim, C. B., M. Kikuchi, A. E. Renold and G. W. Sharp (1977). "Somatostatin- and epinephrine-induced modifications of $^{45}\text{Ca}^{++}$ fluxes and insulin release in rat pancreatic islets maintained in tissue culture." J Clin Invest **60**(5): 1165-1173.
- Wollheim, C. B. and P. Maechler (2002). " β -Cell Mitochondria and Insulin Secretion." Messenger Role of Nucleotides and Metabolites **51**(suppl 1): S37-S42.
- Wolter, J. (2013). "The Notch Signaling Pathway in Embryogenesis." Embryo Project Encyclopedia.

- Wu, L., J. C. Aster, S. C. Blacklow, R. Lake, S. Artavanis-Tsakonas and J. D. Griffin (2000). "MAML1, a human homologue of Drosophila mastermind, is a transcriptional co-activator for NOTCH receptors." Nat Genet **26**(4): 484-489.
- Xu, X., J. D'Hoker, G. Stange, S. Bonne, N. De Leu, X. Xiao, M. Van de Casteele, G. Mellitzer, Z. Ling, D. Pipeleers, L. Bouwens, R. Scharfmann, G. Gradwohl and H. Heimberg (2008). "Beta cells can be generated from endogenous progenitors in injured adult mouse pancreas." Cell **132**(2): 197-207.
- Yang, Q., K. Yamagata, K. Fukui, Y. Cao, T. Nammo, H. Iwahashi, H. Wang, I. Matsumura, T. Hanafusa, R. Bucala, C. B. Wollheim, J. Miyagawa and Y. Matsuzawa (2002). "Hepatocyte nuclear factor-1alpha modulates pancreatic beta-cell growth by regulating the expression of insulin-like growth factor-1 in INS-1 cells." Diabetes **51**(6): 1785-1792.
- Yang, Y. H., J. E. Manning Fox, K. L. Zhang, P. E. MacDonald and J. D. Johnson (2013). "Intra-islet SLIT-ROBO signaling is required for beta-cell survival and potentiates insulin secretion." Proc Natl Acad Sci U S A **110**(41): 16480-16485.
- Yates, A., W. Akanni, M. R. Amode, D. Barrell, K. Billis, D. Carvalho-Silva, C. Cummins, P. Clapham, S. Fitzgerald, L. Gil, C. G. Giron, L. Gordon, T. Hourlier, S. E. Hunt, S. H. Janacek, N. Johnson, T. Juettemann, S. Keenan, I. Lavidas, F. J. Martin, T. Maurel, W. McLaren, D. N. Murphy, R. Nag, M. Nuhn, A. Parker, M. Patricio, M. Pignatelli, M. Rahtz, H. S. Riat, D. Sheppard, K. Taylor, A. Thormann, A. Vullo, S. P. Wilder, A. Zadissa, E. Birney, J. Harrow, M. Muffato, E. Perry, M. Ruffier, G. Spudich, S. J. Trevanion, F. Cunningham, B. L. Aken, D. R. Zerbino and P. Flicek (2016). "Ensembl 2016." Nucleic Acids Res **44**(D1): D710-716.
- Ye, L., M. A. Robertson, D. Hesselton, D. Y. Stainier and R. M. Anderson (2015). "Glucagon is essential for alpha cell transdifferentiation and beta cell neogenesis." Development **142**(8): 1407-1417.
- Yin, D. D., L. H. You, Q. X. Yuan, X. D. Liang, N. Wang, L. T. Wang, L. Yuan, K. M. Wang and W. De (2014). "Mesothelin promotes cell proliferation in the remodeling of neonatal rat pancreas." World J Gastroenterol **20**(22): 6884-6896.
- Yu, R., D. Dhall, N. N. Nissen, C. Zhou and S.-G. Ren (2011). "Pancreatic Neuroendocrine Tumors in Glucagon Receptor-Deficient Mice." PLOS ONE **6**(8): e23397.
- Zhang, C., T. Moriguchi, M. Kajihara, R. Esaki, A. Harada, H. Shimohata, H. Oishi, M. Hamada, N. Morito, K. Hasegawa, T. Kudo, J. D. Engel, M. Yamamoto and S. Takahashi (2005). "MafA is a key regulator of glucose-stimulated insulin secretion." Mol Cell Biol **25**(12): 4969-4976.
- Zhang, H., Y. Fujitani, C. V. E. Wright and M. Gannon (2005). "Efficient recombination in pancreatic islets by a tamoxifen-inducible Cre-recombinase." genesis **42**(3): 210-217.
- Zheng, C., W. Jia, Y. Tang, H. Zhao, Y. Jiang and S. Sun (2012). "Mesothelin regulates growth and apoptosis in pancreatic cancer cells through p53-dependent and -independent signal pathway." Journal of Experimental & Clinical Cancer Research **31**(1): 1-14.
- Zhou, Q., A. C. Law, J. Rajagopal, W. J. Anderson, P. A. Gray and D. A. Melton (2007). "A multipotent progenitor domain guides pancreatic organogenesis." Dev Cell **13**(1): 103-114.

IV. ACKNOWLEDGEMENTS

In den folgenden Zeilen möchte ich die Chance ergreifen allen Personen zu danken, die mir auf dem Weg zu dieser Arbeit geholfen und beigestanden haben. Mein besonderer Dank geht vor allem an Prof. Dr. Martin Hrabě de Angelis, der mir überhaupt erst die Möglichkeit gegeben hat in seiner Gruppe an diesem spannenden Projekt zu arbeiten und mich stets mit Rat und Tat in meinem wissenschaftlichen Vorhaben unterstützt hat. Ich kann mir keinen besseren Doktorvater vorstellen.

Natürlich möchte ich auch Dr. Gerhard Przemek für seine großartige Unterstützung und Einsatz, den er mir in den vergangenen Jahren entgegengebracht hat, danken. Nicht zuletzt für die beste Korrektur, die man sich vorstellen kann! Vielen Dank auch an die Mitglieder meine Prüfungskommission, mit Prof. Dr. Siegfried Scherer als Vorsitzenden und Prof. Dr. Angelika Schnieke als 2. Prüferin, die bereitwillig diese Ämter übernommen haben. Hier zu nennen ist auch Prof. Dr. Heiko Lickert, der durch seine konstruktive Kritik im Rahmen der Thesis Committee Meetings einen wesentlichen Beitrag zu dieser Arbeit beigetragen hat.

Selbstverständlich möchte ich mich besonders auch bei Nirav Chhabra bedanken, der nicht nur mit mir zusammen sämtliche Freuden und Sorgen der letzten Jahre erlebt hat, sondern mir auch wie ein Bruder ans Herz gewachsen ist. Maßgebend für die großartige Zeit, sind natürlich auch die anderen Gruppenmitglieder Sandra Hoffmann, Andreas Mayer und Michael Schulz, sowie Dr. Anna Diller und Dr. Andras Franko. Danke für die tolle Zusammenarbeit und Stimmung im Team! Ich hatte viel Spaß mit euch!

Bedanken möchte ich mich auch bei meinen zwei Officemädels Daniela und Selina, die nicht nur im Turbogang diese Arbeit Korrektur gelesen haben, sondern sich auch stets für eine Kaffeepause zum „wissenschaftlichen“ Austausch zur Verfügung gestellt haben.

Dank geht auch an die Mitglieder der Beckers Gruppe mit Dr. Martin Irmeler, Dr. Peter Huypens, Mareike Bamberger und Prof. Dr. Johannes Becker für die tolle Zusammenarbeit und Hilfe bei den whole genome transcriptomics Experimenten für meine Arbeit.

Herzlichen Dank geht natürlich auch an alle anderen Kollegen des IEGs, die mich die während der letzten Jahre begleitet haben und an das Deutsche Zentrum für Diabetes (DZD), welches

mir durch finanzielle Unterstützung viele Konferenzen und Fortbildungen ermöglicht hat. Auch möchte ich mich bei meinen lieben Kollegen bei den DINI und HELENA bedanken, es hat mir stets Spaß gemacht mit euch zusammen zu arbeiten.

Außerdem möchte ich selbstverständlich bei allen meinen Freunden bedanken, besonders dir lieber Benny für deine physische und psychische Unterstützung und weil du immer für mich da bist.

Last but not least, geht ein großes Dankeschön natürlich an meine Familie, besonders an meine Eltern, Carmen und Walter, die mich nicht nur stets zu jedem Schritt ermutigt haben, sondern mit allen Kräften unterstützt haben. Ohne euch würde es diese Arbeit nicht geben!

VIELEN LIEBEN DANK AN EUCH!

V. AFFIRMATION

Ich erkläre hiermit an Eides statt, dass ich die vorliegende Arbeit selbstständig, ohne unzulässige fremde Hilfe und ausschließlich mit den angegebenen Quellen und Hilfsmitteln angefertigt habe.

Die verwendeten Literaturquellen sind im Literaturverzeichnis (References) vollständig zitiert.

Diese Arbeit hat in dieser oder ähnlicher Form noch keiner anderen Prüfungsbehörde vorgelegen.

München, den 16.05.2017

Marina Fütterer

VI. PUBLICATIONS, TALKS AND POSTERS

***Dll1-* and *Dll4-*mediated Notch signaling in adult pancreatic β -cells is essential for insulin secretion downstream of the adenylyl cyclase**

Marina Fütterer, Nirav Florian Chhabra', Daniel Gradinger, Davide Cavanna, Martin Irmler, Johannes Beckers, Gerhard K. H. Przemeck, Martin Hrabě de Angelis

Manuscript in preparation

Role of Pax6 in glucose homeostasis and energy metabolism in adult mouse

Nirav Florian Chhabra, Davide Cavanna, Daniel Gradinger, Marina Fütterer, Moya Wu, Birgit Rathkolb, Magdalena Götz, Jovica Ninkovic, Katrin Pfulmann, Paul Pfluger, Susanne Seitz, Anja Zeigerer, Martin Irmler, Johannes Beckers, Jan Rozman, Gerhard K. H. Przemeck, Martin Hrabě de Angelis

Manuscript in preparation

Severe defects in pancreatic islets, hyperglycemia and reduced survival time in *Pdia6* mutant mice

Nirav F Chhabra, Sibylle Sabrautzki, Laura Brachthäuser, Marina Fütterer, Gerhard Przemeck, Bettina Lorenz-Depiereux, Susanne Diener, Thomas Wieland, Birgit Rathkolb, Tim-Matthias Strom, Frauke Neff, Martin Hrabě de Angelis

Manuscript in preparation

***Dll1-* and *Dll4-*mediated Notch signaling in adult pancreatic β -cells is essential for the structural integrity of the islets of Langerhans and maintenance of glucose homeostasis**

Marina Fütterer, Nirav Florian Chhabra', Martin Irmler, Johannes Beckers, Gerhard K. H. Przemeck, Martin Hrabě de Angelis

The Allied Genetics Conference 2016, 13.-16.07.2016, Orlando, Florida, USA, oral and poster presentation

***Dll1-* and *Dll4-*mediated Notch signaling in adult pancreatic β -cells is essential for the structural integrity of the islets of Langerhans and maintenance of glucose homeostasis**

Marina Fütterer, Nirav Florian Chhabra', Martin Irmler, Johannes Beckers, Gerhard K. H. Przemeck, Martin Hrabě de Angelis

EASD Munich 2016, 14.09.2016, München, poster presentation

***Dll1-* and *Dll4-*mediated Notch signaling in adult pancreatic β -cells is essential for the structural integrity of the islets of Langerhans and maintenance of glucose homeostasis**

Marina Fütterer, Natalie Wossidlo, Andreas Mayer, Sandra Hoffmann, Gerhard K. H. Przemeck, Martin Hrabě de Angelis

DZD Workshop, 26.04.2016, Düsseldorf, poster presentation

VII. CURRICULUM VITAE

Name: Marina Helga Fütterer
Geburtstag 21. September 1987
Geburtsort Neustadt an der Waldnaab
Nationalität deutsch

Seit 04/2013 **Promotion am Institut für experimentelle Genetik**
Helmholtz Zentrum München
Deutsches Zentrum für Diabetesforschung (DZD)
AG Martin Hrabě de Angelis
Titel: *In vivo* and *in vitro* analysis of Dll1 and Dll4 function in adult murine pancreatic islets

06/2012 - **Masterarbeit**
03/2013 Department of Chemical Engineering and Biotechnology
University of Cambridge, UK
AG Sabine Bahn
Erasmus gefördert
Titel: *Ex vivo* functional blood biomarkers of immune and metabolic function in PBMC subsets

10/2010 - **Master of Science in Biochemie**
05/2012 Ludwig-Maximilian-Universität, München

08/2010- **Bachelorarbeit in Biochemie**
11/2010 Genzentrum München
AG Cramer
Titel: Cloning, Validation and analysis of TAP-tagged RNA polymerase II associated factors in *Saccharomyces cerevisiae*

10/2007 – **Bachelor of Science in Chemie und Biochemie**
11/2010 Ludwig-Maximilian-Universität, München

09/1998 – **Abitur**
06/2007 Gymnasium Neustadt an der Waldnaab